

Axiomata sive Leges Motus

Lex I.

omne per se movere in flatu suo
directum, nisi quatenus a
veniente.

perforant in motibus suis
lucidantibus et in gravitate inf
secundo profectus retrahuntur
non nisi quatenus a
veniente et Cometae
venientes in flatu
inf.

Lex II.

omnes motus perfecti
sunt lineam rectam
na motum quatenus
generabit, sine fin
profecta fuerit. Et
in cum in generatibus delect
atur, motus eius vel cessat
l oblique oblique adjuvitur et
minutionem componitur.

Lex III.

contractionem promptam et equaliter
in actionem in se motus per
vires divigi
promittit vel trahit alterum
valitur. Siquis lapidem digito
e lapide. Si equus lapidem q
are et equus equaliter in le
eodem relaxandi se corat
m, ac lapidem trahit equus
et quantum promovet pro
in corpus aliud impingent.
mutaverit, idem quoque imp
tionem in factum contra
reflexionem multum subit. Hoc

Oliver Krol

Thermo-Mechanical Modelling of Solids and Interfaces – Theory, Numerics and Applications –

Bibliografische Information Der Deutschen Bibliothek

Die Deutsche Bibliothek verzeichnet diese Publikation in der Deutschen Nationalbibliografie; detaillierte bibliografische Daten sind im Internet über <http://dnb.ddb.de> abrufbar.

Bibliographic information published by Die Deutsche Bibliothek

Die Deutsche Bibliothek lists this publication in the Deutsche Nationalbibliografie; detailed bibliographic data is available in the Internet at <http://dnb.ddb.de>.

Herausgeber: Fachbereich Maschinenbau und Verfahrenstechnik
Lehrstuhl für Technische Mechanik
Postfach 3049
Technische Universität Kaiserslautern
D-67653 Kaiserslautern

Verlag: Technische Universität Kaiserslautern

Druck: Technische Universität Kaiserslautern
ZBT – Abteilung Foto-Repro-Druck

D-386

© by Oliver Krol 2007

This work is subject to copyright. All rights are reserved, whether the whole or part of the material is concerned, specifically the rights of translation, reprinting, reuse of illustrations, recitation, broadcasting, reproduction on microfilm or in any other way, and storage in data banks. Duplication of this publication or parts thereof is permitted in connection with reviews or scholarly analysis. Permission for use must always be obtained from the author.

Alle Rechte vorbehalten, auch das des auszugsweisen Nachdrucks, der auszugsweisen oder vollständigen Wiedergabe (Photographie, Mikroskopie), der Speicherung in Datenverarbeitungsanlagen und das der Übersetzung.

Als Manuskript gedruckt. Printed in Germany.

ISSN 1610-4641
ISBN 978-3-939432-45-6

Thermo-Mechanical Modelling of Solids and Interfaces

- Theory, Numerics and Applications-

vom Fachbereich Maschinenbau und Verfahrenstechnik der
Technischen Universität Kaiserslautern
zur Verleihung des akademischen Grades
Doktor-Ingenieur (Dr.-Ing.)
genehmigte Dissertation

von

Dipl.-Ing. Oliver Krol

Hauptreferent:	Prof. Dr.-habil. P. Steinmann
Koreferenten:	Prof. tekn. dr. R. Larsson
	Prof. dr. ir. H. Askes
Vorsitzender:	Prof. Dr-Ing. D.-H. Hellmann
Dekan:	Prof. Dr.-Ing. I. Aurich

Tag der Einreichung:	22. März 2006
Tag der mündl. Prüfung:	5. Juli 2006

Mai 2007
D 386

Zusammenfassung

In der vorliegenden Arbeit soll die Modellierung und numerische Handhabung von Diskontinuitäten in thermo-mechanischen Festkörpern untersucht und auf unterschiedliche Problemstellungen angewendet werden. Aus dieser Aufgabenstellung ergibt sich ein zweigeteilter Aufbau, wobei sich der erste Teil mit der Beschreibung thermo-mechanischer Prozesse in Kontinua befasst und die Grundlage für die Beschreibung von Diskontinuitäten und Grenzsichten (Interfacen) bildet, die im zweiten Teil schließlich in den kontinuumsmechanischen und thermodynamischen Rahmen eingebettet werden.

Die Festkörper-Modellierung baut auf einer ausführlichen Darstellung der geometrisch nichtlinearen Kinematik auf, die auf unterschiedliche nichtlineare Verzerrungs- und Spannungsmaße für die Referenz- und Momentankonfiguration führt. Dementsprechend resultieren daraus auch unterschiedliche Formulierungen der mechanischen und thermodynamischen Bilanzgleichungen. Ausgehend von diesen Grundlagen wird zunächst mit Hilfe der Konzepte der Plastizitätstheorie ein thermodynamisch konsistentes elasto-plastisches Prototyp-Modell abgeleitet, das sukzessive erweitert wird. Insbesondere werden Schädigungsmodelle unter Berücksichtigung ratenabhängigen Materialverhaltens dargestellt. Im nächsten Schritt erfolgt eine Erweiterung der isothermen Material-Modelle auf thermo-mechanisch gekoppelte Probleme, wobei auch der Sonderfall adiabater Prozesse diskutiert wird. Bei der Darstellung der unterschiedlichen konstitutiven Gesetze wurde auf einen modularen Aufbau Wert gelegt.

Des Weiteren wird die numerische Handhabung des isothermen und des gekoppelten Problems in Hinblick auf eine Anwendung der Finite-Elemente-Methode ebenfalls umfassend beleuchtet. Dazu werden die schwachen Formen bezüglich der unterschiedlichen Konfigurationen und ihre entsprechenden Linearisierungen hergeleitet und diskretisiert. Anhand einiger numerischer Beispiele wurden die Material-Modelle dargestellt und hinsichtlich ihrer Plausibilität überprüft.

Zur Berücksichtigung der Diskontinuitäten wird zunächst eine geeignete Kinematik eingeführt und die mechanischen und thermodynamischen Bilanzgleichungen entsprechend modifiziert. Die numerische Beschreibung der Diskontinuitäten geschieht mit Hilfe einer speziellen Finite-Elemente-Formulierung (Interface-Elemente), denen eine adäquate Diskretisierung zugrunde liegt. Dabei sollen im Folgenden zwei grundsätzliche Anwendungsgebiete der Interface-Elemente unterschieden werden. Zum einen dienen sie zur Beschreibung von post-kritischen Vorgängen bei Lokalisierungsproblemen, die auch Materialtrennung zulassen und eignen sich daher zur Beschreibung von Trennvorgängen. Hier sollen wiederum die gebietsabhängige und die gebietsunabhängige Formulierung behandelt werden, die sich im Wesentlichen in der Definition des Verzerrungsmaßes in der Grenzsicht unterscheiden. Im zweiten Fall werden den Diskontinuitäten materielle Eigenschaften zugeordnet, bei gleichzeitig geringer räumlicher Ausdehnung, sodass sich hier ein typisches Anwendungsfeld in der Modellierung von Verbundwerkstoffen findet. Für beide Anwendungsgebiete wird die thermo-mechanisch

gekoppelte Formulierung hergeleitet. Anhand entsprechender Beispiele werden die unterschiedlichen Interface-Formulierungen bezüglich ihrer Plausibilität überprüft.

Abstract

In the present work the modelling and numerical treatment of discontinuities in thermo-mechanical solids is investigated and applied to diverse physical problems. From this topic a structure for this work results, which considers the formulation of thermo-mechanical processes in continua in the first part and which forms the mechanical and thermodynamical framework for the description of discontinuities and interfaces, that is performed in the second part.

The representation of the modelling of solid materials bases on the detailed derivation of geometrically nonlinear kinematics, that yields different strain and stress measures for the material and spatial configuration. Accordingly, this results in different formulations of the mechanical and thermodynamical balance equations. On these foundations we firstly derive by means of the concepts of the plasticity theory an elasto-plastic prototype-model, that is extended subsequently. In the centre of interest is the formulation of damage models in consideration of rate-dependent material behaviour. In the next step follows the extension of the isothermal material models to thermo-mechanically coupled problems, whereby also the special case of adiabatic processes is discussed. Within the representation of the different constitutive laws, the importance is attached to their modular structure. Moreover, a detailed discussion of the isothermal and the thermo-mechanically coupled problem with respect to their numerical treatment is performed. For this purpose the weak forms with respect to the different configurations and the corresponding linearizations are derived and discretized. The derived material models are highlighted by numerical examples and also proved with respect to plausibility.

In order to take discontinuities into account appropriate kinematics are introduced and the mechanical and thermodynamical balance equations have to be modified correspondingly. The numerical description is accomplished by so-called interface-elements, which are based on an adequate discretization. In this context two application fields are distinguished. On the one side the interface elements provide a tool for the description of postcritical processes in the framework of localization problems, which include material separation and therefore they are appropriate for the description of cutting processes. Here in turn one has to make the difference between the domain-dependent and the domain-independent formulation, which mainly differ in the definition of the interfacial strain measure. On the other side material properties are attached to the interfaces whereas the spatial extension is neglectable. A typical application of this type of discontinuities can be found in the scope of the modelling of composites, for instance. In both applications the corresponding thermo-mechanical formulations are derived. Finally, the different interface formulations are highlighted by some numerical examples and they are also proved with respect to plausibility.

Danksagung

Als ich im Jahr 2000 als wissenschaftlicher Mitarbeiter meine Arbeit am Lehrstuhl für technische Mechanik der Universität Kaiserslautern aufnahm, war ich mir nicht sicher, ob ich der Richtige für die Arbeit sei. Die zu bearbeitende Thematik befasste sich im Rahmen eines DFG Forschungsprojektes mit den Schneid- und Reißvorgängen duktiler Materialien und war zwar interessant, aber auch schwierig und verlangte ein Handwerkszeug, das ich mir erst im Laufe der Zeit aneignen musste, da ich ursprünglich aus dem Bereich Kraft- und Arbeitsmaschinen kam; ein Bereich in dem eher Lärm, Rauch und Qualm auf der Tagesordnung standen als Tensorrechnung und Programmieren. Ich bin Professor Steinmann sehr dankbar für das mir entgegen gebrachte Vertrauen, die Geduld und seine wissenschaftliche Unterstützung bei meiner Arbeit, deren Abschluss diese Dissertation bildet. Ich habe sehr viel gelernt.

Des Weiteren bedanke ich mich für das mir von Professor R. Larsson und Professor H. Askes entgegengebrachte Interesse und für die Übernahme der Koreferate. Ich bin sehr froh über ihre konstruktive Kritik, die ich gerne in die Arbeit eingeflochten habe.

Insgesamt bedanke ich mich bei allen Mitarbeitern des LTM, die zu einer angenehmen Arbeitssphäre beigetragen haben und mit denen ich eine gute Zeit verbringen durfte.

Auch meinen Eltern und meiner Familie sei ein Dank ausgesprochen, dafür, dass sie meine Ausbildung jederzeit unterstützt haben und für ihre stete Sorge um mein Wohlergehen.

Zuletzt danke ich meiner Frau, die mich während des gesamten Schaffensprozesses des Zusammenschreibens mit ihrer ganzen Geduld und Liebe begleitet hat.

Oliver Krol

Karlsruhe, Mai 2007

Notation

\mathfrak{B}	body
\mathcal{B}	configuration
$\partial\mathcal{B}$	boundary
$\mathcal{B}_0, \partial\mathcal{B}_0$	reference configuration and boundary
$\mathcal{B}_t, \partial\mathcal{B}_t$	spatial configuration and boundary
$\mathcal{B}_p, \partial\mathcal{B}_p$	intermediate configuration and boundary
$\mathcal{V}, \partial\mathcal{V}$	body and boundary
\mathcal{S}	subconfiguration
$\partial\mathcal{S}$	boundary
\mathcal{I}	interface
$\partial\mathcal{I}$	interfacial boundary
W	strain energy function
W_{vol}	volumetric contribution of an elastic potential
W_{iso}	isochoric contribution of an elastic potential
W_{mic}	hardening potential
W_{eth}	thermo-elastic potential
W_{th}	thermal potential
Ψ	free Helmholtz energy
\dot{Q}	heat power
\overline{Q}	entropy input
P	mechanical power
P_{int}	internal mechanical power
P_{ext}	external mechanical power
K	kinetic energy
U	internal energy
u	specific internal energy
r	specific heat sources
S	entropy
s	specific entropy
Y	entropy production
η	specific entropy production
g	specific entropy source
D	dissipation
D_{loc}	local dissipation
D_{con}	convective dissipation

\mathfrak{F}	generalized thermodynamic flux
\mathfrak{S}	generalized thermodynamic source
\mathfrak{P}	generalized thermodynamic production
\mathcal{G}	mechanical virtual work
\mathcal{U}	thermal virtual work
φ	motion
\mathbf{F}^{\natural}	deformation tensor
\mathbf{f}^{\natural}	inverse deformation tensor
$J = \det \mathbf{F}^{\natural}$	determinant of deformation gradient
\mathbf{H}^{\natural}	displacement gradient
$\mathbf{g}^{\natural}, [\mathbf{g}^{\natural}]^{-1}$	mixed variant metric tensor
\mathbf{P}^{\natural}	1. Piola-Kirchhoff stress
$\mathbf{F}_{iso}^{\natural}$	isochoric deformation tensor
$\mathbf{F}_{vol}^{\natural}$	volumetric deformation tensor
\mathbf{F}_e^{\natural}	elastic deformation tensor
\mathbf{F}_p^{\natural}	plastic deformation tensor
\mathbf{Q}^{\natural}	proper orthogonal transformation tensor
\mathbf{R}^{\natural}	proper orthogonal rotation tensor
$\Delta \mathbf{F}^{\natural}$	deformation tensor increment
$\mathbf{F}_e^{\natural, trial}$	trial deformation tensor
$\bar{\mathbf{L}}$	velocity gradient in \mathcal{B}_p
$\bar{\mathbf{L}}_e, \bar{\mathbf{L}}_p$	elastic and plastic velocity gradient in \mathcal{B}_p
$\bar{\mathbf{D}}$	symmetric deformation rate tensor in \mathcal{B}_p
$\bar{\mathbf{D}}_p^{\natural}$	plastic deformation rate tensor in \mathcal{B}_p
$\bar{\mathbf{W}}_p^{\natural}$	skewsymmetric plastic spin in \mathcal{B}_p
$\bar{\mathbf{M}}_p^{\natural}$	Mandel stress tensor in \mathcal{B}_p
\mathbf{S}^{\sharp}	contravariant stress tensor in \mathcal{B}_p
\mathbf{X}	material placement vector
$\mathbf{G}^{\sharp}, \mathbf{G}^{\flat}$	contra- and covariant metric tensor
$\text{Grad}[\bullet]$	material gradient operator
$\text{Div}[\bullet]$	material divergence operator
\mathbf{U}^{\natural}	right stretch tensor
\mathbf{V}^{\natural}	left stretch tensor
\mathbf{C}^{\flat}	right Cauchy Green tensor
\mathbf{C}_{vol}^{\flat}	volumetric right Cauchy-Green tensor
$\bar{\mathbf{C}}^{\flat}, \mathbf{C}_{iso}^{\flat}$	isochoric right Cauchy Green tensor
$\bar{\mathbf{C}}_e^{\flat}$	elastic right Cauchy-Green tensor
$\bar{\mathbf{C}}_p^{\flat}$	plastic right Cauchy-Green tensor
$\bar{\mathbf{B}}_p^{\sharp}, [\bar{\mathbf{C}}_p^{\flat}]^{-1}$	inverse plastic right Cauchy-Green tensor
\mathbf{E}^{\flat}	Green-Lagrange strain tensor
\mathbf{S}^{\sharp}	2. Piola-Kirchhoff stress
\mathbf{t}_0	initial traction vector
\mathbf{b}_0	initial volume forces
\mathbf{Q}	material heat flux vector
\mathbf{H}	material entropy flux vector

N	initial normal vector
ν	material yield surface normal tensor
x	spatial placement vector
u	displacement vector
g^\sharp, g^\flat	contra- and covariant metric tensor on \mathcal{B}_t
g_i, g^i	co- and contravariant tangent vectors on \mathcal{B}_t
G_i, G^i	co- and contravariant tangent vectors on \mathcal{B}_0
\bar{g}_i, \bar{g}^i	co- and contravariant base vectors on \mathcal{B}_p
$\bar{g}^\sharp, \bar{g}^\flat$	contra- and covariant metric tensor on \mathcal{B}_p
v	velocity tensor
$\text{Grad}[\bullet]$	spatial gradient operator
$\text{Div}[\bullet]$	spatial divergence operator
c^\flat	inverse left Cauchy Green tensor
b^\sharp	left Cauchy Green tensor
b_e^\sharp	elastic left Cauchy Green tensor
l^\sharp	velocity gradient
l_e^\sharp	elastic velocity gradient
l_p^\sharp	plastic velocity gradient
d^\sharp	strain rate tensor
w^\sharp	spin tensor
e^\flat	Almansi tensor
τ^\sharp	Kirchhoff stress tensor
$\tilde{\tau}^\sharp$	deviatoric Kirchhoff stress tensor
σ^\sharp	Cauchy stress
t	spatial traction vector
b	spatial volume forces
r	distance vector
q	spatial heat flux vector
h	spatial entropy flux vector
n	spatial normal vector
ν	spatial yield surface normal tensor
ν_α	coefficient of yield surface normal tensor
I_α	invariants
λ_α	eigenvalues
$\tilde{\lambda}_\alpha$	deviatoric eigenvalues
$\Delta\lambda_\alpha$	eigenvalue increment
N^α	material eigenvector
M^α	material eigenbase
m^α	spatial eigenbase
n^α	spatial eigenvector
$\varphi_{\alpha\beta}$	coefficient matrix
m	mass
ρ	mass density
ρ_0	initial mass density
Θ	temperature
Θ_0	reference temperature

p	pressure
d	damage variable
q	hardening variable
ξ_i	internal variable
Y_0	initial yield stress
Y_n	resulting yield stress
h	linear hardening modulus
κ	nonlinear hardening modulus
Φ	yield function
Φ^{pla}	plastic potential
Φ^{dam}	damage potential
γ	plastic multiplier
S_0	energy release rate
R	damage energy release rate
s_0	damage exponent
η	viscosity
μ	shear modulus
κ	bulk modulus
t	Time
$\Delta t, \Delta \tau$	time increment
ω_h, ω_y	temperature coefficients
c_p	heat capacity
κ_0	material heat conduction tensor
κ	spatial heat conduction tensor
α	heat expansion coefficient
N_a	shape function of mechanical subproblem
M_b	shape function of thermal subproblem
$\nabla_X N_a$	gradient of N_a with respect to \mathbf{X}
$\nabla_x N_a$	gradient of N_a with respect to \mathbf{x}
$D_x[\bullet]$	linearization of $[\bullet]$
$\Delta[\bullet]$	increment of $[\bullet]$
$\delta[\bullet]$	variation of $[\bullet]$
\mathbf{M}	mass matrix
\mathbf{L}	external contributions
\mathbf{T}	internal contributions
\mathbf{K}_e	element stiffness matrix
$\mathbf{K}_e^{\Theta \mathbf{u}}, \mathbf{K}_e^{\mathbf{u} \Theta}$	mixed element stiffness matrix
$\mathbf{K}_e^{\mathbf{u} \mathbf{u}}$	mechanical element stiffness matrix
$\mathbf{K}_e^{\Theta \Theta}$	thermal element stiffness matrix
\mathbf{u}	discrete displacement vectors
\mathbf{F}_e	discrete element deformation gradient
\mathbf{S}_e	material discrete element stress vector
\mathbf{E}_e	material discrete element strain vector
\mathbf{S}_e	material discrete element stress vector
\mathbf{E}_e	material discrete element strain vector
σ_e	spatial discrete element stress vector
\mathbf{e}_e	spatial discrete element strain vector

Θ	discrete temperature vector
\mathbf{J}_e	finite element transformation matrix
\mathbf{B}_e	element B-matrix
ε	strain tensor (lin. theory)
σ	Cauchy stress
$\tilde{\sigma}$	interfacial stress
\mathbf{m}	normal vector across interfaces
$\hat{\mathbf{n}}$	interface tangent vector
$\hat{\mathbf{b}}$	interfacial volume force
$\hat{\mathbf{t}}$	interfacial traction vector
\mathbf{t}_α	tangent vector
\mathbf{P}	projection tensor (2^{nd} order)
\mathbf{I}	unit tensor (2^{nd} order)
$\widetilde{\text{div}}$	interfacial divergence operator
$\{\bullet\}$	average of $[\bullet]$
$[\![\bullet]\!]$	jump of $[\bullet]$
$[\![q]\!]$	heat flux vector across the interface
\hat{q}	heat flux vector along the interface
\tilde{r}	interfacial heat sources
$[\![h]\!]$	entropy flux vector across the interface
\hat{h}	entropy flux vector along the interface
$\hat{\eta}$	interfacial entropy production
\hat{g}	interfacial entropy sources
\hat{s}	interfacial entropy
$\hat{\Psi}$	Interface free Helmholtz energy
$\tilde{\alpha}, \hat{\alpha}$	interfacial heat expansion coefficients
$\tilde{\kappa}, \hat{\kappa}$	interfacial heat conduction coefficients
$\hat{\rho}$	interfacial mass density
$\hat{\Theta}$	interfacial temperature
$\hat{\Theta}_0$	interfacial reference temperature
\hat{D}	interfacial dissipation
\hat{c}	interfacial heat capacity
\hat{E}, \tilde{E}	interfacial elasticity tensor
$\tilde{E}_\perp, \tilde{E}_\parallel$	elastic constants
\mathbb{C}	spatial fourth order material tensor
\mathbb{C}	material fourth order material tensor
\mathbb{i}	spatial fourth order unit tensor
\mathbb{I}	material fourth order unit tensor
\mathbb{I}_{vol}	volumetric fourth order projection tensor
$\mathbb{I}_{iso}, \mathbb{I}_{dev}$	isochoric/ deviatoric fourth order projection tensor
\mathbb{R}	set of real numbers
\mathbb{V}^3	three-dimensional vector-space
\mathbb{E}^3	three-dimensional Euclidian space
$T\mathcal{B}_0$	tangent space on \mathcal{B}_0
$T\mathcal{B}_t$	tangent space on \mathcal{B}_t
$T^*\mathcal{B}_0$	cotangent space on \mathcal{B}_0
$T^*\mathcal{B}_t$	cotangent space on \mathcal{B}_t

\mathcal{M}	manifold
P	material point
Θ^i	convected coordinates in \mathcal{B}_0
θ^i	convected coordinates in \mathcal{B}_t
\mathbb{L}^3	space of mappings $\mathbb{R}^3 \rightarrow \mathbb{R}^3$
\mathbb{L}_+^3	subspace of \mathbb{L}^3 with $\det(\mathbf{y}) > 0$
\mathbb{S}^3	subspace of \mathbb{L}^3 with $\mathbf{y} = \mathbf{y}^t$

Contents

Zusammenfassung	iii
Abstract	v
Danksagung	vii
Notation	ix
1 Introduction	1
2 Bulk Modelling in Continuum Mechanics	5
2.1 Overview	5
2.2 Description of Nonlinear Deformations	6
2.2.1 Kinematics and Strain Measures	6
2.2.2 Material Objectivity and Strain Rates	12
2.3 Balance Principles in Mechanics	14
2.3.1 Material and Spatial Time Derivatives	14
2.3.2 Conservation of Mass	16
2.3.3 Balance of Linear Momentum	16
2.3.4 Balance of Angular Momentum	18
2.3.5 Balance of Mechanical Energy	18
2.4 Thermodynamical Balances	20
2.4.1 1 st Law in Continuum Thermodynamics	20
2.4.2 2 nd Law in Continuum Thermodynamics	22
2.4.3 Clausius-Duhem Inequality	23
2.5 The Concept of Elasticity	24
2.5.1 Stresses in Elastic Materials	24
2.5.2 Volumetric- Isochoric Decomposition	28
2.5.3 Elasticity Tensor	31
2.6 Concepts of Inelasticity	34
2.6.1 Remarks to Linear Elasto-Plasticity	34

2.6.2	Kinematics of nonlinear Elasto-Plasticity	40
2.6.3	Principle of Maximum Plastic Dissipation	42
2.6.4	Evolution Equations	44
2.6.5	Incremental Kinematics	46
2.6.6	Integration of Evolution Equations	48
2.6.7	Elasto-plastic Material Tensor	50
2.6.8	Isotropic Hardening	53
2.7	Inelastic Constitutive Models	54
2.7.1	The Model of Gurson	54
2.7.2	The Model of Lemaitre	58
2.7.3	Rate-dependent Formulations	60
2.8	Numerical Aspects of Elasticity and Inelasticity for Finite Deformations	61
2.8.1	The Weak Form in Terms of the Cauchy Stress	61
2.8.2	The Weak Form in Terms of the Piola Stress	63
2.8.3	Linearization of the Weak Form	64
2.8.4	Discretization of the Weak Form in Terms of the Piola Stress	67
2.8.5	Discretization of the Weak Form in Terms of the Cauchy Stress	73
2.9	Thermo-Mechanical Problems	74
2.9.1	Temperature Evolution	76
2.9.2	The Thermomechanically Coupled Problem	78
2.9.3	Weak Form of the Thermomechanical Problem	79
2.9.4	Linearization and Discretization of the Thermomechanical Problem	80
2.9.5	Adiabatic Processes	85
2.10	Applications	86
2.10.1	Thermo-Elasto-Plasticity	86
2.10.2	The Lemaitre Model and the Gurson Model	89
2.10.3	Deepdrawing Process	90
3	Interface Formulations	99
3.1	Overview	99
3.2	Introduction	99
3.3	Modified Balance Equations	102
3.3.1	Momentum Balance Equations	102
3.3.2	Balance of Mechanical Energy	104
3.4	Thermodynamical Modifications	105
3.4.1	The 1 st Law in Consideration of Interfaces	105
3.4.2	The 2 nd Law in Consideration of Interfaces	105
3.4.3	Modified Clausius-Duhem Inequality	106
3.4.4	Remarks on the Interface Temperature	107
3.5	Weak Form of the Coupled Problem	109
3.5.1	Mechanical Subproblem	109
3.5.2	The Thermal Subproblem based on Hypothesis I	109
3.5.3	The Thermal Subproblem based on Hypothesis II	110
3.5.4	The Thermal Subproblem in Terms of Temperature	111
3.6	Numerical Aspects	113

4	Interfaces in Localisation Problems	117
4.1	Overview	117
4.2	Localization Requirement	118
4.3	Domain-Dependent Interfaces	119
4.3.1	Kinematical Aspects	119
4.3.2	Constitutive Equations	121
4.3.3	Thermo-mechanical Extension	121
4.4	Domain-Independent Interfaces	122
4.4.1	Kinematical Aspects	123
4.4.2	Constitutive Modifications	125
4.4.3	Adiabatic Extension	125
4.5	Weak Form for localization problems	127
4.5.1	Weak Form of the Mechanical Subproblem	127
4.5.2	Weak Form of the Thermal Subproblem	128
4.6	Nonlinear Formulation	130
4.7	Applications	133
4.7.1	Problem of Jointed Sheets	133
4.7.2	Cutting Problems	138
5	Interfaces with Extra-Energy Contributions	145
5.1	Overview	145
5.2	Constitutive Equations	145
5.3	Applications	147
5.3.1	Mechanical Problem	148
5.3.2	Thermal Problems	149
5.3.3	Coupled Problems	153
6	Summary and Conclusions	157
A	Appendix	161
A.1	Spectral Decomposition	161
A.2	Differentiation of Base Tensors	163
A.3	Convexity	165

1 Introduction

Some Remarks on Terminology This thesis is concerned with the modelling of discontinuities and interfaces within thermo-mechanical solids. At first we want to define the given terms, in particular the difference between discontinuities and interfaces. The comprehension of discontinuities in the present text is that a mechanical or non-mechanical field or a property is not smooth but obeys a jump. Therefore the particular quantity is discontinuous and an interface relates a mechanical or non-mechanical quantity to this jump. Since we are going to consider thermo-mechanical behaviour, we are interested in displacement jumps that are related to the corresponding tractions by the interfaces. In analogy to this, the thermal subproblem is governed by the jump of the temperature for instance and the interfaces relates it to the corresponding heat flux. Due to the possibility to handle discontinuities by interfaces these are also the perfect tools to describe the separation of materials occurring in cutting and tearing processes. Other applications arise if not only the jump contributions are taken into account but also tangential contributions within the discontinuity that can be described by averaged values. These formulations are capable to the description of composites including fibres which can be modelled by interfaces as well.

Another focus of this work is the description of thermo-mechanical materials, whereby here especially inelastic material behaviour is taken into account that should be combined with thermal effects. This includes elasto-plastic material behaviour where the elastic range is exceeded and permanent strains are induced, such that deformations remain after unloading. In the case of metals, for instance, additionally hardening effects can occur that make increase the stress-strain-curve over the initial yield stress. The stresses increase to a maximum but due to the nucleation of microcracks or voids the material is weakened leading to the macroscopic decrease of the stress-strain-curve. Rate-dependent formulations are taken into account if the deformation is not superposed quasistatically but by means of high load velocities. The thermal problem can be divided into two subcases, namely a locally coupled or adiabatic problem and a globally coupled problem. The more general case is the globally coupled one, since here in contrast to the adiabatic case the heat transfer is taken into account. To combine these different effects and to adopt them the interface formulation will be one of the main tasks of this thesis.

Motivation This work emanated from a project which was concerned with the modelling of cutting and tearing processes by numerical methods. Hereby one problem was to describe the different physical effects which occur in a combined manner during the loading process of a cutting probe. The process starts when the blade contacts the probe and the probe becomes deformed, whereby the modelling of a two-body problem is very complex on its own. By focusing on the behaviour of the probe it behaves elastic in the first phase of the process but one soon observes permanent

plastic deformations of the material. In the next phase the probe is damaged due to the loading, induced by the development of microcracks. This effect is usually modelled by a reduction of the elasticity module. Nearly at the same time the blade also penetrates the material resulting into a discrete separation of the material. These phases can be observed quite clearly as long as the deformation is superposed quasi-statically. As soon as the loading velocity increases these phases can not be separated as clear as before. In this case the material behaves rate-dependent and also thermal effects have to be taken into account. These effects are related to each other such that the higher the cutting velocity the higher is the temperature occurring in the cutting zone. These temperatures again induce an increased damaging of the material, such that the damaging is temperature-dependent and the temperature depends on the deformation rate, such that finally also the damage depends on the loading velocity. All these effects have to be covered by a material model, combining mechanical and thermal influences and their interaction.

A particular problem is how to model the cutting zone where additionally the penetration of the blade and the discrete failure of the material takes place. These effects can be modelled only by interface elements which have to be equipped with the before mentioned features. In particular the extension to thermal effects have to be taken into account since with higher loading velocities the thermal subproblem plays the dominant role. In particular if non-metallic materials are considered due to the high temperatures occurring at the cutting zone the materials start to melt. These effects can hardly be described by numerical methods.

The application of interfaces with respect to material separation is not the only field this feature is useful for. Another application of interfaces is the treatment of discontinuities as they occur in composites. In the last few years in material sciences one emphasis was placed on investigations with respect to fiber-reinforced composite materials. Since it was nearly impossible to model the materials and especially the fibres this accurately, the properties of the different components were averaged as long as the numerical results and the experimental curves agreed. Also here the interface elements are very promising since they feature the possibility to model the fibres and they also cover the interaction of fibres and matrix material quite easily. Of course, it does not make any sense to discretize every fibre in detail, but one can assemble a number of fibres to a bundle, for instance, which is represented by an interfacial element.

In general interfaces are always useful in the context of discontinuities and therefore the potential number of applications is quite high. However this kind of feature is not implemented in most of the commercial software packages in spite of its high potential. This requires that a lot of problems have to be modelled by numerically very expensive contact elements, which always need the solution of a variation problem with an inequality side condition. This procedure sometimes is necessary but in some applications it would be much more elegant to apply interface elements instead. It would decrease the numerical costs and deliver better results.

Aim of this work Essentially there is more than one objective the author wants to follow up in this work. At first a framework should be created, where different interface formulations and applications can be integrated. Therefore a clear and capacious description of thermo-mechanically coupled problems is intended, whereby the combination with different inelastic effects like plasticity, viscoplasticity and damage are considered. Since the different material model formulations base on the same mechanical and thermodynamical principles, it is possible to combine them in an arbitrary way. For emphasizing this fact a modular representation of the different models is attempted and the elementary realization and combination of the models is illustrated by means of simple or less complicated examples. Furthermore, the numerical treatment of the theoretical material formulations within the finite element formulation should be derived and tested in corresponding realistic

applications.

In the next step the representation of discontinuities and their integration into the continuous background we developed before should be performed. This requires the reformulation of the governing mechanical and thermodynamical balance equations in consideration of discontinuous displacement and temperature fields, yielding a comprehensive theory. Finally, different discontinuous phenomena are presented and it is shown how their theoretical description emerges from the generalized theory and which assumptions have to be made to arrive at the corresponding formulation. Naturally, the formulations have to be transformed into appropriate numerical forms and the corresponding primary variables have to be discretized, such that it can be applied to realistic problems. In particular the subject of postcritical localization material behaviour and the modelling of composites are investigated by means of the extended formulation.

Structure of this work As mentioned before the discontinuity and interfaces are embedded within a surrounding (matrix) material, which has to be equipped at first with the thermo-mechanical properties, i.e. definition of the material properties. This should be topic of **chapter 2**. In order to assure a certain generality the material description is given in terms of geometrically nonlinear deformations. That requires to distinguish between the initial state of the considered body and its current state, which are connected by a nonlinear map. The detailed definitions are given in the following chapter. According to this we obtain different nonlinear strain measures and the corresponding stress fields. With this at hand the governing mechanical and thermodynamical balance equations can be formulated from which important restrictions for the modelling of materials emerge. The simplest and most important class of material models are elastic models and a lot of achievements in mechanics base on the studies of elastic materials. However, we want to extend the number of material models by taking inelastic effects into account. Another important class of material models are plastic models. In this work we present a prototype plastic material law and as we will see this model provides a good foundation for the description of other inelastic effects like viscosity and damage. An intention of this work here is to emphasize the modular character of the presented constitutive models. In order to work with the derived material models the corresponding numerical aspects have to be highlighted. The main task there is to derive the corresponding weak formulation in terms of the initial and the instantaneous configuration and since we consider nonlinear balance equations we need to linearize them, such that the resulting algebraic equations system can be solved by a standard Newton-Raphson iteration scheme. In the last section we like to extend the given formulations to the consideration of thermal effects. Here the distinction between adiabatic and global thermomechanically coupled materials has to be performed. Hereby the main difference is that in the adiabatic case the temperature is defined as an additional internal variable, whereas in thermo-mechanically coupled problems the temperature field is introduced as a further primary variable, that allows the consideration of heat fluxes. In order to perform simulations, the thermo-mechanical model has also transformed to the weak form and accordingly linearized.

The consideration of the discontinuities or interfaces, respectively, is performed in **chapter 3**. Here we restricted ourselves to the linear theory, since the main aspects can be conceived there more easily. The emphasis here is on the derivation of the governing balance equations in consideration of interfaces. In particular we introduce the interface quantities $\tilde{\mathbf{u}}$ and $\hat{\mathbf{u}}$ denoting the displacement jump and the average displacement across and along the interface. From these definitions emerge modifications of the linear momentum balance equation, the 1st and 2nd law of thermodynamics and the corresponding weak formulations for the numerical implementation. Finally we want to discuss two possible definitions of the interface temperature which lead to different formulations of the entropy rate. In order to cover the numerical aspects of the interface formulation the chapter is

finished by the discretization of the primary interface variables in space and time.

In the next step, in **chapter 4** we want to apply the given interface formulation to localization problems whereby firstly the appearance of localization phenomena has to be defined. For this the so-called localization tensor or acoustic tensor is introduced that coincides with the double contraction of the material tensor with the interface normal vector. It can be shown that localization occurs if the acoustic tensor becomes singular. From the mathematical point of view the critical point corresponds with a change of the differential equation type from elliptic to hyperbolic. If the critical point is reached the interfaces are needed to describe the postcritical behaviour of the material. There are two different interface formulations which have to be distinguished. On the one hand we want to present the domain-dependent interface formulation, where the interface constitutive law is taken from the ambient material by projecting it into the discontinuity. On the other hand we introduce the domain-independent interface formulation where the discontinuity is described by an extra interface constitutive law that mainly bases on the concepts of plasticity, which will have been already introduced in chapter 2. Here the yield function is replaced by a slip function indicating the failure of the particular interface and the onset of slip. Both formulations are presented here and afterwards extended to thermo-mechanical/adiabatic problems. The application of the two formulations to numerical examples show the advantages and disadvantages of both formulations. In the last step a geometrically nonlinear approach of the domain-dependent formulation is presented. In **chapter 5** the complete interface formulation introduced in chapter 3 is applied to the modelling of composites in consideration of thermo-mechanically coupled problems. For the simulation we need to specify the corresponding constitutive laws for the interfaces, whereby we restrict ourselves to the case of linear elasticity and thermo-elasticity. To investigate the influence of the different interface contributions across and along the interface we present different numerical examples considering elastic, thermal and thermo-elastic problems and vary the corresponding material parameters. In **chapter 6** a concluding consideration is made, where we summarize and evaluate the main results of this work. This discussion also yields the existing problems and aspects of future research.

2 Bulk Modelling in Continuum Mechanics

2.1 Overview

In this chapter we want to focus on the modelling of materials in the framework of large deformations. In contrast to the formulation in terms of small strains, this requires a kinematical description, that normally leads to nonlinear relations, representing a generalization of the linear theory. A crucial quantity in this context is the so-called mixed-variant *deformation gradient* \mathbf{F}^b , that connects line elements in the material configuration to line elements in the spatial configuration. From this emanates a variety of conceivable nonlinear strain measures and strain rates, that are associated with different *configurations*. The aim of the first section is the representation of how they are related to each other and which requirements have to be fulfilled to obtain physically reasonable formulations. The kinematics constitute the fundament for the mechanical balance equations like the continuity equation, linear and angular momentum balance equation and the balance of mechanical energy. From the variety of strain measures emanates different representations of the balance equations. Since we want to take care deriving thermodynamically consistent constitutive equations we resume the 1st and 2nd law of thermodynamics in terms of continuum mechanics. By appropriate transformations we can derive the Clausius-Duhem-Inequality, a specific representations of the 2nd law of thermodynamics, yielding restrictions for the theory of material modelling. With this at hand we are able to develop the concept of stress as it emanates from an elastic potential, that is introduced by *strain energy function*. In the next step we modify the theory of elasticity in the sense, that we introduce side conditions accounting for inelastic effects, whereby firstly we give a brief review of the concepts of linear elastoplasticity before applying them to the large strain formulation. In respect of the implementation the emphasis is placed on the derivation of the *material tensor* or the *consistent tangent operator/matrix*. The described elastoplastic material model serves as a prototype model which can be enriched by additional inelastic effects or rate dependent formulations. In particular we introduce formulations of the Gurson type and the Lemaitre type for the description of ductile damage and the elasto-viscoplastic effects are recorded by the Perzyna model. Here we want to emphasize the modular character, since all previously presented material models can be considered as extensions of the prototype model of the von-Mises type. For the solution of nonlinear structures in consideration of inelastic constitutive material behaviour we resort to the standard finite element method. Since the numerical solution method is based on variational formulations we apply the variational calculus to the governing differential equations to obtain finally the weak form, that is equivalent to the initial problem. The solution of the resulting set of nonlinear algebraic equations by the standard Newton-Raphson iteration scheme requires a linearization and a discretization of the weak form. Finally we extend the isothermal inelastic models to thermo-mechanically coupled

formulations taking into account temperature dependent constitutive material behaviour and introducing the temperature as an additional global primary variable, whose evolution is determined by the energy balance equation in terms of the internal energy. A specific thermo-mechanical formulation assumes the process velocity this high, that any heat exchange of the system and the environment is negligible, such that *adiabatic conditions* are given. Therefore there is no necessity to consider the temperature as a global variable anymore, but it can be 'reduced' to an internal variable. This completes the theoretical formulation of thermo-mechanical materials including inelastic effects.

The kinematical description of elastic deformations in terms of large strains is state of the art and for an exhaustive introduction of this subject and the theoretical foundations we want to refer to the monographs of Eringen [Eri67], Wang & Truesdell [WT73], Becker & Bürger [BB75], Marsden & Hughes [MH94], Altenbach & Altenbach [AA94], Ogden [Ogd97], Podio-Guidugli [PG00], Holzapfel [Hol01], Greve [Gre03].

There are a lot of publications covering the subject of nonlinear elasto-plasticity and we just refer here to a small number of them. The beginning of inelastic material formulations in terms of large deformation usually is accredited to Green & Naghdi [GN64] and Lee [Lee67]. A comprehensive work taking into account the theoretical and the numerical treatment of inelastic deformations in terms of large strains was contributed by Simo in the papers [Sim88a] and [Sim88b]. Furthermore we like to refer to the papers of Miehe & Stein [MS92], Miehe [Mie98a] and [Mie98b], Weber & Anand [WA90], Naghdi [Nag90], Simo [Sim92]. Monographs about the subject of linear and nonlinear elasto-plasticity are published by Simo & Hughes [SH98], Haupt [Hau02], Parisch [Par03], Miehe [Mie92], Lubliner [Lub90] and Han & Reddy [HR99].

An overview of further literature corresponding to the subject of numerical realisation and thermo-mechanical extension is given at the beginning of the particular sections.

2.2 Description of Nonlinear Deformations

In this section we firstly want to consider the fundamental concepts of nonlinear elastic material theory, which are applied to elasto-plastic problems later on. The concepts presented here are the kinematics, material objectivity or frame-indifference, respectively, and the concept of stress, combined with the fundamental ideas of elasticity theory. We start with the definition of a material body in its different configurations and the corresponding deformation tensors and strain measures that are related by the deformation gradient. After that we derive the strain rates and discuss the matter of objectivity before we declare the terms of Cauchy elasticity, hyper-elasticity and the different stress formulations that refer to the configurations.

2.2.1 Kinematics and Strain Measures

Manifolds, Configurations and Metrics A *material body* \mathfrak{B} is represented by a differentiable manifold \mathcal{M} of finite dimension that consists of a set of *material points* P . At different times $t \in \mathcal{I} \subset \mathbb{R}_+$ the material points $P \in \mathfrak{B}$ can be identified with different subsets of the Euclidean point space \mathbb{E}^3 . The states the body passes through at different times t are called *configurations* and the smooth family of configurations with t as the family parameter we call *motion*. During its motion every material point P describes a curve that can be characterised by time-dependent position vectors $\mathbf{x}(t) \in \mathbb{V}^3$ or coordinate functions $x^k(t) \in \mathbb{R}^3, k = 1, 2, 3$. \mathbb{V}^3 denotes the three-dimensional Euclidean vector-space and the mapping $(\mathcal{M}, t) \rightarrow \mathbf{x}(t) \in \mathbb{V}^3$ is called *placement*, i.e. the placement of \mathfrak{B} at time t defines the corresponding configuration. The motion of the material

body can be easily described by the change from one configuration to the other, so it is useful to determine a *reference* or *material* configuration of the material body at a certain time t_0 , to which we can refer the other configurations. This configuration can be chosen arbitrarily, but it makes sense to choose a stress-free one. So we identify the reference configuration by $(\mathfrak{B}, t_0) \rightarrow \mathcal{B}(t_0) = \mathcal{B}_0 \subset \mathbb{E}^3$ and accordingly the spatial reference configuration by $(\mathfrak{B}, t) \rightarrow \mathcal{B}(t) = \mathcal{B}_t \subset \mathbb{E}^3$. Placements in the reference configuration are denoted by $\mathbf{X} \in \mathcal{B}_0$ and placements in the spatial configuration are denoted by $\mathbf{x}(t) \in \mathcal{B}_t$ and both are connected by the nonlinear mapping $\varphi(\mathbf{X}, t) : \mathcal{B}_0 \times \mathbb{R} \rightarrow \mathcal{B}_t$. Since the placement in the reference configuration is uniquely determined in time and space and following Haupt [Hau02], it also can be interpreted as a *designation*. The mapping $\mathbf{x}(t) = \varphi(\mathbf{X}, t) : \mathcal{B}_0 \times \mathbb{R} \rightarrow \mathcal{B}_t$ describes the position of a particular material point named \mathbf{X} at time t in \mathbb{E}^3 . By fixing two of the three coordinates x^k , respectively, the vector $\mathbf{x}(x^i, t), i \neq k$ describes a curvilinear coordinate line in \mathbb{E}^3 , which are called *convected coordinates*. The convected coordinates in the reference configuration are denoted by $\Theta^i = \theta^i(\mathbf{X}, t_0)$. With this at hand we can define a system of natural base vectors $\mathbf{g}_i = \partial_{\theta^i} \mathbf{x}(t)$, respectively $\mathbf{G}_i = \partial_{\Theta^i} \mathbf{X}$, that are tangent vectors to $\theta^i(\mathbf{x}, t)$, respectively $\Theta^i(\mathbf{X})$ and that span the tangent spaces $(T\mathcal{B}_t, T\mathcal{B}_0)$. According to that we can define a dual base of cotangent base vectors $\mathbf{g}^i = \partial_{\mathbf{x}} \theta^i$ and $\mathbf{G}^i = \partial_{\mathbf{X}} \Theta^i$ spanning the cotangent spaces $T^*\mathcal{B}_t, T^*\mathcal{B}_0$. In a precise mathematical notation we write

$$\begin{aligned} \mathbf{g}_i &= \partial_{\theta^i} \mathbf{x} \in \mathbb{R}^3 : T^*\mathcal{B}_t \rightarrow \mathbb{R}, & \mathbf{g}^i &= \partial_{\mathbf{x}} \theta^i \in \mathbb{R}^3 : T\mathcal{B}_t \rightarrow \mathbb{R}, \\ \mathbf{G}_i &= \partial_{\Theta^i} \mathbf{X} \in \mathbb{R}^3 : T^*\mathcal{B}_0 \rightarrow \mathbb{R}, & \mathbf{G}^i &= \partial_{\mathbf{X}} \Theta^i \in \mathbb{R}^3 : T\mathcal{B}_0 \rightarrow \mathbb{R} \end{aligned} \quad (2.2.1)$$

for the tangent and cotangent base vectors, whereby the $\theta^i(\mathbf{x}, t)$ of the spatial configuration and the $\Theta^i(\mathbf{X})$ of the reference configuration are connected by $\theta^i(\mathbf{x}, t) = \Theta^i(\mathbf{X}) \circ \varphi^{-1}(\mathbf{x}, t)$, respectively by $\Theta^i(\mathbf{X}) = \theta^i(\mathbf{x}, t) \circ \varphi(\mathbf{x}, t)$ with $\varphi^{-1}(\mathbf{x}, t) : \mathcal{B}_t \times \mathbb{R} \rightarrow \mathcal{B}_0$. Naturally we can identify $T^{**}\mathcal{B}_t$ and $T^{**}\mathcal{B}_0$ with $T\mathcal{B}_t$ and $T\mathcal{B}_0$. The natural base vectors \mathbf{g}_i and \mathbf{G}_i define contra-variant fields, whereas the cotangent base vectors \mathbf{g}^i and \mathbf{G}^i denote covariant vector fields, that are usually interpreted as normal vectors on $\theta^i(\mathbf{x}, t)$. Accordingly we define the covariant and contravariant metric tensors by

$$\begin{aligned} \mathbf{g}^b &= g_{ij} \quad \mathbf{g}^i \otimes \mathbf{g}^j \in \mathbb{S}_+^3 : T\mathcal{B}_t \times T\mathcal{B}_t \rightarrow \mathbb{R}, & g_{ij} &= \mathbf{g}_i \cdot \mathbf{g}_j, \\ \mathbf{g}^\sharp &= g^{ij} \quad \mathbf{g}_i \otimes \mathbf{g}_j \in \mathbb{S}_+^3 : T^*\mathcal{B}_t \times T^*\mathcal{B}_t \rightarrow \mathbb{R}, & g^{ij} &= \mathbf{g}^i \cdot \mathbf{g}^j, \\ \mathbf{G}^b &= G_{ij} \quad \mathbf{G}^i \otimes \mathbf{G}^j \in \mathbb{S}_+^3 : T\mathcal{B}_0 \times T\mathcal{B}_0 \rightarrow \mathbb{R}, & G_{ij} &= \mathbf{G}_i \cdot \mathbf{G}_j, \\ \mathbf{G}^\sharp &= G^{ij} \quad \mathbf{G}_i \otimes \mathbf{G}_j \in \mathbb{S}_+^3 : T^*\mathcal{B}_0 \times T^*\mathcal{B}_0 \rightarrow \mathbb{R} & G^{ij} &= \mathbf{G}^i \cdot \mathbf{G}^j \end{aligned} \quad (2.2.2)$$

whereby here and subsequently $[\bullet]^b$ and $[\bullet]^\sharp$ denote covariant and contravariant tensors. The set of metric tensors is complemented by the following mixed-variant tensors

$$\mathbf{g}^\natural = \mathbf{g}_i \otimes \mathbf{g}^i : T^*\mathcal{B}_t \times T\mathcal{B}_t \rightarrow \mathbb{R} \text{ and } \mathbf{G}^\natural = \mathbf{G}_i \otimes \mathbf{G}^i : T^*\mathcal{B}_0 \times T\mathcal{B}_0 \rightarrow \mathbb{R}, \quad (2.2.3)$$

that can be identified as the spatial and material identity tensors.

Deformation gradient and nonlinear strains The difference of the position vectors of a material point P in the spatial and the material configuration

$$\mathbf{u}(\mathbf{X}, t) = \varphi(\mathbf{X}, t) - \mathbf{X} \in \mathbb{V}^3 \quad (2.2.4)$$

is called displacement field. Following the linear theory, we can define the non-symmetric displacement gradient tensor \mathbf{H}^\natural by differentiating the displacement field with respect to \mathbf{X} . That yields

$$\mathbf{H}^\natural(\mathbf{X}, t) = \partial_{\mathbf{X}} \mathbf{u} = \partial_{\mathbf{X}} \varphi(\mathbf{X}, t) - \mathbf{G}^\natural = \mathbf{F}^\natural - \mathbf{G}^\natural \in \mathbb{L}^3 \quad (2.2.5)$$

and the quantity $\mathbf{F}^\natural(\mathbf{X}, t) \in \mathbb{L}_+^3 : T\mathcal{B}_0 \rightarrow T\mathcal{B}_t$ denotes the *deformation gradient tensor*. $\mathbf{F}^\natural(\mathbf{X}, t)$ is a mixed-variant two-point tensor of second order and involves points in two different configurations. This property makes it able to link elements of $T\mathcal{B}_t$ to elements of $T\mathcal{B}_0$. In addition to that the Jacobian of the deformation gradient is always positive, such that the inverse $\mathbf{f}^\natural(\mathbf{x}, t) = [\mathbf{F}^\natural]^{-1}(\mathbf{X}, t) \in \mathbb{L}_+^3 : T\mathcal{B}_t \rightarrow T\mathcal{B}_0$ is defined. If we consider the transposed deformation gradient tensor $[\mathbf{F}^\natural]^t \in \mathbb{L}_+^3 : T^*\mathcal{B}_0 \rightarrow T^*\mathcal{B}_t$ and the transposed of the inverse deformation gradient $[\mathbf{f}^\natural]^t \in \mathbb{L}_+^3 : T^*\mathcal{B}_t \rightarrow T^*\mathcal{B}_0$ we are also able to transform elements of the cotangential spaces in different configurations to each other. The collection

$$\begin{aligned} \mathbf{F}^\natural(\mathbf{X}, t) &= \mathbf{g}_i \otimes \mathbf{G}^i \in \mathbb{L}_+^3 : T\mathcal{B}_0 \rightarrow T\mathcal{B}_t, \\ [\mathbf{F}^\natural]^t(\mathbf{X}, t) &= \mathbf{G}^i \otimes \mathbf{g}_i \in \mathbb{L}_+^3 : T^*\mathcal{B}_0 \rightarrow T^*\mathcal{B}_t, \\ \mathbf{f}^\natural(\mathbf{x}, t) &= \mathbf{G}_i \otimes \mathbf{g}^i \in \mathbb{L}_+^3 : T\mathcal{B}_t \rightarrow T\mathcal{B}_0, \\ [\mathbf{f}^\natural]^t(\mathbf{x}, t) &= \mathbf{g}^i \otimes \mathbf{G}_i \in \mathbb{L}_+^3 : T^*\mathcal{B}_t \rightarrow T^*\mathcal{B}_0 \end{aligned} \quad (2.2.6)$$

shows possible mappings of line elements $d\mathbf{X}$ or $d\mathbf{x}$, respectively. The deformation described by the deformation gradient generally includes a rotation of the line elements, such that the deformation gradient can be decomposed uniquely in two different ways, namely $\mathbf{F}^\natural = \mathbf{R} \cdot \mathbf{U}^\natural = [\mathbf{g}_a \otimes \tilde{\mathbf{G}}^a] \cdot [\tilde{\mathbf{G}}_a \otimes \mathbf{G}^a]$ and $\mathbf{F}^\natural = \mathbf{V}^\natural \cdot \mathbf{R} = [\mathbf{g}_a \otimes \tilde{\mathbf{g}}^a] \cdot [\tilde{\mathbf{g}}_a \otimes \mathbf{G}^a]$, whereby $\tilde{\mathbf{g}}_a$, $\tilde{\mathbf{g}}^a$, $\tilde{\mathbf{G}}_a$ and $\tilde{\mathbf{G}}^a$ denote base systems in a fictitious intermediate configuration and $\mathbf{R} \in \mathbb{S}^3$ is a proper orthogonal rotation tensor, whereas $\mathbf{U}^\natural \in \mathbb{S}_+^3$ and $\mathbf{V}^\natural \in \mathbb{S}_+^3$ describe the stretches and accordingly they are called the *right* and *left stretch tensors*. Both decompositions lead to the same mapping but the order of rotation and stretching are exchanged. Since the rotation tensor is proper orthogonal, it can be shown, that the eigenvalues of the stretch tensors coincide, but they live in different configurations. Nevertheless, the deformation gradient $\mathbf{F}^\natural(\mathbf{X}, t)$ and also the displacement gradient $\mathbf{H}^\natural(\mathbf{x}, t)$ are no useful strain measures in nonlinear kinematics, since they include rotational transformations. Therefore we follow the definition of normal strains in linear theory ($\mathbf{x} = \mathbf{X}$), where the strains coincide with the symmetric displacement gradient $[\partial_X \mathbf{u}]^{sym}$

$$\begin{aligned} \varepsilon = \frac{|d\mathbf{x}| - |d\mathbf{X}|}{|d\mathbf{X}|} &\implies d\mathbf{x} \cdot d\mathbf{x} = [\varepsilon + 1]^2 d\mathbf{X} \cdot d\mathbf{X} = d\mathbf{X} \cdot [[\mathbf{F}^\natural]^t \cdot \mathbf{g}^b \cdot \mathbf{F}^\natural] \cdot d\mathbf{X} \\ &= d\mathbf{X} \cdot \mathbf{C}^b \cdot d\mathbf{X} \end{aligned} \quad (2.2.7)$$

and obtain the right *Cauchy-Green tensor* $\mathbf{C}^b = g_{ij} \mathbf{G}^i \otimes \mathbf{G}^j \in \mathbb{S}_+^3 : T\mathcal{B}_0 \times T\mathcal{B}_0 \rightarrow \mathbb{R}$. The double contraction of this second order tensor with the initial line element $d\mathbf{X}$ yields the squared length of the stretched spatial line element $d\mathbf{x}$ and moreover this excludes the rotational contributions. Another interpretation of the right Cauchy-Green tensor is given by considering it as the spatial metric \mathbf{g}^b applied to the reference configuration¹. Nevertheless, solving eqn. 2.2.7 for all terms including ε

$$\left[\varepsilon + \frac{1}{2}\varepsilon^2 \right] d\mathbf{X} \cdot d\mathbf{X} = \frac{1}{2} d\mathbf{X} \cdot [\mathbf{C}^b - \mathbf{G}^b] \cdot d\mathbf{X} := d\mathbf{X} \cdot \mathbf{E}^b \cdot d\mathbf{X} \implies \mathbf{E}^b = \frac{1}{2} [\mathbf{C}^b - \mathbf{G}^b] \quad (2.2.8)$$

renders the *Green-Lagrange tensor* $\mathbf{E}^b = \frac{1}{2} [g_{ij} - G_{ij}] \mathbf{G}^i \otimes \mathbf{G}^j \in \mathbb{S}^3 : T\mathcal{B}_0 \times T\mathcal{B}_0 \rightarrow \mathbb{R}$, that can be identified as a proper strain tensor recording obviously the effects of nonlinearity. This can also be interpreted as the difference of the spatial and material metric with respect to the reference

¹This so-called *pull back* operation $\varphi^*(\mathbf{x}, t)$ is often used to express spatial quantities in terms of the reference configuration. The opposed operation from the reference configuration to the spatial one is called *push forward* operation $\varphi_*(\mathbf{X}, t)$.

configuration. For the shear strain of two material line elements $d\mathbf{x}_1$ and $d\mathbf{x}_2$ the Green-Lagrange strain tensor accordingly yields

$$\begin{aligned} 2d\mathbf{X}_1 \cdot \mathbf{E}^b \cdot d\mathbf{X}_2 &= [d\mathbf{x}_1 \cdot d\mathbf{x}_2 - d\mathbf{X}_1 \cdot d\mathbf{X}_2] \\ &= |d\mathbf{x}_1||d\mathbf{x}_2| \cos \gamma_{12} - |d\mathbf{X}_1||d\mathbf{X}_2| \cos \gamma_{12}^R \\ &= [\varepsilon_1 + 1][\varepsilon_2 + 1] \cos \gamma_{12} - \cos \gamma_{12}^R |d\mathbf{X}_1||d\mathbf{X}_2|, \end{aligned} \quad (2.2.9)$$

that records the change of the length and the angle to each other. The Green-Lagrange strain tensor can also be expressed in terms of the displacement gradient \mathbf{H}^\natural

$$\begin{aligned} \mathbf{E}^b &= \left[[\mathbf{H}^\natural + \mathbf{G}^\natural]^t \cdot \mathbf{g}^b \cdot [\mathbf{H}^\natural + \mathbf{G}^\natural] - \mathbf{G}^b \right] \\ &= \left[\underbrace{[\mathbf{H}^\natural]^t \cdot \mathbf{g}^b \cdot \mathbf{H}^\natural}_{\mathbf{E}_{nonl}^b} + \underbrace{[\mathbf{H}^\natural]^t \cdot \mathbf{g}^b \cdot \mathbf{G}^\natural + [\mathbf{G}^\natural]^t \cdot \mathbf{g}^b \cdot \mathbf{H}^\natural}_{\mathbf{E}_{lin}^b} - \mathbf{G}^b \right] \end{aligned} \quad (2.2.10)$$

whereby \mathbf{E}_{lin}^b denotes the linear part of the Green-Lagrange strain tensor, whereas the nonlinear part is detected by \mathbf{E}_{nonl}^b .

In analogy to the right Cauchy Green tensor, that lives purely in the material configuration, we can define the so-called *left Cauchy-Green* tensor $\mathbf{b}^\sharp = G^{ij} \mathbf{g}_i \otimes \mathbf{g}_j \in \mathbb{S}_+^3 : T^*\mathcal{B}_t \times T^*\mathcal{B}_t \rightarrow \mathbb{R}$, that lives in the spatial configuration. In addition it is conceivable to define the inverse tensors denoted by $\mathbf{B}^\sharp = [\mathbf{C}^b]^{-1}$ and $\mathbf{c}^b = [\mathbf{b}^\sharp]^{-1}$, so that we get the following collection

$$\begin{aligned} \mathbf{C}^b &= [\mathbf{F}^\natural]^t \cdot \mathbf{g}^b \cdot \mathbf{F}^\natural = g_{ij} \mathbf{G}^i \otimes \mathbf{G}^j \in \mathbb{S}_+^3 : T\mathcal{B}_0 \times T\mathcal{B}_0 \rightarrow \mathbb{R}, \\ \mathbf{B}^\sharp &= \mathbf{f}^\natural \cdot \mathbf{g}^\sharp \cdot [\mathbf{f}^\natural]^t = g^{ij} \mathbf{G}_i \otimes \mathbf{G}_j \in \mathbb{S}_+^3 : T^*\mathcal{B}_0 \times T^*\mathcal{B}_0 \rightarrow \mathbb{R}, \\ \mathbf{c}^b &= [\mathbf{f}^\natural]^t \cdot \mathbf{G}^b \cdot \mathbf{f}^\natural = G_{ij} \mathbf{g}^i \otimes \mathbf{g}^j \in \mathbb{S}_+^3 : T\mathcal{B}_t \times T\mathcal{B}_0 \rightarrow \mathbb{R}, \\ \mathbf{b}^\sharp &= \mathbf{F}^\natural \cdot \mathbf{G}^\sharp \cdot [\mathbf{F}^\natural]^t = G^{ij} \mathbf{g}_i \otimes \mathbf{g}_j \in \mathbb{S}_+^3 : T^*\mathcal{B}_t \times T^*\mathcal{B}_t \rightarrow \mathbb{R} \end{aligned} \quad (2.2.11)$$

With these kinematical quantities it is also possible to define *generalized* co- and contravariant strain measures in different configurations. In the following set the different types of nonlinear strain measures are compiled in a generalized way

$$\begin{aligned} n\mathbf{E}_{(n)}^b &= [\mathbf{C}^b]^{\frac{n}{2}} - \mathbf{G}^b = n[E_{(n)}]_{ij} \mathbf{G}^i \otimes \mathbf{G}^j \in \mathbb{S}^3 : T^*\mathcal{B}_t \times T^*\mathcal{B}_t \rightarrow \mathbb{R}, \\ n\mathbf{A}_{(n)}^\sharp &= \mathbf{G}^\sharp - [\mathbf{B}^\sharp]^{\frac{n}{2}} = n[A_{(n)}]^{ij} \mathbf{G}_i \otimes \mathbf{G}_j \in \mathbb{S}^3 : T\mathcal{B}_t \times T\mathcal{B}_t \rightarrow \mathbb{R}, \\ ne_{(n)}^b &= \mathbf{g}^b - [\mathbf{c}^b]^{\frac{n}{2}} = n[e_{(n)}]_{ij} \mathbf{g}^i \otimes \mathbf{g}^j \in \mathbb{S}^3 : T^*\mathcal{B}_t \times T^*\mathcal{B}_t \rightarrow \mathbb{R}, \\ na_{(n)}^\sharp &= [\mathbf{b}^\sharp]^{\frac{n}{2}} - \mathbf{g}^\sharp = n[a_{(n)}]^{ij} \mathbf{g}_i \otimes \mathbf{g}_j \in \mathbb{S}^3 : T\mathcal{B}_t \times T\mathcal{B}_t \rightarrow \mathbb{R} \end{aligned} \quad (2.2.12)$$

A particular strain measure that can be also derived from this set of generalized strain measures is the *logarithmic* or *natural strains*. Since these strain measures are essential for the numerical treatment of elastoplasticity, we mention them here explicitly

$$\begin{aligned} \mathbf{E}_{(0)}^b &= \frac{1}{2} \ln \mathbf{C}^b \in \mathbb{S}^3 : T^*\mathcal{B}_t \times T^*\mathcal{B}_t \rightarrow \mathbb{R}, \\ \mathbf{A}_{(0)}^\sharp &= -\frac{1}{2} \ln \mathbf{B}^\sharp \in \mathbb{S}^3 : T\mathcal{B}_t \times T\mathcal{B}_t \rightarrow \mathbb{R}, \\ \mathbf{e}_{(0)}^b &= -\frac{1}{2} \ln \mathbf{c}^b \in \mathbb{S}^3 : T^*\mathcal{B}_t \times T^*\mathcal{B}_t \rightarrow \mathbb{R}, \\ \mathbf{a}_{(0)}^\sharp &= \frac{1}{2} \ln \mathbf{b}^\sharp \in \mathbb{S}^3 : T\mathcal{B}_t \times T\mathcal{B}_t \rightarrow \mathbb{R}. \end{aligned} \quad (2.2.13)$$

Furthermore it can be shown, that all these different strain measures are equal to first order and therefore they coincide in the case of small strains, such that $\mathbf{C}^b \rightarrow \mathbf{G}^b$, $\mathbf{B}^\sharp \rightarrow \mathbf{G}^\sharp$, $\mathbf{c}^b \rightarrow \mathbf{g}^b$ and $\mathbf{b}^\sharp \rightarrow \mathbf{g}^\sharp$.

Spectral decomposition All the previously established kinematical quantities are tensors of second order and if they are symmetric, they can be represented by the spectral decomposition as it is represented in the appendix. For the (nonsymmetric) deformation tensor \mathbf{F}^\natural the described decomposition is not valid, but following Parisch [Par03] it consists of an rotation tensor and an stretch tensor in the subsequent way

$$\mathbf{F}^\natural = \sum_{\alpha=1}^3 \lambda_\alpha \mathbf{n}^\alpha \otimes \mathbf{N}^\alpha = \sum_{\alpha=1}^3 \mathbf{n}^\alpha \otimes \widetilde{\mathbf{N}}^\alpha \cdot \sum_{\alpha=1}^3 \lambda_\alpha \widetilde{\mathbf{N}}^\alpha \otimes \mathbf{N}^\alpha = \mathbf{R} \cdot \mathbf{U}^\natural \quad (2.2.14)$$

$$= \sum_{\alpha=1}^3 \lambda_\alpha \mathbf{n}^\alpha \otimes \mathbf{N}^\alpha = \sum_{\alpha=1}^3 \lambda_\alpha \mathbf{n}^\alpha \otimes \widetilde{\mathbf{n}}^\alpha \cdot \sum_{\alpha=1}^3 \widetilde{\mathbf{n}}^\alpha \otimes \mathbf{N}^\alpha = \mathbf{V}^\natural \cdot \mathbf{R} \quad (2.2.15)$$

for the polar decomposed form and it is obvious, that the right and left stretch tensor $\mathbf{U}^\natural = \sum_{\alpha=1}^3 \lambda_\alpha \widetilde{\mathbf{N}}^\alpha \otimes \mathbf{N}^\alpha$ and $\mathbf{V}^\natural = \sum_{\alpha=1}^3 \lambda_\alpha \mathbf{n}^\alpha \otimes \widetilde{\mathbf{n}}^\alpha$ have the same eigenvalues, which can be considered as the stretches in the principal directions and therefore they are called *principal stretches*. The difference between the stretch tensors can be found in the eigenbase, since the right stretch tensor exists in the material configuration whereas the left stretch tensor exists in the spatial configuration. Since the right Cauchy-Green tensor \mathbf{C}^b and accordingly the left Cauchy-Green tensor \mathbf{b}^\sharp can be expressed in terms of the stretch tensors it ensures that also the deformation tensors possess the same eigenvalues.

$$\mathbf{C}^b = [\mathbf{U}^\natural]^2 = \sum_{\alpha=1}^3 \lambda_\alpha^2 \mathbf{N}^\alpha \otimes \mathbf{N}^\alpha, \quad \mathbf{b}^\sharp = [\mathbf{V}^\natural]^2 = \sum_{\alpha=1}^3 \lambda_\alpha^2 \mathbf{n}^\alpha \otimes \mathbf{n}^\alpha, \quad (2.2.16)$$

which coincide with the squared principal stretches. As mentioned before the deformation tensors can be related to each other by the push-forward Φ_* and pull-back Φ^* operations, whereby only the eigenvectors are transformed and the eigenvalues remain untouched. For this transformation we take eqn. 2.2.15 into account and rewrite it as

$$\lambda_\alpha \mathbf{N}^\alpha = \mathbf{n}^\alpha \cdot \mathbf{F}^\natural. \quad (2.2.17)$$

Hence, we obtain

$$\begin{aligned} \mathbf{C}^b &= \sum_{\alpha=1}^3 \lambda_\alpha^2 \mathbf{N}^\alpha \otimes \mathbf{N}^\alpha = \sum_{\alpha=1}^3 [\mathbf{F}^\natural]^t \mathbf{n}^\alpha \otimes \mathbf{n}^\alpha \cdot \mathbf{F}^\natural \\ &= [\mathbf{F}^\natural]^t \cdot \sum_{\alpha=1}^3 \mathbf{n}^\alpha \otimes \mathbf{n}^\alpha \cdot \mathbf{F}^\natural = [\mathbf{F}^\natural]^t \cdot \mathbf{g}^b \cdot \mathbf{F}^\natural. \end{aligned} \quad (2.2.18)$$

Since the principal stretches of the right and left Cauchy-Green tensors are the same, it follows from eqn. A.1.5, that also the principal invariants are the same. Of course, for the calculation of the invariants of the deformation tensors the squares of the principal stretches have to be considered. The invariants can be expressed in the following representations

$$\begin{aligned} I_1(\mathbf{C}^b) &= \mathbf{G}^\sharp : \mathbf{C}^b &= \lambda_1^2 + \lambda_2^2 + \lambda_3^2 &= \mathbf{g}^b : \mathbf{b}^\sharp &= I_1(\mathbf{b}^\sharp) \\ I_2(\mathbf{C}^b) &= \frac{1}{2} [I_1^2 - \mathbf{G}^\sharp : [\mathbf{C}^b]^2] &= \lambda_1^2 \lambda_2^2 + \lambda_2^2 \lambda_3^2 + \lambda_1^2 \lambda_3^2 &= \frac{1}{2} [I_1^2 - \mathbf{g}^b : [\mathbf{b}^\sharp]^2] &= I_2(\mathbf{b}^\sharp) \\ I_3(\mathbf{C}^b) &= \det [\mathbf{C}^b] &= \lambda_1^2 \lambda_2^2 \lambda_3^2 &= \det [\mathbf{b}^\sharp] &= I_3(\mathbf{b}^\sharp). \end{aligned} \quad (2.2.19)$$

Transformation formulas We want to stop here considering eigenvalue problems, but therefore we would like to give some useful tools for the transformation of surface elements and volume elements from the referential configuration to the current one and vice versa. For this we firstly have to introduce some additional quantities, like permutation tensor $\mathbf{E} = \varepsilon_{ijk} \mathbf{g}^i \otimes \mathbf{g}^j \otimes \mathbf{g}^k$ that possess the following properties

$$\varepsilon_{ijk} = \begin{cases} 1, & \text{with } (i, j, k) \in \{(1, 2, 3), (2, 3, 1), (3, 1, 2)\} \\ -1, & \text{with } (i, j, k) \in \{(1, 3, 2), (3, 2, 1), (2, 1, 3)\} \\ 0, & \text{otherwise} \end{cases} \quad (2.2.20)$$

With this at hand we can define the vector product of two vectors \mathbf{u} and \mathbf{v} given by

$$\mathbf{u} \times \mathbf{v} = \varepsilon_{ijk} u_i v_j \mathbf{g}^k \quad (2.2.21)$$

and the triple product of three vectors \mathbf{u} , \mathbf{v} and \mathbf{w}

$$v = \mathbf{u} \cdot [\mathbf{v} \times \mathbf{w}] = \varepsilon_{ijk} u^i v^j w^k \quad (2.2.22)$$

that yields a scalar quantity, that can be identified with the volume enclosed by the three vectors. Applying this relation to the material and spatial base vectors renders the infinitesimal volume elements $dV = d\mathbf{X}_1 \cdot [d\mathbf{X}_2 \times d\mathbf{X}_3] = \mathbf{G}_1 dX^1 \cdot [\mathbf{G}_2 dX^2 \times \mathbf{G}_3 dX^3]$ and $dv = d\mathbf{x}_1 \cdot [d\mathbf{x}_2 \times d\mathbf{x}_3] = \mathbf{g}_1 dx^1 \cdot [\mathbf{g}_2 dx^2 \times \mathbf{g}_3 dx^3]$. For the transformation rules describing the relation between both volumes, we firstly need the definition of the determinant that is given by

$$\varepsilon_{ijk} \varepsilon^{lmn} = \det \begin{pmatrix} g_i^l & g_i^m & g_i^n \\ g_j^l & g_j^m & g_j^n \\ g_k^l & g_k^m & g_k^n \end{pmatrix}. \quad (2.2.23)$$

Applying this definition to the deformation gradient we obtain

$$J = \det(\mathbf{F}^\natural) = \frac{1}{6} \varepsilon^{ijk} \varepsilon_{IJK} F_i^I F_j^J F_k^K \rightsquigarrow J \varepsilon^{IJK} = \varepsilon^{ijk} F_i^I F_j^J F_k^K. \quad (2.2.24)$$

The meaning of this relation for the transformation becomes clear if we consider the spatial volume element dv

$$dv = d\mathbf{x}_i \cdot [d\mathbf{x}_j \times d\mathbf{x}_k] = \varepsilon^{ijk} dx^i dx^j dx^k \quad (2.2.25)$$

$$= \varepsilon^{ijk} F_i^I F_j^J F_k^K dX_I dX_J dX_K = J \varepsilon^{IJK} dX_I dX_J dX_K = J dV. \quad (2.2.26)$$

From this result it is derivable that scalar quantities in principle transform by the Jacobian of the deformation gradient J , such that the initial and current density are related by

$$\rho_0 dV = \rho dv = \rho J dV \rightsquigarrow \rho_0 = J \rho. \quad (2.2.27)$$

Another important transformation rule is called the Nanson formula, that transforms surface elements from the material to the spatial configuration. A material surface element can be represented by its normal vector in the form $d\mathbf{A} = \mathbf{N} dA$. Since $\mathbf{N} = \mathbf{G}^I$ is defined on the cotangential space it cannot be transformed by the deformation tensor but by its inverse $\mathbf{g}^i = \mathbf{f}^\natural \cdot \mathbf{G}^I$. For the derivation of the Nanson formula we start from the following relation for the material surface element

$$d\mathbf{A} = \mathbf{G}^3 dA = \mathbf{G}_1 \times \mathbf{G}_2 d\Theta^1 d\Theta^2 = \mathbf{G}^3 [\mathbf{G}_1 d\Theta^1 \times \mathbf{G}_2 d\Theta^2] \cdot \mathbf{G}_3 = \mathbf{G}^3 d\Theta^1 d\Theta^2 dV. \quad (2.2.28)$$

In analogy to the material description the spatial surface elements can be derived and by applying the transformation rules for the contravariant base vectors and the volume elements we obtain the so-called Nansons formula

$$d\mathbf{a} = \mathbf{g}^3 da = \mathbf{g}^3 d\Theta^1 d\Theta^2 dv = [\mathbf{f}^{\natural}]^t \cdot \mathbf{G}^3 d\Theta^1 d\Theta^2 J dV = J [\mathbf{f}^{\natural}]^t \cdot d\mathbf{A} \quad (2.2.29)$$

whereby here the material surface description was taken into account. These transformation rules appear quite often and are very useful tools. At this point we like to remark, that for the particular case the body \mathfrak{B} carries out a pure rotation, the volume remains unchanged in eqn. 2.2.15 : $\mathbf{F}^{\natural} = \mathbf{R} \implies \det(\mathbf{F}^{\natural}) = 1$.

2.2.2 Material Objectivity and Strain Rates

Objectivity For the formulation of the mechanical and the thermodynamical balance equations as well as for the constitutive laws, the rates of quantities are needed, such that it is also necessary to know the rates of the non-linear strain measures derived in the section before. The problem here is, that these strain rates have to fulfill the constraint of *material objectivity* or *material frame-indifference*, in the following sense. Two different observers at different positions observing the same deformation of the body \mathfrak{B} at time t and $t' = t - a$, are expected to see the properly transformed result. A deformation observed by two observers at position \mathbf{o} and $\tilde{\mathbf{o}}$ is related by

$$\tilde{\mathbf{x}} = \mathbf{Q}^{\natural}(t) \cdot \mathbf{x} + \mathbf{c}(t), \quad (2.2.30)$$

whereby $\mathbf{Q} \in \mathbb{S}\mathbb{O}^3$ is a proper orthogonal transformation tensor and $\mathbf{c}(t)$ denotes a distance vector between \mathbf{o} and $\tilde{\mathbf{o}}$. Another point of view is to regard eqn. 2.2.30 as a rigid body motion that is superimposed on \mathfrak{B} at a particular configuration \mathcal{C} and leading to the new configuration $\tilde{\mathcal{C}}$. If the state of a quantity transforms properly from \mathcal{C} to $\tilde{\mathcal{C}}$, it is called *objective* or *frame-indifferent*. In general there is hardly no other subject in solid mechanics, where the minds are less conform than in the definition of objectivity. Usually, the objectivity of a scalar a , a vector \mathbf{a} or a tensor \mathbf{A} is ensured, if they transform in the following way

$$\tilde{a}(\tilde{\mathbf{x}}, \tilde{t}) = a(\mathbf{x}, t), \quad \tilde{\mathbf{a}}(\tilde{\mathbf{x}}, \tilde{t}) = \mathbf{Q}^{\natural} \cdot \mathbf{a}(\mathbf{x}, t), \quad \tilde{\mathbf{A}}(\tilde{\mathbf{x}}, \tilde{t}) = \mathbf{Q}^{\natural} \cdot \mathbf{A}(\mathbf{x}, t) \cdot [\mathbf{Q}]^t \quad (2.2.31)$$

The new deformation gradient $\tilde{\mathbf{F}}^{\natural} = \partial_{\mathbf{X}} \tilde{\varphi}(\mathbf{X}, t)$ can be obtained by the derivative of eqn. 2.2.30 with respect to \mathbf{X} that yields

$$\tilde{\mathbf{F}}^{\natural} = \mathbf{Q} \cdot \mathbf{F}^{\natural}. \quad (2.2.32)$$

Comparing this expression with the transformation rule in eqn. 2.2.31₃, the deformation gradient has to be assumed as a non-objective quantity.² By applying this transformation to the tangent vector $d\mathbf{x}$ of the spatial configuration

$$d\tilde{\mathbf{x}} = \tilde{\mathbf{F}}^{\natural} \cdot d\mathbf{X} = \mathbf{Q}(t) \cdot \mathbf{F}^{\natural} \cdot d\mathbf{X} = \mathbf{Q}(t) \cdot d\mathbf{x} \quad (2.2.33)$$

we see that it causes a rigid body rotation of the spatial tangent vector $d\mathbf{x}$. Therefore the tangent vector $d\mathbf{x}$ can be considered as an objective quantity. Furthermore the transformed Jacobian \tilde{J} is

²In some textbooks the deformation gradient is considered as an objective tensor, since it is a twofield tensor consisting of a spatial and a material base vector, which is „intrinsically independent of the observer“ (s. Holzapfel [Hol01]). In this spirit the transformation of the deformation tensor also yields an objective quantity, since the rotation is applied to the spatial base vector.

equal to the original one, because $\mathbf{Q}(t)$ is a proper orthogonal tensor and the transformation results in

$$\tilde{J} = \det(\tilde{\mathbf{F}}^\sharp) = \det(\mathbf{Q}) \det(\mathbf{F}^\sharp) = 1 \det(\mathbf{F}^\sharp) = \det(\mathbf{F}). \quad (2.2.34)$$

Now we investigate the nonlinear strain measures with respect to the objectivity requirements given in eqn. 2.2.31. Taking the objectivity of the spatial covariant metric tensor $\mathbf{g}^b = \mathbf{Q}^t \tilde{\mathbf{g}}^b \mathbf{Q}$ into account, we can easily show, that the right Cauchy-Green tensor keeps completely untouched by an change of observer

$$\tilde{\mathbf{C}}^b = [\tilde{\mathbf{F}}^\sharp]^t \cdot \tilde{\mathbf{g}}^b \cdot \tilde{\mathbf{F}}^\sharp = [\mathbf{F}^\sharp]^t \cdot \mathbf{Q}^t \cdot \tilde{\mathbf{g}}^b \cdot \mathbf{Q} \cdot \mathbf{F}^\sharp = [\mathbf{F}^\sharp]^t \cdot \mathbf{g}^b \cdot \mathbf{F}^\sharp = \mathbf{C}^b, \quad (2.2.35)$$

since both base vectors are defined on the material configuration, which are independent of the observer. Therefore we refer to the right Cauchy-Green tensor as non-objective, because it does not fulfill the objectivity requirement in eqn. 2.2.31₃. But since it is not influenced by the rigid body motion, it is an (*observer-*) *invariant* quantity. Inserting the transformation rule of the deformation gradient into the definition of the left Cauchy-Green tensor we obtain

$$\tilde{\mathbf{b}}^\sharp = \tilde{\mathbf{F}}^\sharp \cdot \mathbf{G}^\sharp \cdot [\tilde{\mathbf{F}}^\sharp]^t = \mathbf{Q} \cdot \mathbf{F}^\sharp \cdot \mathbf{G}^\sharp \cdot [\mathbf{F}^\sharp]^t \cdot \mathbf{Q}^t = \mathbf{Q} \cdot \mathbf{b}^\sharp \cdot \mathbf{Q}^t. \quad (2.2.36)$$

The transformation of the left Cauchy-Green tensor \mathbf{b}^\sharp coincides with the objectivity requirements in eqn. 2.2.30 and can be identified as an objective tensor. For completeness we want to mention here, that also the inverse quantities are either invariant or objective, respectively, such that we obtain for the inverse right Cauchy-Green tensor

$$\tilde{\mathbf{B}}^\sharp = \tilde{\mathbf{f}}^\sharp \cdot \tilde{\mathbf{g}}^\sharp \cdot [\tilde{\mathbf{f}}^\sharp]^t = \mathbf{f}^\sharp \cdot \mathbf{Q}^t \cdot \tilde{\mathbf{g}}^\sharp \cdot \mathbf{Q} \cdot [\mathbf{f}^\sharp]^t = \mathbf{f}^\sharp \cdot \mathbf{g}^\sharp \cdot [\mathbf{f}^\sharp]^t, \quad (2.2.37)$$

that is invariant and the inverse left Cauchy-Green tensor

$$\tilde{\mathbf{c}}^b = [\tilde{\mathbf{f}}^\sharp]^t \cdot \tilde{\mathbf{G}}^b \cdot \tilde{\mathbf{f}}^\sharp = \mathbf{Q} \cdot [\mathbf{f}^\sharp]^t \cdot \mathbf{G}^b \cdot \mathbf{f}^\sharp \cdot \mathbf{Q}^t = \mathbf{Q} \cdot \mathbf{c}^b \cdot \mathbf{Q}^t, \quad (2.2.38)$$

is also objective. Analogously all the corresponding strain measures in eqn. 2.2.12 can be proofed with respect to objectivity and invariance. In general one can say, that symmetric material tensor quantities are invariant, whereas spatial symmetric quantities are objective.

Strain Rates Now we consider the rates of the deformation tensor and the corresponding strain measures. We start with the time derivative of the Green-Lagrange strain tensor

$$2\dot{\mathbf{E}}^b = \partial_t \left[[\mathbf{F}^\sharp]^t \cdot \mathbf{g}^b \cdot \mathbf{F}^\sharp - \mathbf{G}^b \right] = \left[[\dot{\mathbf{F}}^\sharp]^t \cdot \mathbf{g}^b \cdot \mathbf{F}^\sharp + [\mathbf{F}^\sharp]^t \cdot \mathbf{g}^b \cdot \dot{\mathbf{F}}^\sharp \right] = \dot{\mathbf{C}}^b \quad (2.2.39)$$

whereby of course the material metric tensor is constant in time. Eqn. 2.2.39 includes the time derivative of the deformation tensor that is defined by

$$\dot{\mathbf{F}}^\sharp = \partial_t \varphi(\mathbf{X}, t) = \frac{\partial}{\partial t} \frac{\partial \mathbf{x}}{\partial \mathbf{X}} = \frac{\partial}{\partial \mathbf{X}} \frac{\partial \mathbf{x}}{\partial t} = \frac{\partial \mathbf{v}}{\partial \mathbf{X}} = \frac{\partial \mathbf{v}}{\partial \mathbf{x}} \cdot \frac{\partial \mathbf{x}}{\partial \mathbf{X}} = \text{grad} \mathbf{v} \cdot \mathbf{F}^\sharp = \mathbf{l}^\sharp \cdot \mathbf{F}^\sharp. \quad (2.2.40)$$

Here $\mathbf{l}^\sharp = l_j^\sharp \mathbf{g}_i \otimes \mathbf{g}^j \in \mathbb{L}^3 : T^* \mathcal{B}_t \times T \mathcal{B}_t \rightarrow \mathbb{R}$ denotes the *spatial velocity gradient*. $\dot{\mathbf{F}}^\sharp$ relates the spatial velocity gradient $\text{grad} \mathbf{v}$ to the material configuration, that often is specified as *material velocity gradient* $\text{Grad} \mathbf{v}$. Inserting this in eqn. 2.2.39 renders

$$\begin{aligned} \dot{\mathbf{E}}^b &= \frac{1}{2} \left[[\mathbf{F}^\sharp]^t \cdot [\mathbf{l}^\sharp]^t \cdot \mathbf{g}^b \cdot \mathbf{F}^\sharp + [\mathbf{F}^\sharp]^t \cdot \mathbf{g}^b \cdot \mathbf{l}^\sharp \cdot \mathbf{F}^\sharp \right] = \frac{1}{2} [\mathbf{F}^\sharp]^t \cdot \left[[\mathbf{l}^\sharp]^t \cdot \mathbf{g}^b + \mathbf{g}^b \cdot \mathbf{l}^\sharp \right] \cdot \mathbf{F}^\sharp \\ &= [\mathbf{F}^\sharp]^t \cdot \mathbf{d}^b \cdot \mathbf{F}^\sharp \end{aligned} \quad (2.2.41)$$

whereby $\mathbf{d}^b = d^{ij} \mathbf{g}_i \otimes \mathbf{g}_j \in \mathbb{S}^3 : T\mathcal{B}_t \times T\mathcal{B}_t \rightarrow \mathbb{R}$ denotes the *strain rate tensor* and corresponds to the symmetric part of the spatial velocity tensor, whereas the skewsymmetric part $\mathbf{w}^b = \frac{1}{2} [\mathbf{l}^b \cdot \mathbf{g}^b - \mathbf{g}^b \cdot [\mathbf{l}^b]^t] \in \mathbb{L}^3 : T\mathcal{B}_t \times T\mathcal{B}_t \rightarrow \mathbb{R}$ is called *spin tensor*. To investigate the objectivity of the material strain rate tensor we apply again a rigid body motion

$$\dot{\tilde{\mathbf{E}}}^b = [\tilde{\mathbf{F}}^b]^t \cdot \tilde{\mathbf{d}}^b \cdot \tilde{\mathbf{F}}^b = [\mathbf{F}^b]^t \cdot \mathbf{Q}^t \cdot \tilde{\mathbf{d}}^b \cdot \mathbf{Q} \cdot \mathbf{F}^b = [\mathbf{F}^b]^t \cdot \mathbf{d}^b \cdot \mathbf{F}^b = \dot{\mathbf{E}}^b \quad (2.2.42)$$

and find that it is an invariant quantity, since $\tilde{\mathbf{d}}^b = \mathbf{Q}^t \cdot \mathbf{d}^b \cdot \mathbf{Q}$ fullfills the requirement of material objectivity. In the case of the Almansi-tensor we found that it is also an objective strain measure, because of the identity $\tilde{\mathbf{e}}^b = \mathbf{Q} \cdot \mathbf{e}^b \cdot \mathbf{Q}^t$. However, the time derivative

$$\dot{\tilde{\mathbf{e}}}^b = \dot{\mathbf{Q}} \cdot \mathbf{e}^b \cdot \mathbf{Q}^t + \mathbf{Q} \cdot \dot{\mathbf{e}}^b \cdot \mathbf{Q}^t + \mathbf{Q} \cdot \mathbf{e}^b \cdot \dot{\mathbf{Q}} \neq \mathbf{Q}^t \cdot \dot{\mathbf{e}}^b \cdot \mathbf{Q} \quad (2.2.43)$$

is obviously not objective. In general one can say that rates of spatial quantities are not objective, since also their base system are time-dependent, whereas the material base system is fixed. But it is possible to construct objective spatial strain rates by the Lie-derivative, that is denoted by $\mathcal{L}_t[\bullet]$. With this method an objective time derivative of spatial variables is constructed by pulling back the particular spatial quantity on the reference configuration, where the time derivative is performed and the resulting expression is pushed forward again to the spatial configuration. Applying this scheme to the Almansi strain tensor renders

$$\mathcal{L}_t(\mathbf{e}^b) = \varphi_* [\partial_t \varphi^*(\mathbf{e}^b)] = [\mathbf{f}^b]^t \cdot \dot{\mathbf{E}}^b \cdot \mathbf{f}^b = [\mathbf{f}^b]^t \cdot \left[[\mathbf{F}^b]^t \cdot \mathbf{d}^b \cdot \mathbf{F}^b \right] \cdot \mathbf{f}^b = \mathbf{d}^b \quad (2.2.44)$$

and we find that the objective deformation rate tensor \mathbf{d}^b is the Lie-derivative of the Almansi-strain tensor. The subject of objective time-derivative of spatial quantities is not only important for the formulation of strain rates, but also in the context of stresses. There is a variety of different objective stress rates, that were constructed in the past and for example the Olroyd stress rate can be identified with the Lie time derivative of the Cauchy stress [Hol01].

2.3 Balance Principles in Mechanics

In this section we will briefly summarize the main balance principles in mechanics: the conservation of mass, the linear and the angular momentum balance equation and the mechanical energy balance equation. In the framework of the linear momentum balance equation we will anticipate the concept of stress. Therefore we will introduce the stresses in an abstract manner, before we will give a more precise definition in the subsequent section. For brevity we will not discuss every balance equation in detail for the reference and the current configuration, but the most important relations will be given. A tool that is needed in all the following considerations are the spatial and material time derivatives, that we introduce at first.

2.3.1 Material and Spatial Time Derivatives

According to the different configurations we have to distinguish two kinds of time derivatives. A time derivative of a smooth material field $\mathcal{F}(\mathbf{X}, t)$ parameterized in material coordinates \mathbf{X} , denoted by $D[\bullet]/Dt$, is defined by

$$\frac{D\mathcal{F}}{Dt} =: \dot{\mathcal{F}}(\mathbf{X}, t) = \left. \frac{\partial \mathcal{F}(\mathbf{X}, t)}{\partial t} \right|_{\mathbf{X}}, \quad (2.3.1)$$

whereby \mathbf{X} is fixed. In analogy to the material time derivative we can define the spatial time derivative of a smooth spatial field $\mathcal{F}(\mathbf{x}, t)$ parameterized in \mathbf{x} by

$$\frac{d\mathcal{F}}{dt} =: \dot{\mathcal{F}}(\mathbf{x}, t) = \left. \frac{\partial \mathcal{F}(\mathbf{x}, t)}{\partial t} \right|_{\mathbf{x}}. \quad (2.3.2)$$

This time the spatial coordinate \mathbf{x} is fixed. At last we consider the material time derivative of a smooth spatial field $\mathcal{F}(\mathbf{x}, t)$, that is very crucial in the context of balance equations. The corresponding time derivative is given by

$$\frac{D\mathcal{F}(\mathbf{x}, t)}{Dt} = \frac{\mathcal{F}(\mathbf{x}, t)}{\partial t} + \left. \frac{\partial \mathcal{F}(\mathbf{x}, t)}{\partial \mathbf{x}} \right|_t \cdot \left. \frac{\partial \boldsymbol{\varphi}(\mathbf{X}, t)}{\partial t} \right|_{\mathbf{X}=\boldsymbol{\varphi}^{-1}(\mathbf{x}, t)}. \quad (2.3.3)$$

A particular application of the material time derivative can be found in the so-called Reynolds theorem. This theorem allows to compute the material time derivative of a spatial quantity field $I(\mathbf{x}, t)$ defined by the integral of $\Phi(\mathbf{x}, t)$ over the current configuration \mathcal{B}_t , such that we obtain

$$\frac{DI(\mathbf{x}, t)}{Dt} = \frac{D}{Dt} \int_{\mathcal{B}_t} \Phi(\mathbf{x}, t) dv. \quad (2.3.4)$$

For being able to perform the time derivative we need to transform the relation to the fixed material configuration, such that the time derivative and the integral can be exchanged

$$\begin{aligned} \frac{D}{Dt} \int_{\mathcal{B}_t} \Phi(\mathbf{x}, t) dv &= \frac{D}{Dt} \int_{\mathcal{B}_0} J \Phi(\mathbf{x}, t) dV \\ &= \int_{\mathcal{B}_0} \frac{D}{Dt} [J \Phi(\mathbf{x}, t)] dV \\ &= \int_{\mathcal{B}_0} [\dot{J} \Phi(\mathbf{x}, t) + J \dot{\Phi}(\mathbf{x}, t)] dV \end{aligned} \quad (2.3.5)$$

For the time derivative of the Jacobian J we start with the definition of $J = \det \mathbf{F}^{\natural}$ and differentiating it with respect to time we obtain

$$\dot{J} = \frac{\partial J}{\partial \mathbf{F}^{\natural}} \cdot \dot{\mathbf{F}}^{\natural} = J [\mathbf{f}^{\natural}]^t : [\mathbf{l}^{\natural} \mathbf{F}^{\natural}] = J \operatorname{div} \mathbf{v} \quad \text{with} \quad \frac{\partial J}{\partial \mathbf{F}^{\natural}} = J [\mathbf{f}^{\natural}]^t, \quad (2.3.6)$$

whereby here eqn. 2.2.40 was taken into account. The time derivative of $\Phi(\mathbf{x}, t)$ is given by eqn. 2.3.3, such that we finally obtain

$$\begin{aligned} \frac{D}{Dt} \int_{\mathcal{B}_t} \Phi(\mathbf{x}, t) dv &= \int_{\mathcal{B}_0} J [\partial_t \Phi(\mathbf{x}, t) + \operatorname{grad} \Phi(\mathbf{x}, t) \cdot \mathbf{v} + \Phi(\mathbf{x}, t) \operatorname{div} \mathbf{v}] dV \\ &= \int_{\mathcal{B}_t} [\partial_t \Phi(\mathbf{x}, t) + \operatorname{div}(\Phi(\mathbf{x}, t) \mathbf{v})] dv. \end{aligned} \quad (2.3.7)$$

In the last step the transformation back to the current configuration is performed.

2.3.2 Conservation of Mass

The law of mass conservation states that the mass m of a system does not change during a deformation process. Since the mass is defined by the product of mass density and the volume, we can formulate the total mass in the reference and the current configuration by

$$m = \int_{\mathcal{B}_0} \rho_0 dV = \int_{\mathcal{B}_0} \rho J dV = \int_{\mathcal{B}_t} \rho dv. \quad (2.3.8)$$

This relation more or less was already introduced in eqn. 2.2.27 and contains the relation between the mass densities in the reference and the current configuration $\rho_0 = J\rho$. An equivalent representation of the *continuity mass equation* is given by the constraint, that the current mass alteration in time has to be zero. The corresponding time derivative can be obtained if we apply the Reynolds theorem in eqn. 2.3.7, whereby $\Phi(x, t) = \rho(x, t)$ is taken into account, such that applies

$$\dot{m} = \int_{\mathcal{B}_t} \partial_t [\rho(\mathbf{x}, t) J(\mathbf{X}, t)] dV = \int_{\mathcal{B}_t} [J\dot{\rho} + J \text{grad} \rho \cdot \mathbf{v}(\mathbf{x}, t) + \dot{J}\rho] dV = 0. \quad (2.3.9)$$

Here the time derivative of the Jacobian that was performed in eqn. 2.3.6 is inserted into eqn. 2.3.9 and we can rewrite the time derivative as

$$\dot{m} = \int_{\mathcal{B}_t} [\partial_t \rho + \text{div}[\rho \mathbf{v}]] dv = 0. \quad (2.3.10)$$

If we apply the Gauss theorem to the second term we obtain the mass continuity equation for closed systems

$$\int_{\mathcal{B}_t} \partial_t \rho dv = - \int_{\partial \mathcal{B}_t} \rho \mathbf{v} \cdot \mathbf{n} da, \quad (2.3.11)$$

that coincides with the idea, that the mass within a control volume alters with the flux over the boundary of the system or the control volume, respectively.

2.3.3 Balance of Linear Momentum

The balance equation of linear momentum is the basic equation in solid mechanics, from which the weak form for the finite element method is derived. It states, that the change of the linear momentum in time emanates from the sum of the external forces, whereby we distinguish between forces acting on the surface of the body and the volume forces. In the current configuration it takes the standard form

$$\frac{\partial}{\partial t} \int_{\mathcal{B}_t} \rho \mathbf{v} dv = \int_{\mathcal{B}_t} \mathbf{b} dv + \int_{\partial \mathcal{B}_t} \mathbf{t} da, \quad (2.3.12)$$

whereby \mathbf{b} here describes a *force per unit volume* and \mathbf{t} denotes the *traction vector*. Usually the Cauchy theorem $\mathbf{t} = \boldsymbol{\sigma}^\# \cdot \mathbf{n}$ can be applied to the traction vector, whereby $\boldsymbol{\sigma}^\#$ denotes the spatial stress tensor, that will be defined later on. In consideration of the application of the Cauchy

theorem we can replace the integral over the surface by an integral over the volume. This leads to the representation

$$\frac{\partial}{\partial t} \int_{\mathcal{B}_t} \rho \mathbf{v} dv = \int_{\mathcal{B}_t} [\mathbf{b} + \text{div} \boldsymbol{\sigma}^\#] dv \quad \text{with} \quad \text{div} \boldsymbol{\sigma}^\# = \sigma_{ij,j}, \quad (2.3.13)$$

and by shrinking the volume to zero we obtain the local linear momentum balance equation

$$\rho \dot{\mathbf{v}} = \mathbf{b} + \text{div} \boldsymbol{\sigma}^\#. \quad (2.3.14)$$

In quasistatics the applied velocity field is assumed to be constant such that its time derivative gets zero and we find the relation

$$\mathbf{b} + \text{div} \boldsymbol{\sigma}^\# = \mathbf{0}. \quad (2.3.15)$$

The material formulation of the linear momentum balance equation can be obtained by relating the terms in eqn. 2.3.13 with respect to the reference volume V . The transformation of the body force can be found by

$$\int_{\mathcal{B}_t} \mathbf{b} dv = \int_{\mathcal{B}_0} \mathbf{b} J dV = \int_{\mathcal{B}_0} \mathbf{b}_0 dV \quad (2.3.16)$$

The transformation of the forces per current unit area we again take into account the Cauchy theorem and apply the Nansons formula in eqn. 2.2.29 such that we get

$$\int_{\partial \mathcal{B}_t} \mathbf{t} da = \int_{\partial \mathcal{B}_t} \boldsymbol{\sigma}^\# \cdot \mathbf{n} da = \int_{\mathcal{B}_0} J \boldsymbol{\sigma}^\# \cdot [\mathbf{f}^\natural]^t \cdot \mathbf{N} dA = \int_{\mathcal{B}_0} \text{Div} \mathbf{P}^\natural dA. \quad (2.3.17)$$

Here \mathbf{P}^\natural is the corresponding stress field in the reference configuration, that is denoted by *1. Piola-Kichhoff stress*. \mathbf{P}^\natural is a two-field tensor and it measures the actual stress with respect to a surface element of the reference configuraion. Finally we need to rewrite the inertia forces with respect to the reference unit volume. This happens taking eqn. 2.2.27 into account and we get

$$\int_{\mathcal{B}_t} \rho \dot{\mathbf{v}} dv = \int_{\mathcal{B}_0} \rho \dot{\mathbf{v}} J dV = \int_{\mathcal{B}_0} \rho_0 \dot{\mathbf{v}} dV. \quad (2.3.18)$$

With this at hand we are finally able to formulate the linear momentum balance equation with respect to the material configuration by inserting the results from eqn. 2.3.16 -2.3.18 into eqn. 2.3.13, such that we obtain

$$\int_{\mathcal{B}_0} \rho_0 \dot{\mathbf{v}} dV = \int_{\mathcal{B}_0} [\mathbf{b}_0 + \text{Div} \mathbf{P}^\natural] dV. \quad (2.3.19)$$

The performing terms in eqn. 2.3.19 depend on the place \mathbf{X} in the reference configuration and on time t . The local formulation can be derived by shrinking the volume to zero again and for the case of elastostatics the velocity has \mathbf{v} to be set to zero.

2.3.4 Balance of Angular Momentum

The result of the angular momentum balance equation yields the symmetry of the Cauchy stress $\boldsymbol{\sigma}^\sharp$. For completeness the derivation should be sketched here briefly. The proposition of the angular momentum balance equation can be formulated analogously to the linear momentum balance equation. The change of the angular momentum in time is equal to the resultant external moments acting on the body about a particular point \mathbf{x}_0 . This can be derived by writing eqn. 2.3.12 in a vector product with an vector \mathbf{r} such that we get

$$\frac{D}{Dt} \int_{\mathcal{B}_t} \mathbf{r} \times \rho \mathbf{v} dv = \int_{\partial \mathcal{B}_t} \mathbf{r} \times \mathbf{t} da + \int_{\mathcal{B}_t} \mathbf{r} \times \mathbf{b} dv. \quad (2.3.20)$$

This equation can also be rewritten in consideration of the Cauchy theorem and applying the divergence theorem to the surface integral renders

$$\int_{\partial \mathcal{B}_t} \mathbf{r} \times \mathbf{t} da = \int_{\partial \mathcal{B}_t} \mathbf{r} \times \boldsymbol{\sigma}^\sharp \cdot \mathbf{n} da = \int_{\partial \mathcal{B}_t} [\mathbf{r} \times \text{div} \boldsymbol{\sigma}^\sharp + \mathbf{E} : [\boldsymbol{\sigma}^\sharp]^t] dv, \quad (2.3.21)$$

whereby here \mathbf{E} denotes the permutation tensor, which was already introduced in eqn. 2.2.20. Considering the linear momentum balance equation we find

$$\int_{\partial \mathcal{B}} \mathbf{r} \times [\rho \dot{\mathbf{v}} - \mathbf{b} - \text{div} \boldsymbol{\sigma}^\sharp] dv = \mathbf{0} = \int_{\partial \mathcal{B}_t} [\boldsymbol{\sigma}^\sharp]^{axl} dv. \quad \text{with} \quad [\boldsymbol{\sigma}^\sharp]^{axl} = \mathbf{E} : [\boldsymbol{\sigma}^\sharp] \quad (2.3.22)$$

and this equation is only fulfilled if the Cauchy stress $\boldsymbol{\sigma}^\sharp$ is symmetric, i.e. $\boldsymbol{\sigma}^\sharp = [\boldsymbol{\sigma}^\sharp]^t$. For the 1. Piola-Kirchhoff stress tensor the symmetry cannot be derived, but the product $\mathbf{P}^\natural \cdot [\mathbf{F}^\natural]^t$ is symmetric as well. Furthermore $[\boldsymbol{\sigma}^\sharp]^{axl}$ denotes the axial vector, that becomes zero, if the stresses are symmetric.

2.3.5 Balance of Mechanical Energy

Starting point for the derivation of the kinetic energy balance equation is the balance of linear momentum. If eqn. 2.3.14 is multiplied by the spatial velocity vector \mathbf{v} and the product is integrated over \mathcal{B}_t such that we obtain

$$\int_{\mathcal{B}_t} \rho \mathbf{v} \cdot \dot{\mathbf{v}} dv = \int_{\mathcal{B}_t} [\mathbf{v} \cdot \text{div} \boldsymbol{\sigma}^\sharp + \mathbf{v} \cdot \mathbf{b}] dv. \quad (2.3.23)$$

which can be identified with mechanical powers. Furthermore the first contribution on the right hand side can be integrated partially yielding

$$\int_{\mathcal{B}_t} \mathbf{v} \cdot \text{div} \boldsymbol{\sigma}^\sharp dv = \int_{\mathcal{B}_t} [\text{div}(\mathbf{v} \cdot \boldsymbol{\sigma}^\sharp) - \text{grad} \mathbf{v} : \boldsymbol{\sigma}^\sharp] dv \quad (2.3.24)$$

and after applying the Gauss theorem to the term containing the divergence operator we can rewrite the balance as

$$\int_{\mathcal{B}_t} \rho \mathbf{v} \cdot \dot{\mathbf{v}} dv = \int_{\mathcal{B}_t} \mathbf{v} \cdot \mathbf{b} dv + \int_{\partial \mathcal{B}_t} \mathbf{v} \cdot \mathbf{t} da - \int_{\mathcal{B}_t} \text{grad} \mathbf{v} : \boldsymbol{\sigma}^\sharp dv. \quad (2.3.25)$$

In this expression we can identify the left-hand side with the time derivative of the kinetic energy

$$D_t K = \int_{B_t} \rho \mathbf{v} \cdot \dot{\mathbf{v}} dv = D_t \int_{B_0} \frac{1}{2} \rho_0 \mathbf{v} \cdot \mathbf{v} dV. \quad (2.3.26)$$

On the right handside we can summarize the contributions due to external forces

$$P_{ext} = \int_{B_t} \mathbf{v} \cdot \mathbf{b} dv + \int_{\partial B_t} \mathbf{v} \cdot \mathbf{t} da, \quad (2.3.27)$$

whereby P_{ext} denotes the external power. The last term in eqn. 2.3.25 describes the power due to internal forces such that it is called the internal power

$$P_{int} = \int_{B_t} \text{grad} \mathbf{v} : \boldsymbol{\sigma}^\# dv = \int_{B_t} \boldsymbol{\sigma}^\# : \mathbf{d}^\flat dv. \quad (2.3.28)$$

With these abbreviations at hand we can rewrite the balance of kinetic energy as

$$D_t K = P_{ext} - P_{int} \quad (2.3.29)$$

This balance shows that the power due to external force which are applied to a system and which is not transformed to internal power contributes to a change of kinetic energy. In analogy to the rate of kinetic energy we can express the internal power and external power with respect to the material configuration. The transformation leads to

$$\frac{D}{Dt} \int_{B_0} \frac{1}{2} \rho_0 \mathbf{v} \cdot \mathbf{v} dV + \int_{B_0} \mathbf{P}^\natural : \dot{\mathbf{F}}^\natural dV = \int_{\partial B_0} \mathbf{t}_0 \cdot \mathbf{v} dA + \int_{B_0} \mathbf{b}_0 \cdot \mathbf{v} dV, \quad (2.3.30)$$

whereby the traction vector $\mathbf{t}_0 = \mathbf{t}_0(\mathbf{X}, t)$, the volume force per unit reference volume $\mathbf{b}_0 = \mathbf{b}_0(\mathbf{X}, t)$ and the velocity vector $\mathbf{v} = \mathbf{v}(\mathbf{X}, t)$ here depends on the material placement \mathbf{X} . We solely want to discuss here the transformation of the stress power in detail. Using the transformation rules in eqn. 2.2.27 - 2.2.29 the stress power in terms of the 1. Piola-Kirchhoff stress can be derived as follows

$$P_{int} = \int_{B_t} \boldsymbol{\sigma}^\# : \mathbf{d}^\flat dv = \int_{B_t} \boldsymbol{\sigma}^\# : [\dot{\mathbf{F}}^\natural \cdot \mathbf{f}^\natural] dv = \int_{B_0} J \boldsymbol{\sigma}^\# \cdot [\mathbf{f}^\natural]^t : \dot{\mathbf{F}}^\natural dV = \int_{B_0} \mathbf{P}^\natural : \dot{\mathbf{F}}^\natural dV. \quad (2.3.31)$$

By expressing the strain rate tensor in terms of the Euler Lagrange strain tensor \mathbf{E}^\flat it is possible to rewrite the stress power also in terms of an purely material stress tensor $\mathbf{S}^\#$, such that we obtain

$$\begin{aligned} P_{int} &= \int_{B_t} \boldsymbol{\sigma}^\# : \mathbf{d}^\flat dv = \int_{B_t} \boldsymbol{\sigma}^\# : [\mathbf{f}^\natural]^t \cdot \dot{\mathbf{E}}^\flat \cdot \mathbf{f}^\natural dv = \int_{B_0} J [\mathbf{f}^\natural \cdot \boldsymbol{\sigma}^\# \cdot [\mathbf{f}^\natural]^t] : \dot{\mathbf{E}}^\flat dV \\ &= \int_{B_0} \mathbf{S}^\# : \dot{\mathbf{E}}^\flat dV. \end{aligned} \quad (2.3.32)$$

These different representations with respect to different configurations and coordinates describe always the same stress power, since it is an scalar expression and therefore independent of the

particular configuration. Rewriting the energy balance equation for the case of quasistatics we integrate it over the time and assume that the velocity gets zero such that we obtain

$$\int_{\mathcal{B}_t} \boldsymbol{\sigma}^\sharp : [\text{grad} \Delta \mathbf{u}]^{sym} dv = \int_{\partial \mathcal{B}_t} \mathbf{t} \cdot \Delta \mathbf{u} da + \int_{\mathcal{B}_t} \mathbf{b} \cdot \Delta \mathbf{u} dv, \quad (2.3.33)$$

whereby the velocity on the right hand side is replaced by the incremental displacement or later on by the test function within variational formulations. During the deformation the other quantities are assumed to be time independent.

2.4 Thermodynamical Balances

Thermodynamics forms the framework in which the phenomenological mechanical theories (and other sciences) are embedded and yields additional constraints for the material theory for instance. Moreover, as the name makes us assume, thermodynamics considers also thermal processes and introduces the temperature as another primary variable. Here we want to present the *first law* of thermodynamics which emanates from the consideration of *reversible* processes. However the *second law* of thermodynamics deals with *irreversible* process and yields a tool to measure the irreversibility. This tool is called *entropy*. For the theory of materials the second law is needed in a particular form that is denoted as *Clausius-Duhem-Inequality*. This inequality allows to derive the crucial constraints, that a material model has to fulfill ensuring the thermodynamic consistency.

2.4.1 1st Law in Continuum Thermodynamics

As mentioned before the first law of thermodynamics extends the mechanical energy balance equation whereby here non-mechanical quantities, as *heat* and *temperature* in particular, are introduced. These non-mechanical quantities can also effect the mechanical behaviour and vice versa. Therefore we want to start by assuming that except for the kinetic energy, the complete energy, of the considered system (or body in particular) occupying a certain volume V is described by the so-called *internal energy* U . This internal energy is a state variable that can be expressed by

$$U = \int_{\mathcal{B}_t} \rho u dv = \int_{\mathcal{B}_0} \rho_0 u dV \quad (2.4.1)$$

The sum of the internal energy and the kinetic energy characterizes the total energy of the system. The change of the total energy depends on the external mechanical power P_{ext} and thermal power Q such that we can make up the balance of energy by

$$\frac{d}{dt} [K + U] = Q + P_{ext}. \quad (2.4.2)$$

In the case of a pure mechanical process the thermal effects are neglected, such that the thermal power Q becomes zero. Following Greve [Gre03] the change of every physical quantity $\xi(\omega, t)$ in time within a control volume ω in general consists of three contributions, namely

- flux terms \mathfrak{F} over the boundary $\partial\omega$,
- source terms \mathfrak{S} in ω and

- production terms \mathfrak{P} in ω ,

such that by formulating the balance we obtain

$$\frac{d}{dt}\xi(\omega, t) = \mathfrak{F}(\partial\omega, t) + \mathfrak{S}(\omega, t) + \mathfrak{P}(\omega, t). \quad (2.4.3)$$

Since the flux is assumed to show in direction of the environment and usually in thermodynamics all quantities are assumed positive if they enter the body, the flux terms usually get negative. For conserving quantities as energy, for instance, the production term is zero. Furthermore it is assumed, that the flux term depends on the normal vector linearly and can be expressed by

$$\mathfrak{F} = \int_{\partial\omega} f(\mathbf{x}, \mathbf{n}, t) da. \quad (2.4.4)$$

On this relation the Cauchy theorem is applicable such that we finally can rewrite it as an integral over the domain ω by using the divergence theorem.

$$\mathfrak{F} = - \int_{\partial\omega} \phi(\mathbf{x}, t) \mathbf{n} da. \quad (2.4.5)$$

This procedure was already applied to the traction vector when the linear momentum balance equation was introduced. Therefore in the linear momentum balance equation, for instance, the traction vector can be identified by the flux term, whereas the volume forces correspond to the source terms. Since the linear momentum is a conserving quantity no production terms can be found. This structure can be also applied to the non-mechanical power Q , that only consists of the heat flux q_n and the heat source r , but without heat production. We obtain

$$Q = \int_{\partial\omega} q_n(\mathbf{x}, t, \mathbf{n}) da + \int_{\omega} \rho r(\mathbf{x}, t) dv \quad (2.4.6)$$

whereby the heat flux, following the upper remarks, can be rewritten by the Cauchy theorem as

$$q_n(\mathbf{x}, \mathbf{n}, t) = -\mathbf{q}(\mathbf{x}, t) \cdot \mathbf{n}. \quad (2.4.7)$$

Inserting these non-mechanical flux and source terms in eqn. 2.4.2 the spatial formulation of the first law of thermodynamics is given by

$$\frac{d}{dt} \int_{\mathcal{B}_t} \left[\frac{1}{2} \rho \mathbf{v} \cdot \mathbf{v} + \rho u \right] dv = \int_{\partial\mathcal{B}_t} [\mathbf{t} \cdot \mathbf{v} + q_n] da + \int_{\mathcal{B}_t} [\mathbf{b} \cdot \mathbf{v} + \rho r] dv. \quad (2.4.8)$$

Here the change of the total energy of a thermodynamic system not only depends on the external mechanical power P_{ext} , that is done by the surface tractions and the volume forces, but also of the thermal power that is caused by the heat fluxes and the heat sources. With this relation at hand, processes can be described where a transformation of one form of energy to another one takes place, i.e. thermomechanical processes can be taken into account. Taking eqn. 2.3.29 into account we can reformulate eqn. 2.4.2 in terms of the internal mechanical power, such that the rate of internal energy coincides with the internal mechanical power. In the case of a general thermodynamical process the change of the internal energy also depends on the heat power, such that we get

$$\frac{d}{dt} U = P_{ext} + Q. \quad (2.4.9)$$

This identity can be rewritten by inserting the particular terms that were derived before and that finally renders

$$\frac{d}{dt} \int_{\mathcal{B}_t} \rho u dv = \int_{\mathcal{B}_t} [\boldsymbol{\sigma}^\sharp : \mathbf{d}^\flat - \operatorname{div} \mathbf{q} + \rho r] dv \quad (2.4.10)$$

the so-called balance of internal energy in the spatial configuration. By shrinking the volume to zero the local form of the first law can be obtained. The material representation of the first law of thermodynamics is given by

$$\frac{d}{dt} \int_{\mathcal{B}_0} [\frac{1}{2} \rho_0 \mathbf{v} \cdot \mathbf{v} + \rho_0 u_R] dV = \int_{\partial \mathcal{B}_0} [\mathbf{t}_0 \cdot \mathbf{v} + Q_N] dA + \int_{\mathcal{B}_0} [\mathbf{b}_0 \cdot \mathbf{v} + \rho_0 r] dV, \quad (2.4.11)$$

whereby the Nansons formula relates the material heat flux and the spatial one. This renders the according pull back operation

$$- \int_{\partial \mathcal{B}_t} \mathbf{q} \cdot \mathbf{n} da = - \int_{\partial \mathcal{B}_0} J \mathbf{q} \cdot [\mathbf{f}^\sharp]^t \cdot \mathbf{N} dA = - \int_{\partial \mathcal{B}_0} \mathbf{Q} \cdot \mathbf{N} dA = \int_{\partial \mathcal{B}_0} Q_N dA. \quad (2.4.12)$$

In analogy to eqn. 2.4.10 the balance of energy includes also the non-mechanical contributions such that

$$\frac{d}{dt} \int_{\partial \mathcal{B}_0} \rho_0 u dV = \int_{\mathcal{B}_0} [\mathbf{P}^\sharp : \dot{\mathbf{F}}^\sharp - \operatorname{Div} \mathbf{Q} + \rho_0 r] dV \quad (2.4.13)$$

describes the total internal energy with respect to the material coordinates. In this relation the divergence theorem was used to transform the surface integral to an integral over the volume.

2.4.2 2nd Law in Continuum Thermodynamics

While the first law of thermodynamics quantifies the energy transfer of a process the second law provides a tool to predict the direction that a process will take. For this the so-called entropy is introduced that is a non-conserving quantity, i.e. an additional production term has to be considered. This production term Υ can be calculated by the difference of the total entropy rate \dot{S} and the entropy input \bar{Q}

$$\Upsilon = \frac{d}{dt} S - \bar{Q} \geq 0, \quad (2.4.14)$$

whereby here \bar{Q} determines the entropy supply and includes the flux and source terms, such that we obtain the same structure that was installed in the section before. The entropy of the system is a state variable and it can be written as

$$S = \int_{\mathcal{B}_t} \rho s dv = \int_{\mathcal{B}_0} \rho_0 s dV \quad (2.4.15)$$

for the current and the reference configuration, respectively. Denoting the entropy flux by h_n and the entropy sources by g we can write the total entropy production as the difference

$$\Upsilon = \frac{d}{dt} \int_{\mathcal{B}_t} \rho s dv - \int_{\mathcal{B}_t} \rho g dv + \int_{\partial \mathcal{B}_t} \mathbf{h} \cdot \mathbf{n} da \geq 0. \quad (2.4.16)$$

Here it is taken into account, that analogously to the heat flux the Cauchy theorem can be applied to the entropy flux and it is defined by

$$h_n = -\mathbf{h} \cdot \mathbf{n}. \quad (2.4.17)$$

As long as the total entropy production is zero the process is reversible whereas if it becomes greater than zero the process is irreversible. The case $Y < 0$ is not admissible. Therefore the system will follow this direction of a process, in which it can increase its entropy. For the material formulation we assume that the entropy flux also transforms by the Nansons formula such that we obtain

$$Y = \frac{d}{dt} \int_{B_0} \rho_0 s dV - \int_{B_0} \rho_0 g dV + \int_{\partial B_0} \mathbf{H} \cdot \mathbf{N} dA \geq 0. \quad (2.4.18)$$

All natural and spontaneously proceeding processes are irreversible and following Zemansky [Zem68] they are indicated by the fact that they do not pass through equilibrium states and they are causing dissipative effects like friction or inelasticity. The given representations are very general and for material theory a specified formulation is used that is called the *Clausius-Duhem inequality* which is derived in the following subsection.

2.4.3 Clausius-Duhem Inequality

The entropy fluxes and entropy sources are not measurable quantities and the entropy input \bar{Q} usually is related to the rate of thermal heat Q . For this the heat power is divided by the absolute temperature that is denoted by Θ , such that the total entropy input is determined by

$$\bar{Q} = - \int_{\partial B_t} \frac{\mathbf{q}}{\Theta} \cdot \mathbf{n} da + \int_{B_t} \rho \frac{r}{\Theta} dv, \quad (2.4.19)$$

whereby the entropy flux and the entropy sources are identified with

$$\mathbf{h} = \frac{\mathbf{q}}{\Theta}, \quad g = \frac{r}{\Theta}. \quad (2.4.20)$$

These relations are valid for equilibrium processes and for processes close to equilibrium they are good approximations [Hau02]. Nevertheless, the approaches are not useful for the description of gas dynamics or diffusion processes, but in order to characterise the behaviour of materials they work satisfactorily. The relation which results from these approaches is the so-called Clausius-Duhem inequality, which was firstly studied intensively by Coleman & Noll [CN63]. In terms of the spatial coordinates we obtain

$$Y = \frac{d}{dt} \int_{B_t} \rho s dv + \int_{\partial B} \frac{\mathbf{q}}{\Theta} \cdot \mathbf{n} da - \int_B \rho \frac{r}{\Theta} dv \geq 0 \quad (2.4.21)$$

and by taking into account the Nansons formula the corresponding representation in the reference configuration can be derived. In order to derive the local form of these relations we need to transform the surface integral to a volume integral again by the divergence theorem. However, here we have to consider the quotient of the heat flux and temperature, thus we finally obtain

$$\rho \dot{s} + \frac{1}{\Theta} \operatorname{div} \mathbf{q} - \frac{1}{\Theta^2} \mathbf{q} \cdot \operatorname{grad} \Theta - \rho \frac{r}{\Theta} \geq 0. \quad (2.4.22)$$

This equation can be multiplied by Θ and taking into account eqn. 2.4.10, such that the heat source is replaced, we obtain the following representation of the second law of thermodynamics

$$\rho\Theta\dot{s} - \rho\dot{u} + \boldsymbol{\sigma}^\sharp : \mathbf{d}^b - \nabla \ln \Theta \cdot \mathbf{q} \geq 0. \quad (2.4.23)$$

If finally the rate of the internal energy is rewritten by using the Legendre transformation $u = \Psi + s\Theta$ that in general replaces the variables with their conjugate variables, we find the representation of the Clausius-Duhem inequality in the form of

$$-\rho\dot{\Psi} - \rho\dot{\Theta}s + \boldsymbol{\sigma}^\sharp : \mathbf{d}^b - \nabla \ln \Theta \cdot \mathbf{q} \geq 0. \quad (2.4.24)$$

whereby Ψ denotes the Helmholtz energy. With eqn. 2.4.24 a relation is given connecting thermodynamical restrictions to the material behaviour that is defined by the free Helmholtz energy Ψ . While the Clausius-Duhem inequality demands to be non-negative for the sum of all terms in eqn. 2.4.24, a stronger restriction separates the heat conduction term from the rest in eqn. 2.4.24 and requires from both terms to be non-negative separately. Therefore this proceeding yields the heat conduction inequality on the one hand

$$D_{con} = -\nabla \ln \Theta \cdot \mathbf{q} \geq 0, \quad (2.4.25)$$

that also is identified with the *nonlocal* or *convective dissipation* D_{con} and on the other hand we find the so-called Clausius-Planck inequality

$$D_{loc} = \boldsymbol{\sigma}^\sharp : \mathbf{d}^b - \rho\dot{\Psi} - \rho\dot{\Theta}s \geq 0, \quad (2.4.26)$$

whereby D_{loc} defines the *internal* or *local dissipation*. Eqn. 2.4.25 yields a restriction to the heat flux vector \mathbf{q} . Since the temperature gradient of the system can be negative or positive the simplest choice of \mathbf{q} to fulfill the inequality in any case is given by $\mathbf{q} = -\boldsymbol{\kappa} \cdot \text{grad}\Theta$, that accords to a Fourier-type law. $\boldsymbol{\kappa}$ denotes the heat conduction coefficient tensor of order two and in isotropic applications it reduces to $\boldsymbol{\kappa} = k\mathbf{b}^\sharp$.

The Clausius-Planck inequality presents the fundamental restriction that materials have to fulfill such that thermodynamical consistency can be ensured. In the isothermal case the last term in eqn. 2.4.26 vanishes and the local dissipation solely depends on the rate of the free Helmholtz energy. A matter in material theory is to decide in which variables the free energy must be formulated to record the effects it should describe. While in isotropic hyperelasticity of homogenous bodies the material solely depends on the actual deformation, in plasticity it also depends on the *history of deformation*, for instance, such that the free energy has to be enriched by additional variables. Before we continue presenting this method we firstly have a look at the kinematics of inelastic deformations in the next section. Finally we want to mention here, that the presented method by Coleman & Noll is not the only one and there are "...no generally valid and universally acknowledged formulations of the second law so far for expressing a general principle of irreversibility..." [Hau02]. A detailed discussion of different theories of thermodynamics with respect to material theory is also given by Hutter [Hut77].

2.5 The Concept of Elasticity

2.5.1 Stresses in Elastic Materials

Definition of stress In this section we want to consider *constitutive relations*, which describe the behaviour of a body \mathfrak{B} consisting of a certain material and undergoing external loads like forces or

heat fluxes. Here at first, we solely restrict ourselves to forces. The work done by these forces on the considered body during a certain deformation process is partially stored in the body. This stored energy is denoted by W , that we like to call *stored energy function* or *strain energy function*. Since the strain energy depends on the deformation given by \mathbf{F}^b , we can write $W = W(\mathbf{F}^b(\mathbf{X}, t), \mathbf{X})$, that is called a *scalar-valued tensor function*. If the material behaves the same way at every \mathbf{X} it is called *homogenous* and therefore we can reduce the arguments of the work function as $W = W(\mathbf{F}^b(\mathbf{X}, t))$. Furthermore it is called *elastic* if it behaves completely *reversible*, i.e. after withdrawing the external loading the material returns to its initial state³. Is the state of the body additionally independent of the way of deformation the strain energy function defines a potential and we refer to the material as *hyper-elastic* or *Green-elastic*. In the case of isothermal elastic deformations the strain energy function coincides with the free Helmholtz energy Ψ

$$W(\mathbf{F}^b(\mathbf{X}, t)) = \Psi(\mathbf{F}^b(\mathbf{X}, t)) = \rho_0 \psi(\mathbf{F}^b(\mathbf{X}, t)). \quad (2.5.27)$$

and is referred to reference volume V . Another restriction we want to introduce here, is called *isotropy*, which means that the properties of a material does not change with the direction. For the investigation of this property we consider a particular point in the reference configuration \mathbf{X} undergoing a certain motion $\mathbf{x} = \varphi(\mathbf{X}, t)$, which generates a strain-energy $W(\mathbf{F}^b(\mathbf{X}, t))$. If we apply a rigid-body motion (consisting of a translation and rotation) to the reference configuration, such that we attain at the point \mathbf{X}^* and afterwards additionally employ the deformation $\mathbf{x}^* = \varphi(\mathbf{X}^*, t)$, in general we would expect to obtain another strain-energy $W(\mathbf{F}^b(\mathbf{X}^*, t))$. A material is called *isotropic*, if and only if the expressions of the strain energy function for different \mathbf{X} and \mathbf{X}^* do not differ. We have to emphasize here that there has to be distinguished between *isotropy* and *frame-indifference*. We want to oppose both restrictions at the example of the strain energy function $W(\mathbf{F}(\mathbf{X}, t))$. For this we firstly recall the constraint of frame indifference, where a rigid body motion is superimposed on the current configuration and the deformation gradient \mathbf{F}^b is multiplied on the left by $\mathbf{Q} \in SO^3$. To check if the strain energy function fullfills the constraint of objectivity, we like to consider a particular choice of \mathbf{Q} , namely the transposed of the proper orthogonal rotation tensor \mathbf{R}^t

$$W(\mathbf{F}^b) = W(\mathbf{R}^t \cdot \mathbf{F}^b) = W(\mathbf{R}^t \cdot \mathbf{R} \cdot \mathbf{U}^b) = W(\mathbf{U}^b). \quad (2.5.28)$$

This is the necessary and sufficient condition for the strain energy to be objective. Usually however, the strain energy function is formulated in terms of of the right Cauchy-Green deformation tensor $\mathbf{C}^b = [\mathbf{U}^b]^2$ or the Green-Lagrange strain tensor $2\mathbf{E}^b = [\mathbf{U}^b]^2 - \mathbf{G}^b$. Therefore an objective strain energy function is given by

$$W = W(\mathbf{C}^b). \quad (2.5.29)$$

In contrast to this for the proof of isotropy the deformation gradient \mathbf{F}^b is multiplied on the right hand side by \mathbf{Q}^t

$$W(\mathbf{F}^b) = W(\mathbf{F}^{b*}) = W(\mathbf{F}^b \cdot \mathbf{Q}^t), \quad (2.5.30)$$

namely in the reference configuration. Applying this relation to the strain energy function in terms of the right Cauchy-Green tensor

$$W(\mathbf{C}^b) = W([\mathbf{F}^{b*}]^t \cdot \mathbf{F}^{b*}) = W(\mathbf{Q} \cdot [\mathbf{F}^b]^t \cdot \mathbf{F}^b \cdot \mathbf{Q}^t) = W(\mathbf{Q} \cdot \mathbf{C}^b \cdot \mathbf{Q}^t) \quad (2.5.31)$$

³The exact definition of elastic materials says, that during an elastic deformation no entropy is produced

we can identify the strain energy function as an isotropic tensor function. The topic of isotropic and anisotropic material description is quite difficult and detailed discussion of anisotropic material modelling is given by Menzel [Men02].

Now we consider the rate of the strain-energy function

$$\dot{W} = \frac{\partial W}{\partial \mathbf{F}^b} : \dot{\mathbf{F}}^b, \quad \text{with} \quad \frac{\partial W}{\partial \mathbf{F}^b} = \rho_0 \frac{\partial \psi}{\partial \mathbf{C}^b} \cdot \frac{\partial \mathbf{C}^b}{\partial \mathbf{F}^b} = 2\rho_0 \mathbf{g}^b \cdot \mathbf{F}^b \cdot \frac{\partial \psi}{\partial \mathbf{C}^b} = \mathbf{g}^b \cdot \mathbf{F}^b \cdot \mathbf{S}^\sharp, \quad (2.5.32)$$

that is called *stress power* and the expression $2\rho_0 \frac{\partial \psi}{\partial \mathbf{C}^b}$ defines the 2. Piola-Kirchhoff stress tensor $\mathbf{S}^\sharp = S^{ij} \mathbf{G}_i \otimes \mathbf{G}_j \in \mathbb{S}^3 : T^* \mathcal{B}_0 \times T^* \mathcal{B}_0 \rightarrow \mathbb{R}$. \mathbf{S}^\sharp is called work conjugated to the right Cauchy-Green deformation tensor or the Green Lagrange tensor \mathbf{E}^b as we already have seen in eqn. 2.3.32 and has no physical meaning. Nevertheless, it is a very crucial quantity, since it lives solely in the reference configuration and therefore it can be used for the formulation of objective stress rates. Moreover, the expression $\mathbf{g}^\sharp \cdot \partial_{\mathbf{F}^b} W$ derived in eqn. 2.5.32 can be interpreted as a stress that commonly is called the 1. Piola-Kirchhoff stress or *nominal stress*. This two-point tensor was also already introduced in eqn. 2.3.31 and we denoted it by $\mathbf{P}^b = P_i^j \mathbf{g}^i \otimes \mathbf{G}_j \in \mathbb{L}^3 : T^* \mathcal{B}_0 \rightarrow T^* \mathcal{B}_t$. As we can learn from eqn. 2.3.31 the 1. Piola-Kirchhoff stress is work-conjugated to the deformation tensor \mathbf{F}^b and can be interpreted as a measure for the actual forces in the current configuration with respect to surface elements in the reference configuration. With this at hand eqn. 2.5.32 can also be interpreted as a transformation equation between both stress formulations that are related by the push forward and pull back operations, as

$$\mathbf{P}^b = \mathbf{g}^b \cdot \mathbf{F}^b \cdot \mathbf{S}^\sharp. \quad (2.5.33)$$

Both stress formulations can be identified with derivatives of the strain energy function with respect to the deformation gradient \mathbf{F}^b or the right Cauchy-Green tensor \mathbf{C}^b , respectively. Therefore we need different formulations for the strain energy function W , namely in terms of \mathbf{F}^b or \mathbf{C}^b . Accordingly we obtain these two different stress formulations derived before, whereby the 2. Piola-Kirchhoff stress can be assumed as an frame-indifferent stress tensor whereas the 1. Piola-Kirchhoff stress is not objective. For the engineering practice the stresses at the current configuration are of most interest. By applying the push forward operation to the 1. Piola-Kirchhoff stress \mathbf{P}^b

$$\boldsymbol{\tau}^\sharp = \mathbf{g}^\sharp \cdot \mathbf{P}^b \cdot [\mathbf{F}^b]^t \quad (2.5.34)$$

we obtain the so-called *Kirchhoff stress* $\boldsymbol{\tau}^\sharp = \tau^{ij} \mathbf{g}_i \otimes \mathbf{g}_j \in \mathbb{S}^3 : T^* \mathcal{B}_t \times T^* \mathcal{B}_t \rightarrow \mathbb{R}$. Sometimes it is also called the weighted Cauchy stress tensor because the Cauchy stress or true stress $\boldsymbol{\sigma}^\sharp$ can be obtained from $\boldsymbol{\tau}^\sharp$ by multiplying the Kirchhoff stress by the inverse Jacobian J^{-1} . Finally we get the following relations between the different stress quantities in the different configurations

$$\boldsymbol{\sigma}^\sharp = J^{-1} \boldsymbol{\tau}^\sharp = J^{-1} \mathbf{P}^b \cdot [\mathbf{F}^b]^t = J^{-1} \mathbf{F}^b \cdot \mathbf{S}^\sharp \cdot [\mathbf{F}^b]^t. \quad (2.5.35)$$

Since the stored energy function is invariant under rotation, like $W(\mathbf{C}^b)$, it can also be expressed in terms of the principal invariants I_1, I_2 and I_3 . Therefore the 2. Piola-Kirchhoff stress tensor can be rewritten as

$$\mathbf{S}^\sharp = 2 \left[\frac{\partial W}{\partial I_1} \frac{\partial I_1}{\partial \mathbf{C}^b} + \frac{\partial W}{\partial I_2} \frac{\partial I_2}{\partial \mathbf{C}^b} + \frac{\partial W}{\partial I_3} \frac{\partial I_3}{\partial \mathbf{C}^b} \right]. \quad (2.5.36)$$

The derivatives of the principal invariants with respect to the right Cauchy-Green tensor can be derived from eqn. 2.2.19

$$\frac{\partial I_1}{\partial \mathbf{C}^b} = \mathbf{G}^\sharp, \quad \frac{\partial I_2}{\partial \mathbf{C}^b} = I_1 \mathbf{G}^\sharp - \mathbf{G}^\sharp \cdot \mathbf{C}^b \cdot \mathbf{G}^\sharp, \quad \frac{\partial I_3}{\partial \mathbf{C}^b} = I_3 [\mathbf{C}^b]^{-t}. \quad (2.5.37)$$

Since \mathbf{C}^b is symmetric it is sufficient to calculate the inverse of \mathbf{C}^b in eqn. 2.5.37₃, but in general the derivative of the Jacobian is given in the form that is presented here. Inserting the derivatives in eqn. 2.5.36 we obtain an equation for the material 2. Piola-Kirchhoff stress in terms of the invariants.

$$\mathbf{S}^\sharp = 2 \left[\left[\frac{\partial W}{\partial I_1} + I_1 \frac{\partial W}{\partial I_2} \right] \mathbf{G}^\sharp - \frac{\partial W}{\partial I_2} \mathbf{G}^\sharp \cdot \mathbf{C}^b \cdot \mathbf{G}^\sharp + I_3 \frac{\partial W}{\partial I_3} [\mathbf{C}^b]^{-1} \right] \quad (2.5.38)$$

This representation is only valid for isotropic hyperelastic materials. By pushing forward this representation in the manner of eqn. 2.5.35 and by taking eqn. A.1.9 into account we get the representation of the Kirchhoff stress in terms of principal invariants

$$\boldsymbol{\tau}^\sharp = 2 \left[\frac{\partial W}{\partial I_1} \mathbf{b}^\sharp + \left[I_2 \frac{\partial W}{\partial I_2} + I_3 \frac{\partial W}{\partial I_3} I_3 \right] \mathbf{g}^\sharp - I_3 \frac{\partial W}{\partial I_2} [\mathbf{b}^\sharp]^{-1} \right], \quad (2.5.39)$$

which is analogous to the representation of the 2. Piola-Kirchhoff stress in eqn. 2.5.38. In this context we like to present another important result with respect to equivalent stress representations. If we assume, that the strain energy depends only on the spatial left Cauchy Green tensor and it is objective in \mathbf{b}^\sharp the strain energy rate can be expressed by

$$\dot{W} = \frac{\partial W}{\partial \mathbf{b}^\sharp} : \dot{\mathbf{b}}^\sharp = \frac{\partial W}{\partial \mathbf{b}^\sharp} : [\mathbf{l}^\sharp \cdot \mathbf{b}^\sharp + [\mathbf{l}^\sharp \cdot \mathbf{b}^\sharp]^t] = 2 \left[\frac{\partial W}{\partial \mathbf{b}^\sharp} \cdot \mathbf{b}^\sharp \right] : \mathbf{l}^\sharp = [\mathbf{g}^\sharp \cdot \boldsymbol{\tau}^\sharp] : \mathbf{l}^\sharp \quad (2.5.40)$$

On the other hand we consider the strain energy in terms of the material Euler Lagrange strain tensor \mathbf{E}^b , such that the push forward of the 2. Piola-Kirchhoff stress to the spatial configuration yields

$$\boldsymbol{\tau}^\sharp = \Phi^*(\mathbf{S}^\sharp) = \mathbf{F}^\sharp \cdot \frac{\partial W}{\partial \mathbf{e}^b} : \frac{\partial \mathbf{e}^b}{\partial \mathbf{E}^b} \cdot [\mathbf{F}^\sharp]^t = \frac{\partial W}{\partial \mathbf{e}^b}. \quad (2.5.41)$$

If we finally consider the derivative of the strain energy function with respect to the spatial metric tensor \mathbf{g}^b , taking the result from eqn. 2.5.41 into account, we obtain

$$\frac{\partial W}{\partial \mathbf{g}^b} = \frac{\partial W}{\partial \mathbf{e}^b} \cdot \frac{\partial \mathbf{e}^b}{\partial \mathbf{g}^b} = \frac{1}{2} \boldsymbol{\tau}^\sharp. \quad (2.5.42)$$

The last three equations render three different but equivalent constitutive laws for the spatial Kirchhoff stress tensor. We want to summarize these results here in one equation

$$\boldsymbol{\tau}^\sharp = \frac{\partial W}{\partial \mathbf{e}^b} = 2 \frac{\partial W}{\partial \mathbf{g}^b} = 2 \mathbf{g}^\sharp \cdot \frac{\partial W}{\partial \mathbf{b}^\sharp} \cdot \mathbf{b}^\sharp. \quad (2.5.43)$$

Stresses in terms of principal stretches Since in the case of isotropy the invariants depend on the eigenvalues, stress tensors can also be represented in terms of the principal directions, that is crucial for the numerical treatment. We start with the definition of the 2. Piola Kirchhoff stress \mathbf{S}^\sharp

$$\mathbf{S}^\sharp = 2 \frac{\partial W}{\partial \mathbf{C}^b} = 2 \frac{\partial W}{\partial \lambda_\alpha} \frac{\partial \lambda_\alpha}{\partial \mathbf{C}^b}, \quad (2.5.44)$$

whereby the derivative of the eigenvalue with respect to the right Cauchy-Green deformation tensor can be derived as follows. We consider the derivative of the right Cauchy Green tensor with respect to itself

$$\frac{\partial \mathbf{C}^b}{\partial \mathbf{C}^b} = \frac{\partial \mathbf{C}^b}{\partial \lambda_\alpha} \otimes \frac{\partial \lambda_\alpha}{\partial \mathbf{C}^b} = \mathbb{I}^{sym} \rightsquigarrow \frac{\partial C_{ij}}{\partial C_{kl}} = \frac{1}{2} [\delta_i^k \delta_j^l + \delta_i^l \delta_j^k], \quad (2.5.45)$$

that defines the symmetric material fourth order identity tensor $\mathbb{I}^{sym} = \mathbf{G}^i \otimes \mathbf{G}_k \otimes \mathbf{G}^j \otimes \mathbf{G}_l \in \mathbb{S}^{3 \times 3} : T\mathcal{B}_0 \times T\mathcal{B}_0 \times T^*\mathcal{B}_0 \times T^*\mathcal{B}_0 \rightarrow \mathbb{R}$. In eqn. 2.5.45₂ we used the chain rule and considering the derivative of the right Cauchy-Green tensor with respect to the eigenvalues, that can be easily determined from the spectral decomposed representation of the right Cauchy-Green tensor (eqn. 2.2.18₁), such that we obtain

$$\frac{\partial \mathbf{C}^b}{\partial \lambda_\alpha} = 2\lambda_\alpha \mathbf{N}^\alpha \otimes \mathbf{N}^\alpha. \quad (2.5.46)$$

Inserting this relation in eqn. 2.5.45 and solving for $\frac{\partial \lambda_\alpha}{\partial \mathbf{C}^b}$ renders

$$\frac{\partial \lambda_\alpha}{\partial \mathbf{C}^b} = \frac{1}{2} \lambda_\alpha \mathbf{M}^\alpha, \quad \text{with} \quad \mathbf{M}^\alpha = \lambda_\alpha^{-2} \mathbf{N}^\alpha \otimes \mathbf{N}^\alpha \quad (2.5.47)$$

such that we can rewrite the relation for the 2. Piola-Kirchhoff stress in terms of the eigenvalues as

$$\mathbf{S}^\sharp = \sum_{\alpha=1}^3 \frac{\partial W}{\partial \lambda_\alpha} \lambda_\alpha^{-1} \mathbf{N}^\alpha \otimes \mathbf{N}^\alpha = \sum_{\alpha=1}^3 \frac{\partial W}{\partial \lambda_\alpha} \lambda_\alpha \mathbf{M}^\alpha. \quad (2.5.48)$$

Taking eqn. 2.5.35 and 2.5.36 into account, we can also determine the 1. Piola-Kirchhoff stress \mathbf{P}^\sharp , the Kirchhoff stress $\boldsymbol{\tau}^\sharp$ and the true stress $\boldsymbol{\sigma}^\sharp$ in terms of the principal directions by pushing forward the relation in eqn. 2.5.48. Of course we have to consider the deformation gradient in eigenvalue representation as well. Therefore the stress tensors can be calculated by

$$\mathbf{P}^\sharp = \sum_{\alpha=1}^3 \frac{\partial W}{\partial \lambda_\alpha} \mathbf{n}^\alpha \otimes \mathbf{N}^\alpha, \quad \boldsymbol{\tau}^\sharp = \sum_{\alpha=1}^3 \frac{\partial W}{\partial \lambda_\alpha} \lambda_\alpha \mathbf{m}^\alpha \quad \boldsymbol{\sigma}^\sharp = J^{-1} \sum_{\alpha=1}^3 \frac{\partial W}{\partial \lambda_\alpha} \lambda_\alpha \mathbf{m}^\alpha, \quad (2.5.49)$$

whereby

$$\mathbf{m}^\alpha = \mathbf{n}^\alpha \otimes \mathbf{n}^\alpha \quad (2.5.50)$$

denotes the eigenbasis on the current configuration. An essential result that can be recognized in all stress representations is that their principal directions coincide with the principal directions of the corresponding work-conjugated deformation tensors. We want to emphasize here, that this is only valid for isotropy and therefore in the sequel we restrict ourselves to isotropic formulations.

2.5.2 Volumetric- Isochoric Decomposition

In modelling of materials it is a quite common idea, that the deformation can be decomposed into a part that describes the volumetric change of the material body and another part that records the change of its shape. The latter one is thought to be volume-preserving or isochoric. This idea is reflected in the additive decomposition of the strain energy function into an *volumetric* and an *isochoric* part

$$W(\mathbf{C}^b) = W_{vol}(J) + W_{iso}(\tilde{\mathbf{C}}^b). \quad (2.5.51)$$

This proposition firstly was made by Lee [Lee67] and it is straight forward that the volumetric part only depends on the Jacobian J of the deformation gradient, that describes the volumetric change

of the body within a deformation process. The isochoric part depends on $\tilde{\mathbf{C}}^b$ that consequently only denotes the isochoric part of the right Cauchy-Green tensor. For the determination of the isochoric part the following crucial assumption is made that says that also the deformation gradient can be decomposed multiplicatively into a volumetric part and an isochoric part

$$\mathbf{F}^b = \mathbf{F}_{vol}^b \cdot \mathbf{F}_{iso}^b. \quad (2.5.52)$$

Since the volumetric change is described by the principal stretches, which are assumed to be equal as long as we consider isotropic materials, it is clear that the volumetric part of the deformation gradient can be described by

$$\mathbf{F}_{vol}^b = J^{\frac{1}{3}} \mathbf{g}^b. \quad (2.5.53)$$

and from eqn. 2.5.52 we can also easily determine the isochoric part of \mathbf{F}^b by

$$\mathbf{F}_{iso}^b = \tilde{\mathbf{F}}^b = J^{-\frac{1}{3}} \mathbf{F}^b. \quad (2.5.54)$$

With this at hand it is also possible to determine the decomposition of \mathbf{C}^b by inserting this expression into the definition of the right Cauchy-Green tensor. Here we obtain the two parts

$$\mathbf{C}_{vol}^b = J^{\frac{2}{3}} \mathbf{G}^b, \quad \mathbf{C}_{iso}^b = \tilde{\mathbf{C}}^b = J^{-\frac{2}{3}} \mathbf{C}^b. \quad (2.5.55)$$

Alternatively the free energy function can also be formulated in terms of the left Cauchy-Green tensor

$$W(\mathbf{b}^\sharp) = W_{vol}(J) + W_{iso}(\tilde{\mathbf{b}}^\sharp), \quad \text{with} \quad \mathbf{b}_{vol}^\sharp = J^{\frac{1}{3}} \mathbf{g}^\sharp \quad \text{and} \quad \mathbf{b}_{iso}^\sharp = \tilde{\mathbf{b}}^\sharp = J^{-\frac{2}{3}} \mathbf{b}^\sharp \quad (2.5.56)$$

whereby the two formulations coincide to each other since the left and right Cauchy-Green tensor depend on the same eigenvalues. Therefore it makes sense to formulate the strain energy function in terms of the eigenvalues directly. Taking into account the volumetric-isochoric decomposition the free energy function in terms of the eigenvalues can be written as

$$W(\lambda_\alpha) = W_{vol}(J) + W_{iso}(\tilde{\lambda}_\alpha), \quad \text{with} \quad \tilde{\lambda}_\alpha = \lambda_{\alpha,iso} = J^{-\frac{1}{3}} \lambda_\alpha \quad (2.5.57)$$

Here the terms $\tilde{\lambda}_\alpha$ denote the eigenvalues of the isochoric part. To give some examples for hyper-elastic strain energy functions we like to refer to the *Mooney-Rivlin* model and to the *neo-Hookean* model, which are applied to incompressible materials like rubber for instance. The Mooney-Rivlin model is represented by the strain energy function

$$W = c_1[I_1 - 3] + c_2[I_2 - 3] \quad (2.5.58)$$

whereby the constants c_1 and c_2 are material parameters. The Neo-Hooke model can be obtained from the Mooney-Rivlin model by setting the second term to zero, such that it reduces to

$$W = c_1[I_1 - 3]. \quad (2.5.59)$$

Here the constant c_1 is identified with the shear modulus μ . These models can be extended to compressible materials by adding a contribution in terms of J , such that volumetric changes are treatable. The compressible modification of the Mooney-Rivlin, for instance, could look like

$$W = c_3[J - 1]^2 - d \ln J + c_1[I_1 - 3] + c_2[I_2 - 3], \quad \text{with} \quad d = 2[c_1 + 2c_2] \quad (2.5.60)$$

as it was proposed similarly by Ciarlet & Geymonat [Cia82]. Here c_3 is another given material parameter. Another free Helmholtz energy function we want to mention here is the modified *St. Venant-Kirchhoff*-model

$$W = \frac{1}{2}\kappa[\ln J]^2 + \frac{1}{4}\mu \sum_{\alpha} [\ln \tilde{\lambda}_{\alpha}^2]^2, \quad (2.5.61)$$

which is well known from the geometrically linear theory. For the nonlinear case the linear strains are replaced by the logarithmic strain measure, such that the additive structure of the geometrically linear formulation of the Hookean material law can be maintained. κ and μ are material parameters denoting the bulk and the shear modulus. This material model is very crucial with respect to hyperelasto-plastic material formulations, since it forms the starting point for the von-Mises formulation, as we will see later on. Here we just want to point out that this energy function is also decomposed into a volumetric and an isochoric contribution. An overview on the most important geometrically nonlinear elastic material models and their modifications with respect to rate-dependent and damage formulations is given in [Hol01].

The consequence of the volumetric-isochoric decomposition of the strain energy function is that we obtain a decomposed stress formulations. For this we firstly consider the 2. Piola Kirchhoff stress \mathbf{S}^{\sharp} in terms of the eigenvalues and in its decomposed form we get the contributions

$$\mathbf{S}_{vol}^{\sharp} = 2 \frac{\partial W_{vol}}{\partial J} \frac{\partial J}{\partial \lambda_{\alpha}} \frac{\partial \lambda_{\alpha}}{\partial \mathbf{C}^b}, \quad \mathbf{S}_{iso}^{\sharp} = 2 \frac{\partial W_{iso}}{\partial \tilde{\lambda}_{\alpha}} \frac{\partial \tilde{\lambda}_{\alpha}}{\partial \lambda_{\alpha}} \frac{\partial \lambda_{\alpha}}{\partial \mathbf{C}^b}, \quad (2.5.62)$$

that we want to investigate separately. The derivative of J with respect to \mathbf{C}^b can be derived from eqn. 2.5.37₃, such that we rewrite the volumetric part of the 2. Piola-Kirchhoff stress as

$$\mathbf{S}_{vol}^{\sharp} = J \frac{\partial W_{vol}}{\partial J} \sum_{\alpha=1}^3 \mathbf{M}^{\alpha} \quad \text{with} \quad \sum_{\alpha=1}^3 \mathbf{M}^{\alpha} = [\mathbf{C}^b]^{-1} \quad (2.5.63)$$

Computing the isochoric part is more complicated since the derivative of the isochoric eigenvalues with respect to λ_{α} needs to be evaluated, whereby the relation $\tilde{\lambda}_{\alpha} = J^{-\frac{1}{3}} \lambda_{\alpha}$, as already introduced in eqn. 2.5.57, is consulted. From this the derivative of the isochoric eigenvalues with respect to the original eigenvalues λ_{α} is given by

$$\frac{\partial \tilde{\lambda}_{\alpha}}{\partial \lambda_{\beta}} = J^{-\frac{1}{3}} \left[\delta_{\alpha\beta} - \frac{1}{3} \lambda_{\beta}^{-1} \lambda_{\alpha} \right], \quad (2.5.64)$$

such that by taking eqn. 2.5.47 into account, the isochoric stress contribution $\mathbf{S}_{iso}^{\sharp}$ can be determined by

$$\mathbf{S}_{iso}^{\sharp} = \left[\frac{\partial W_{iso}}{\partial \tilde{\lambda}_{(\beta)}} \tilde{\lambda}_{(\beta)} - \sum_{\alpha=1}^3 \frac{1}{3} \tilde{\lambda}_{\alpha} \frac{\partial W_{iso}}{\partial \tilde{\lambda}_{\alpha}} \right] \mathbf{M}^{\beta} = \tilde{\tau}_{\beta} \mathbf{M}^{\beta}. \quad (2.5.65)$$

In this representation the reader can see that the isochoric part of the 2. Piola-Kirchhoff stress is decomposed into the eigenbase \mathbf{M}^{β} and the coefficient denoted by $\tilde{\tau}_{\beta}$, that coincide with the isochoric eigenvalues of the Kirchhoff stress. The brackets of the index β indicate that no summation takes place here. An alternative representation of the isochoric part of the 2. Piola-Kirchhoff stress is common use, whereby the last two factors are merged to the material eigenbase, that renders

$$\mathbf{S}_{iso}^{\sharp} = \left[\frac{\partial W_{iso}}{\partial \tilde{\lambda}_{(\beta)}} \tilde{\lambda}_{(\beta)} - \sum_{\eta=1}^3 \frac{1}{3} \tilde{\lambda}_{\eta} \frac{\partial W_{iso}}{\partial \tilde{\lambda}_{\eta}} \right] \lambda_{\beta}^{-2} \tilde{\mathbf{M}}^{\alpha}, \quad \text{with} \quad \tilde{\mathbf{M}}^{\alpha} = \mathbf{N}^{\alpha} \otimes \mathbf{N}^{\alpha}. \quad (2.5.66)$$

It follows from eqn. A.1.3 and 2.2.16 that the sum of the material eigenbases

$$\sum_{\alpha=1}^3 M^{\alpha} = \sum_{\alpha=1}^3 \lambda_{\alpha}^{-2} \widetilde{M}^{\alpha} = [C^b]^{-1} \quad (2.5.67)$$

defines the inverse of the right Cauchy-Green tensor.

At the end of this section we want to introduce projection tensors which extract the volumetric or the isochoric part, respectively, of a given second order tensor \mathbf{A} . The volumetric part of a tensor can be calculated from

$$\mathbf{A}_{vol} = \mathbb{I}_{vol} : \mathbf{A} \quad \text{with} \quad \mathbb{I}_{vol} = \frac{1}{3} \mathbf{I} \otimes \mathbf{I} \quad (2.5.68)$$

and \mathbb{I}_{vol} denotes the volumetric fourth order projection tensor. The deviatoric part of \mathbf{A} can be determined by

$$\mathbf{A}_{dev} = \widetilde{\mathbf{A}} = \mathbb{I}_{dev} : \mathbf{A}, \quad \text{with} \quad \mathbb{I}_{dev} = \mathbb{I}^{sym} - \frac{1}{3} \mathbf{I} \otimes \mathbf{I} \quad (2.5.69)$$

whereby \mathbb{I}_{dev} is the deviatoric projection tensor of fourth order, that is defined by the difference between the fourth order unit tensor \mathbb{I}^{sym} and the volumetric projection tensor. Therefore the sum of the volumetric and the isochoric part of \mathbf{A} yields the tensor itself.

2.5.3 Elasticity Tensor

In the framework of numerical calculations the deformation of the body is applied incrementally, that means that the loading is imposed stepwise. For a given loading step the crucial task is to find a set of primary variables, i.e. the displacements \mathbf{u} for instance, such that the configuration describes a state of equilibrium. The stress of the particular configuration is determined by its integral over the time from t_n to t_{n+1}

$$\mathbf{S}_{n+1} = \mathbf{S}_n + \int_{t_n}^{t_{n+1}} d\mathbf{S}, \quad \text{with} \quad d\mathbf{S} = \frac{\partial \mathbf{S}}{\partial t} dt. \quad (2.5.70)$$

whereby \mathbf{S}_n describes the stress at the time t_n for a given equilibrium state. The time integration can be replaced by an equivalent integration over the strains, whereby a constitutive relation

$$\mathbb{C} = \frac{d\mathbf{S}}{d\mathbf{E}} \quad (2.5.71)$$

relating the differential of the total strains and the differential of the stresses. The resulting quantity represents the forth order *material tensor* and in general it contains inelastic material behaviour as well. In the case of pure elasticity the material tensor is also called *elasticity tensor*. Firstly we want to consider the elastic case, since the derivation of the elasticity tensor includes a lot of aspects which are also needed for the inelastic material formulations. Therefore we want to have a detailed view to the derivation of the elasticity tensor as well in the initial as in the current configuration.

Material Description If we consider hyperelastic materials, the continuous elasticity tensor coincides with the second derivative of the strain energy function with respect to the applied strain measure, such that we obtain

$$\dot{\mathbf{S}}^\# = 2 \frac{\partial \mathbf{S}^\#}{\partial \mathbf{C}^b} : \dot{\mathbf{C}}^b = 4 \frac{\partial W}{\partial \mathbf{C}^b \otimes \mathbf{C}^b} : \dot{\mathbf{C}}^b = \mathbb{C}^e : \dot{\mathbf{C}}^b \quad (2.5.72)$$

for the rate of the 2. Piola-Kirchhoff stress tensor. Here $\mathbb{C}^e = \mathcal{C}^{ijkl} \mathbf{G}_i \otimes \mathbf{G}_j \otimes \mathbf{G}_k \otimes \mathbf{G}_l \in \mathbb{S}^{3 \times 3}$ denotes the continuous fourth order elasticity tensor in the reference configuration. In general this elasticity tensor possess the minor symmetry, i.e. the first and the second index are exchangeable and the third and fourth as well. This attribute is valid for all materials, whereas the major symmetry is restricted to hyperelastic materials. This kind of symmetry means that the first pair of indices and the second pair are also exchangeable. This can also be considered as a definition of hyperelastic materials, to which we like to restrict ourselves subsequently. The introduced tangent modulus lives in the material configuration, accordingly we can define a spatial tangent modulus or elasticity tensor $\mathbb{C}^e = \mathcal{C}^{ijkl} \mathbf{g}_i \otimes \mathbf{g}_j \otimes \mathbf{g}_k \otimes \mathbf{g}_l \in \mathbb{S}^{3 \times 3}$. This current elasticity tensor can be obtained by the Piola transformation of the four base vectors of the material elasticity tensor

$$\mathbb{C}^e = J^{-1} \boldsymbol{\varphi}^* (\mathbb{C}^e). \quad (2.5.73)$$

If the free Helmholtz energy W is decomposed into a volumetric and an isochoric part, the material tensor consists of a volumetric and an isochoric part accordingly, since it emanates from the derivative of the stress tensor, which itself can be decomposed in this way. We obtain for the material elasticity tensor

$$\mathbb{C}^e = \mathbb{C}_{vol}^e + \mathbb{C}_{iso}^e \quad (2.5.74)$$

Following eqn. 2.5.57 it is conceivable to determine the material tensor in terms of the eigenvalues, that we like to discuss in detail here. The volumetric and isochoric contributions of the 2. Piola-Kirchhoff stress tensor in the representations above, we can derive the consistent tangent operator and as mentioned before, we obtain two contributions for the material tensor. Firstly we consider the volumetric part of the material tensor

$$\mathbb{C}_{vol}^e = J \left[\frac{\partial W_{vol}}{\partial J} + J \frac{\partial^2 W_{vol}}{\partial J^2} \right] [\mathbf{C}^b]^{-1} \otimes [\mathbf{C}^b]^{-1} - 2J \frac{\partial W_{vol}}{\partial J} \mathbb{I}_{C^{-1}}^{sym} \quad (2.5.75)$$

that is independent of the eigenbases, whereas the isochoric contribution depends on the eigenbases, as the reader can easily see in eqn. 2.5.65. This makes the calculation of the tangent operator quite complex and starting from eqn. 2.5.66 we obtain for the isochoric part

$$\mathbb{C}_{iso}^e = \sum_{\alpha=1} \mathbf{M}^\alpha \otimes \frac{\partial \tilde{\tau}_\alpha}{\partial \mathbf{C}^b} + 2 \tilde{\tau}_\alpha \frac{\partial \mathbf{M}^\alpha}{\partial \mathbf{C}^b}. \quad (2.5.76)$$

Here the first term describes the stress alteration because of a change of the eigenvalues, whereas the second term records the stress rate due to (geometrical) changes of the eigenvectors. Using eqn. 2.5.47 and 2.5.64 the contribution due to the changing eigenvalues can be evaluated by

$$2 \frac{\partial \tilde{\tau}_\alpha}{\partial \mathbf{C}^b} = \varphi_{\alpha\beta} \mathbf{M}^\beta, \quad \text{with} \quad \varphi_{\alpha\beta} = \frac{\partial \tilde{\tau}_\alpha}{\partial \tilde{\lambda}_\alpha} \frac{\partial \tilde{\lambda}_\alpha}{\partial \lambda_\beta} \lambda_\beta. \quad (2.5.77)$$

Here we introduce the coefficient matrix $\varphi_{\alpha\beta}$ that denotes the derivative of the principal Kirchhoff stress with respect to the principal stretches. This abbreviation makes the subsequent proceeding more comprehensible. The only term that still needs to be determined are the derivatives of the eigenvalues $\tilde{\tau}_\alpha$ of the second Piola-Kirchhoff stress with respect to the isochoric principal stretches, such that a symmetric 3×3 - matrix will be obtained. The coefficients of the isochoric 2. Piola-Kirchhoff stress are defined in eqn. 2.5.66, whereby the index was exchanged by α and its derivative can be determined by the product rule, such that we obtain

$$\frac{\partial \tilde{\tau}_\alpha}{\partial \tilde{\lambda}_\beta} = \frac{\partial^2 W_{iso}}{\partial \tilde{\lambda}_\alpha \partial \tilde{\lambda}_\beta} \tilde{\lambda}_\alpha + \frac{\partial W_{iso}}{\partial \tilde{\lambda}_\alpha} \delta_{\alpha\beta} - \frac{1}{3} \left[\frac{\partial W_{iso}}{\partial \lambda_\gamma} + \frac{\partial^2 W_{iso}}{\partial \tilde{\lambda}_\eta \partial \tilde{\lambda}_\beta} \tilde{\lambda}_\eta \right] \quad (2.5.78)$$

Inserting this derivative and the results from eqn. 2.5.47 and 2.5.64 into eqn. 2.5.77 yields the coefficient matrix $\varphi_{\alpha\beta}$ and taking it into account we can rewrite eqn. 2.5.76 as

$$\mathbb{C}_{iso}^e = \sum_{\gamma=1}^3 \sum_{\alpha=1}^3 \varphi_{\alpha\gamma} \mathbf{M}^\gamma \otimes \mathbf{M}^\alpha + 2\tilde{\tau} \frac{\partial \mathbf{M}^\alpha}{\partial \mathbf{C}^b}. \quad (2.5.79)$$

The last step is to determine the derivative of the eigenbase \mathbf{M}^α with respect to the right Cauchy Green tensor \mathbf{C}^b , that is summarized in the appendix.

Spatial Description In the spatial setting the elasticity tensor \mathbb{C} can be obtained in a similar procedure as the material tensor for the reference configuration, by differentiating the strain energy function with respect to the spatial metric tensor or the corresponding strain measure. On the other hand the spatial elasticity tensor can also be determined by pushing forward (eqn. 2.5.73) the essential results of the material description. Using this approach maintains the additive structure of the stress tensor and the material tensor consisting of volumetric and isochoric parts. Therefore we firstly consider the volumetric part of the material elasticity tensor in eqn. 2.5.75 and apply the push forward operation, such that we obtain

$$\mathbb{C}_{vol}^e = \left[\frac{\partial W}{\partial J} + J \frac{\partial^2 W}{\partial J^2} \right] \mathbf{g}^\sharp \otimes \mathbf{g}^\sharp - 2 \frac{\partial W}{\partial J} \mathbb{I}_{\mathbf{g}^\sharp}, \quad (2.5.80)$$

whereby $\mathbb{I}_{\mathbf{g}^\sharp} = \mathbf{g}_i \otimes \mathbf{g}_k \otimes \mathbf{g}_j \otimes \mathbf{g}_l \in \mathbb{S}^{3 \times 3}$ denotes the push forward of $\mathbb{I}_{C^{-1}}^{sym}$. We want to note here, that the coefficients remain unaltered here, only the base tensors are transformed. Accordingly, the deviatoric part of the material elasticity tensor in eqn. 2.5.79 can also be transformed, such that we get

$$\mathbb{C}_{iso}^e = \sum_{\alpha=1}^3 \sum_{\gamma=1}^3 \frac{1}{J} \varphi_{\alpha\gamma} \mathbf{m}^\gamma \otimes \mathbf{m}^\alpha + \sum_{\alpha=1}^3 \frac{2}{J} \tilde{\tau}_\alpha \varphi^* \left(\frac{\partial \mathbf{M}^\alpha}{\partial \mathbf{C}^b} \right), \quad \text{with} \quad \mathbf{m}^\alpha = \mathbf{F}^\sharp \cdot \mathbf{M}^\alpha \cdot [\mathbf{F}^\sharp]^t \quad (2.5.81)$$

The derivative of the material eigenbase with respect to the right Cauchy Green tensor was derived in eqn. A.2.16 and one can show, that its pushing forward is equivalent to the derivative of the spatial base tensor with respect to the spatial metric tensor. A more detailed discussion is given in the appendix. Finally we want note, that the derived expressions will also be used for the derivation of the inelastic material tensors.

Example of an elastic material To give an example the derived relations are applied to the model defined by eqn. 2.5.61. The volumetric and isochoric eigenvalues of the Kirchhoff stress are given then by

$$\tilde{\tau}_{vol,\alpha} = \frac{\partial W_{vol}}{\partial \lambda_\alpha} \lambda_\alpha = \kappa \ln J, \quad \text{and} \quad \tilde{\tau}_{iso,\alpha} = \frac{\partial W_{iso}}{\partial \tilde{\lambda}_\alpha} \tilde{\lambda}_\alpha = \mu \ln \tilde{\lambda}_\alpha^2. \quad (2.5.82)$$

The coefficient matrix $\varphi_{\alpha\beta}$ for the isochoric part of the tangent operator, which was defined in eqn. 2.5.77 reduces to

$$\varphi_{\alpha\beta} = 2\mu \left[\delta_{\alpha\beta} - \frac{1}{3} \right] \quad (2.5.83)$$

such that by taking the volumetric part into account the complete spatial elasticity tensor is given by

$$\mathbb{C}^e = \sum_{\alpha=1}^3 \sum_{\beta=1}^3 \frac{1}{J} \varphi_{\alpha\beta}^e \mathbf{m}^\beta \otimes \mathbf{m}^\alpha + \sum_{\alpha=1}^3 \frac{2}{J} \tilde{\tau}_\alpha \frac{\partial \mathbf{m}^\alpha}{\partial \mathbf{g}^p}, \quad \text{with} \quad \varphi_{\alpha\beta}^e = \kappa + 2\mu \left[\delta_{\alpha\beta} - \frac{1}{3} \right] \quad (2.5.84)$$

This elasticity tensor is modified in the framework of hyper-elastoplasticity, whereby usually the main structure remains unchanged. Only the coefficients are adopted to the elasto-plastic problem. Therefore these described results are very essential for the consideration of inelastic deformations. Finally we want to note here for completeness, that the calculation of the tangent operator analytically can be a bad exercise or nearly impossible, such that in a lot of applications it is preferable to determine the tangent operator numerically, whereby the system is perturbed by a small number $\epsilon \ll 1$ and the derivative is approximated by the difference quotient. Moreover, the numerical tangent operator can sometimes be a very helpful tool for the determination of the analytical one. The main problem in the numerical approach is to find the best perturbation parameter ϵ . A detailed discussion can be found in [DS96] and [Wri01].

2.6 Concepts of Inelasticity

2.6.1 Remarks to Linear Elasto-Plasticity

Plastic strains and the yield function The theory of elasto-plasticity is based on macroscopic observations that can be understood in the simplest way by investigating the uniaxial tension test. In fig. 2.1 a typical stress-strain curve is depicted and there we find essentially three different domains:

1. The elastic domain that is indicated by the linear branch of the curve determined by the *Young modulus*.
2. The domain where the material changes from purely elastic to elasto-plastic behaviour that is indicated by the *yield stress* Y_0 and that is followed by a further increase of strength which is denoted by *hardening*. This hardening effect goes back to microscopic processes like moving dislocations and imperfections.
3. The domain of *softening* where the strength of the material decreases from the maximum to the point of disruption.

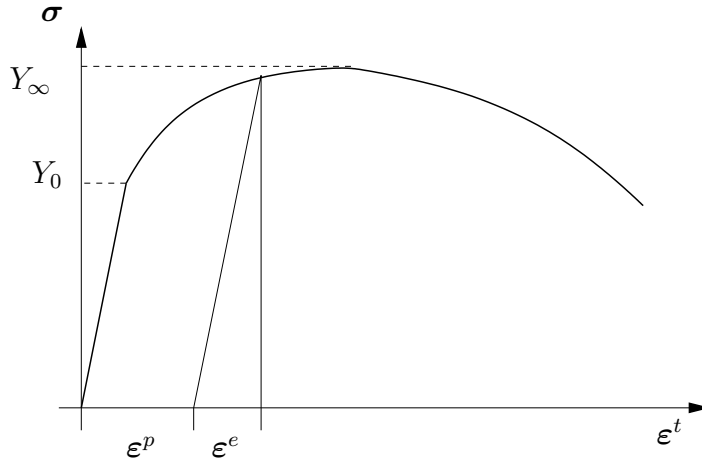


Figure 2.1. Stress-strain-Curve of an uniaxial tension-test

Before we continue with the kinematical description of nonlinear elasto-plastic deformations we want to give an idea of the basic concepts within the framework of the linear theory. While in elasticity the total strains coincide with the elastic strains, in plasticity we have to differ between the elastic and the plastic strains. The elastic strains vanishes as soon as the external loading vanishes, whereas the plastic strains remain permanently after unloading. Therefore in the linear theory the total strain is given by the sum

$$\epsilon^t = \epsilon^e + \epsilon^p. \quad (2.6.1)$$

To describe this inelastic effect and other phenomena like hardening and softening it is necessary to introduce additional variables, such that the strain energy does not solely depend on the strains (or the deformation gradient in the nonlinear theory) and the temperature θ anymore, but also on the so-called *internal variables* ξ_i , which can also be merged into a vector ξ . Subsequently we will firstly neglect the temperature and restrict our considerations to isothermal processes, but the reader should keep in mind, that there are no temperature independent plastic deformations. The concepts of plasticity will be extended to temperature dependent processes in the last section of this chapter. Now we want to focus our attention on how these internal variables can be used to describe plasticity. For the sake of clarity subsequently we want to restrict our considerations only to one internal variable ξ , that is sufficient to describe hardening effects and therefore it is often denoted by *hardening variable*. The regard of hardening effects is reflected in the free energy function

$$W = W_{vol}(\epsilon_{vol}^e) + W_{iso}(\epsilon_{dev}^e) + W_{mic}(\xi), \quad (2.6.2)$$

that is extended by the hardening potential W_{mic} , that records micromechanical processes like moving dislocations, that are considered as responsible for hardening effects. This potential solely depends on the internal variable ξ .

As mentioned before, plastic strains solely occur if a certain threshold stress, the yield stress Y_0 , is reached during the loading. Because of this we introduce a function comparing the current stress state σ with the yield stress Y_0 and indicating if the proceeding deformation is inelastic or not. This function is called yield function Φ and as derived before, it depends on the current stress state σ and the initial yield stress Y_0 . In general the yield stress is not constant but it increases due to hardening effects, such that it is reasonable to introduce a resulting yield stress Y_n that consists of the initial yield stress and a function $H(\xi)$ that describes the hardening effects

$$Y_n(\xi) = Y_0 + H(\xi). \quad (2.6.3)$$

Taking this into account, the corresponding yield function depends on the current stress state σ and the resulting yield stress Y_n , but since the initial yield stress is constant the yield condition usually is written as

$$\Phi = \Phi(\sigma, H). \quad (2.6.4)$$

The initial yield stress Y_0 depends on the considered material and in the case of an uniaxial tension this parameter is simple to measure. In the three dimensional case this threshold must be extended to a so-called *yield surface* that incloses all possible stress states. The interior of this yield surface describes the elastic range whereas stress states on the surface cause plastic deformations. Stress states beyond the surface are not admissible so far. This means if the yield surface can be described by the yield function Φ we obtain the following constraints

$$\Phi(\sigma, H) \begin{cases} < 0 \rightsquigarrow \text{elastic} \\ = 0 \rightsquigarrow \text{plastic} \\ > 0 \rightsquigarrow \text{not admissible} \end{cases} \quad (2.6.5)$$

Since plastic strains induce an alteration of the shape of the body these deformations are assumed to be caused by the isochoric or *deviatoric* stresses, whereby this assumption is only valid for metallic materials. Therefore the yield function $\Phi(\sigma_{dev}, H)$ is usually formulated in terms of the deviatoric stresses and the volumetric contributions are neglected. In the case of metallic materials this is a good approximation. However, the yield function Φ detects the transition from the elastic to the inelastic range.

The principle of maximum dissipation Another important constraint in the framework of plasticity ensuring the thermodynamical consistency is the *principle of maximum dissipation*, that states that the current stress state always maximizes the dissipation. Applying this principle we consider the isothermal Clausius-Planck inequality for geometrically linear deformations

$$D_{loc} = \sigma : \dot{\epsilon}^t - \dot{W}(\epsilon^e, \xi) \geq 0, \quad (2.6.6)$$

where the dissipation has to be maximized. The conditions in eqn. 2.6.5 and 2.6.6 can be considered as a problem of finding the extremal value with side condition that coincides with the yield condition. This kind of problem is solved by the Lagrange-formalism, whereby both constraints are written as a Lagrange functional

$$\mathcal{L}(\sigma, H) = -D_{loc} + \dot{\gamma}\Phi(\sigma_{dev}, H) \longrightarrow \text{stat.} \quad (2.6.7)$$

that is demanded to get stationary and where $\dot{\gamma}$ denotes the Lagrange multiplier. In this relation we inserted the negative dissipation to guarantee a positive multiplier, such that we obtain a minimization problem with a side condition. This condition of becoming stationary is fulfilled if the first variation of the Lagrange functional gets zero for any σ_{dev} and Y_0

$$\delta\mathcal{L}(\sigma, Y_0) = \frac{\partial\mathcal{L}}{\partial\sigma_{dev}} : \delta\sigma_{dev} + \frac{\partial\mathcal{L}}{\partial H}\delta H = 0. \quad (2.6.8)$$

Since the product of free energy $\Psi(\epsilon^e, \xi)$ times the density ρ yields the strain energy W we can rewrite the Clausius-Planck inequality as

$$D_{loc} = \frac{\partial W}{\partial \epsilon^e} : \dot{\epsilon}^p + \underbrace{\left[\sigma - \frac{\partial W}{\partial \epsilon^e} \right]}_{=0} : \dot{\epsilon}^e - \frac{\partial W}{\partial \xi} \dot{\xi} \geq 0, \quad (2.6.9)$$

whereby the stress σ is work conjugated to the elastic strains and it can be determined from the free energy function W , such that the second terms in eqn. 2.6.9 vanishes. Since the free energy function also depends on the internal variable ξ we can define it work conjugated to the current hardening stress

$$H(\xi) = -\frac{\partial W}{\partial \xi}. \quad (2.6.10)$$

Inserting eqn. 2.6.9 in consideration of 2.6.10 into eqn. 2.6.7, this relation is solely fulfilled for any σ and H if the partial derivatives of the Lagrange functional in eqn. 2.6.8 is zero. From this postulate the so-called *evolution equations* follow

$$\dot{\epsilon}^p = \dot{\gamma} \frac{\partial \Phi}{\partial \sigma} \quad \text{and} \quad \dot{\xi} = \dot{\gamma} \frac{\partial \Phi}{\partial H}, \quad (2.6.11)$$

which describe the development of the plastic strain rate ϵ^p and the rate of the hardening variable ξ in time. With eqn. 2.6.11 and 2.6.5 the so-called *Kuhn-Tucker conditions* can be formulated, describing the loading/ unloading behaviour

$$\left. \begin{array}{ll} \dot{\gamma} = 0, & \text{if } \Phi < 0 \\ \dot{\gamma} \geq 0, & \text{if } \Phi = 0 \end{array} \right\} \dot{\gamma} \Phi = 0$$

$$\dot{\gamma} \dot{\Phi} = 0. \quad (2.6.12)$$

These relations express that there is no plastic flow $\dot{\gamma} = 0$ as long as the material behaves elastic $\Phi < 0$, whereas we get plastic deformations $\dot{\gamma} > 0$ when the yield condition becomes zero $\Phi = 0$. Therefore the product of the Lagrange multiplier and the yield function becomes always zero. According to this, assuming a state of plastic loading $\Phi = 0$ the consistency condition (eqn. 2.6.12₃) applies because

- if the yield function changes to elastic unloading ($\dot{\Phi} < 0$), there is no plastic flow $\dot{\gamma} = 0$.
- if there is no change in the yield function ($\dot{\Phi} = 0$), it means that we still have plastic loading and there is plastic flow $\dot{\gamma} > 0$.

The J_2 -plasticity For the determination of the evolution equations it is crucial what kind of yield function is given. There are a lot of propositions and one of the most important is the *von-Mises* yield function, that is reviewed here. As mentioned before, the yield condition compares the current (deviatoric) stress state with the yield stress. Therefore one of the simplest conceivable form of a yield function is given by

$$\Phi = |\sigma_{dev}| - Y_0 \leq 0. \quad (2.6.13)$$

Here the yield surface in the three-dimensional stress space coincides with a cylinder that is oriented in direction along the space diagonal. Von-Mises modified this yield function and proposed that in the case of a three-dimensional stress state the material starts yielding as soon as the second invariant of the deviatoric stress $J_2 = -\frac{1}{2} \sigma_{dev} : \sigma_{dev}$ reaches the second invariant of the one-dimensional deviatoric stress that can be identified with the yield stress Y_0 determined by the one-dimensional tension test. Therefore we obtain the identity

$$-\frac{1}{2} \sigma_{dev} : \sigma_{dev} = -\frac{1}{3} Y_0^2. \quad (2.6.14)$$

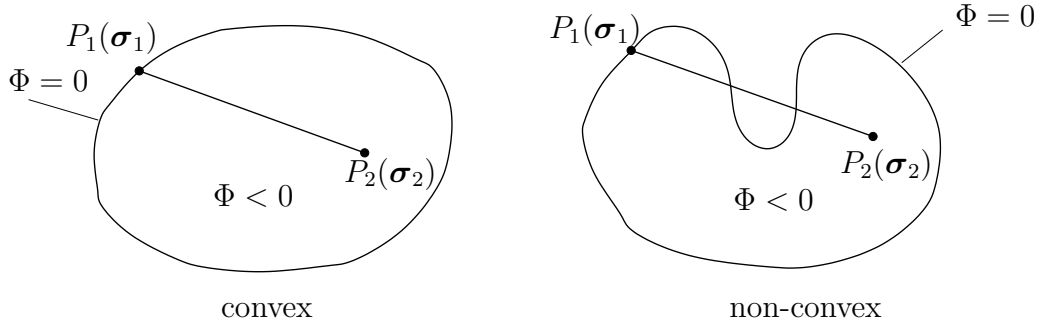


Figure 2.2. Convex and non-convex domain of a yield function

Multiplying eqn. 2.6.14 by -1 and after some simple algebra we finally obtain the von-Mises yield condition

$$\Phi(\boldsymbol{\sigma}_{dev}, Y_0) = |\boldsymbol{\sigma}_{dev}| - \sqrt{\frac{2}{3}} Y_0 \leq 0 \quad (2.6.15)$$

Since this yield condition is derived from the second invariant of the deviatoric stress field that is usually denoted by J_2 , this yield condition is often called *J_2 -Plasticity*. As mentioned before, in general the yield stress is not constant but it changes in time, since it depends on the internal variable ξ . Therefore usually the resulting yield stress $Y_n(\xi)$ (eqn. 2.6.3) has to be taken into account here. If we evaluate the evolution equations in eqn. 2.6.11 and calculate the derivative of this yield function with respect to the deviatoric stress tensor or the yield stress, respectively, we obtain

$$\dot{\epsilon}^p = \dot{\gamma} \tilde{\nu} \quad \text{and} \quad \dot{\xi} = \sqrt{\frac{2}{3}} \dot{\gamma}. \quad (2.6.16)$$

Here $\tilde{\nu}$ denotes the corresponding normal tensor, which is a deviatoric quantity as well and its direction coincides with the deviatoric stress. This means that the direction of the plastic flow always coincides with the direction of deviatoric stress. Therefore the evolution equation of the plastic strain is also denoted by *normality rule* or *flow rule*. Since the plastic strain rate is proportional to the gradient of the yield function with respect to the stress field, the yield condition can be considered as a plastic potential. If the plastic strain rate can be derived from a plastic potential, it is called *associated*.⁴

Constraint of Convexity From the circumstance, that the plastic flow is normal to the yield condition, emanates a very important property, the yield function has to fulfill and that is also very crucial for numerical aspects. Namely, the yield function has to be convex as it is illustrated in fig. 2.2. In simple terms, convexity means that every line connecting two possible stress states on the surface must lie completely within the enclosed surface. Since the yield surface resulting from the von-Mises yield condition is a circle the convexity condition is ensured.

This yield function needs to be convex since in numerical computations firstly the current stress state

⁴Of course, since the rate of hardening variable is also proportional to the gradient of the plastic potential Φ with respect to the yield stress, it is also associated. Admittedly this term of *associated evolution equations* is reserved with respect to plastic potentials. As we will see in the sequel the same proceeding can be also applied to damage mechanics, where a damage potential is introduced and the evolution equation is derived from that, but they are not denoted by being associated.

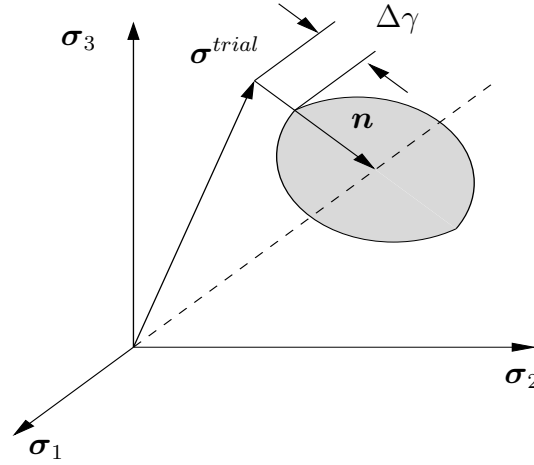


Figure 2.3. Radial return mapping

is approximated by the so-called trial stress σ_{dev}^{trial} . This trial stress can lie in the non-admissible domain $\Phi > 0$ and by projecting it on the yield surface along the normal direction we obtain the current stress σ_{dev} . In the case of a non-convex yield surface the projection is not unique. The mathematical requirement of convexity demanded from the yield surface is equivalent to the principle of maximum dissipation, that says, that the current stress state σ always maximizes the dissipation compared to any other possible stress state σ^* . Therefore the plastic work done by the actual stress state has to be greater than the plastic work done by any other possible stress state for a given plastic flow $\dot{\epsilon}^p$. We finally obtain the relation

$$[\sigma - \sigma^*] : \dot{\epsilon}_p = \dot{\gamma} [\sigma - \sigma^*] : \frac{\partial \Phi}{\partial \sigma} \geq 0 \quad (2.6.17)$$

and by taking into account the Kuhn-Tucker optimality condition, $\dot{\gamma}\Phi = 0$ and assuming a homogeneity of degree one for Φ we can rewrite the principle of maximum dissipation as

$$\dot{\gamma} [\sigma - \sigma^*] : \frac{\partial \Phi}{\partial \sigma} \geq \dot{\gamma} [\Phi(\sigma) - \Phi(\sigma^*)]. \quad (2.6.18)$$

The argumentation is as follows:

1. If there is no plastic flow, i.e. $\dot{\gamma} = 0$, there is pure elastic loading and the inequality holds trivially.
2. If plastic flow takes place, i.e. $\dot{\gamma} > 0$ and $\Phi(\sigma) = 0$ results

$$[\sigma^* - \sigma] : \frac{\partial \Phi}{\partial \sigma} \leq \Phi(\sigma^*) - \Phi(\sigma) = \Phi(\sigma^*), \quad (2.6.19)$$

whereby we multiplied the inequality by -1 and we can identify this expression with the convexity condition as it is derived in appendix 1 (eqn. A.3.22).

A more descriptive reasoning to derive the normality rule from the principle of maximum dissipation is that eqn. 2.6.17₁ only holds if σ is collinear to $\dot{\epsilon}^p$, as it was derived in eqn. 2.6.16.

Radial return The common method to calculate the plastic flow in linear theory is the radial return method. This method takes the convexity of the yield surface into account, that allows an unique determination of the plastic flow. If this constraint is not fulfilled, the calculation of plastic strains is not possible. We consider fig. 2.3 that shows the stress space, whereby the stress states along the diagonal denote volumetric stress states, whereas the stresses that lie on a plane orthogonal to the space diagonal denote the deviatoric stress contributions. Therefore the decomposition of a given stress state is unique. The yield function limits the deviatoric „stress plane” to the yield surface. If a given stress state (trial stress) lies outside the yield surface it coincides with a violation of the yield condition $\Phi \leq 0$, this stress state is projected on the yield surface, namely in orthogonal direction $\tilde{\nu}$ to the yield surface, such that the yield condition is fulfilled again. The distance $\Delta\sigma$ of the trial stress state to the yield surface is assumed to be proportional to the plastic flow. The plastic flow itself is defined by eqn. 2.6.16₁ and depends on $\dot{\gamma}$ proportionally, that is determined iteratively within numerical calculations.

In the subsequent sections the presented concepts will be transformed from the linear to the nonlinear theory. There are the Kuhn-Tucker loading/unloading conditions, the associated flow rule, the convexity of the yield function and the radial return method, which are taken one by one from the linear theory. The kinematics of nonlinear elastoplasticity do not seem to be appropriate for the application of the described concepts of linear elastoplasticity. But as we will see the nonlinear kinematics can be modified, such that the methods of the linear theory can be adapted to the nonlinear case.

2.6.2 Kinematics of nonlinear Elasto-Plasticity

In the linear theory the basic assumption was the additive decomposition of the total strains into an elastic and a plastic contribution. This idea is transformed to the nonlinear theory by introducing an additional configuration, that is called the *intermediate configuration*. This plastic configuration \mathcal{B}_p is inserted among the reference and the current configuration. In the case of unloading the body from the current configuration the permanent strains remain, which are cumulated in the intermediate configuration. The additive decomposition of the total strains is not possible anymore because of the nonlinear contributions in the strain measures. But by the introduction of the plastic configuration a *multiplicative decomposition* of the deformation gradient can be installed

$$\mathbf{F}^{\natural} = \mathbf{F}_e^{\natural} \cdot \mathbf{F}_p^{\natural}, \quad (2.6.20)$$

whereby here the order of the terms is essential. In the linear theory the plastic deformations are assumed to be isochoric and therefore the plastic strain is a deviatoric quantity. This assumption is adopted to the non-linear theory, that is represented by

$$\det \mathbf{F}^{\natural} = \det [\mathbf{F}_e^{\natural}] \cdot \det [\mathbf{F}_p^{\natural}] = \det [\mathbf{F}_e^{\natural}], \quad \text{with} \quad \det [\mathbf{F}_p^{\natural}] = 1. \quad (2.6.21)$$

Here and in the sequel we assume the plastic deformations as isochoric. This multiplicative decomposition works analogously to the volumetric-isochoric decomposition of the deformation, that was introduced for elastic problems (s. section 1.2.4). Furthermore it requires additional base systems, but since this configuration is not compatible, they can not be defined by the tangent and cotangent spaces. Therefore we want to define the co- and contravariant metric tensors on \mathcal{B}_p , as follows

$$\begin{aligned} \bar{\mathbf{g}}^{\flat} &= [\bar{g}]_{ij} \bar{\mathbf{g}}^i \otimes \bar{\mathbf{g}}^j \in \mathbb{S}^+ : T\mathcal{B}_p \times T\mathcal{B}_p \rightarrow \mathbb{R}, & [\bar{g}]_{ij} &= \bar{\mathbf{g}}_i \cdot \bar{\mathbf{g}}_j \\ \bar{\mathbf{g}}^{\sharp} &= [\bar{g}]^{ij} \bar{\mathbf{g}}_i \otimes \bar{\mathbf{g}}_j \in \mathbb{S}^+ : T^*\mathcal{B}_p \times T^*\mathcal{B}_p \rightarrow \mathbb{R}, & [\bar{g}]^{ij} &= \bar{\mathbf{g}}^i \cdot \bar{\mathbf{g}}^j. \end{aligned} \quad (2.6.22)$$

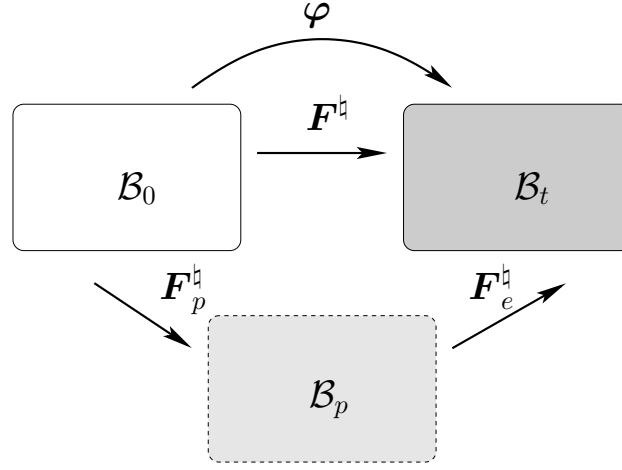


Figure 2.4. Multiplicative Decomposition of elasto-plastic Deformations

\mathcal{B}_p constitutes the current configuration with respect to the reference configuration and with respect to the current configuration it forms the material configuration. For calculating the pure elastic deformation we solve eqn. 2.6.20 for the elastic deformation gradient \mathbf{F}_e^h and insert this into the definition of the left Cauchy Green tensor in eqn. 2.2.11₄

$$\mathbf{b}_e^\sharp = \mathbf{F}_e^h \cdot \bar{\mathbf{g}}^\sharp \cdot [\mathbf{F}_e^h]^t = [\mathbf{F}^h \cdot \mathbf{f}_p^\sharp] \cdot \bar{\mathbf{g}}^\sharp \cdot [\mathbf{F}^h \cdot \mathbf{f}_p^\sharp]^t = \mathbf{F}^h \cdot \mathbf{B}_p^\sharp \cdot [\mathbf{F}^h]^t. \quad (2.6.23)$$

This corresponds to the pull back of the metric in the intermediate configuration to the reference configuration, that is followed by the push forward to the current configuration. Therefore the elastic left Cauchy Green tensor can be understood as the push forward of the inverse plastic right Cauchy Green tensor $\bar{\mathbf{B}}_p^b$. On the other hand it is possible to define a strain measure on the intermediate configuration, that is denoted by elastic right Cauchy Green tensor $\bar{\mathbf{C}}_e^b$. It can be obtained by pulling back the current covariant metric tensor to the intermediate configuration, such that we obtain

$$\bar{\mathbf{C}}_e^b = [\mathbf{F}_e^h]^t \cdot \mathbf{g}^b \cdot \mathbf{F}_e^h, \quad (2.6.24)$$

that corresponds to a Riemann metric on \mathcal{B}_p . For the rates of the introduced strain measures in the intermediate configurations we consider the time derivative of the deformation gradient as it was reformulated in eqn. 2.6.20

$$\dot{\mathbf{F}}^h = \dot{\mathbf{F}}_e^h \cdot \mathbf{F}_p^h + \mathbf{F}_e^h \cdot \dot{\mathbf{F}}_p^h. \quad (2.6.25)$$

Multiplying this expression by \mathbf{f}^h and comparing it with eqn. 2.2.40 we find the definition of the spatial velocity gradient \mathbf{l}^h as

$$\mathbf{l}^h = \dot{\mathbf{F}}^h \cdot \mathbf{f}^h = \mathbf{l}_e^h + \mathbf{l}_p^h, \quad \text{with} \quad \mathbf{l}_e^h = \dot{\mathbf{F}}_e^h \cdot \mathbf{f}_e^h \quad \text{and} \quad \mathbf{l}_p^h = \mathbf{F}_e^h \cdot \bar{\mathbf{L}}_p^h \cdot \mathbf{f}_e^h \quad (2.6.26)$$

Here we see an additive decomposition of the strain evolution into a purely elastic part and a plastic contribution, $\bar{\mathbf{L}}_p^h = \dot{\mathbf{F}}_p^h \cdot \mathbf{f}_p^h$ define the plastic mixed-variant velocity gradient on the intermediate configuration and applying the push forward operations to them yields the corresponding plastic and elastic velocity gradients on the spatial configuration. Performing a pull back of the spatial velocity gradient to the intermediate configuration

$$\bar{\mathbf{L}}^h = [\mathbf{f}_e^h] \cdot \mathbf{l}^h \cdot \mathbf{F}_e^h = \mathbf{f}_e^h \cdot \dot{\mathbf{F}}_e^h + \dot{\mathbf{F}}_p^h \cdot \mathbf{f}_p^h = \bar{\mathbf{L}}_e^h + \bar{\mathbf{L}}_p^h \quad (2.6.27)$$

we can preserve the additive structure of the strain evolution as it was known from the linear theory. Moreover, both contributions are completely decoupled from each other, since $\bar{\mathbf{L}}_e^{\natural}$ only depends on \mathbf{F}_e^{\natural} , whereas the plastic strain rate $\bar{\mathbf{L}}_p^{\natural}$ only depends on the plastic deformation gradient \mathbf{F}_p^{\natural} . With this at hand we are also able to derive the strain rate formulations of the elastic right Cauchy Green tensor

$$\dot{\bar{\mathbf{C}}}_e^b = [\dot{\mathbf{F}}_e^{\natural}]^t \cdot \mathbf{g}^b \cdot \mathbf{F}_e^{\natural} + [\mathbf{F}_e^{\natural}]^t \cdot \mathbf{g}^b \cdot \dot{\mathbf{F}}_e^{\natural} + [\mathbf{F}_e^{\natural}]^t \cdot \dot{\mathbf{g}}^b \cdot \mathbf{F}_e^{\natural} = [\bar{\mathbf{L}}_e^{\natural}]^t \cdot \bar{\mathbf{C}}_e^b + \bar{\mathbf{C}}_e^b \cdot \bar{\mathbf{L}}_e^{\natural}, \quad (2.6.28)$$

whereby the time derivative of the spatial covariant metric tensor becomes zero. These derived relations in terms of the intermediate configurations enables one to install the plasticity theory in the nonlinear context, whereby the anisotropic case is still included.

Of course we can also consider the elastic left Cauchy Green tensor \mathbf{b}_e^{\sharp} and with the given definitions its rate formulation can be written as

$$\dot{\mathbf{b}}_e^{\sharp} = \dot{\mathbf{F}}_e^{\natural} \cdot \bar{\mathbf{g}}^{\sharp} \cdot [\mathbf{F}_e^{\natural}]^t + \mathbf{F}_e^{\natural} \cdot \bar{\mathbf{g}}^{\sharp} \cdot [\dot{\mathbf{F}}_e^{\natural}]^t = \mathbf{l}_e^{\natural} \cdot \mathbf{b}_e^{\sharp} + \mathbf{b}_e^{\sharp} \cdot [\mathbf{l}_e^{\natural}]^t \quad (2.6.29)$$

On the other side if we start from the definition in eqn. 2.6.23₃ we obtain a formulation where the Lie-derivative of \mathbf{b}_e^{\sharp} occurs, that coincides with the plastic part of the rate

$$\dot{\mathbf{b}}_e^{\sharp} = \mathbf{l}^{\natural} \cdot \mathbf{b}_e^{\sharp} + \mathbf{b}_e^{\sharp} \cdot [\mathbf{l}^{\natural}]^t + \mathcal{L}_t(\mathbf{b}_e^{\sharp}) \quad (2.6.30)$$

with

$$\mathcal{L}_t(\mathbf{b}_e^{\sharp}) = \mathbf{F}_e^{\natural} \cdot \partial_t [\mathbf{f}_p^{\natural} \cdot \bar{\mathbf{g}}^{\sharp} \cdot [\mathbf{f}_p^{\natural}]^t] \cdot [\mathbf{F}_e^{\natural}]^t = -\mathbf{l}_p^{\natural} \cdot \mathbf{b}_e^{\sharp} - \mathbf{b}_e^{\sharp} \cdot [\mathbf{l}_p^{\natural}]^t, \quad (2.6.31)$$

whereby eqn. 2.6.26 and $\dot{\mathbf{f}}_p^{\natural} = -\mathbf{f}_p^{\natural} \cdot \bar{\mathbf{L}}_p^{\natural}$ was taken into account. This is an alternative nonlinear formulation, where the anisotropic contributions are also included.

2.6.3 Principle of Maximum Plastic Dissipation

In this section we want to transform the principle of maximum dissipation to a formulation in terms of finite deformations and in consideration of the yield function Φ as a side condition. For the purpose to obtain a general formulation we assume the elastic potential W depending on the covariant strain measure $\bar{\mathbf{C}}_e^b$. Considering the time derivative of the elastic potential the corresponding work-conjugated contravariant stress measure $\bar{\mathbf{S}}^{\sharp}$ can be identified with the derivative of the elastic potential with respect to the $\bar{\mathbf{C}}_e^b$

$$\dot{W}(\bar{\mathbf{C}}_e^b) = 2 \frac{\partial W}{\partial \bar{\mathbf{C}}_e^b} : \dot{\bar{\mathbf{C}}}_e^b = \bar{\mathbf{S}}^{\sharp} : \dot{\bar{\mathbf{C}}}_e^b = 2 \bar{\mathbf{C}}_e^b \cdot \frac{\partial W}{\partial \bar{\mathbf{C}}_e^b} : \bar{\mathbf{L}}_e^{\natural} \quad \text{with} \quad \bar{\mathbf{S}}^{\sharp} = 2 \frac{\partial W}{\partial \bar{\mathbf{C}}_e^b}. \quad (2.6.32)$$

In the last expression the product of the elastic right Cauchy Green strain tensor $\bar{\mathbf{C}}_e^b$ and the contravariant stress tensor $\bar{\mathbf{S}}^{\sharp}$ defines a mixed-variant stress tensor $\bar{\mathbf{M}}^{\natural} = \bar{\mathbf{C}}_e^b \cdot \bar{\mathbf{S}}^{\sharp}$ that is denoted by Mandel stress tensor and that is work-conjugated to the mixed-variant velocity gradient $\bar{\mathbf{L}}_e^{\natural}$ on \mathcal{B}_p . In literature the principle of maximum plastic dissipation on \mathcal{B}_p is usually formulated in terms of $\bar{\mathbf{L}}_e^{\natural}$, whereby the elastic velocity gradient can be replaced by the difference of the total velocity gradient tensor and the plastic contribution $\bar{\mathbf{L}}_p^{\natural}$, that was defined in eqn. 2.6.26. In analogy to the

linear theory we assume that the elastic potential also depends on the internal variable ξ , such that we obtain

$$D_{loc} = \left[\bar{\mathbf{M}}^{\sharp} - 2\bar{\mathbf{C}}_e^b \cdot \frac{\partial W}{\partial \bar{\mathbf{C}}_e^b} \right] : \bar{\mathbf{L}}^{\sharp} + 2\bar{\mathbf{C}}_e^b \cdot \frac{\partial W}{\partial \bar{\mathbf{C}}_e^b} : \bar{\mathbf{L}}_p^{\sharp} + H\dot{\xi} \geq 0, \quad \text{with} \quad H = \frac{\partial W}{\partial \xi} \quad (2.6.33)$$

Here Y_0 also denotes the yield stress as it was introduced in the linear theory. Since the product of $\bar{\mathbf{C}}_e^b$ and $2\partial W/\partial \bar{\mathbf{C}}_e^b$ commutes, the corresponding product coinciding with the mixed-variant Mandel stress $\bar{\mathbf{M}}^{\sharp}$, is a symmetric quantity. Like in the linear theory the plastic velocity gradient $\bar{\mathbf{L}}_p^{\sharp}$ can be decomposed into a symmetric and skew-symmetric part, such that

$$\bar{\mathbf{L}}_p^{\sharp} = \mathbf{D}_p^{\sharp} + \mathbf{W}_p^{\sharp}, \quad \text{with} \quad \mathbf{D}_p^{\sharp} = [\bar{\mathbf{L}}_p^{\sharp}]^{sym} \quad \text{and} \quad \mathbf{W}_p^{\sharp} = [\bar{\mathbf{L}}_p^{\sharp}]^{skw}. \quad (2.6.34)$$

However we want to follow the proposal of Miehe & Stein [MS92], who considered the formulation of the dissipation inequality in terms of $\bar{\mathbf{S}}^{\sharp}$, such that we obtain

$$D_{loc} = \left[\bar{\mathbf{S}}^{\sharp} - 2\frac{\partial W}{\partial \bar{\mathbf{C}}_e^b} \right] : [\bar{\mathbf{C}}_e^b \cdot \bar{\mathbf{L}}^{\sharp}] + 2 \cdot \frac{\partial W}{\partial \bar{\mathbf{C}}_e^b} : [\bar{\mathbf{C}}_e^b \cdot \bar{\mathbf{L}}_p^{\sharp}] + H\dot{\xi} \geq 0, \quad \text{with} \quad H = -\frac{\partial W}{\partial \xi} \quad (2.6.35)$$

The advantage of this formulation becomes clearer as soon as we decompose the kinematical quantity $[\bar{\mathbf{C}}_e^b \cdot \bar{\mathbf{L}}_p^{\sharp}]$ a symmetric and a skewsymmetric part

$$[\bar{\mathbf{C}}_e^b \cdot \bar{\mathbf{L}}_p^{\sharp}] = \bar{\mathbf{D}}_p^{\sharp} + \bar{\mathbf{W}}_p^{\sharp} \quad \text{with} \quad \bar{\mathbf{D}}_p^{\sharp} = [\bar{\mathbf{C}}_e^b \cdot \bar{\mathbf{L}}_p^{\sharp}]^{sym} \quad \text{and} \quad \bar{\mathbf{W}}_p^{\sharp} = [\bar{\mathbf{C}}_e^b \cdot \bar{\mathbf{L}}_p^{\sharp}]^{skw} = \mathbf{0} \quad (2.6.36)$$

$\bar{\mathbf{C}}_e^b$ is a symmetric quantity, such that only the symmetric contribution of velocity gradient $\bar{\mathbf{D}}_p^{\sharp}$ has to be considered and any contributions due to the skew-symmetric part $\bar{\mathbf{W}}_p^{\sharp}$ becomes zero whereas from the decomposition of the velocity gradient $\bar{\mathbf{L}}_p^{\sharp}$ emanate two contributions where the skewsymmetric part does not disappear. The consequence of this fact is that also in eqn. 2.6.35 only the symmetric contributions have to be taken into account, such that we automatically obtain an isotropic non-linear elasto-plastic constitutive law. If we transform the derived equations from the intermediate configuration \mathcal{B}_t to the spatial one, this also yields an isotropic formulation on \mathcal{B}_p . Taking eqn. 2.6.24 and performing the particular push forward operations

$$\mathbf{d}_p^{\sharp} = \mathbf{f}_e^{\sharp} \cdot \bar{\mathbf{D}}_p^{\sharp} \cdot \mathbf{F}_e^{\sharp} \quad \text{and} \quad \bar{\mathbf{S}}^{\sharp} = \mathbf{f}_e^{\sharp} \cdot \boldsymbol{\tau}^{\sharp} \cdot [\mathbf{f}_e^{\sharp}]_e^t, \quad (2.6.37)$$

the principle of maximum dissipation yields the resulting plastic dissipation inequality

$$D_{loc} = \boldsymbol{\tau}^{\sharp} : [\mathbf{g}^b \cdot \mathbf{d}_p^{\sharp}] + H\dot{\xi} \geq 0 \quad \text{with} \quad H = \frac{\partial W}{\partial \xi}, \quad (2.6.38)$$

whereby \mathbf{d}_p^{\sharp} defines the spatial plastic deformation rate tensor on \mathcal{B}_p .

On the other hand the elastic potential W can also be assumed depending on \mathbf{b}_e^{\sharp} , such that the derivative of W with respect to \mathbf{b}_e^{\sharp} has to yield the equivalent formulation on the current configuration. If isotropy is assumed the derivative $\partial W/\partial \mathbf{b}_e^{\sharp}$ and the elastic left Cauchy Green tensor \mathbf{b}_e^{\sharp}

commute such that the time derivative of W can be written as

$$\begin{aligned}
 \dot{W}(\mathbf{b}_e^\sharp) &= \frac{\partial W}{\partial \mathbf{b}_e^\sharp} : \dot{\mathbf{b}}_e^\sharp = \left[\frac{\partial W}{\partial \mathbf{b}_e^\sharp} \cdot \mathbf{b}_e^\sharp \right] : \mathbf{l}^\sharp + \left[[\mathbf{b}_e^\sharp]^t \cdot \frac{\partial W}{\partial \mathbf{b}_e^\sharp} \right] : [\mathbf{l}^\sharp]^t + \frac{\partial W}{\partial \mathbf{b}_e^\sharp} : \mathcal{L}_t(\mathbf{b}_e^\sharp) \\
 &= \left[2\mathbf{g}^\sharp \cdot \frac{\partial W}{\partial \mathbf{b}_e^\sharp} \cdot \mathbf{b}_e^\sharp \right] : \mathbf{g}^\flat \cdot \mathbf{d}^\sharp + \left[2\mathbf{g}^\sharp \cdot \frac{\partial W}{\partial \mathbf{b}_e^\sharp} \cdot \mathbf{b}_e^\sharp \right] : \left[\frac{1}{2}\mathbf{g}^\flat \cdot \mathcal{L}_t(\mathbf{b}_e^\sharp) \cdot [\mathbf{b}_e^\sharp]^{-1} \right] \\
 &= \boldsymbol{\tau}^\sharp : \mathbf{g}^\flat \cdot \mathbf{d}^\sharp - \boldsymbol{\tau}^\sharp : \left[\frac{1}{2}\mathbf{g}^\flat \cdot \mathcal{L}_t(\mathbf{b}_e^\sharp) \cdot [\mathbf{b}_e^\sharp]^{-1} \right].
 \end{aligned} \tag{2.6.39}$$

For being able to factor out the covariant strain rate tensor we multiplied the expression by the unit tensor $\mathbf{I} = \mathbf{g}^\sharp = \mathbf{g}^\flat \cdot \mathbf{g}^\flat$ and after some algebra we find the definition of the Kirchhoff stress tensor from eqn. 2.5.43. Comparing eqn. 2.6.36 and eqn. 2.6.37 it is easy to find the identity ⁵

$$\mathbf{d}_p^\sharp = -\frac{1}{2}\mathcal{L}_t(\mathbf{b}_e^\sharp) \cdot [\mathbf{b}_e^\sharp]^{-1} \tag{2.6.40}$$

whereby we have to emphasize here, that in the first case the isotropy of the spatial formulation emanates from the transformation of the isotropic formulation in the intermediate configuration in terms of $\bar{\mathbf{C}}_e^\flat$, whereas in the second case the isotropy was postulated before. The given definitions can be inserted into the dissipation inequality in terms of the Kirchhoff stress

$$D_{loc} = \boldsymbol{\tau}^\sharp : \mathbf{d}_p^\flat + H\dot{\xi} \geq 0 \quad \text{with} \quad H = -\frac{\partial W}{\partial \xi} \quad \text{and} \quad \mathbf{d}_p^\flat = \mathbf{g}^\flat \cdot \mathbf{d}_p^\sharp. \tag{2.6.41}$$

In the next step we want to derive the evolution equations for the plastic strains and the hardening variable by formulating the dissipation inequality as a Lagrange functional with the yield function as side condition.

2.6.4 Evolution Equations

For the derivation of the evolution equations we proceed analogously to eqn. 2.6.7, where we considered the local dissipation inequality as a minimization problem. By taking into account the yield function as side condition we rewrite the two constraints as a Lagrange functional. In terms of the intermediate configuration, the Lagrange functional can be written as

$$\mathcal{L}(\bar{\mathbf{M}}^\sharp, Y_0) = \bar{\mathbf{M}}^\sharp : \bar{\mathbf{L}}_p^\sharp - Y_0\dot{\xi} + \dot{\gamma}\Phi(\bar{\mathbf{M}}^\sharp, Y_0) \rightarrow \text{stat.} \tag{2.6.42}$$

and it becomes stationary if the partial derivatives of the functional with respect to the Mandel stress and the yield stress becomes zero. In analogy to the linear theory we obtain the evolution equations for the plastic deformations and the internal variable by solving the derivatives for the rates of the plastic strain measure and the internal variable

$$\bar{\mathbf{L}}_p^\sharp = \dot{\gamma} \frac{\partial \Phi}{\partial \bar{\mathbf{M}}^\sharp} \quad \dot{\xi} = \dot{\gamma} \frac{\partial \Phi}{\partial H}. \tag{2.6.43}$$

⁵This relation can also be shown as follows:

$$\mathcal{L}_t(\mathbf{b}_e^\sharp) = -\mathbf{l}_p^\sharp \cdot \mathbf{b}_e^\sharp - \mathbf{b}_e^\sharp \cdot [\mathbf{l}_p^\sharp]^t = -\mathbf{b}_e^\sharp \cdot [\mathbf{l}_p^\sharp + [\mathbf{l}_p^\sharp]^t] = -2\mathbf{b}_e^\sharp \cdot \mathbf{d}_p^\sharp$$

Here $\bar{\mathbf{L}}_p^{\sharp}$ includes also skewsymmetric contributions, such that this formulation is not restricted to isotropy. But if we rewrite the Lagrange functional and the yield function $\Phi(\bar{\mathbf{S}}^{\sharp}, \bar{\mathbf{C}}_e^b, Y_0)$ on \mathcal{B}_p in terms of $\bar{\mathbf{C}}_e^b$ and the contravariant stress measure $\bar{\mathbf{S}}^{\sharp}$ we find the resulting flow rule by

$$\bar{\mathbf{D}}_p^{\sharp} = [\bar{\mathbf{C}}_e^b \cdot \bar{\mathbf{L}}_p^{\sharp}] = \dot{\gamma} \frac{\partial \Phi}{\partial \bar{\mathbf{S}}^{\sharp}}. \quad (2.6.44)$$

Finally we like to formulate the flow function in terms of the current configuration. Therefore we can derive the flow function by inserting the transformed isotropic local dissipation into the Lagrange functional and in analogy to the linear theory we assume the yield function depending on the Kirchhoff stress, such that we obtain the Lagrange functional

$$\mathcal{L}(\boldsymbol{\tau}^{\sharp}, H) = \boldsymbol{\tau}^{\sharp} : \left[-\frac{1}{2} \mathbf{g}^b \cdot \mathcal{L}_t(\mathbf{b}_e^{\sharp}) \cdot [\mathbf{b}_e^{\sharp}]^{-1} \right] + H\dot{\xi} + \dot{\gamma} \Phi(\boldsymbol{\tau}^{\sharp}, H) \rightarrow \text{stat.}, \quad (2.6.45)$$

that has to become stationary. This is fulfilled if the partial derivatives with respect to the actual stress and the yield stress becomes zero and solving again the resulting equations for the plastic flow and the internal variable, respectively, we obtain the evolution equations

$$-\frac{1}{2} \mathbf{g}^b \cdot \mathcal{L}_t(\mathbf{b}_e^{\sharp}) \cdot [\mathbf{b}_e^{\sharp}]^{-1} = \dot{\gamma} \frac{\partial \Phi}{\partial \boldsymbol{\tau}^{\sharp}}, \quad \dot{\xi} = \dot{\gamma} \frac{\partial \Phi}{\partial H}. \quad (2.6.46)$$

That means, that we can specify the Lie derivative of the left Cauchy-Green tensor in terms of the derivative of the yield function with respect to $\boldsymbol{\tau}^{\sharp}$ and the Lagrange multiplier. Therefore the total rate of the left Cauchy-Green tensor in eqn. 2.6.30 can be rewritten as

$$\dot{\mathbf{b}}_e = [\mathbf{l}^{\sharp} \cdot \mathbf{b}_e^{\sharp} + \mathbf{b}_e^{\sharp} \cdot [\mathbf{l}^{\sharp}]^t] - 2\dot{\gamma} \boldsymbol{\nu} \cdot \mathbf{b}_e^{\sharp}, \quad \text{with} \quad \boldsymbol{\nu} = \mathbf{g}^{\sharp} \cdot \frac{\partial \Phi}{\partial \boldsymbol{\tau}^{\sharp}}. \quad (2.6.47)$$

In this equation we can interpret the expression in brackets as an elastic predictor describing the rate of the elastic left Cauchy-Green tensor if a pure elastic deformation occurs. Whereas in the case of inelastic deformations additionally plastic flow occurs and the first term leads to a virtual state, that can be identified with the trial state, that lies in the non-admissible range beyond the yield surface. Therefore the last term in eqn. 2.6.47 can be understood as a corrector that projects this trial stress state back on the yield surface, namely in direction of the gradient of the yield surface, that coincides with the normal direction on the yield surface. This term becomes zero if no plastic flow emerges. This time derivatives of the elastic left Cauchy-Green tensor can also be derived in terms of incremental kinematics, that is described in the next subsection and that allows a more comprehensible view of the evolution equation of the plastic strains. Of course we can reformulate the plastic flow also in terms of $\bar{\mathbf{B}}_p^b$. For this we simply perform a pull back operation of the Lie-derivative of \mathbf{b}_e^{\sharp} to the material configuration and obtain

$$\partial_t \bar{\mathbf{B}}_p^b = -2\dot{\gamma} \boldsymbol{\nu} \cdot \bar{\mathbf{B}}_p^b, \quad \text{for} \quad \boldsymbol{\nu} = \mathbf{f}^{\sharp} \cdot \mathbf{g}^{\sharp} \cdot \frac{\partial \Phi}{\partial \boldsymbol{\tau}^{\sharp}} \cdot \mathbf{F}^{\sharp}. \quad (2.6.48)$$

Here we want to note that the normal direction $\partial_{\boldsymbol{\tau}^{\sharp}} \Phi$ in the spatial configuration is transformed to the material configuration and it seems straightforward that the normal direction in the material configuration is given by $\partial_{\mathbf{S}^{\sharp}} \Phi$. In the next step these determined evolution equations need to be integrated. But before we continue we want to note here that eqn. 2.6.46 and 2.6.47 once more show that the material behaviour depends crucially on the kind of yield function, since it prescribes

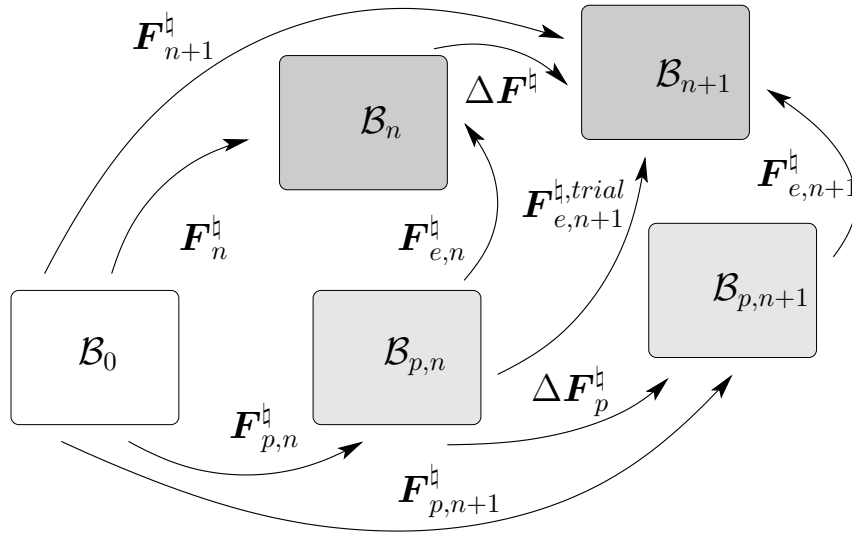


Figure 2.5. Incremental Kinematics of inelastic Deformations

the direction of plastic flow. The yield function still must fulfill the properties as they were discussed in the framework of linear theory. There are the Kuhn-Tucker conditions detecting the frontier between the elastic and inelastic range. Furthermore there is the convexity condition, that ensures the unique direction of the plastic flow, that usually coincides with the direction of the current stress field (normality rule). There are a lot of conceivable yield functions and it always depends on what the model has to describe. The J_2 -plasticity that was introduced before is a prototype of elasto-plastic models and some models that we want to present here, are based on von-Mises plasticity. Before we discuss some of these more involved material models we want to describe the numerical treatment of the derived relations. For this we will refer subsequently to the von-Mises yield condition as it was presented in eqn. 2.6.15.

2.6.5 Incremental Kinematics

Since plastic deformations are dissipative and therefore path-dependent it is necessary to subdivide the loading into increments denoted by $\Delta \mathbf{F}^\sharp$, such that the stress-strain curve can be retraced more precisely. From this emanates an incremental kinematic, illustrated in fig. 2.5, that starts with the assumption that the strain tensors $\mathbf{b}_{e,n}^\sharp, \bar{\mathbf{B}}_{p,n}^\sharp, \xi_n$ for the last load and time step n are known and that they describe an equilibrium state. Furthermore the multiplicative decomposition described in the upper paragraph can also be adopted to incremental kinematics, such that the new deformation gradient \mathbf{F}_{n+1}^\sharp can be represented by

$$\mathbf{F}_{n+1}^\sharp = \Delta \mathbf{F}^\sharp \cdot \mathbf{F}_n^\sharp. \quad (2.6.49)$$

Since we start from the intermediate configuration we firstly need to consider the pull back from the intermediate configuration to the material one, such that the corresponding deformation gradient is given by

$$\mathbf{F}_{n+1}^{\sharp, trial} = \Delta \mathbf{F}^\sharp \cdot \mathbf{F}_{e,n}^\sharp = \Delta \mathbf{F}^\sharp \cdot \mathbf{F}_n^\sharp \cdot [\mathbf{F}_p^\sharp]_n^{-1} = \mathbf{F}_{n+1}^\sharp \cdot [\mathbf{F}_p^\sharp]_n^{-1}. \quad (2.6.50)$$

This deformation gradient describes the deformation starting from the plastic configuration of the old load step $\mathcal{B}_{p,n}$ to the current configuration of the new load step $\mathcal{B}_{t_{n+1}}$, that includes also plastic

deformations. Since we do not know the plastic flow due to the new load increment this deformation gradient describes a trial state. If we consider the elastic left Cauchy-Green tensor by taking into account the new increment we obtain

$$\mathbf{b}_e^{\sharp, trial} = \mathbf{F}_{n+1}^{\natural, trial} \cdot \mathbf{g}_p^{\sharp} \cdot [\mathbf{F}_{n+1}^{\natural, trial}]^t = \Delta \mathbf{F}^{\natural} \cdot \mathbf{b}_{e, n}^{\sharp} \cdot [\Delta \mathbf{F}^{\natural}]^t = \mathbf{F}_{n+1}^{\natural} \cdot \mathbf{B}_{p, n}^{\sharp} \cdot [\mathbf{F}_{n+1}^{\natural}]^t \quad (2.6.51)$$

Furthermore, if we consider the time derivative of the elastic left Cauchy-Green tensor, on the one hand we obtain the expression that was already derived in eqn. 2.6.47. On the other hand we can derive the time derivative from eqn. 2.6.51₄ that renders

$$\dot{\mathbf{b}}_e^{\sharp, trial} = \Delta \dot{\mathbf{F}}^{\natural} \cdot \mathbf{b}_{e, n}^{\sharp} \cdot [\Delta \mathbf{F}^{\natural}]^t + \Delta \mathbf{F}^{\natural} \cdot \mathbf{b}_{e, n}^{\sharp} \cdot [\Delta \dot{\mathbf{F}}^{\natural}]^t = \mathbf{l}^{\natural} \cdot \mathbf{b}_{e, n+1}^{\sharp} + \mathbf{b}_{e, n+1}^{\sharp} \cdot [\mathbf{l}^{\natural}]^t. \quad (2.6.52)$$

Here the deformation is assumed as purely elastic, whereas in eqn. 2.6.47 also the alteration of the plastic metric in time is taken into account. Therefore we can also identify the Lie derivative of the plastic metric as the contribution that describes the plastic flow. This plastic strain rate goes into the deformation increment that consists of an elastic and a plastic contribution, which is reflected in the multiplicative decomposition of the incremental deformation gradient

$$\mathbf{F}_{e, n+1}^{\natural, trial} = \mathbf{F}_{e, n+1}^{\natural} \cdot \Delta \mathbf{F}_p^{\natural}. \quad (2.6.53)$$

This split of the deformation increment can be found in Bonet & Wood [BWed] or in Parisch [Par03]. Following eqn. 2.2.15 the incremental trial deformation gradient can be represented in terms of the eigenvalues and the eigenvectors as well as the total deformation gradient $\mathbf{F}_{n+1}^{\natural}$. The spectral decomposition of the elastic trial deformation gradient in consideration of the multiplicative split in eqn. 2.6.53 leads to

$$\mathbf{F}_{e, n+1}^{\natural, trial} = \sum_3 [\lambda_{e, \alpha}^{trial, n+1}] \mathbf{n}_{e, n+1}^{\alpha} \otimes \mathbf{n}_{p, n}^{\alpha} = \sum_3 [\lambda_{e, \alpha}^{n+1}] [\Delta \lambda_{p, \alpha}^{n+1}] \mathbf{n}_{e, n+1}^{\alpha} \otimes \mathbf{n}_{p, n}^{\alpha}. \quad (2.6.54)$$

According to this the elastic trial tensor can also be rewritten in terms of the principal directions and the principal stretches, such that we obtain the representation of the trial tensor

$$\mathbf{b}_{e, n+1}^{\sharp, trial} = \sum_3 [\lambda_{e, \alpha}^{n+1}]^2 \cdot [\Delta \lambda_{p, \alpha}^{n+1}]^2 \mathbf{n}_{e, n+1}^{\alpha} \otimes \mathbf{n}_{e, n+1}^{\alpha} = \sum_3 [\lambda_{e, \alpha}^{trial, n+1}]^2 \mathbf{n}_{e, n+1}^{\alpha} \otimes \mathbf{n}_{e, n+1}^{\alpha}. \quad (2.6.55)$$

We want to emphasize here, that the elastic trial tensor only depends on the principal direction of the actual configuration $\mathbf{n}_{e, n+1}^{\alpha}$. For the determination of the plastic strains we start from eqn. 2.6.48 that coincides with a ordinary differential equation can be solved by an exponential update algorithm of the Euler-backward type. We finally obtain the actual plastic strains in terms of the material configuration by

$$[\bar{\mathbf{B}}_p^b]_{n+1} = \exp[-2\Delta\gamma\boldsymbol{\nu}] \cdot [\bar{\mathbf{B}}_p^b]_n. \quad (2.6.56)$$

Performing a push forward operation to the spatial configuration leads to the integration scheme of the left Cauchy-Green tensor

$$\begin{aligned} [\mathbf{b}_e^{\sharp}]_{n+1} &= \exp[-2\Delta\gamma\boldsymbol{\nu}] \cdot \mathbf{b}_{e, n}^{\sharp, trial} \\ &= \exp[-2\Delta\gamma\nu_{\alpha}\mathbf{n}^{\alpha} \otimes \mathbf{n}^{\alpha}] [\lambda_{e, \alpha}^{trial, n+1}]^2 \mathbf{n}_{e, n+1}^{\alpha} \otimes \mathbf{n}_{e, n+1}^{\alpha}. \end{aligned} \quad (2.6.57)$$

Since the spectral decomposition of the elastic left Cauchy Green tensor \mathbf{b}_e^{\sharp} is unique and the spectral representation of $\boldsymbol{\nu}$ and $\mathbf{b}_e^{\sharp, trial}$ are unique as well, their principal directions have to coincide

$\mathbf{n}^\alpha = \mathbf{n}_{e,n+1}^\alpha$. Moreover the exponential expression can be represented by a power series. Since all the series terms possess the same eigenbase, it can be extracted, such that the following relation results

$$\mathbf{F}_{n+1}^\sharp \cdot \exp[\bullet] \cdot \mathbf{f}_{n+1}^\sharp = \exp[\mathbf{F}_{n+1}^\sharp \cdot [\bullet] \cdot \mathbf{f}_{n+1}^\sharp]. \quad (2.6.58)$$

Therefore the resulting representation of the actual left Cauchy Green tensor in terms of the principal directions can be rewritten as

$$\mathbf{b}_{e,n+1}^\sharp = \sum_{\alpha=1}^3 \exp[-2\Delta\gamma\nu_\alpha] [\lambda_{\alpha}^{trial,n+1}]^2 \mathbf{n}^\alpha \otimes \mathbf{n}^\alpha. \quad (2.6.59)$$

Here it is easy to identify the eigenvalue of the incremental plastic strains with $[\Delta\lambda_{p,\alpha}^{n+1}]^2 = \exp[2\Delta\gamma\nu_\alpha]$. If we apply the logarithmic strain measure we can transform the multiplicative structure of the coefficients into an additive form

$$2 \ln[\lambda_{e,\alpha}^{n+1}] = -2\Delta\gamma\nu_\alpha + 2 \ln[\lambda_{e,\alpha}^{trial,n+1}], \quad (2.6.60)$$

whereby the eigenbase remains untouched by this operation. From this equation it is straight forward to determine the principal deviatoric Kirchhoff stresses

$$\tau_\alpha = 2\mu [\ln[\Delta\lambda_{\alpha,e}^{trial}] - \Delta\gamma\nu_\alpha]. \quad (2.6.61)$$

In this relation we can see, that the trial stress is a kind of predictor, whereas the second term acts as a corrector that is conditioned by the increment of the Lagrangian multiplier $\Delta\gamma$. The main result of this subsection is that we transformed the multiplicative structure to an additive one by the introduction of logarithmic strains. Therefore we can apply the methods of the linear theory also to nonlinear formulations. Moreover, we performed a transition from the continuous setting to the discrete one, which is very crucial for the numerical treatment. Therefore the aim of the next subsection is the introduction of numerical methods to determine the Lagrange multiplier.

2.6.6 Integration of Evolution Equations

For the treatment of inelastic deformations the crucial task is to determine the accumulated permanent deformations, expressed by $\mathbf{B}_p^\sharp = [\mathbf{C}_p^\flat]^{-1}$ for instance, that occur if a particular load is applied. These plastic contributions can be calculated by integration of the evolution equations. These evolution equations that are derived from the principle of maximum dissipation, generally constitute a system of ordinary differential equations (ode's) with inequality constraints. There are some conceivable integration schemes that can be applied to the solution of the system of ode's.

Implicit Euler integration scheme The standard integration scheme that is usually applied to the integration of the evolution equations is the implicit Euler backward method. For a scalar-, vector- or tensor-valued function $\mathbf{d}(t)$, which is known at the time step t_n the evolution can be described by a differential equation

$$\dot{\mathbf{d}}(t) = \partial_t \mathbf{d} = \mathbf{f}(\mathbf{d}(t)). \quad (2.6.62)$$

We like to know the function value \mathbf{d}_{n+1} at the current time t_{n+1} . For this we rewrite the system of ordinary differential equations as a residual in terms of the discrete time increment $\Delta t = t_{n+1} - t_n$ and the function values of \mathbf{d} at these times, such that we finally obtain

$$\mathbf{d}_{n+1} = \mathbf{d}_n + \Delta t \mathbf{f}(\mathbf{d}_{n+1}) \quad \rightsquigarrow \quad \mathbf{r} = \mathbf{d}_n - \mathbf{d}_{n+1} + \Delta t \mathbf{f}(\mathbf{d}_{n+1}) = \mathbf{0} \quad (2.6.63)$$

This generally nonlinear problem can be solved by a Newton-Raphson iteration algorithm. Within this method we approximate the residual by a Taylor series, such that we obtain the following structure

$$\mathbf{r}_{n+1} \approx \mathbf{r}_n + \mathbf{J} \cdot \Delta \mathbf{d}, \quad \text{with} \quad \mathbf{J} = \frac{\mathbf{r}_{n+1}}{\mathbf{d}_{n+1}}, \quad (2.6.64)$$

whereby \mathbf{J} denotes the Jacoby-Matrix and by solving this equation for \mathbf{d}_{n+1} we obtain an equation to determine the new function value at the new iteration step $n + 1$

$$\mathbf{d}_{n+1} = \mathbf{d}_n - [\mathbf{J}]^{-1} \cdot \Delta \mathbf{d}. \quad (2.6.65)$$

The new values are inserted in eqn. 2.6.64 and if the new quantities fulfill the residual sufficiently we can stop the iteration process, otherwise we repeat this procedure as long as the constraint is fulfilled. The accuracy of the Euler backward scheme is of first order and if the starting point is sufficiently close to the solution the Newton Raphson algorithm converges quadratically. The only problem is the determination of the entries of the Jacoby matrix.

Integration of evolution equations In the case of the integration of the evolution equations given in eqn. 2.6.46 the time increment can be eliminated easily and we only need to determine the increment of the Lagrange multiplier. Therefore we chose the yield function as the first residual to determine the Lagrange multiplier and we reformulate the evolution equation as the second residual, such that we obtain

$$\begin{aligned} r_1 &= |\tilde{\boldsymbol{\tau}}^{\sharp, trial}| - 2\Delta\gamma\mu - \sqrt{\frac{2}{3}}Y_0(\xi) \\ r_2 &= \xi_n - \xi_{n-1} + \sqrt{\frac{2}{3}}\Delta\gamma \end{aligned} \implies \mathbf{J} = \begin{bmatrix} \partial_{\Delta\gamma} r_1 & \partial_{\xi} r_1 \\ \partial_{\Delta\gamma} r_2 & \partial_{\xi} r_2 \end{bmatrix}. \quad (2.6.66)$$

With this procedure we have collected all tools so far, that are needed to describe and solve inelastic deformations. Subsequently, we present the algorithm for the determination of the plastic flow and the rate of the hardening variable, which are needed to update the actual elastic and accumulated plastic strains and the current stress, respectively. For this we assume, as mentioned before, that the deformation gradient $\mathbf{F}_{n+1}^{\sharp}$ of the new load step is known as well as the plastic strains of the last time or load step that are given by the plastic inverse right Cauchy-Green tensor $\mathbf{B}_{p,n}^{\sharp}$. Additionally, the stress of the old time step $\boldsymbol{\tau}_n^{\sharp}$ is known. With this at hand we can start the algorithm that is determined by the subsequent steps:

1. Computing the current elastic left Cauchy-Green trial tensor.
2. Spectral decomposition of $\mathbf{b}_{e,n+1}^{\sharp, trial} = \sum_{\alpha} \lambda_{\alpha,e}^{trial} \mathbf{n}^{\alpha} \otimes \mathbf{n}^{\alpha}$, whereby the principal trial stretches consists of an elastic and plastic contribution, as it was derived in eqn. 2.6.54.
3. Transforming the multiplicative structure of the principal trial stretches into an additive one, by applying the logarithmic strain measure.
4. Calculation of trial stress $\boldsymbol{\tau}_{n+1}^{\sharp, trial}$ from the modified St. Venant- Kirchhoff strain-energy function (eqn. 2.5.61). Isolating the deviatoric part of the trial stress.
5. Evaluating the yield-function Φ ⁶ and checking the yield condition, such that the following two possibilities arise:

⁶As mentioned before, we firstly restrict ourselves to the von-Mises yield-function, that was already introduced in eqn. 2.6.15.

- (a) $\Phi \leq 0$, i.e. the trial stress coincides with the new actual stress state: $\tau_{n+1}^{\#,trial} = \tau_{n+1}^{\#}$ and from eqn. 2.6.46 emanates that the plastic flow is zero: $\dot{\gamma} = 0$.
- (b) $\Phi > 0$, i.e. the trial state lies beyond the admissible range, such that we need to iterate the plastic flow and the rate of the hardening variable defined by the evolution equations in eqn. 2.6.46. For this we reformulate the evolution equations as residuals and determine the Lagrange multiplier $\dot{\gamma}$ by applying the implicit Euler backward scheme. If $\dot{\gamma}$ is known, the hardening variable can be updated.
6. Calculation of the new actual stress state $\tau_{n+1}^{\#}$.
7. Update of $\ln \lambda_{e,\alpha}^{n+1}$ and retransformation to non-logarithmic strain measure $b_{e,n+1}^{\#}$.
8. Updating and storing the new accumulated plastic strains $B_{p,n+1}^{\#}$.
9. Evaluating the elasto-plastic tangent operator.

This algorithm describes the complete procedure solving problems of nonlinear elasto-plastic deformations by the J_2 -plasticity. The used equations are collected once more in the Box 1.5.1. The last task that is left to do now, is the derivation of the material tensor, whereby we can employ some results from elasticity.

2.6.7 Elasto-plastic Material Tensor

In section 1.2.4 we introduced a free energy function with completely decoupled volumetric and isochoric contributions, that gave rise to a stress formulation, which could be decomposed analogously. Also the elasticity tensor could be splitted into a volumetric and an isochoric part as well. In analogy to the linear theory in the case of hyper-elastoplasticity with hardening effects we have to complement an additional contribution in the free energy function considering the hardening behaviour (s. eqn. 2.6.2). This part depends on the hardening variable ξ , such that we obtain a free energy function

$$W(\lambda_\alpha, \xi) = W_{vol}(J) + W_{iso}(\tilde{\lambda}_\alpha) + W_{mic}(\xi), \quad (2.6.67)$$

whereby the hardening potential is indicated by 'mic', since the hardening phenomena is assumed to be based on microscopic effects. We will specify the hardening potential later on. Here we just want to keep in mind, that it has to be considered for the description of hardening effects. The aim of this section is the calculation of the material tensor. We start from the free energy function in eqn. 2.5.61, that is formulated in terms of the principal stretches or the isochoric eigenvalues, respectively. For the elastic case the corresponding stress was already determined in eqn. 2.5.82 and the spatial elasticity tensor is given by eqn. 2.5.82. In the inelastic case the volumetric part of the elasticity tensor remains unchanged and in the isochoric material tensor only the coefficient matrix changes, whereby also the inelastic contributions have to be considered, which results in the modified formulation of the deviatoric principal Kirchhoff stresses

$$\tilde{\tau}_\alpha = \mu \ln \tilde{\lambda}_\alpha^2 - 2\mu \Delta\gamma \nu_\alpha. \quad (2.6.68)$$

Computing the derivatives of the deviatoric principal Kirchhoff stresses with respect to the principal stretches yields the coefficient matrix

$$\frac{\partial \tilde{\tau}_\alpha}{\partial \lambda_\beta} \lambda_\beta = \varphi_{\alpha\beta} = \frac{\partial \mu \ln \tilde{\lambda}_\alpha^2}{\partial \lambda_\beta} + 2\mu \left[\frac{\partial \Delta\gamma}{\partial \lambda_\beta} \nu_\alpha + \Delta\gamma \frac{\partial \nu_\alpha}{\partial \lambda_\beta} \right]. \quad (2.6.69)$$

Here the last two terms needed to be determined, whereby the ν_α denotes the components of the normal direction tensor, that is defined by $\nu_\alpha = \tilde{\tau}_\alpha^{trial} / \|\tilde{\tau}^\#, trial\|$ and from this definition emanates the derivative

$$\frac{\partial \nu_\alpha}{\partial \lambda_\beta} = \frac{2\mu}{\|\tilde{\tau}^\#, trial\|} [\delta_{\alpha\beta} - \nu_\alpha \nu_\beta] \quad (2.6.70)$$

that coincides with the results in the linear theory. Furthermore, the derivative of the Lagrange multiplier $\Delta\gamma$ with respect to the principal stretches needs to be determined, that can also be obtained from the consistency condition and that yields

$$\frac{\partial \Delta\gamma}{\partial \lambda_\beta} = \frac{2\mu \nu_\beta}{[2\mu + \sqrt{\frac{2}{3}} \frac{\partial Y_0}{\partial \xi} \frac{\partial \xi}{\partial \Delta\gamma}]}, \quad (2.6.71)$$

that also has the analogous structure as in the linear theory. With these modifications we can adopt the spatial elasticity tensor in eqn. 2.5.84 to the hyper-elastoplastic formulation and obtain the consistent elasto-plastic algorithmic tangent operator

$$\mathbb{C}^{ep} = \sum_{\alpha=1}^3 \sum_{\beta=1}^3 \varphi_{\alpha\beta} \mathbf{m}^\alpha \otimes \mathbf{m}^\beta + \sum_{\alpha=1}^3 2\tilde{\tau}_\alpha \frac{\partial \mathbf{m}^\alpha}{\partial \mathbf{g}^b}, \quad \text{with} \quad (2.6.72)$$

$$\varphi_{\alpha\beta} = \varphi_{\alpha\beta}^e - \frac{4\mu^2 \Delta\gamma}{\|\tilde{\tau}^\#\|} [\delta_{\alpha\beta} - \nu_\alpha \nu_\beta] - 2\mu \left[1 + \frac{1}{3} \frac{Y'_0}{\mu} \right]^{-1} \nu_\alpha \nu_\beta$$

if a Newton-Raphson iteration scheme is supposed. This algorithmic tangent operator completes the numerical formulation of a prototype model, that can be used as a starting point for an amount of material models including inelastic effects. In the subsequent sections some additional models are introduced that are based on the J_2 -plasticity model and which take into account additional attributes of material behaviour like viscosity and damage.

1. Computing

$$\mathbf{b}_{e,n+1}^{\sharp,trial} : \quad \mathbf{b}_{e,n+1}^{\sharp,trial} = \mathbf{F}_{n+1}^{\natural} \cdot \mathbf{B}_{p,n}^{\sharp} \cdot [\mathbf{F}^{\natural}]_{n+1}^t$$

2. Spectral decomposition in terms of logarithmic strains:

$$\mathbf{b}_e^{\sharp,trial} = \sum_{\alpha=1}^3 \ln [\lambda_{e,\alpha}^{trial}] \mathbf{m}^{\alpha}$$

3. Calculate the deviatoric trial stress:

$$\tilde{\boldsymbol{\tau}}^{\sharp,trial} = \sum_{\alpha=1}^3 \tilde{\tau}_{\alpha} \mathbf{n}^{\alpha} \otimes \mathbf{n}^{\alpha} \quad \tilde{\tau}_{\alpha} = 2\mu \ln \tilde{\lambda}_{e,\alpha}^{trial}$$

4. Evaluate the yield function

$$\Phi(\tilde{\boldsymbol{\tau}}^{\sharp}, \sigma_y) = \|\tilde{\boldsymbol{\tau}}^{\sharp,trial}\| - \sqrt{\frac{2}{3}} Y_n(\xi)$$

5. Iteration of Lagrange multiplier and internal variables from residuals, if $\Phi(\tilde{\boldsymbol{\tau}}^{\sharp,trial}) > 0$

$$r_1 = |\boldsymbol{\tau}^{\sharp,trial}| - 2\mu \Delta\gamma - \sqrt{\frac{2}{3}} \sigma_y(\xi) \quad r_2 = \xi_n - \xi_{n+1} + \sqrt{\frac{2}{3}} \Delta\gamma$$

6. Update of the principal Kirchhoff stresses

$$\tilde{\tau}_{\alpha} = 2\mu [\ln \tilde{\lambda}_{e,\alpha}^{trial}] - \Delta\gamma \nu_{\alpha}$$

7. Update of the principal stretches and retransformation

$$\mathbf{b}_{e,n+1}^{\sharp} = \sum_{\alpha=1}^3 \exp[-2\Delta\gamma \nu_{\alpha}] [\lambda_{e,\alpha}^{trial}]^2 \mathbf{m}^{\alpha}$$

8. Update of the accumulated plastic strains

$$\mathbf{B}_{p,n+1}^{\sharp} = \mathbf{f}_{n+1}^{\natural} \cdot \mathbf{b}_{e,n+1}^{\sharp} \cdot [\mathbf{f}^{\natural}]_{n+1}^t$$

9. Consistent elasto-plastic tangent operator

$$\mathbb{C}^{ep} = \sum_{\alpha=1}^3 \sum_{\beta=1}^3 \varphi_{\alpha\beta} \mathbf{m}^{\alpha} \otimes \mathbf{m}^{\beta} + \sum_{\beta=1}^3 2\tilde{\tau}_{\alpha} \frac{\partial \mathbf{m}^{\alpha}}{\partial \mathbf{g}^{\beta}}, \quad \text{with}$$

$$\varphi_{\alpha\beta} = \varphi_{\alpha\beta}^e - \frac{4\mu^2}{\|\tilde{\boldsymbol{\tau}}^{\sharp}\|} \Delta\gamma [\delta_{\alpha\beta} - \nu_{\alpha} \nu_{\beta}] - 2\mu \left[1 + \frac{1}{3} \frac{Y'_n}{\mu} \right]^{-1} \nu_{\alpha} \nu_{\beta}$$

Box 1.5.1: Integration algorithm for the kinematical state variables

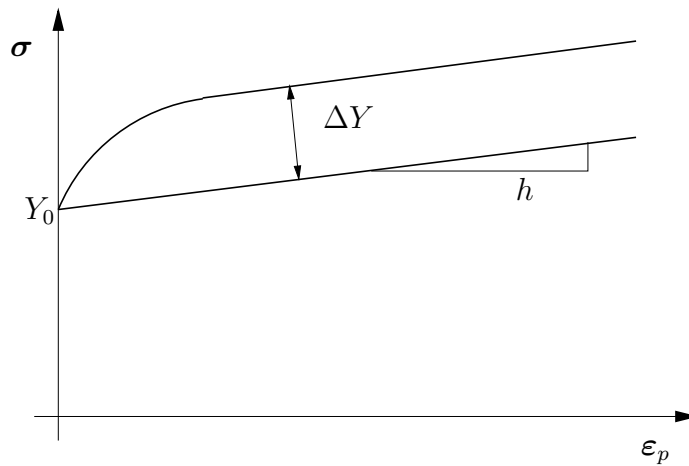


Figure 2.6. Superposition of linear and nonlinear hardening

2.6.8 Isotropic Hardening

In the sections before we derived the equations for the description of inelastic deformations, whereby we introduced the yield function, which compares the actual stress state with a so-called yield stress and in case the difference becomes greater than zero, plastic flow takes place and the material behaviour changes from elastic to an inelastic one. We introduced the resulting yield stress Y_0 and defined it by the derivative of the free energy function with respect to the hardening variable ξ (eqn. 2.6.10), for which we formulated an evolution equation. In general ξ alters during the deformation process and is not constant, but it is possible to describe hardening effects as they were mentioned in the introduction to this section. Here we want to give an example for a potential $W_{mic}(\xi)$ describing the hardening effects, that were mentioned before. The simplest approach for a hardening potential is given by

$$W_{mic}^{lin} = \frac{1}{2} h \xi^2 \quad (2.6.73)$$

that leads to a linear hardening in the yield function, whereby h denotes the linear hardening modulus. The application of this hardening formulation yields a very unsatisfying description of real deformation processes, such that it is quite common to upgrade the linear model by a nonlinear approach like

$$W_{mic}^{nonl} = [Y_\infty - Y_0] \left[\xi + \frac{1}{\varkappa} \exp[-\varkappa \xi] \right]. \quad (2.6.74)$$

The superposition of the linear and the nonlinear hardening potential yields a resulting yield stress $Y_n(\xi)$ that can be obtained by differentiation of the hardening potential with respect to the according variable ξ , such that the yield function finally can be specified as

$$\Phi(\tilde{\tau}^\#, Y_n) = \|\tilde{\tau}^\#\| - \sqrt{\frac{2}{3}} Y_n(\xi), \quad \text{with} \quad Y_0(\xi) = Y_0 + h\xi + [Y_\infty - Y_0] [1 - \exp[-\varkappa \xi]]. \quad (2.6.75)$$

The quantities Y_0 , Y_∞ and \varkappa are material specific parameters, whereby Y_0 defines the initial yield stress, namely when the material starts to plastify. The nonlinear hardening curve finally approximates a parallel to the linear hardening law, whereby the difference $\Delta Y = [Y_\infty - Y_0]$ determines the

distance to the linear hardening curve that goes through the initial yield stress Y_0 . The parameter \varkappa determines how fast the nonlinear root approximates the linear model. In the given description we assumed an isothermal deformation process, but in general these parameters are temperature dependent. This causes a softening material behaviour, since the resulting yield stress $Y_n(\xi, \Theta)$ decreases when the temperature increases. Therefore, the nonlinear hardening parameters Y_0, Y_∞ and the linear hardening modulus h are assumed to be linearly temperature dependent, such that we obtain

$$\left. \begin{aligned} \tilde{Y}_0(\Theta) &= Y_0 \Big|_{\Theta_0} [1 - \omega_y \Delta\vartheta], \\ \tilde{Y}_\infty(\Theta) &= Y_\infty \Big|_{\Theta_0} [1 - \omega_h \Delta\vartheta], \\ \tilde{h}(\Theta) &= h \Big|_{\Theta_0} [1 - \omega_h \Delta\vartheta], \end{aligned} \right\} \quad \text{with} \quad \Delta\vartheta = \Theta - \Theta_0. \quad (2.6.76)$$

Here ϑ_0 denotes a reference temperature, where the parameters have their initial values and the quantities ω_y and ω_h denote further material specific parameters. They describe how strong the thermal softening process takes place. The nonlinear hardening parameter \varkappa is assumed as not temperature dependent.

2.7 Inelastic Constitutive Models

In this section we like to present some isotropic inelastic models considering additional effects to plasticity. In particular we want to present two models taking ductile damage into account and which can be understood as an extension of the J_2 -model. Furthermore we want to discuss a model, by which rate-independent hyperelasto-plastic material formulations can be transformed into an elasto-viscoplastic material model. The representation of the governing equations are analogous to the von-Mises plasticity and therefore the models are not discussed in detail. Where the methods differ, an closer consideration takes place, but otherwise we restricted ourselves to present the governing equations and giving some remarks on the numerical aspects.

2.7.1 The Model of Gurson

Governing equations Originally this model was derived by Gurson [Gur77], who derived a yield potential for porous plastic materials for simple cell models. As the term 'porous' suggests, the key idea here is that the material contains voids, that arise from fracture of particles or micro-cracks in the surrounding matrix material. This process is denoted by *nucleation*. These microscopic voids can grow with further loading, such that microscopic holes evolve. If these holes reach a particular volume they can coalesce with each other and the softening process of the material gets accelerated. These mechanisms are recorded by the Gurson model, where the void evolution is described by the so-called *void-volume-ratio*,

$$d = \frac{V_v}{V_A} \quad (2.7.1)$$

that is introduced as an additional internal variable and where V_v denotes the void volume and V_A is the elementary volume of the material. Improvements of the model with respect to the predictions at low void-volume-ratios and a better representation of final void coalescence were performed by Tvergaard & Needleman [TN84]. A nonlinear formulation of the Gurson model was proposed

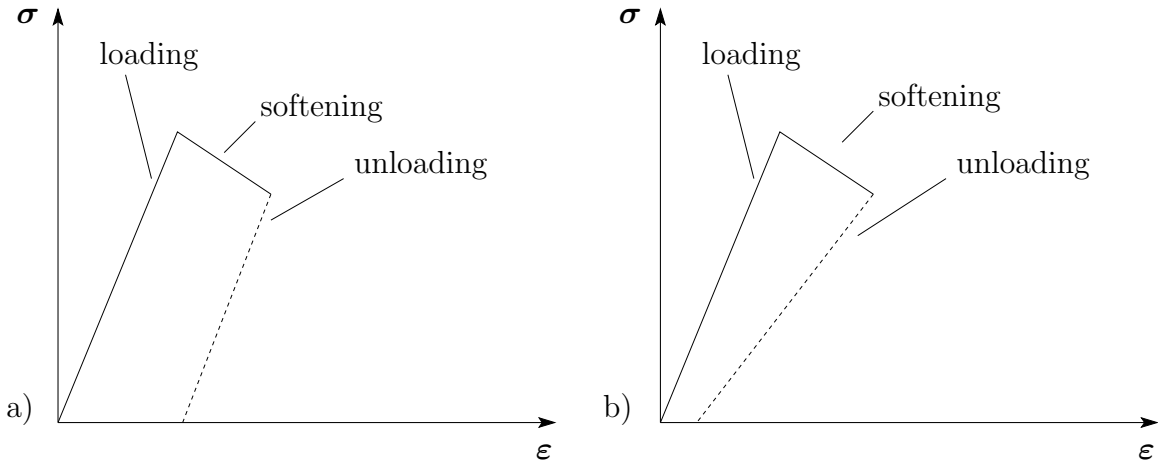


Figure 2.7. Differences of the a) Gurson-type model and b) a damage model of the Lemaitre-type

by Steinmann, Miehe & Stein [SMS94] and further improvement with respect to the numerical treatment and identification of the models parameter was proposed by Mahnen [Mah99]. Here we want to refer to the latter formulation, whereby we neglect the nucleation process and assume that the material initially contains already micro-voids.

It has to be emphasized here, that the Gurson model is not a real damage model since only the yield stress is reduced, but not the effective stress. Therefore within a cycling loading the slope of the elastic part of stress-strain curve would not be effected due to damaging, whereas in real damage models it would. This effect is scetched in fig. 2.7 where a softening can be observed, but the stiffness of the remaining 'undamaged' material is not effected by that. In comparison to that the Lemaitre-type model incorporates this effect and the stiffness decreases. Furthermore we have to mention here, that the 'damage effects' only occur for tension, otherwise the voids are decreasing due to pressure loading. Therefore this material model is predestinated for the description of concrete where damage effects are mainly initiated due to tension loading.

The Gurson model describes *porous elasto-plastic materials* including a kind of damaging, that is reflected in the reduction of the resulting yields stress by a scalar-valued function φ , that itself depends on the modified void volume ratio \hat{d} . Therefore the yield function, as we introduced it in the previous sections, gets the subsequent representation

$$\begin{aligned} \Phi &= \|\tilde{\tau}\| - \sqrt{\frac{2}{3}} \text{sign}(\varphi) \sqrt{|\varphi|} JY_n(\xi), & \text{with} \\ \varphi &= 1 + q_3 \hat{d} - 2q_1 \hat{d} \text{Cosh}v, & v = \left[\frac{3q_2 p}{2JY_n} \right], & \text{with} \\ \hat{d} &= d + (k-1)(d-d_c)\varsigma(d, d_c, \Delta d). \end{aligned} \quad (2.7.2)$$

The factors q_i are material parameters and $p = \text{tr}(\tilde{\tau}^\#)/3$ denotes the Kirchhoff pressure. The void volume function \hat{d} describes the change of the initial void growth to the increased growth due to coalescence, when a crucial void volume d_c is reached. Here k denotes the new slope and the function ς is defined by

$$\varsigma(d, d_c, \Delta d) = \begin{cases} 0 & , \text{ with } d \leq d_c \\ \frac{1}{2} \left[1 + \sin \left[\frac{d-d_c}{\Delta d} \pi - \frac{\pi}{2} \right] \right] & , \text{ with } d_c < d < d_c + \Delta d \\ 1 & , \text{ with } d_c + \Delta d \leq d, \end{cases} \quad (2.7.3)$$

that provides a smooth transition and numerical troubles due to the discontinuity can be avoided. Also the Cosh- function is modified for numerical reasons, since initially it coincides with the standard cosh-function, but if its argument reaches a crucial value v_c it is modified as follows

$$\text{Cosh} = \begin{cases} \cosh v & , \quad \text{with } v \leq v_c \\ \cosh v_c + [v - v_c] \sinh v_c + \frac{1}{2} [v - v_c]^2 \cosh v_c & , \quad \text{with } v > v_c. \end{cases} \quad (2.7.4)$$

These modifications lead to a better control of particular effects of the model, but with that an increasing number of parameters comes along.

Evolution equations As we learned in the previous section the evolution of the plastic strains is proportional to the derivative of the yield function Φ with respect to the Kirchhoff stress. Since also the function φ depends on the Kirchhoff stress or the Kirchhoff pressure, respectively, the evolution equation of the plastic strains become more complicate. Therefore the plastic flow emanates from eqn. 2.6.46 as

$$-\frac{1}{2} \mathcal{L}_t(\mathbf{b}_e^\#) \cdot \mathbf{c}_e^\flat = \dot{\gamma} \mathbf{g}^\# \cdot \frac{\partial \Phi}{\partial \boldsymbol{\tau}^\#} = \dot{\gamma} \boldsymbol{\nu} + \frac{1}{3} \dot{\gamma} s \mathbf{I}, \quad \text{with } s = \left[\sqrt{\frac{2}{3}} q_1 q_2 \hat{d} \text{Sinh} v \right] \quad (2.7.5)$$

whereby $\text{Sinh} v$ denotes the derivative of the $\text{Cosh} v$. We want to emphasise, that in contrast to the J_2 -plasticity, where the volumetric stress remained untouched by the local iteration scheme, that here the plastic flow is not purely deviatoric anymore. Therefore we also need to update the volumetric stress contributions.

The evolution equation for the hardening variable can also be derived from the dissipation equation, whereby the hardening potential is modified, such that the resulting yield stress can be introduced by

$$\frac{\partial \mathcal{W}}{\partial \xi} = \tilde{Y}_n = [1 - d] Y_n(\xi). \quad (2.7.6)$$

Inserting this into the Lagrange functional and differentiating it with respect to the associated stress-like quantity \tilde{Y}_n we obtain

$$\partial_{Y_n} \mathcal{L} = -[1 - d] \dot{\xi} + \dot{\gamma} \frac{\partial \Phi}{\partial Y_n} = 0. \quad (2.7.7)$$

This relation can be solved for the rate of the hardening variable and its evolution equation can finally be written as

$$\dot{\xi} = \frac{1}{[1 - d]} \left[\dot{\gamma} \sqrt{\frac{2}{3}} |\varphi| \text{sign } \varphi + \frac{ps}{Y_n} \right]. \quad (2.7.8)$$

In opposition to the plastic strains and the hardening variable the evolution of the void-volume-ratio is not derived from the dissipation inequality, but from the balance equation of mass. The total mass density ρ consists of the matrix material ρ_m and the mass of the included voids ρ_v . Since the mass of the voids can be neglected and the matrix material is assumed to be incompressible ($\dot{\rho}_m = 0$) we obtain for the balance equation of mass and its evolution

$$\rho = [1 - d] \rho_m \quad \text{and} \quad \dot{\rho} = -\dot{d} \rho_m. \quad (2.7.9)$$

Otherwise we know from the mass balance in eqn. 2.3.10 that the mass rate can be expressed by

$$\dot{\rho} = -\rho \operatorname{div} \mathbf{v} = -\rho \mathbf{l}^\sharp : \mathbf{I} = -\rho [\mathbf{l}_e^\sharp + \mathbf{l}_p^\sharp] : \mathbf{I} \quad (2.7.10)$$

whereby the elastic contributions in the mass balance $\mathbf{l}_e^\sharp : \mathbf{g}^\sharp = 0$ can be neglected. Comparing both mass rate formulations we can identify the rate of the void volume ratio with

$$\dot{d} = [1 - d] \mathbf{l}_p^\sharp : \mathbf{g}^\sharp = [1 - d] \dot{\gamma} s. \quad (2.7.11)$$

For the numerical iteration of the internal variables we have to rewrite these evolution equations as residuals and apply the Newton-Raphson iteration scheme. As mentioned before, also the volumetric Kirchhoff stress, respectively, needs to be updated, such that the subsequent four residuals can be derived

$$r_1 = \operatorname{sign}(\varphi) \|\tilde{\boldsymbol{\tau}}^{\sharp, trial}\| - 2\mu \Delta\gamma - \sqrt{\frac{2}{3}} Y_n(\xi) \quad (2.7.12)$$

$$r_2 = \xi_n - \xi + \frac{1}{[1 - d]} \left[\Delta\gamma \sqrt{\frac{2}{3}} |\varphi| \operatorname{sign} \varphi + \frac{ps}{Y_n} \right] \quad (2.7.13)$$

$$r_3 = d_n - d + [1 - d] \Delta\gamma \left[\sqrt{\frac{2}{3}} q_1 q_2 d^* \operatorname{Sinh} v \right] \quad (2.7.14)$$

$$r_4 = p - p^{trial} + \kappa \Delta\gamma \left[\sqrt{\frac{2}{3}} q_1 q_2 d^* \operatorname{Sinh} v \right]. \quad (2.7.15)$$

For the further proceeding we need to determine the entries of the Jacoby-matrix $J_{ij} = \partial_{x_j} r_i$, where x_i denotes the vector of four unknowns $\mathbf{x} = [\Delta\gamma, \xi, d, p]$. The inverse Jacobian is inserted into eqn. 2.6.65 and an updated set of the unknowns can be obtained. This procedure is repeated until the residuals are sufficient small. Some additional features for a better convergence are introduced by Mahnken, which are not presented here.

Algorithmic tangent operator Due to the additional dependency of the volumetric stresses on the plastic flow, the general representation of the spatial algorithmic tangent operator has to be modified for the Gurson-model

$$\mathbb{C}^{ep} = \sum_{\alpha=1}^3 \sum_{\beta=1}^3 \frac{1}{J} \varphi_{\alpha\beta} \mathbf{m}^\beta \otimes \mathbf{m}^\alpha + \sum_{\alpha=1}^3 \frac{2}{J} \tilde{\tau}_\alpha \frac{\partial \mathbf{m}^\alpha}{\partial \mathbf{g}^p} + \sum_{\alpha=1}^3 \frac{\partial \tau_\alpha}{\partial J} \mathbf{m}^\alpha \otimes \mathbf{g}^\sharp. \quad (2.7.16)$$

This representation can be obtained from the principal Kirchhoff stress, that can be rewritten as follows

$$\tau_\alpha = \tau_{\alpha, vol} + \tau_{\alpha, dev}, \quad \text{with} \quad \tau_{\alpha, vol} = \kappa [\ln J - \Delta\gamma s] \quad \text{and} \quad \tau_{\alpha, dev} = 2\mu [\ln \tilde{\lambda}_\alpha - \Delta\gamma \nu_\alpha]. \quad (2.7.17)$$

Following eqn. 2.5.77 the coefficient matrix $\varphi_{\alpha\beta}$ is defined by the derivative of the principal Kirchhoff stresses with respect to the principal stretches, that yields

$$\varphi_{\alpha\beta} = \kappa - \kappa s \frac{\partial \Delta\gamma}{\partial \tilde{\lambda}_\beta} - \kappa \Delta\gamma \frac{\partial s}{\partial \tilde{\lambda}_\beta} + 2\mu \left[\delta_{\alpha\beta} - \frac{1}{3} \right] - 2\mu \Delta\gamma \frac{\partial \nu_\alpha}{\partial \tilde{\lambda}_\beta} - 2\mu \frac{\partial \Delta\gamma}{\partial \tilde{\lambda}_\beta} \nu_\alpha \quad (2.7.18)$$

The derivative of the Kirchhoff stress with respect to the Jacobian yields

$$\frac{\partial \tau_\alpha}{\partial J} = \kappa \frac{\partial \ln J}{\partial J} - \kappa s \frac{\partial \Delta \gamma}{\partial J} - \kappa \Delta \gamma \frac{\partial s}{\partial J} - 2\mu \frac{\partial \Delta \gamma}{\partial J} \nu_\alpha. \quad (2.7.19)$$

We want to dispense with details here on the calculation of the appearing derivatives. We just want to note here, that also the volumetric part of the stresses are touched by the local iteration process and because of that, we have to take some care of the linearization of the stress formulation.

2.7.2 The Model of Lemaitre

Governing equations This damage model was firstly introduced by Lemaitre in his papers [Lem84] and [Lem85], whereby we mainly refer to the first publication. The idea of the elasto-plastic damage models of the Lemaitre-type is, that during the deformation the supporting cross section decreases, such that an effective stress $\hat{\tau}^\sharp$ can be defined. In the original proposition the effective stress includes volumetric parts as well as isochoric contributions, whereas Steinmann, Miehe & Stein [SMS94] suggest, that only the deviatoric part is affected by the damage effect. Therefore the strain energy function is assumed as

$$W(\mathbf{b}^\sharp, \xi, d) = W_{vol}(J) + [1 - d] W_{iso}(\tilde{\lambda}_\alpha) + W_{mic}(\xi), \quad (2.7.20)$$

such that we obtain the effective deviatoric stress by

$$\hat{\tau}^\sharp = \frac{1}{[1 - d]} \tau^\sharp, \quad (2.7.21)$$

whereby τ^\sharp denotes the deviatoric Kirchhoff stress as it was defined within the elastic framework. Here $0 \leq d \leq 1$ denotes the damage variable, and the material disrupts completely, if the denominator in eqn. 2.7.21 gets zero. Furthermore, from eqn. 2.7.21 emanates the stress-like quantity

$$R = -\frac{\partial W}{\partial d} = W_{iso}(\tilde{\lambda}_\alpha), \quad (2.7.22)$$

which is thermodynamically conjugated to the damage variable and that is denoted by *damage energy release rate* R .

Evolution equations With this at hand we can write the Lagrange functional in consideration of the side conditions as

$$\mathcal{L}(\tilde{\tau}, Y_n, R) = -\tau^\sharp : \left[\frac{1}{2} \mathbf{g}^b \cdot \mathcal{L}_t(\mathbf{b}_e^\sharp) \cdot \mathbf{c}_e^b \right] + Y_n \dot{\xi} - R \dot{d} + \dot{\gamma} \Phi^{pla} \geq 0, \quad \text{with} \quad (2.7.23)$$

$$\Phi = \Phi^{pla}(\tilde{\tau}^\sharp, Y_n) + \Phi^{dam}(R)$$

whereby here the side condition consists of the plastic potential as it was introduced in eqn. 2.6.15. In the yield function we have to take into account, that the resulting yield stress of the undamaged material is compared with the absolute value of the effective stress. Therefore the yield function becomes

$$\Phi^{pla} = \frac{\|\tilde{\tau}\|}{[1 - d]} - \sqrt{\frac{2}{3}} Y_n(\xi). \quad (2.7.24)$$

The damage potential is assumed to be a function of the damage energy release rate R , that is related to an value S_0 , that can be denoted by reference damage energy release rate of the undamaged material. The original damage potential given by Lemaitre was assumed by

$$\Phi^{dam} = \frac{S_0}{[1-d][s_0+1]} \left[\frac{-R}{S_0} \right]^{s_0+1}, \quad (2.7.25)$$

but in Steinmann, Miehe & Stein $s_0 = 1$ is assumed, that we also want to adopt here. From these potentials the following evolution equations emanate

$$-\frac{1}{2} \mathbf{g}^b \cdot \mathcal{L}_t(\mathbf{b}_e^\#) \cdot \mathbf{c}_e^b = \dot{\gamma} \frac{\partial \Phi^{pla}}{\partial \tilde{\boldsymbol{\tau}}^\#}, \quad \dot{\xi} = \dot{\gamma} \frac{\partial \Phi^{pla}}{\partial Y_n}, \quad \dot{d} = \dot{\gamma} \frac{\partial \Phi^{dam}}{\partial R}. \quad (2.7.26)$$

The concept, that the evolution equation of the internal variable is derived from the plastic potential by differentiating it with respect to the associated variable is called *hypothesis of associativity*. Since this procedure is adopted here to the damage variable, whereby the plastic potential is replaced by the damage potential, it is denoted by hypothesis of *generalized associativity*. From the evolution equations of the internal variables, as they are formulated in the continuous setting, we can derive the corresponding residuals in an incremental representation as they are needed for the Newton-Raphson iteration scheme. We obtain three residuals, whereby the first one coincides with the yield condition and

$$\begin{aligned} r_1 &= \frac{\|\tilde{\boldsymbol{\tau}}^\#\|}{[1-d]} - \frac{2\mu\Delta\gamma}{[1-d]} - \sqrt{\frac{2}{3}} Y_n, \\ r_2 &= \xi_n - \xi + \sqrt{\frac{2}{3}} \Delta\gamma, \\ r_3 &= d_n - d - \frac{\Delta\gamma}{[1-d]} \left[\frac{-R}{S_0} \right]. \end{aligned} \quad (2.7.27)$$

To install again a Newton-Raphson iteration scheme for the iteration of the internal variables, we have to calculate the entries of the Jacobi matrix, which correspond to the derivatives of the residuals with respect to the internal variables.

Algorithmic tangent operator In contrast to the Gurson-type damage model here only the deviatoric Kirchhoff stress is attracted by the damage effects, such that we can adopt the structure of the tangent operator of the v.-Mises formulation

$$\mathbb{C}^{ep} = \sum_{\alpha=1}^3 \sum_{\beta=1}^3 \frac{1}{J} \hat{\varphi}_{\alpha\beta} \mathbf{m}^\alpha \otimes \mathbf{m}^\beta + \sum_{\alpha=1}^3 \frac{2}{J} [1-d] \tilde{\tau}_\alpha \frac{\partial \mathbf{m}^\alpha}{\partial \mathbf{g}^b} \quad \text{with}$$

$$\hat{\varphi}_{\alpha\beta} = \frac{\partial \hat{\tau}}{\partial \lambda_\beta} = \kappa + [1-d] \left[2\mu \left[\delta_{\alpha\beta} - \frac{1}{3} \right] - 2\mu \left[\frac{\partial \Delta\gamma}{\partial \lambda_\beta} \nu - \alpha - \Delta\gamma \frac{\partial \nu_\alpha}{\partial \lambda_\beta} \right] \right] - \tilde{\tau}_\alpha \frac{\partial d}{\partial \Delta\gamma} \frac{\partial \Delta\gamma}{\partial \lambda_\beta}, \quad (2.7.28)$$

whereby $\hat{\varphi}_{\alpha\beta}$ denotes the coefficient matrix obtained from the derivatives of the principal stretches with respect to the principal stretches. From the derivative of eqn. 2.7.27₃ with respect to the Lagrange multiplier we obtain the term, that is needed for the derivation of the damage variable with respect to the principal stretches. Since the plastic potential depends on the effective stress, also

the Lagrange multiplier depends on the plastic potential. Therefore the derivative of the Lagrange multiplier with respect to the principal stretches

$$\frac{\partial \Delta \gamma}{\partial \lambda_\beta} = \frac{2\mu}{\left[2\mu + \frac{2}{3}Y'_n + \frac{1}{[1-d]} \left[\frac{-R}{S_0} \right] \right]} \nu_\beta. \quad (2.7.29)$$

gets modified by a contribution of the damage potential in the denominator. This completes the algorithmic tangent operator and we want to emphasize here once more that the volumetric stress contribution is not affected by the damage effects.

2.7.3 Rate-dependent Formulations

The inelastic models, as they were presented so far, are rate-independent. However, in general the material behaviour depends on the loading velocity and therefore we need an approach that records this effect, that is usually denoted by *viscosity*. We want to introduce an approach made by Perzyna in [Per63], [Per66] and [PW68], that allows an over-stress, in contrast to the rate-independent models, such that a stress state in the non-admissible domain ($\Phi > 0$) is possible. The material behaves elastic as long as the yield condition is not violated. After that plastic flow occurs superposed by a rate-dependent effect. In rheological models this effect is motivated by a dash-pot that acts parallel to the friction element, that describes the effects due to plasticity. The derivation of the elasto-viscoplastic material behaviour can also be effected from the principle of maximum dissipation, where the inequality of dissipation is enforced by a penalty term that replaces the side condition in the Lagrange functional in eqn. 2.6.7. Therefore the dissipation equation takes the following shape

$$\mathcal{L} = -\tilde{\boldsymbol{\tau}}^\# : \mathbf{d}^\flat + \dot{W}(\mathbf{b}^\#, \xi) + \frac{1}{2} \zeta [\Phi(\tilde{\boldsymbol{\tau}}^\#)]^2, \quad \text{with} \quad \Phi > 0 \quad (2.7.30)$$

Here ζ denotes the penalty parameter and if we consider the gradient of the dissipation with respect to the deviatoric Kirchhoff stress, we obtain a formulation for the viscoplastic strain-rate

$$-\frac{1}{2} \mathbf{g}^\flat \cdot \mathcal{L}_t(\mathbf{b}_e^\#) \cdot \mathbf{c}_e^\flat = \frac{1}{\eta} \langle \Phi \rangle \frac{\partial \Phi}{\partial \tilde{\boldsymbol{\tau}}^\#}, \quad \text{with} \quad \zeta = \frac{1}{\eta} \quad (2.7.31)$$

whereby the McCauley brackets are defined by

$$\langle \Phi \rangle = \frac{1}{2} [\Phi + |\Phi|] = \begin{cases} \Phi, & \text{for } \Phi > 0 \\ 0, & \text{for } \Phi \leq 0. \end{cases} \quad (2.7.32)$$

Moreover we replaced the penalty parameter by the inverse of the *viscosity* η , that describes the viscoplastic material behaviour. If we compare eqn. 2.7.31 and eqn. 2.6.16 we realize, that the Lagrange multiplier was replaced by a constitutive approach

$$\dot{\gamma} = \frac{\langle \Phi \rangle}{\eta}. \quad (2.7.33)$$

To transform the rate-independent into a rate-dependent J_2 -plasticity formulation, we solve this relation for the yield function, that finally yields

$$\Phi = \|\tilde{\boldsymbol{\tau}}^{\#,trial}\| - 2\mu\Delta\gamma - \sqrt{\frac{2}{3}}Y_n(\xi) - \frac{\eta}{\Delta t}\Delta\gamma \quad \text{with} \quad \dot{\gamma} = \frac{\Delta\gamma}{\Delta t} \quad (2.7.34)$$

whereby we installed an incremental description, where Δt denotes the time increment, by which the dependence on time is realised explicitly. This modification also involves a simple addition in the spatial algorithmic tangent operator as it was derived for the rate-independent formulation in eqn. 2.6.72. The only alteration takes place in the derivative of the plastic multiplier with respect to the principal stretches in eqn. 2.6.71

$$\mathbb{C}^{ep} = \sum_{\alpha=1}^3 \sum_{\beta=1}^3 \frac{1}{J} \varphi_{\alpha\beta} \mathbf{m}^\alpha \otimes \mathbf{m}^\beta + \sum_{\alpha=1}^3 \frac{2}{J} \tilde{\tau}_\alpha \frac{\partial \mathbf{m}^\alpha}{\partial g^b}, \quad \text{with}$$

$$\varphi_{\alpha\beta} = \varphi_{\alpha\beta}^e - \frac{4\mu^2 \Delta\gamma}{\|\tilde{\tau}^\# \|} [\delta_{\alpha\beta} - \nu_\alpha \nu_\beta] - 2\mu \left[1 + \frac{\eta}{2\mu\Delta\bar{\tau}} + \frac{1}{3} \frac{Y'_n}{\mu} \right]^{-1} \nu_\alpha \nu_\beta. \quad (2.7.35)$$

This viscous description shows a modular character and can be integrated into every hyper-elasto-plastic material formulation, such that a rate-independent formulation can easily be transformed into a rate-dependent one.

2.8 Numerical Aspects of Elasticity and Inelasticity for Finite Deformations

In this section we discuss the numerical realization of the derived material models within the framework of the finite element method. And we want to develop the procedure from the continuous balance equation to the set of linear equations step by step. Starting point here is the balance of linear momentum, that needs to be transformed into the weak form. The derived equation is nonlinear, since we consider nonlinear strain measures and therefore we need to perform a linearization, such that a Newton- Raphson iteration scheme is applicable. In the sequel we will discretize the equations by standard Lagrange element formulations and finally we will construct the *element stiffness matrix* and the corresponding *element load vector*. The assembling procedure is described briefly and the numerical integration methods, as there are the *Gauss quadrature* or the *Newton-Cotes quadrature*, are briefly summarized. The used numerical methods are common standard, such that they are not discussed in detail, but for completeness the main ideas are represented. The emphasis is placed on the weak form in the different configurations, the corresponding linearization and the discretization. The number of publications on the finite element method is quite large, such that it is not difficult to give a link to further reading. A very fine introduction into the linear finite element method is given by Hughes [Hug00], Reddy [Red93] or Rappaz, Bellet & Deville [RBD03]. These authors focus on the representation of the main steps to get a finite element formulation, whereas Oden & Reddy [OR76] highlight the mathematical basics of the Finite element method. A nice compromise between theory and application can be found in Jung & Langer [JL01]. Formulation of the finite element method with respect to nonlinear problems can be found in Oden [Ode72], Bonet & Wood [BWed], Wriggers [Wri01] or in Belytschko, Liu & Moran [BLM00]. The standard work containing the representation of linear and nonlinear problems is published by Zienkiewics & Taylor [ZT02a], [ZT02b] and [ZT02c].

2.8.1 The Weak Form in Terms of the Cauchy Stress

Point of departure is the spatial formulation of the linear momentum balance equation in eqn. 2.3.14, whereby the corresponding initial boundary value problem requires additional information about the

initial values of the deformation and the velocity and the given conditions at the boundary of the considered domain. The complete description of the strong formulation in terms of the reference and the current configuration is given by

$$\rho_0 \partial_t \mathbf{v} = \text{Div} \mathbf{P}^\sharp + \mathbf{b}_0, \quad \rho \partial_t \mathbf{v} = \text{div} \boldsymbol{\sigma}^\sharp + \mathbf{b} \quad (2.8.1)$$

with the initial values of the deformation and the velocity

$$\boldsymbol{\varphi}(t_0) = \boldsymbol{\varphi}_0 \text{ in } \mathcal{B}_0, \quad \mathbf{v}(t_0) = \mathbf{v}_0 \text{ in } \mathcal{B}_0 \quad (2.8.2)$$

and the Dirichlet and Neumann boundary conditions

$$\mathbf{u} = \bar{\mathbf{u}} \text{ on } \partial \mathcal{B}_{0u}, \quad \boldsymbol{\sigma}^\sharp \cdot \mathbf{n} = \bar{\mathbf{t}} \text{ on } \partial \mathcal{B}_{0\sigma}, \quad (2.8.3)$$

where $\bar{\mathbf{u}}$ and $\bar{\mathbf{t}}$ prescribed displacements and tractions at the boundary, respectively. By these presettings the problem is wellposed and the next step is to derive the *weak form* of the linear momentum balance equation, which is completely equivalent to the strong representation, but here some of the boundary conditions are already included within the formulation. But in contrast to the strong form the restrictions on the solution with respect to smoothness are weaker. To obtain firstly the variational form of the differential equation, it is multiplied by a so-called *test function* or *weight function* $\delta \mathbf{u} \in H^1(\mathcal{B}_t)$ ⁷ and by integrating the resulting equation over the domain of \mathcal{B}_t we transform it to a functional \mathcal{G} , that is called *variational form*. The test function has to be continuous and becomes zero at the boundaries. The weak form can be represented as

$$\mathcal{G} = \int_{\mathcal{B}_t} [\text{div} \boldsymbol{\sigma}^\sharp + \mathbf{b} - \rho \dot{\mathbf{v}}] \cdot \delta \mathbf{u} dv = 0 \quad (2.8.4)$$

whereby we can apply the partial integration to the first term and in consideration of the test function it can be rewritten as

$$\int_{\mathcal{B}_t} \text{div} \boldsymbol{\sigma}^\sharp \cdot \delta \mathbf{u} dv = \int_{\mathcal{B}_t} [\text{div} [\boldsymbol{\sigma}^\sharp \cdot \delta \mathbf{u}]] dv - \int_{\mathcal{B}_t} \boldsymbol{\sigma}^\sharp : \text{grad} \delta \mathbf{u} dv. \quad (2.8.5)$$

⁷There are two important function spaces, which are needed in the framework of the finite element method and that are fundamental to it. The first one is the set of quadratically integrable functions, that usually are defined by

$$L_2(\Omega) = \{\mathbf{u} : \exists \int_{\Omega} (\mathbf{u}(\mathbf{x}))^2 d\mathbf{x} < \infty\},$$

such that L_2 includes all functions \mathbf{u} , for which the integral over Ω exists and becomes finite. Therefore L_2 is denoted by *space of quadratically integrable functions*. For a function $\mathbf{u} \in H_2^1(\Omega)$ one demands that also the integral of the first *generalized derivative* over Ω exists and gets a finite value as well, such that it is also an element of $L_2(\Omega)$. $H_2^1(\Omega)$ is called *Sobolev space*, which is a subspace of L_2 . The generalized derivative can be derived from the partial integration, where the function $\mathbf{u}(\mathbf{x}) \in C^1(\Omega)$ is weighted by the continuous function $\varphi(\mathbf{x}) \in C^1(\Omega) | \varphi(\partial\Omega) = 0$, such that we can write

$$\int_{\Omega} \mathbf{u}(\mathbf{x}) \varphi'(\mathbf{x}) dv = - \int_{\Omega} \mathbf{u}'(\mathbf{x}) \varphi(\mathbf{x}) dv + \underbrace{\mathbf{u}(\mathbf{x}) \varphi(\mathbf{x})}_{=0} \Big|_{\partial\Omega}.$$

This generalized derivative was introduced by Sobolev and it is fundamental for the derivation of the weak formulations.

Furthermore we can apply the Gauss theorem to the first term in eqn. 2.9.59 and include the Neumann boundary conditions, such that we can write

$$\int_{\mathcal{B}_t} \operatorname{div} [\boldsymbol{\sigma}^\# \cdot \delta \mathbf{u}] dv = \int_{\partial \mathcal{B}_t} \mathbf{n} \cdot \boldsymbol{\sigma}^\# \cdot \delta \mathbf{u} da = \int_{\partial \mathcal{B}_{t,\sigma}} \mathbf{t} \cdot \delta \mathbf{u} da. \quad (2.8.6)$$

Inserting this into eqn. 2.9.59 we finally obtain the so-called *weak form*

$$\mathcal{G} = \int_{\mathcal{B}_t} \boldsymbol{\sigma}^\# : \operatorname{grad} \delta \mathbf{u} dv - \int_{\mathcal{B}_t} [\mathbf{b} - \rho \dot{\mathbf{v}}] \cdot \delta \mathbf{u} dv - \int_{\partial \mathcal{B}_{t,\sigma}} \mathbf{t} \cdot \delta \mathbf{u} da = 0. \quad (2.8.7)$$

This equation represents the weak form of the linear momentum balance equation in terms of the spatial configuration. This formulation coincides with the variational formulation that emanates from the *principle of virtual work*. Therefore the particular terms in the variational formulation

$$\mathcal{G} = \underbrace{\int_{\mathcal{B}_t} \boldsymbol{\sigma}^\# : \delta \mathbf{e}^b dv}_{\mathcal{G}^{int}} - \underbrace{\int_{\mathcal{B}_t} \mathbf{b} \cdot \delta \mathbf{u} dv - \int_{\partial \mathcal{B}_{t,\sigma}} \mathbf{t} \cdot \delta \mathbf{u} da}_{\mathcal{G}^{ext}} + \underbrace{\int_{\mathcal{B}_t} \rho \dot{\mathbf{v}} \cdot \delta \mathbf{u} dv}_{\mathcal{G}^{dyn}} = 0 \quad (2.8.8)$$

can be interpreted as virtual work, whereby the first one describes the virtual work due to internal forces. The rest records the virtual work done by the external forces, acting at the surface and the volume, and the inertial forces.

2.8.2 The Weak Form in Terms of the Piola Stress

The weak formulation of the material representation of the momentum balance equation can be derived analogously to the spatial one, whereby here the work-conjugated strain measure accords to the deformation gradient. With this at hand the variational form can be written as

$$\mathcal{G} = \int_{\mathcal{B}_0} [\operatorname{Div} \mathbf{P}^\natural + \mathbf{b}_0 - \rho_0 \dot{\mathbf{v}}] \cdot \delta \mathbf{u} dV = 0 \quad (2.8.9)$$

To this expression we can apply the same transformations as in the spatial description, only with respect to the material configurations, such that we finally obtain for the material weak formulation

$$\mathcal{G} = \underbrace{\int_{\mathcal{B}_0} \mathbf{P}^\natural : \delta \mathbf{F}^\natural dV}_{\mathcal{G}^{int}} - \underbrace{\int_{\mathcal{B}_0} \mathbf{b}_0 \cdot \delta \mathbf{u} dV - \int_{\partial \mathcal{B}_{0,\sigma}} \mathbf{t}_0 \cdot \delta \mathbf{u} dA}_{\mathcal{G}^{ext}} + \underbrace{\int_{\mathcal{B}_0} \rho_0 \dot{\mathbf{v}} \cdot \delta \mathbf{u} dV}_{\mathcal{G}^{dyn}} = 0, \quad \text{with} \quad \delta \mathbf{F}^\natural = \operatorname{Grad} \delta \mathbf{u} \quad (2.8.10)$$

whereby here the surface and volume forces are transformed by $\mathbf{t}_0 = \mathbf{t} dA/da$ and $\mathbf{b}_0 = J\mathbf{b}$, respectively, and the internal virtual work is expressed in terms of the 1. Piola-Kirchhoff stress. An equivalent representation in terms of the 2. Piola-Kirchhoff stress can be obtained by the subsequent transformation

$$\mathcal{G}^{int} = \int_{\mathcal{B}_0} \mathbf{P}^\natural : \delta \mathbf{F}^\natural dV = \int_{\mathcal{B}_0} \mathbf{S}^\# : [[\mathbf{F}^\natural]^t \cdot \mathbf{g}^b \cdot \delta \mathbf{F}^\natural]^{sym} dV = \int_{\mathcal{B}_0} \mathbf{S}^\# : \delta \mathbf{E}^b dV. \quad (2.8.11)$$

Inserting this result in eqn. 2.9.64 yields the weak form of the material momentum balance equation in terms of the symmetric 2. Piola-Kirchhoff stress \mathbf{S}^\sharp , that filters the symmetric part of $[\mathbf{F}^\natural]^t \cdot \mathbf{g}^\flat \cdot \delta \mathbf{F}^\natural$, that coincides with the rate of the Green-Lagrange strain tensor.

The results in eqn. 2.9.64, 2.8.11 and eqn. 2.9.62 describe an energetic state of a given system, that depends on the configuration given by the motion φ . The task is to find the particular configuration, that minimizes the energy in the system, since this coincides with a state of equilibrium. The problem is, that the balance equations represented by the weak forms in terms of the material or the spatial configurations are highly nonlinear and therefore the problem can not be solved directly. For a numerical solution of the given problem the weak formulations need to be *linearized*, i.e. it is approximated by a Taylor expansion, which is truncated after the linear term. If the linearization is performed, finally a numerical iteration algorithm like the Newton-Raphson iteration scheme for instance can be applied to find the particular configuration, that minimizes the systems energy. We have to distinguish between nonlinearities, that are induced by the consideration of large deformations and nonlinearities due to the constitutive equations. The nonlinearity of the given variational formulations is a consequence of both reasons, whereby the linear approximations of the particular stress rates was already performed by derivation of the material or spatial algorithmic tangent operators, such that in the sequel we can assume them as given. Therefore in the subsequent sections we consider the linearization of the variational formulations with respect to the nonlinear strain measures in particular.

2.8.3 Linearization of the Weak Form

Linearization of a function means that a function $\mathbf{f}(\mathbf{x})$ at \mathbf{x} is approximated by a Taylor expansion

$$\mathbf{f}(\mathbf{x}) = \mathbf{f}(\bar{\mathbf{x}}) + \frac{\partial \mathbf{f}}{\partial \mathbf{x}} \Big|_{\bar{\mathbf{x}}} [\mathbf{x} - \bar{\mathbf{x}}] + \frac{1}{2!} \frac{\partial^2 \mathbf{f}}{\partial \mathbf{x}^2} \Big|_{\bar{\mathbf{x}}} [\mathbf{x} - \bar{\mathbf{x}}]^2 + \dots \quad (2.8.12)$$

which is truncated after the second terms, such that we obtain

$$\mathbf{f}(\mathbf{x}) = \mathbf{f}(\bar{\mathbf{x}}) + \frac{\partial \mathbf{f}}{\partial \mathbf{x}} \Big|_{\bar{\mathbf{x}}} [\mathbf{u}] + O(u^2) \quad (2.8.13)$$

a linear approximation of the function \mathbf{f} at $\bar{\mathbf{x}}$, whereby the function value $\mathbf{f}(\bar{\mathbf{x}})$ is given and the second term coincides with the directional derivative of the function $\mathbf{f}(\mathbf{x})$ in direction of \mathbf{u} . \mathbf{u} denotes the difference of the old and the new \mathbf{x} and describes a kind of increment. The directional derivative often is denoted by $\Delta \mathbf{f}$ or $D_x [\mathbf{f}] \mathbf{u}$ and it can also be derived by

$$\Delta \mathbf{f}(\bar{\mathbf{x}}, \mathbf{u}) = D_x [\mathbf{f}(\bar{\mathbf{x}}, \mathbf{u})] \cdot \mathbf{u} = \frac{\partial}{\partial \varepsilon} \mathbf{f}(\bar{\mathbf{x}} + \varepsilon \mathbf{u}) \Big|_{\varepsilon=0} = \frac{\partial \mathbf{f}(\bar{\mathbf{x}} + \varepsilon \mathbf{u})}{\partial \bar{\mathbf{x}} + \varepsilon \mathbf{u}} \cdot \frac{\partial \bar{\mathbf{x}} + \varepsilon \mathbf{u}}{\partial \varepsilon} \Big|_{\varepsilon=0} = \frac{\partial \mathbf{f}}{\partial \mathbf{x}} \Big|_{\varepsilon=0} \cdot \mathbf{u} \quad (2.8.14)$$

where the derivative of \mathbf{f} with respect to $\mathbf{x} = \bar{\mathbf{x}} + \varepsilon \mathbf{u}$ is evaluated at $\bar{\mathbf{x}}$. The last term in eqn. 2.8.13 $O(u^2) \rightarrow 0$ is the remainder, that is characterized by the *Landau order symbol* and it becomes lower the more terms are considered in the Taylor series. We want to apply this linearization procedure to the weak form of the linear momentum balance equation, where we like to consider the different terms in detail now. As mentioned before, we can divide the weak form into an internal virtual work $\mathcal{G}^{int}(\bar{\varphi}, \delta \mathbf{u})$ and an external virtual work $\mathcal{G}^{ext}(\bar{\varphi}, \delta \mathbf{u})$, which depend on the motion $\bar{\varphi}$, that accords to $\bar{\mathbf{x}}$ in the general consideration, and on the variation $\delta \mathbf{u}$. The linearization of a quantity is indicated by the $L[\bullet]$ -operator, that we firstly apply to the internal virtual work.

$$L[\mathcal{G}^{int}(\bar{\varphi}, \delta \mathbf{u})] = \bar{\mathcal{G}}^{int} + \Delta \bar{\mathcal{G}}^{int}(\Delta \mathbf{u}), \quad (2.8.15)$$

whereby $\bar{\mathcal{G}}^{int}$ indicates, that the expression of internal virtual work is evaluated at the last established equilibrium state of the motion denoted by $\bar{\varphi}$. Since the motion is given by $\varphi(\mathbf{X}, t) = \mathbf{x}(\mathbf{X}, t) = \mathbf{X} + \mathbf{u}(\mathbf{X}, t)$, where $\mathbf{u}(\mathbf{X}, t)$ denotes the complete displacements we want to introduce the displacement increment $\Delta \mathbf{u}$. The main task is to determine the directional derivative represented by the second term in eqn. 2.8.15. For the initial configuration we can rewrite it as

$$\begin{aligned} D_x \bar{\mathcal{G}}^{int}(\bar{\varphi}, \delta \mathbf{u}) \Delta \mathbf{u} &= \frac{\partial}{\partial \varepsilon} \int_{\mathcal{B}_0} \mathbf{S}^\#(\mathbf{E}^b(\bar{\varphi} + \varepsilon \Delta \mathbf{u})) : \delta \mathbf{E}^b(\bar{\varphi} + \varepsilon \Delta \mathbf{u}) dV \\ &= \int_{\mathcal{B}_0} \left[D_x \mathbf{S}^\# : \delta \mathbf{E}^b + \mathbf{S}^\# : D_x \delta \mathbf{E}^b : \Delta \mathbf{u} \right] dV. \end{aligned} \quad (2.8.16)$$

In order to determine the linearization of the 2. Piola-Kirchhoff stress, we can use the chain rule that is applicable here, since the directional derivative is a linear operator. This consideration yields

$$D_x [\mathbf{S}^\#(\mathbf{E}^b)] \cdot \Delta \mathbf{u} = \frac{\partial \mathbf{S}^\#}{\partial \mathbf{E}^b} : D_x \mathbf{E}^b(\mathbf{u}) \Delta \mathbf{u} = \mathbb{C} : D_x [\mathbf{E}^b] \cdot \Delta \mathbf{u}, \quad (2.8.17)$$

and we find, that for the linearization of the stress tensor the material tensor of the material description has to be taken into account. Furthermore we need to establish the directional derivative of the Green-Lagrange tensor. For this we firstly investigate the linearization of the deformation gradient, that is

$$D_x [\mathbf{F}^b] \cdot \Delta \mathbf{u} = \frac{\partial}{\partial \varepsilon} \mathbf{F}^b(\bar{\varphi} + \varepsilon \Delta \mathbf{u}) = \frac{\partial}{\partial \varepsilon} \left[\frac{\bar{\varphi} + \varepsilon \Delta \mathbf{u}}{\partial \mathbf{X}} \right] = \frac{\partial}{\partial \mathbf{X}} \left[\frac{\partial [\bar{\varphi} + \varepsilon \Delta \mathbf{u}]}{\partial \varepsilon} \right] = \text{Grad} \Delta \mathbf{u} \quad (2.8.18)$$

where $\text{Grad}[\bullet]$ denotes the gradient with respect to the reference configuration. The application of this result to the linearization of the Green Lagrange strain tensor accordingly yields

$$D_x [\mathbf{E}^b] \cdot \Delta \mathbf{u} = \frac{1}{2} \left[([\mathbf{F}^b]^t \cdot \text{Grad} \Delta \mathbf{u})^t + [\mathbf{F}^b]^t \cdot \text{Grad} \Delta \mathbf{u} \right] \quad (2.8.19)$$

For the complete linearization of the virtual internal work the determination of the linearized variation of the Green Lagrange tensor is required. But before we can perform its linearization we have to determine the variation of the Green Lagrange tensor itself, which can be performed analogously to its linearization, such that we obtain

$$\delta \mathbf{E}^b = \frac{1}{2} \left[([\mathbf{F}^b]^t \cdot \text{Grad} \delta \mathbf{u})^t + [\mathbf{F}^b]^t \cdot \text{Grad} \delta \mathbf{u} \right]. \quad (2.8.20)$$

The corresponding linearization is represented by

$$D_x [\delta \mathbf{E}^b] \cdot \Delta \mathbf{u} = \frac{1}{2} \left[[\text{Grad} \Delta \mathbf{u}]^t \cdot \text{Grad} \delta \mathbf{u} + \text{Grad} \Delta \mathbf{u} \cdot [\text{Grad} \delta \mathbf{u}]^t \right], \quad (2.8.21)$$

such that the directional derivative of the material internal virtual work finally can be rewritten as

$$\begin{aligned} D_x [\bar{\mathcal{G}}^{int}(\bar{\varphi}, \delta \mathbf{u})] \cdot \Delta \mathbf{u} &= \int_{\mathcal{B}_0} \left[\delta \mathbf{E}^b : \mathbb{C} : ([\mathbf{F}^b]^t \cdot \text{Grad} \Delta \mathbf{u}) \right. \\ &\quad \left. + \mathbf{S}^\# : ([\text{Grad} \Delta \mathbf{u}]^t \cdot \text{Grad} \delta \mathbf{u}) \right] dV. \end{aligned} \quad (2.8.22)$$

We want to note here, that the variation of a quantity and its linear approximation both are based on the concept of directional derivatives, such that the symbol of the first variation $\delta [\bullet]$ easily can be replaced by $\Delta [\bullet]$ to obtain the linearization.

The contribution of the external virtual work due to volume forces and surface forces can be assumed as deformation independent⁸. Likewise the contributions due to inertia forces are neglected here, since we consider quasistatic problems such that the corresponding linearization of the external virtual work and the dynamic contribution are given by

$$D_x [\mathcal{G}^{ext}(\bar{\varphi}, \delta \mathbf{u})] \cdot \Delta \mathbf{u} = 0 \quad \text{and} \quad D_x [\mathcal{G}^{dyn}(\bar{\varphi}, \delta \mathbf{u})] \cdot \Delta \mathbf{u} = 0, \quad (2.8.23)$$

such that the linearization of the total virtual work reduces to the internal virtual work.

$$D_x [\mathcal{G}(\bar{\varphi}, \delta \mathbf{u})] \cdot \Delta \mathbf{u} = D_x [\mathcal{G}^{int}(\bar{\varphi}, \delta \mathbf{u})] \cdot \Delta \mathbf{u}. \quad (2.8.24)$$

The linearization of the Cauchy stress formulation can be performed in analogy to the Piola stress formulation. Therefore it makes sense to rewrite the weak form in terms of the Kirchhoff stress

$$\mathcal{G}^{int} = \int_{B_t} \boldsymbol{\sigma}^\# : \delta \mathbf{e}^b dv = \int_{B_0} \boldsymbol{\tau}^\# : \delta \mathbf{e}^b dV. \quad (2.8.25)$$

The linearization of this formulation can be divided into different contributions

$$D_x [\mathcal{G}^{int}(\bar{\varphi}, \delta \mathbf{u})] \cdot \Delta \mathbf{u} = \int_{B_0} [D_x [\boldsymbol{\tau}^\#] \cdot \Delta \mathbf{u} : \delta \mathbf{e}^b + \boldsymbol{\tau}^\# : D_x [\delta \mathbf{e}^b] \cdot \Delta \mathbf{u}] dV. \quad (2.8.26)$$

In order to linearize the Kirchhoff stress we take eqn 2.5.35 into account, such that the linearization can be represented by

$$\begin{aligned} D_x [\boldsymbol{\tau}^\#] \Delta \mathbf{u} &= D_x [\mathbf{F}^\natural \cdot \mathbf{S}^\# \cdot [\mathbf{F}^\natural]^t] \cdot \Delta \mathbf{u} \\ &= \text{grad} \Delta \mathbf{u} \cdot \boldsymbol{\tau}^\# + \boldsymbol{\tau}^\# \cdot [\text{grad} \Delta \mathbf{u}]^t + \mathbf{F}^\natural \cdot D_x [\mathbf{S}^\#] \cdot \Delta \mathbf{u} [\mathbf{F}^\natural]^t. \end{aligned} \quad (2.8.27)$$

⁸However, in general the contributions due to surface forces, like the ambient pressure for instance, or volume forces have to be considered as deformation dependent, since the pressure always acts in normal direction, which can change during the deformation. The concerning term in the weak form can be rewritten as

$$\int_{\partial B_t} \mathbf{t} \cdot \delta \mathbf{u} da = \int_{\partial B_t} p \mathbf{n} \cdot \delta \mathbf{u} da = \int_{B_0} J p [\mathbf{F}^\natural]^{-1} \cdot \mathbf{N} \cdot \delta \mathbf{u} dA,$$

whereby p denotes the scalar value of the pressure and \mathbf{N} is the normal unit vector on the surface in the material configuration. Therefore the directional derivative can be obtained from

$$D_x [\mathbf{n} da] \cdot \Delta \mathbf{u} = D_x [J [\mathbf{F}^\natural]^{-t} \cdot \mathbf{N} da] \cdot \Delta \mathbf{u} = [D_x J [\mathbf{F}^\natural]^{-t} + J D_x [[\mathbf{F}^\natural]^{-t}]] \cdot \mathbf{N} da,$$

whereby the directional derivatives of the different terms are given by

$$D_x [J \cdot] \Delta \mathbf{u} = J \text{div} \mathbf{u}, \quad D_x [[\mathbf{F}^\natural]^{-t}] \cdot \Delta \mathbf{u}.$$

The volume forces can be decomposed into the magnitude and the normed direction vector $\mathbf{b} = b \mathbf{g}$, which is constant, such that the total differential of the external contribution can finally be written as

$$D_x [\mathcal{G}^{ext}] \cdot \Delta \mathbf{u} = \rho_0 D_x [b] \cdot \Delta \mathbf{u} \int_{B_0} \mathbf{g} \cdot \delta \mathbf{u} dV + D_x [p] \cdot \Delta \mathbf{u} \int_{\partial B_t} \mathbf{n} \cdot \delta \mathbf{u} da + \int_{\partial B_t} p [\mathbf{n} \text{div} \mathbf{u} - [\text{grad} \delta \mathbf{u}]^t \mathbf{n}] \cdot \delta \mathbf{u} da.$$

If we insert the linearization of the second Piola stress derived in eqn. 2.8.17 we obtain the corresponding push forward

$$\mathbf{F}^\sharp [\dot{D}_x [\mathbf{S}^\sharp] \cdot \Delta \mathbf{u}] \cdot [\mathbf{F}^\sharp]^t = J \mathbb{C} : [\text{grad} \Delta \mathbf{u}]^{sym}, \quad (2.8.28)$$

whereby in the last step the push forward relation from eqn. 2.5.73 is performed. The linearization of $\delta \mathbf{e}^b$ can also be represented by the push forward of the $\delta \mathbf{E}^b$, such that the linearization is given by

$$\begin{aligned} D_x [\delta \mathbf{e}^b] \cdot \Delta \mathbf{u} &= D_x [\mathbf{f}^\sharp]^t \cdot \delta \mathbf{E}^b \cdot \mathbf{f}^\sharp \cdot \Delta \mathbf{u} \\ &= [\text{grad} \Delta \mathbf{u}]^t \cdot \text{grad} \delta \mathbf{u}]^{sym} - [\text{grad} \Delta \mathbf{u}]^{sym} \cdot \delta \mathbf{e}^b. \end{aligned} \quad (2.8.29)$$

Inserting the results from eqn. 2.8.27, eqn. 2.8.28 and eqn. 2.8.29 into eqn. 2.8.26 yields the linearization of the internal virtual work in terms of the Cauchy stress

$$\begin{aligned} D_x \mathcal{G}^{int} &= \int_{\mathcal{B}_0} [[\text{grad} \Delta \mathbf{u}]^{sym}]^t \cdot \boldsymbol{\tau}^\sharp : \delta \mathbf{e}^b + J \delta \mathbf{e}^b : \mathbb{C} : [\text{grad} \Delta \mathbf{u}]^{sym} \\ &\quad - [[\text{grad} \Delta \mathbf{u}]^{sym}]^t \cdot \boldsymbol{\tau}^\sharp : \delta \mathbf{e}^b + \boldsymbol{\tau}^\sharp : [[\text{grad} \Delta \mathbf{u}]^{sym}]^t \cdot \text{grad} \delta \mathbf{u}]^{sym} dV. \end{aligned} \quad (2.8.30)$$

Here the first and the third term vanishes and the linearized internal virtual work finally reduces to

$$D_x \mathcal{G}^{int} = \int_{\mathcal{B}_0} [J \delta \mathbf{e}^b : \mathbb{C} : [\text{grad} \Delta \mathbf{u}]^{sym} + \boldsymbol{\tau}^\sharp : [[\text{grad} \Delta \mathbf{u}]^{sym}]^t \cdot \text{grad} \delta \mathbf{u}]^{sym} dV. \quad (2.8.31)$$

Eqn. 2.8.31 is the corresponding linearization of the internal virtual work in terms of the Cauchy stress, whereby the linearization of the spatial quantities were performed analogously to the Lie-derivative. We want to note here, that the linearization of the spatial or material strain tensors tend to the linear strain measure we know from the linear theory, where the reference setting coincides with the spatial configuration $\mathbf{X} = \boldsymbol{\varphi}(\mathbf{X}, t) = \mathbf{x}$. Furthermore, we want to remark that the expressions derived due to linearization are symmetric that makes it possible to install more efficient numerical solvers. Within the treatment of thermomechanically coupled problems we will realize, that the symmetry of the tangent matrix can not be ensured anymore.

2.8.4 Discretization of the Weak Form in Terms of the Piola Stress

Within the discretization of the weak form the continuous differential equations are transformed to a system of algebraic equations which are evaluated for a certain material particle \mathbf{X} at a discrete time t_{n+1} and spatial placement \mathbf{x}_{n+1} . For the discrete description of the governing quantities we follow the *isoparametric concept*, where the same shape functions N_a are used for the geometry and the kinematic quantities as well, such that the initial and actual placement of a particle within a *finite element* is given by the interpolations

$$\mathbf{X}_e \approx \sum_{a=1}^n N_a(\xi_i) \mathbf{X}^a, \quad \mathbf{x}_e \approx \sum_{a=1}^n N_a(\xi_i) \mathbf{x}^a. \quad (2.8.32)$$

Here N_a denotes the standard shape functions of the Lagrange type, which depends on the coordinates ξ_i of the reference element, that represents a configuration \mathcal{B}_\square that is never adopted by the

considered body. n is the number of element nodes represented by their particular positions \mathbf{X}_a and \mathbf{x}_a . Since the reference element is of orthonormal structure we can give up distinguishing between covariant and contravariant quantities and derivatives, respectively. According to the isoparametric concept we can introduce the interpolation of the displacements and the corresponding variation by

$$\mathbf{u}_e \approx \sum_{a=1}^n \mathbf{N}_a(\xi_a) \mathbf{u}_a \quad \text{and} \quad \delta \mathbf{u}_e \approx \sum_{a=1}^n \mathbf{N}_a(\xi_a) \delta \mathbf{u}_a. \quad (2.8.33)$$

For the determination of the gradients the main trick of the finite element approach is introduced. Since here the derivatives of the displacement field is not calculated directly, but the derivatives of the shape functions with respect to the coordinates of the reference element. The gradient of the displacements and the corresponding variations with respect to the material and the spatial configuration are approximated by

$$\begin{aligned} \text{Grad} \mathbf{u}_e &= \sum_{a=1}^n \mathbf{u}_a \otimes \nabla_X \mathbf{N}_a, & \text{grad} \mathbf{u} &= \sum_{a=1}^n \mathbf{u}_a \otimes \nabla_x \mathbf{N}_a, \\ \text{Grad} \delta \mathbf{u}_e &= \sum_{a=1}^n \delta \mathbf{u}_a \otimes \nabla_X \mathbf{N}_a, & \text{grad} \delta \mathbf{u} &= \sum_{a=1}^n \delta \mathbf{u}_a \otimes \nabla_x \mathbf{N}_a. \end{aligned} \quad (2.8.34)$$

There is no more information needed, but the displacement of the particular particle. The derivatives of the shape functions with respect to the placement in the material or spatial setting are obtained by

$$\nabla_X \mathbf{N}_a = [\mathbf{J}_e]^{-t} \nabla_\xi \mathbf{N}_a, \quad \nabla_x \mathbf{N}_a = [\mathbf{j}_e]^{-t} \nabla_\xi \mathbf{N}_a, \quad (2.8.35)$$

whereby the \mathbf{J}_e and \mathbf{j}_e are the so-called Jacobi matrices mapping the geometry from the reference element to the material or the spatial configuration and vice versa. Therefore they are defined by

$$\mathbf{J}_e = \sum_{\alpha}^n \mathbf{X}_a \otimes \nabla_\xi \mathbf{N}_a, \quad \mathbf{j}_e = \sum_{\alpha}^n \mathbf{x}_a \otimes \nabla_\xi \mathbf{N}_a \quad (2.8.36)$$

With this at hand we are able to construct the further quantities in discrete form. Therefore we can define the deformation gradient analogously to the gradient of the displacement with respect to the material setting, whereby the spatial placement field is exchanged by the displacement field

$$\mathbf{F}_e = \mathbf{I} + \text{Grad} \mathbf{u}_e = \mathbf{I} + \sum_{a=1}^n \mathbf{u}_a \otimes \nabla_X \mathbf{N}_a. \quad (2.8.37)$$

In the sequel we want to discretize the weak form with respect to the material setting, whereby we only consider the element formulation that is indicated by the fact, that the integration is not performed over the whole body \mathcal{B}_0 , but over the domain of one element denoted by \mathcal{B}_e . Point of departure is the weak form in terms of the 2. Piola Kirchhoff stress

$$\mathcal{G}_e = \int_{\mathcal{B}_e} \mathbf{S}^\# : \delta \mathbf{E}^b d\Omega - \int_{\mathcal{B}_e} [\mathbf{b}_0 - \rho_0 \dot{\mathbf{v}}] \cdot \delta \mathbf{u} d\Omega - \int_{\partial \mathcal{B}_e} \mathbf{t}_0 \cdot \delta \mathbf{u} d\Gamma, \quad (2.8.38)$$

consisting of the expressions of virtual work due to internal, external and inertial forces. We derive the discretization of the different terms separately and start with the internal virtual work. Here the variation of the Green Lagrange strain tensor occurs, whose discretized formulation is obtained by

replacing the corresponding quantities in eqn. 2.8.20 by the discretized approximations as they are given in eqn. 2.8.37 and 2.8.34

$$\delta \mathbf{E}_e = \frac{1}{2} \sum_{a=1}^n [\mathbf{F}_e^t \cdot [\delta \mathbf{u}_a \otimes \nabla_X \mathbf{N}_a] + [\nabla_X \mathbf{N}_a \otimes \delta \mathbf{u}_a] \cdot \mathbf{F}_e] = \sum_{a=1}^n \mathbf{B}_a \cdot \delta \mathbf{u}_a. \quad (2.8.39)$$

In order to implement the formulations the discretized quantities are usually represented by the Voigt notation, where the variation of the Green Lagrange tensor $\delta \mathbf{E}_e$ due to symmetry reduces to a vector with six components $\delta \mathbf{E}_e = \{E_{11}, E_{22}, E_{33}, E_{12}, E_{23}, E_{31}\}$ and the components are determined by

$$\delta E_{AB} = \sum_{a=1}^n [F_{Ak} N_{a,B} + N_{a,A} F_{kB}] \delta u_{ka}. \quad (2.8.40)$$

The product of the deformation gradient and the gradient of the shape function, that is summarized by the \mathbf{B} -matrix and can be written precisely as

$$\mathbf{B}_a = \begin{bmatrix} F_{11} N_{a,1} & F_{21} N_{a,1} & F_{31} N_{a,1} \\ F_{12} N_{a,1} & F_{22} N_{a,1} & F_{32} N_{a,1} \\ F_{13} N_{a,1} & F_{23} N_{a,1} & F_{33} N_{a,1} \\ F_{11} N_{a,2} + F_{12} N_{a,1} & F_{21} N_{a,2} + F_{22} N_{a,1} & F_{31} N_{a,2} + F_{32} N_{a,1} \\ F_{12} N_{a,3} + F_{13} N_{a,2} & F_{22} N_{a,3} + F_{23} N_{a,2} & F_{32} N_{a,3} + F_{33} N_{a,2} \\ F_{11} N_{a,3} + F_{13} N_{a,1} & F_{21} N_{a,3} + F_{23} N_{a,1} & F_{31} N_{a,3} + F_{33} N_{a,1} \end{bmatrix}. \quad (2.8.41)$$

The discretized variation of the Green Lagrange tensor can be inserted into eqn. 2.8.38, such that the internal virtual work can be approximated by

$$\mathcal{G}_e^{int} = \sum_{a=1}^n \delta \mathbf{u}_a \cdot \int_{\mathcal{B}_e} \mathbf{B}_a \cdot \mathbf{S} d\Omega, \quad (2.8.42)$$

where $\mathbf{S} = \{S_{11}, S_{22}, S_{33}, S_{12}, S_{23}, S_{31}\}$ represents the 2. Piola Kirchhoff stress in vectorial notation by exploiting its symmetry and that is already calculated on the constitutive level. For the integration over the element usually the standard *Gauss quadrature* is applied, where the particular „physical element” is transformed to the reference element. On the reference element the integration is performed and afterwards the re-transformations takes place. We do not present this method here, but a detailed description can be found in [Fel93], [Wei96] [Sch97] or [RS99].

The discretization of the external virtual work contribution can be easily performed by inserting the approximation of the virtual displacements into eqn. 2.8.38. We obtain

$$\mathcal{G}_e^{ext} = \int_{\mathcal{B}_e} \sum_{a=1}^n \mathbf{b} \cdot \delta \mathbf{u}_a N_a d\Omega + \int_{\partial \mathcal{B}_e} \sum_{a=1}^n \mathbf{t} \cdot \delta \mathbf{u}_a N_a d\Gamma = \sum_{a=1}^n \delta \mathbf{u}_a^t \cdot \left[\int_{\mathcal{B}_e} \mathbf{b} N_a d\Omega + \int_{\partial \mathcal{B}_e} \mathbf{t} N_a d\Gamma \right] \quad (2.8.43)$$

whereby the contribution due to surface forces only takes place at these element boundaries, which in fact coincides with the boundary of the particular structure $\partial \mathcal{B}_e \subset \partial \mathcal{B}_0$.

Finally, for completeness we want to consider here the inertial contribution to the virtual work

$$\mathcal{G}_e^{dyn} = \int_{\mathcal{B}_e} \rho_0 \dot{\mathbf{v}} \delta \mathbf{u} dv. \quad (2.8.44)$$

The crucial point here is, that it depends on time, such that it has to be discretized not only in space but also in time. Within the isoparametric concept the spatial approximations of the acceleration field are simply given by

$$\dot{\mathbf{v}} = \ddot{\mathbf{u}} = \sum_{a=1}^n \mathbf{N}_a \ddot{\mathbf{u}}_a, \quad (2.8.45)$$

whereby the acceleration field at the different element nodes are approximated by adequate approaches that are treated subsequently. Of course, we also have to replace the virtual displacement by its corresponding interpolation, such that we get

$$\mathcal{G}_e^{dyn} = \int_{\mathcal{B}_e} \rho_0 \sum_{a=1}^n \mathbf{N}_a \delta \mathbf{u}_a \sum_{b=1}^n \mathbf{N}_b \ddot{\mathbf{u}}_b d\Omega = \sum_{a=1}^n \sum_{b=1}^n \delta \mathbf{u}_a^t \cdot \left[\int_{\mathcal{B}_e} \mathbf{N}_a \rho_0 \mathbf{N}_b \mathbf{I} d\Omega \right] \cdot \ddot{\mathbf{u}}_b. \quad (2.8.46)$$

The aim in the sequel is to rewrite the discretized expressions in such a way, that the virtual displacement can be factored out. For this we introduce the following abbreviations

$$\mathbf{T}_a = \int_{\mathcal{B}_e} \mathbf{B} \cdot \mathbf{S}_e d\Omega, \quad \mathbf{L}_a = \int_{\mathcal{B}_e} \mathbf{b} \mathbf{N}_a d\Omega + \int_{\partial \mathcal{B}_e} \mathbf{t} \mathbf{N}_a d\Gamma, \quad \mathbf{M}_{ab} = \int_{\mathcal{B}_e} \mathbf{N}_a \rho_0 \mathbf{N}_b \mathbf{I} d\Omega, \quad (2.8.47)$$

and by inserting these quantities into eqns. 2.8.42, 2.8.43 and 2.8.46 we can write the discrete formulation of the element balance equation as

$$\mathcal{G}_e = \sum_{a=1}^n \sum_{b=1}^n \delta \mathbf{u}_a^t \cdot \mathbf{M}_{ab} \cdot \ddot{\mathbf{u}}_b + \sum_{a=1}^n \delta \mathbf{u}_a^t \cdot \mathbf{T}_a - \sum_{a=1}^n \delta \mathbf{u}_a^t \cdot \mathbf{L}_a. \quad (2.8.48)$$

Since we need the balance equation for the whole body we need to sum up over the whole number of elements n_e ,

$$\mathcal{G} = \bigcup_{e=1}^{n_e} \mathcal{G}_e \quad (2.8.49)$$

that is expressed by the union of all elements. This notation indicates, that the element contributions are organized in a particular manner within an assembly algorithm, that belongs to the standard finite element procedure and that we do not discuss here. The last step, however, leads to

$$\delta \mathbf{u}^t \cdot [\mathbf{M} \cdot \ddot{\mathbf{u}} + \mathbf{T}(\mathbf{u}) - \mathbf{L}] = 0, \quad \forall \delta \mathbf{u} \in \mathbb{R}^{dim \times n}, \quad (2.8.50)$$

that describes the global form of the discretized equilibrium equation. Since the virtual displacements can be chosen arbitrarily, eqn. 2.8.50 is only fulfilled, if the expression within the brackets gets zero

$$\mathbf{M} \cdot \ddot{\mathbf{u}} + \mathbf{T}(\mathbf{u}) - \mathbf{L} = \mathbf{0}. \quad (2.8.51)$$

This set of nonlinear algebraic equations represents the discretized formulation of the momentum balance equation in terms of the material configuration.

So far the time discretization is not taken into account and we just want to sketch a quite simple way to approximate the time dependent quantities. For this we assume a time increment $\Delta t = t_{n+1} - t_n$ and the velocity and acceleration vectors can be approximated by

$$\dot{\mathbf{u}} = \frac{\mathbf{u}_{n+1} - \mathbf{u}_n}{\Delta t} \quad \text{and} \quad \ddot{\mathbf{u}} = \frac{\mathbf{u}_{n+1} - 2\mathbf{u}_n + \mathbf{u}_{n-1}}{[\Delta t]^2}, \quad (2.8.52)$$

as they emanate from the finite difference method. Inserting these approximations into eqn. 2.8.51 it can be reformulated in terms of the displacements

$$\mathbf{M} \cdot [\mathbf{u}_{n+1} - 2\mathbf{u}_n + \mathbf{u}_{n-1}] = [\Delta t]^2 [\mathbf{L} - \mathbf{T}(\mathbf{u}_n)]. \quad (2.8.53)$$

Since the discrete formulation of the virtual work only consists of sum expressions where the displacements can be factored out and the discretized balance of momentum can be rewritten as

$$\mathbf{M} \cdot \mathbf{u}_{n+1} = [\Delta t]^2 [\mathbf{L} - \mathbf{T}(\mathbf{u}_n)] + \mathbf{M} \cdot [2\mathbf{u}_n - \mathbf{u}_{n-1}], \quad (2.8.54)$$

that describes a system of algebraic equations that can be solved directly for the new configuration represented by \mathbf{u}_{n+1} ⁹. In the case of quasistatic deformations the inertial contribution can be neglected, such that the eqn 2.8.51 reduces to

$$\mathbf{T}(\mathbf{u}) - \mathbf{L} = \mathbf{0}, \quad (2.8.55)$$

where no time dependent contributions occur anymore and it solely depends on the displacements. In the sequel we consider quasistatic problems, where the mechanical time dependent contributions are neglected, whereas the heat conduction within the thermal problem is predominant as we will see later on. Both types of problems act on different time scales, such that in the case of thermo-mechanically coupled problems, the 'mechanical time scale' is neglectible, since the mechanical processes go on very much faster than the heat conduction.¹⁰ Furthermore, we want to emphasize here once more that we took the assumption that the external loads are independent of the deformation, such that within the linearization procedure of the virtual work only the contribution caused by internal forces needs to be taken into account. The resulting system of nonlinear equations in eqn. 2.8.55 has to be solved by the Newton-Raphson method, that requires the linearization of the given residual. This linearization was already performed in one of the previous sections, namely with respect to the weak form. Therefore, the only thing left to do is to carry out the discretization of the linearized virtual work. In principle the linearization and discretization can be exchanged, but commonly the presented order is retained. Since we assumed the external virtual work as deformation independent, the linearization is restricted to the internal contribution, as it was derived in eqn. 2.8.22. It consists of two terms

$$D_x [\mathcal{G}^{int}] \cdot \Delta \mathbf{u} = \int_{\mathcal{B}_0} \left[\delta \bar{\mathbf{E}}^b : \bar{\mathbb{C}} : D_x [\bar{\mathbf{E}}^b] \cdot \Delta \mathbf{u} + [\text{Grad} \Delta \mathbf{u}] \cdot \bar{\mathbf{S}}^\# \cdot [\text{Grad} \delta \mathbf{u}] \right] dV \quad (2.8.56)$$

⁹There are better approximations for the time dependent quantities, but the chosen (explicit) approaches in eqn. 2.8.52 serve as a showcase to present exemplarily the common procedure to solve dynamic problems. In general one distinguishes between explicit and implicit methods, which differ from each other by assuming the actual configuration depending on the old time step t_n or considering the quantities $\ddot{\mathbf{u}}_{n+1}$, $\dot{\mathbf{u}}_{n+1}$ and \mathbf{u}_{n+1} as implicitly depending on each other. In this case we need to perform a linearization of the virtual work with respect to the actual configuration for being able to apply the Newton Raphson iteration scheme. However, since the linearization of the dynamic depends on the chosen time integration scheme and the approximations of the time dependent quantities, respectively, it is not possible to give a general representation of the linearization of the virtual work in the case of dynamic investigations. Within the framework of dynamic problems the research is concerned with investigations of efficient time integration schemes, which are energy and momentum conserving and which are sufficiently stable in a numerical sense. Since we do not consider dynamic problems subsequently, we refer to the following publications There is big number of publications dealing with this subject and we just want to mention some of them. There are publications of Simo & Tarnow [ST94], [ST92], Gonzales & Simo [GS00], Gonzales [Gon96a], [Gon96b], [Gon00], Betsch & Steinmann [BS00a], [BS00b], [BS02a], [BS02b] and the work Betsch [Bet02] and Groß [Gro04].

¹⁰This assumption is not valid anymore as soon as the load velocity is of the same order as the dynamical effects like wave propagation effects within the particular structure. High speed cutting or deep drawing processes for instance are dynamic processes, where the effects due to wave propagation possibly is not neglectible anymore.

and analogously to eqn. 2.8.42 we consider the stress tensor \mathbf{S} and the corresponding tangent operator \mathbb{C} as known from the constitutive level. The discretization of $\text{Grad}\Delta\mathbf{u}$ in eqn. 2.8.34 can be also adopted one by one to the interpolation of the incremental displacement, such that we get the approximation

$$\text{Grad}\Delta\mathbf{u}_e = \sum_{a=1}^n \Delta\mathbf{u}_a \otimes \nabla_X \mathbf{N}_a \quad (2.8.57)$$

and the discretization of the linearized Green Lagrange tensor can be derived from eqn. 2.8.39 by substituting the test function by the incremental element displacement vector, such that we obtain

$$\Delta\mathbf{E}_e = \frac{1}{2} \sum_{a=1}^n [\mathbf{F}_e^t \cdot [\Delta\mathbf{u}_a \otimes \nabla_X \mathbf{N}_a] + [\nabla_X \mathbf{N}_a \otimes \Delta\mathbf{u}_a] \cdot \mathbf{F}_e] = \sum_{a=1}^n \mathbf{B}_a \cdot \Delta\mathbf{u}_a. \quad (2.8.58)$$

With this at hand and the discretized virtual strain tensor in eqn. 2.8.39 the discrete linearization of the first term in eqn. 2.8.56 with respect to an element can be written as

$$\int_{\mathcal{B}_e} \delta \bar{\mathbf{E}}^b : \bar{\mathbb{C}} : D_x \bar{\mathbf{E}}^b d\Omega = \sum_{a=1}^n \sum_{b=1}^n \delta \mathbf{u}_a^t \cdot \left[\int_{\mathcal{B}_e} \bar{\mathbf{B}}_a^t \cdot \bar{\mathbf{D}} \cdot \bar{\mathbf{B}}_b d\Omega \right] \cdot \Delta \mathbf{u}_b. \quad (2.8.59)$$

Here $\bar{\mathbf{D}}$ denotes the incremental tangent matrix that corresponds to the algorithmic tangent operator \mathbb{C} and $[\bullet]$ indicates, that the quantity is evaluated at the last iteration step. Taking eqn. 2.8.57 into account the discretization of the second term in eqn. 2.8.56 is straight forward

$$\int_{\mathcal{B}_e} [\text{Grad}\Delta\mathbf{u}] \cdot \bar{\mathbf{S}}^\# \cdot [\text{Grad}\delta\mathbf{u}] d\Omega = \sum_{a=1}^n \sum_{b=1}^n \delta \mathbf{u}_a^t \cdot \left[\int_{\mathcal{B}_e} [\nabla_X \mathbf{N}_a]^t \cdot \mathbf{S}_e \cdot [\nabla_X \mathbf{N}_b] d\Omega \right] \cdot \Delta \mathbf{u}_b. \quad (2.8.60)$$

In both expressions the variation $\delta\mathbf{u}$ and the incremental displacements $\Delta\mathbf{u}$ can be factored out, such that summing up both contributions yields

$$D_x [\mathcal{G}_e^{int}] \cdot \Delta\mathbf{u} = \sum_{a=1}^n \sum_{b=1}^n \delta \mathbf{u}_a^t \cdot \bar{\mathbf{K}}_{e,ab} \cdot \Delta \mathbf{u}_b, \quad \text{with} \quad (2.8.61)$$

$$\bar{\mathbf{K}}_{e,ab} = \int_{\mathcal{B}_e} [[\nabla_X \mathbf{N}_a] \cdot \bar{\mathbf{S}}_e \cdot \nabla_X \mathbf{N}_b + \bar{\mathbf{B}}_a^t \cdot \bar{\mathbf{D}} \cdot \bar{\mathbf{B}}_b] d\Omega$$

whereby $\bar{\mathbf{K}}_e$ denotes the so-called element tangent stiffness matrix. The corresponding arrangement within the assembly procedure leads to the global stiffness matrix

$$\delta \mathbf{u}^t \cdot \mathbf{K} \cdot \Delta \mathbf{u} = \bigcup_{e=1}^{n_e} \sum_{a=1}^n \sum_{b=1}^n \delta \mathbf{u}_a^t \cdot \bar{\mathbf{K}}_{e,ab} \cdot \Delta \mathbf{u}_b. \quad (2.8.62)$$

With this at hand we have found a complete numerical description of the mechanical problem that enables one to find the configuration describing the equilibrium state of a body for given loads. If we consider eqn. 2.8.15 we can write the discrete linear approximation of the linear momentum balance equation as

$$\delta \mathbf{u}^t \cdot [\mathbf{R}(\mathbf{u}) + \mathbf{K} \cdot \Delta \mathbf{u}] = 0, \quad \forall \delta \mathbf{u} \in \mathbb{R}^{dim \times n}. \quad (2.8.63)$$

Here the residual $\mathbf{R}(\mathbf{u}) = \mathbf{T}(\mathbf{u}) - \mathbf{L}$ summarizing the internal and external forces and \mathbf{K} corresponds to the global tangent stiffness matrix, that coincides with the gradient of the given residual. Therefore the Newton-Raphson iteration scheme is applicable to the expression within the brackets

$$\mathbf{K} \cdot \Delta \mathbf{u} = -\mathbf{R}(\mathbf{x}^k), \quad \text{with} \quad \mathbf{x}^{k+1} = \mathbf{x}^k + \Delta \mathbf{u}. \quad (2.8.64)$$

Here the residual expression and the stiffness matrix are evaluated at the last iteration step k within the $n + 1^{st}$ load step.

2.8.5 Discretization of the Weak Form in Terms of the Cauchy Stress

Analogously to the discretization of the weak form in terms of the Piola stress the discretization can be performed in terms of the Cauchy stress setting and some results of the previous section can also be used here. We again start from the weak form in eqn. 2.9.62, but with respect to an element, that is represented by

$$\mathcal{G}_e = \int_{\mathcal{B}_e} \boldsymbol{\sigma}^\# : \delta \mathbf{e}^b d\Omega - \int_{\mathcal{B}_e} [\mathbf{b} - \rho \dot{\mathbf{v}}] \cdot \delta \mathbf{u} d\Omega - \int_{\partial \mathcal{B}_e} \mathbf{t} \cdot \delta \mathbf{u} d\Gamma. \quad (2.8.65)$$

At first we discretize the variation of the Almansi strain tensor in eqn. that is given by

$$\delta \mathbf{e}_e = \frac{1}{2} \sum_{a=1}^n [\delta \mathbf{u} \otimes \nabla_x \mathbf{N}_a + \nabla_x \mathbf{N}_a \otimes \delta \mathbf{u}] = \sum_{a=1} \mathbf{B}_a^s \cdot \delta \mathbf{u}_a, \quad (2.8.66)$$

where eqn. 2.8.34 is taken into account. Comparing eqn. 2.8.66 and eqn. 2.8.39 it is clear, that the \mathbf{B} -matrices in both formulations are different. This is taken into account by the superscript index s and in this present context the \mathbf{B}^s -matrix for a certain node a is defined by

$$\mathbf{B}_a^s = \begin{bmatrix} N_{a,1} & 0 & 0 \\ 0 & N_{a,2} & 0 \\ 0 & 0 & N_{a,3} \\ N_{a,2} & N_{a,1} & 0 \\ 0 & N_{a,3} & N_{a,2} \\ N_{a,3} & 0 & N_{a,1} \end{bmatrix}. \quad (2.8.67)$$

Since this \mathbf{B}^s -matrix has much less entries, this finite element formulation is more efficient than the formulation in terms of the Piola stress. Inserting eqn. 2.8.66 into the spatial internal virtual work we obtain

$$\mathcal{G}_e = \sum_{a=1}^n \delta \mathbf{u}_a^t \cdot \int_{\mathcal{B}_e} [\mathbf{B}_a^s]^t \cdot \boldsymbol{\sigma}_e d\Omega = \sum_{a=1}^n \delta \mathbf{u}_a^t \cdot \mathbf{T}^s, \quad \text{with} \quad \mathbf{T}^s = \int_{\mathcal{B}_e} [\mathbf{B}_a^s]^t \cdot \boldsymbol{\sigma}_e d\Omega, \quad (2.8.68)$$

whereby the Cauchy stress vector $\boldsymbol{\sigma}_e = \{\sigma_{11}, \sigma_{22}, \sigma_{33}, \sigma_{12}, \sigma_{23}, \sigma_{31}\}$ is calculated in the constitutive routine. The interpolation of the external and inertial virtual work contributions do not alter very much from the formulation in terms of the Piola stress except for the factor J . Therefore we can adopt them one by one, such that the discretization of the weak form yields the general form

$$\delta \mathbf{u}^t \cdot [\mathbf{M}^s \cdot \ddot{\mathbf{u}}^s + \mathbf{T}^s(\mathbf{u}) - \mathbf{L}^s] \quad \forall \delta \mathbf{u} \in \mathbb{R}^{dim \times n} \quad (2.8.69)$$

where the index $[\bullet]^s$ indicates, that we consider the formulation in terms of the Cauchy stress. The global formulation is obtained from the summation over all elements within an assembly procedure. As we learned from the previous sections the linearization restricts to the internal virtual work, since we consider quasistatic deformations and the external forces are assumed to be independent of the deformation. The linearized formulation consists of two terms and can be rewritten as

$$D_x [\mathcal{G}^{int}] \cdot \Delta \mathbf{u} = \int_{\mathcal{B}_e} [\text{grad} \delta \mathbf{u} \cdot \boldsymbol{\sigma}^\# \cdot \text{grad} \Delta \mathbf{u} + \text{grad} \delta \mathbf{u} : \mathbb{c} : \text{grad} \Delta \mathbf{u}] d\Omega. \quad (2.8.70)$$

Taking eqn. 2.8.33 and 2.8.57 into account the discretization of the linearized internal virtual work contribution can easily be written as

$$D_x [\mathcal{G}^{int}] \cdot \Delta \mathbf{u} = \sum_{a=1}^n \sum_{b=1}^n \delta \mathbf{u}_a^t \cdot \left[\int_{\mathcal{B}_e} [(\nabla_x \mathbf{N}_a)^t \cdot \bar{\boldsymbol{\sigma}}_e \cdot \nabla_x \mathbf{N}_b + [\mathbf{B}_a^s]^t \cdot \bar{\mathbf{D}}^s \cdot \mathbf{B}_b^s] d\Omega \right] \cdot \Delta \mathbf{u}_b \quad (2.8.71)$$

and the element stiffness matrix can be identified by

$$\mathbf{K}_a^s = \int_{\mathcal{B}_e} [(\nabla_x \mathbf{N}_a)^t \cdot \bar{\boldsymbol{\sigma}}_e \cdot \nabla_x \mathbf{N}_b + [\mathbf{B}_a^s]^t \cdot \bar{\mathbf{D}}^s \cdot \mathbf{B}_a^s] d\Omega. \quad (2.8.72)$$

The global formulation can be derived by assembling all elements into the global tangent stiffness matrix, such that the corresponding system of linearized algebraic equations is given by

$$\mathbf{K}_s \cdot \Delta \mathbf{u} = -\mathbf{R}(\mathbf{x}^k), \quad \text{with} \quad \mathbf{x}^{k+1} = \mathbf{x}^k + \Delta \mathbf{u}. \quad (2.8.73)$$

The solution is performed by the Newton-Raphson iteration scheme, that shows a quadratic convergence behaviour. In the case of constitutive laws considering (ductile) damage, one can recognize a mesh dependence of the finite element solution, that means, the finer the geometry is mapped by the mesh, the smaller the damage zone is represented. To avoid this size effect and the associated ill-posedness of the mathematical problem, so-called regularization methods were developed. Within these methods an intrinsic length scale is introduced, that relates the microscopic processes to the macroscopic continuum description. Furthermore not only the information of the microstructure at a local point is taken into account, but also the state of surrounding points are incorporated, whereby the intrinsic scale determines the considered neighbouring points. This proceeding leads to a non-local material formulation. Important keywords in this context are homogenization or the gradient theory, where hardening or damage variables for instance, are introduced as global variables. This topic is very important in the research of computational mechanics, but to present these theories would extend the aim of this work, such that we restrict ourselves to refer to the work of Askes [Ask00], where the different regularisation methods are introduced. Here the author attempted to circumvent the problem by certain mesh adaptivity strategies within the finite element method or by meshless methods like the element free Galerkin method. Askes & Sluys [AS00] attempted to overcome the problem of strain localisation by appropriate remeshing strategies. In Eringen [Eri02], Askes & Aifantis [AA02] or Liebe [Lie03] the gradient theory is treated in detail.

2.9 Thermo-Mechanical Problems

In many technical processes the temperature is not negligible and the isothermal considerations fail. In particular the production of technical components, as there are machining or deep drawing

processes for instance, requires a better understanding of thermomechanically coupled problems. There are a lot of investigations concerned with providing appropriate constitutive propositions and optimized solution algorithms for this kind of problem. For the description of thermal effects on the concepts of hyperelasticity in terms of large strains we refer to Miehe [Mie95], Holzapfel [Hol01], Wilmanski [Wil99], Reese [Ree01], Ibrahimbegovic *et al.* [ICG01]. Here we want to present a completely thermo-mechanically coupled large strain formulation in consideration of plasticity. A fundamental and exhaustive contribution on this subject is the work of Simo & Miehe [SM92], who present a complete formulation of a model of associated thermoelastoplasticity for large deformations. They introduce a plastic entropy as an independent internal variable and extend the principle of maximum dissipation to thermo-elastoplastic deformations conserving the multiplicative decomposition of the deformation gradient. Based on this they are able to generalize the principle of associativity. Furthermore, the paper presents a product formula algorithm that leads to two step algorithm, where the thermal and the mechanical subproblems are solved separately. Parts of this work can be also found in Miehe [Mie88] and [Mie92]. Other contributions on the matter of thermo-plasticity in terms of large deformations can be found in the work of Argyris & Doltsinis [AD81], Argyris *et al.* [ADPW82], Miehe [Mie94], Celigoj [Cel98], Simo in 1998 [Sim98], Ibrahimbegovic & Chorfi [IC02].

In section 2.4 we introduced the 1st law of thermodynamics, that teaches us that we have to distinguish mechanical and thermal energy and that they can be transformed to each other.

In most technical applications the thermal effects can not be considered separately from the mechanical problem. Therefore the isothermal considerations as we performed them in the previous sections is not realistic and the thermal effects have to be taken into account. In general the processes are thermo-mechanically coupled. In the sequel we distinguish between two kinds of thermo-mechanically processes. In the first case we assume that no heat flux takes place and the system is only effected by internal heat sources and mechanical loads. This kind of process is called *locally coupled* or *adiabatic*, whereas a problem is denoted by *globally coupled*, if also a heat flux has to be taken into account. The dilatation of a body due to external heating is a simple example of a globally coupled problem. An adiabatic process is given if the mechanical loading is performed very fast, such that the heat flux can be neglected during the deformation. In experimental investigations for the identification of parameters for instance, one tries to exclude thermal effects from experiments by superposing the load in a quasi-static manner. The thermal effects due to mechanical loads become stronger the faster the deformation takes place, such that we have to register a relation of deformation velocity and temperature increase. As we mentioned before, the 1st law of thermodynamics is predestinated as a starting point for the derivation of relations, which are able to describe the thermo-mechanical interaction. In particular we need a relation, that determines the temperature evolution due to thermal and mechanical load. In analogy to the pure mechanical case, where the mechanical attributes of a material were described by an elastic potential, it is assumed that its thermal behaviour be described by a potential function as well. Therefore we extend the isotropic strain energy function

$$W(\mathbf{b}_e^\sharp, \xi, \Theta) = \rho_0 \Psi(\mathbf{b}_e^\sharp, \xi, \Theta) \quad (2.9.1)$$

by assuming an additional dependence on the temperature. By the Legendre transformation the free energy can be related to the entropy and the internal energy

$$u = \Psi + \Theta s, \quad (2.9.2)$$

such that it is useful for the subsequent derivations to replace the strain energy function by the product of initial density and free energy. The particular formulation of the thermo-mechanical

potential will be specified later on, but we want to assume that a hyperelasto-plastic material of the von-Mises type with hardening behaviour is considered, such that we have to take an internal variable ξ into account.

2.9.1 Temperature Evolution

In order to derive a evolution equation for the temperature we start from eqn. 2.4.10, that defines the alteration of the internal energy u with respect to time and it is expressed with respect to quantities in the current configuration. We rewrite this balance equation per unit volume of the initial configuration and obtain an expression

$$\rho_0 \dot{u} = \boldsymbol{\tau}^\# : \mathbf{d}^p - J \operatorname{div} \mathbf{q} + \rho_0 r, \quad (2.9.3)$$

that is the local form of the 1. law of thermodynamics in terms of the Kirchhoff stress. Taking the Legendre transformation into account, that we performed in eqn. 2.9.2, we can replace the rate of internal energy by

$$\rho_0 \dot{u} = \rho_0 \dot{\Psi} + \rho_0 s \dot{\Theta} + \rho_0 \Theta \dot{s}. \quad (2.9.4)$$

Inserting this expression for the rate of the internal energy and in consideration of eqn. 2.9.1 we can rewrite the rate of the free energy function by its total differential, such that we can rewrite eqn. 2.9.3 as

$$2\rho_0 \frac{\partial \Psi}{\partial \mathbf{b}_e^\#} \cdot \dot{\mathbf{b}}_e^\# + \rho_0 \frac{\partial \Psi}{\partial \xi} \dot{\xi} + \rho_0 \frac{\partial \Psi}{\partial \Theta} \dot{\Theta} + \rho_0 \Theta \dot{s} + \rho_0 s \dot{\Theta} = \boldsymbol{\tau}^\# : \mathbf{d}^p - J \operatorname{div} \mathbf{q} + \rho_0 r. \quad (2.9.5)$$

In this representation we can identify the Kirchhoff stress and the hardening stress, which were defined by the derivatives of the free energy function with respect to the elastic left Cauchy Green tensor and the internal hardening variable, respectively. In addition to that we now want to define here

$$\frac{\partial \Psi(\mathbf{b}_e^\#, \xi, \Theta)}{\partial \Theta} := -s(\mathbf{b}_e^\#, \xi, \Theta), \quad (2.9.6)$$

that the derivative of the free energy function with respect to the temperature coincides with the negative entropy. With this at hand we can eliminate the entropy-dependent terms in eqn. 2.9.3, but not the terms where the entropy rate is involved. However, we can derive the entropy rate by considering the total differential of eqn. 2.9.6

$$\dot{s} = -\frac{\partial^2 \Psi}{\partial \Theta^2} \dot{\Theta} - \frac{\partial^2 \Psi}{\partial \Theta \partial \mathbf{b}_e^\#} \dot{\mathbf{b}}_e^\# - \frac{\partial^2 \Psi}{\partial \Theta \partial \xi} \dot{\xi}. \quad (2.9.7)$$

Inserting this relation into eqn. 2.9.5 and taking the definition of the local dissipation in eqn. 2.6.41 into account, the eqn. 2.9.3 can be represented by

$$-D_{loc} - \rho_0 \Theta \frac{\partial^2 \Psi}{\partial \Theta^2} \dot{\Theta} - \rho_0 \Theta \frac{\partial^2 \Psi}{\partial \Theta \partial \mathbf{b}_e^\#} \dot{\mathbf{b}}_e^\# - \rho_0 \Theta \frac{\partial^2 \Psi}{\partial \Theta \partial \xi} \dot{\xi} = -J \operatorname{div} \mathbf{q} + \rho_0 r. \quad (2.9.8)$$

At this point we need to specify the form of the strain energy or the free energy function, respectively, since we need to compute the derivatives occurring in the previous equation. Here we want to follow

the suggestion given by Miehe [Mie92], where the thermomechanical potential is assumed to consists of the following five contributions

$$W(\mathbf{b}_e^\sharp, \xi, \Theta) = W_{vol}(J) + W_{iso}(\tilde{\lambda}_\alpha) + W_{mic}(\xi) + W_{eth}(J, \Theta) + W_{th}(\Theta). \quad (2.9.9)$$

The first three terms in eqn. 2.9.9 can be identified by the same contributions as in the isothermal case (eqn. 2.6.67) where we distinguished between the volumetric, the ischoric and the micromechanical contribution taking the hardening effects into account. Furthermore we enriched the strain energy function by two additional temperature dependent terms W_{eth} and W_{th} , whereby one of them additionally depends on the deformation. From this terms emanates the thermal stress, whereby it is of volumetric nature, since it is a function of J . The thermoelastic potential is chosen as

$$W_{eth} = -3\alpha\Delta\vartheta \frac{\partial W_{vol}}{\partial J} = -3\alpha\kappa\Delta\vartheta \ln J, \quad \text{with} \quad \Delta\vartheta = \Theta - \Theta_0, \quad (2.9.10)$$

whereby Θ_0 defines a reference temperature. Of course a strong restriction is made here since we assume that the thermomechanical coupling only depends on the volumetric part of the thermomechanical potential. Of course, in general also the deviatoric part can be defined as temperature-dependent, such that an contribution of the free energy function can be assumed like $\Psi = \Psi(\tilde{\lambda}_\alpha, \Theta)$. But to keep things more simple in our formulation we just introduced an indirect temperature dependence since we assumed that the initial yield stress is reduced due to higher temperatures. These relations were already discussed in section 2.6.8.

The previous assumptions additionally yield the subsequent identities

$$\rho_0\Theta \frac{\partial^2 \Psi}{\partial \xi \partial \Theta} = 0, \quad \text{and} \quad \rho\Theta \frac{\partial^2 \Psi}{\partial J \partial \Theta} = -\frac{3\kappa\alpha\Theta}{J}. \quad (2.9.11)$$

Furthermore, it is common to define the double derivative with respect to the temperature as a constant

$$-\Theta \frac{\partial^2 \Psi}{\partial \Theta \partial \Theta} := c_p, \quad (2.9.12)$$

whereby this quantity is denoted by *heat capacity*. From this definition the corresponding potential can be constructed by integrating eqn.2.9.12 with respect to the temperature, such that we obtain for the purely thermal potential

$$W_{th} = c_p \left[\Theta - \Theta_0 - \Theta \ln \frac{\Theta}{\Theta_0} \right]. \quad (2.9.13)$$

This completes the thermomechanical potential and we are able to specify the internal energy expression, but before we come to that, we want to reformulate the local dissipation in a more comfortable way. For this we rewrite the dissipation inequality in terms of the yield function, such that we obtain

$$D_{loc} = \boldsymbol{\tau}^\sharp : \mathbf{d}_p^\flat - Y_n \dot{\xi} = \dot{\gamma} \sqrt{\frac{2}{3}} H(\Theta), \quad (2.9.14)$$

whereby the yield function has to be zero in the case of plastic flow and in the elastic case no local dissipation takes place. That means, that the local dissipation can be reduced to an expression only depending on the initial yield stress. This does not coincide with experimental observations, which show that the hardening process is indeed a dissipative one, such that the initial yield stress in eqn.

2.9.14 is replaced by the resulting yields stress $Y_n(\xi, \Theta)$ and furthermore it is common to introduce a constant factor $\chi < 1$, that weights the dissipation, such that the temperature evolution can be rewritten as

$$\rho_0 c_p \dot{\Theta} = D_{loc} + Q_{eth} - J \operatorname{div} \mathbf{q} + \rho_0 r + \Theta \partial_{\Theta} D_{loc} \quad \text{with} \quad Q_{eth} = -3\kappa\alpha\Theta \operatorname{tr}(\mathbf{d}^p). \quad (2.9.15)$$

Here we solved for the term including the temperature rate, such that we obtain the temperature evolution equation in consideration of thermomechanical coupling, where elastoplasticity of the von-Mises type is taken into account.

The last term in eqn. 2.9.15 emanates from eqn. 2.6.41 where the definition of the local dissipation for the isothermal case is introduced and that was reformulated in eqn. 2.9.14 in terms of the temperature-dependent resulting Yield Stress. This definition can be recovered again in eqn. 2.9.8 whereby here additionally a derivative with respect to temperature was performed, such that in the end we obtain

$$-\rho\Theta \frac{\partial^2 \Psi}{\partial \Theta \partial \mathbf{b}_e^{\sharp}} : \mathbf{b}_e^{\sharp} \quad (2.9.16)$$

In the case of the inelastic material models of the Gurson-type or the Lemaitre-type the derived equation would have to be specified accordingly. Furthermore we like to note here, that the terms describing the heat power are untouched by all the derivations, that were previously performed.

2.9.2 The Thermomechanically Coupled Problem

Before we try to transform the thermo-mechanical formulation into its weak form and try to prepare it for the finite element method we want to achieve a clear summary of the coupled problem. There are two coupled subproblems consisting of the linear momentum balance equation and the balance of internal energy

$$\begin{aligned} \rho \dot{\mathbf{v}} &= \operatorname{div} \boldsymbol{\sigma}^{\sharp} + \mathbf{b} \\ \rho c_p \dot{\Theta} &= -\operatorname{div} \mathbf{q} + D_{loc} + \rho r + Q_{eth} + \Theta \partial_{\Theta} D_{loc}, \end{aligned} \quad (2.9.17)$$

whereby Q_{eth} describes the thermomechanical coupling. Usually there are no additional heat sources r and the heat only increases due to thermo-mechanical coupled deformations or the heat flux. Since both subproblems are time dependent we have to prescribe initial conditions, for the motion $\boldsymbol{\varphi}(t)$, the velocity $\mathbf{v}(t)$ and the temperature $\Theta(t)$

$$\begin{aligned} \boldsymbol{\varphi}(t = t_0) &= \boldsymbol{\varphi}_0 & \text{in } \mathcal{B}_0 \\ \mathbf{v}(t = t_0) &= \mathbf{v}_0 & \text{in } \mathcal{B}_0 \\ \Theta(t = t_0) &= \Theta_0 & \text{in } \mathcal{B}_0 \end{aligned} \quad (2.9.18)$$

and for the wellposedness of the initial boundary value problem we have to define boundary values of the Dirichlet and the Neumann type for the mechanical and for the thermal field as well

$$\begin{aligned} \mathbf{u} &= \bar{\mathbf{u}} & \text{on } \partial \mathcal{B}_u & \quad \boldsymbol{\sigma}^{\sharp} \cdot \mathbf{n} = \bar{\mathbf{t}} & \text{on } \partial \mathcal{B}_{\sigma} \\ \Theta &= \bar{\Theta} & \text{on } \partial \mathcal{B}_{\Theta} & \quad \mathbf{q} \cdot \mathbf{n} = q_n & \text{on } \partial \mathcal{B}_q. \end{aligned} \quad (2.9.19)$$

Taking the constitutive relations into account completes the description of the problem in its *strong representation* and we can continue to derive the equivalent weak formulation. In the subsequent representation we restrict ourselves to the thermal subproblem, since the mechanical subproblem coincides with isothermal case we discussed in the previous sections. Naturally, the required modifications and extensions are considered.

2.9.3 Weak Form of the Thermomechanical Problem

The aim is to transform the energy balance equation into a weak form to solve the coupled problem numerically by the finite element method. In contrast to the adiabatic case, that we consider at the end of this section, here the temperature and the temperature gradient are introduced as additional primary variables, such that the linearization procedure has to be modified if the Newton-Raphson iteration scheme has to be applied. Point of departure is the strong form of the energy balance equation and we obtain the variational form by testing and integrating it over the considered domain, namely the actual configuration \mathcal{B}_t

$$\mathcal{U} = \int_{\mathcal{B}_t} \left[-\rho c_p \dot{\Theta} - \operatorname{div} \mathbf{q} + \tilde{r} \right] \delta \Theta dv = 0, \forall \delta \Theta \in \mathbb{R}. \quad (2.9.20)$$

Here $\delta \Theta$ is the test function and can be understood as the virtual temperature, analogous to the virtual displacements. \tilde{r} combines all terms which can be considered somehow as „sources“ and therefore it also includes the dissipation and the thermal stress. Furthermore, we can apply the partial integration method to the heat conduction, such that we obtain

$$- \int_{\mathcal{B}_t} \operatorname{div} \mathbf{q} \delta \Theta dv = - \int_{\mathcal{B}_t} \operatorname{div} [\mathbf{q} \delta \Theta] dv + \int_{\mathcal{B}_t} \mathbf{q} \cdot \operatorname{grad} \delta \Theta dv. \quad (2.9.21)$$

Here the Gauss theorem can be applied to the first term in eqn. 2.9.21, such that we can introduce $q_n = -\mathbf{q} \cdot \mathbf{n}$, that defines the boundary condition at $\partial \mathcal{B}_t$ of the Neumann type. The unit vector \mathbf{n} acts in normal direction to the surface, such that an incoming heat flux becomes positiv. With this at hand the virtual thermal energy can be written as

$$\mathcal{U} = \int_{\mathcal{B}_t} \left[-\rho c_p \dot{\Theta} \delta \Theta + \mathbf{q} \cdot \operatorname{grad} \delta \Theta + \tilde{r} \delta \Theta \right] dv + \int_{\partial \mathcal{B}_t} q_n \delta \Theta da = 0, \forall \delta \Theta \in \mathbb{R}. \quad (2.9.22)$$

This represents the weak form of the energy balance equation in terms of the spatial configuration, whereby also here the equation can be splitted into an internal and an external contribution

$$\mathcal{U} = \mathcal{U}^{int} - \mathcal{U}^{ext}$$

$$\mathcal{U}^{int} = \int_{\mathcal{B}_t} \left[-\rho c_p \dot{\Theta} \delta \Theta + \mathbf{q} \cdot \operatorname{grad} \delta \Theta \right] dv, \quad \mathcal{U}^{ext} = - \int_{\partial \mathcal{B}_t} q_n \delta \Theta da - \int_{\mathcal{B}_t} \tilde{r} \delta \Theta dv. \quad (2.9.23)$$

Here we can insert the Fourier heat conduction law where the heat flux vector is proportional to the negative temperature gradient, such that we obtain for the virtual energy contribution due to heat conduction

$$\mathcal{U}_{con} = - \int_{\mathcal{B}_t} \operatorname{grad} \delta \Theta \cdot \boldsymbol{\kappa} \cdot \operatorname{grad} \Theta dv. \quad (2.9.24)$$

The transformation to the corresponding material formulation can be obtained by a pull back operation of the spatial temperature gradient

$$\operatorname{Grad} \Theta = [\mathbf{F}^{\natural}]^t \cdot \operatorname{grad} \Theta \quad (2.9.25)$$

Applying this transformation also to the gradient of the virtual temperature field we can rewrite the energy balance equation (eqn. 2.9.22) with respect to the reference configuration and obtain

$$\mathcal{U} = \int_{\mathcal{B}_0} \left[-\rho_0 c_p \dot{\Theta} \delta \Theta - [\text{Grad} \Theta]^t \cdot \boldsymbol{\kappa}_0 \cdot \text{Grad} \delta \Theta + J \tilde{r} \delta \Theta \right] dV - \int_{\partial \mathcal{B}_0} Q_n \delta \Theta dA = 0, \forall \delta \Theta \in \mathbb{R}. \quad (2.9.26)$$

Here the material heat conduction tensor $\boldsymbol{\kappa}_0 = J \mathbf{f}^\sharp \cdot \boldsymbol{\kappa} \cdot [\mathbf{f}^\sharp]^t$ includes the transformation to the reference configuration and if we assume an isotropic heat conduction behaviour in the undeformed configuration we replace the spatial heat conduction tensor by

$$\boldsymbol{\kappa} = \varkappa \mathbf{b}^\sharp, \quad (2.9.27)$$

such that the energy contribution due to heat conduction in terms of the material setting is represented by

$$\mathcal{U}_{con} = -\varkappa_0 \int_{\mathcal{B}_0} \text{Grad} \Theta \cdot \mathbf{G}^\sharp \cdot \text{Grad} \delta \Theta dV \quad \text{with} \quad \varkappa_0 = J \varkappa. \quad (2.9.28)$$

This relation shows that the spatial heat conduction term depends on the deformation and a corresponding linearization with respect to the displacement field has to be performed.

2.9.4 Linearization and Discretization of the Thermomechanical Problem

The weak formulation of the thermal subproblem needs to be linearized in analogy to the linear momentum balance equation. Since we have to consider the coupling between both subproblems, we have to perform the linearization not only with respect to the temperature, but also with respect to the displacements, such that we obtain

$$D[\mathcal{U}] = D_\Theta[\mathcal{U}] \Delta \Theta + D_x[\mathcal{U}] \cdot \Delta \mathbf{u}. \quad (2.9.29)$$

Naturally, we also have to extend the linearization of the linear momentum balance equation by an thermal contribution describing the alteration of the mechanical subproblem due to temperature changes. But at first we want to consider the linearization of the thermal problem. In this case it is useful to approximate the temperature rate by

$$\dot{\Theta} \approx \frac{\Theta_{n+1} - \Theta_n}{\Delta t} \quad (2.9.30)$$

and in contrast to the mechanical problem, we want to perform the discretization before the linearization procedure. For this we introduce the interpolation of the temperature and its variation

$$\Theta = \sum_{a=1}^n \mathbf{M}_a \Theta_a, \quad \delta \Theta = \sum_{a=1}^n \mathbf{M}_a \delta \Theta_a \quad (2.9.31)$$

and the corresponding gradient formulations with respect to the spatial and the material setting are approximated by

$$\begin{aligned} \text{Grad} \Theta &= \sum_{a=1}^n \nabla_X \mathbf{M}_a \Theta_a, & \text{Grad} \delta \Theta &= \sum_{a=1}^n \nabla_X \mathbf{M}_a \delta \Theta_a, \\ \text{grad} \Theta &= \sum_{a=1}^n \nabla_x \mathbf{M}_a \Theta_a, & \text{grad} \delta \Theta &= \sum_{a=1}^n \nabla_x \mathbf{M}_a \delta \Theta_a. \end{aligned} \quad (2.9.32)$$

The insertion of these approximations into the weak form yields the discretized form of the thermal balance equation, whereby we restrict ourselves again to a single finite element of the body $\mathcal{B}_e \subset \mathcal{B}_t$. For the internal contribution we obtain

$$\mathcal{U}_e^{int} = \int_{\mathcal{B}_e} \sum_{a=1}^n \left[\frac{\rho c_p}{\Delta t} [\Theta_{n+1} - \Theta_n] M_a \delta \Theta_a - \text{grad}_x \Theta \cdot \boldsymbol{\kappa} \cdot \nabla_x M_a \delta \Theta_b \right] d\Omega \quad (2.9.33)$$

and the linearization of this term with respect to the temperature increment renders

$$D_{\Theta} [\mathcal{U}^{int}] \Delta \Theta = \sum_{a=1}^n \sum_{b=1}^n \delta \Theta_a \int_{\mathcal{B}_e} \left[\frac{\rho c_p}{\Delta t} M_a M_b - \nabla_x M_a \cdot \boldsymbol{\kappa} \cdot \nabla_x M_b \right] \Delta \Theta_b d\Omega \quad (2.9.34)$$

For the discretization of the external contribution we replace the abbreviation \tilde{r} again and by inserting the interpolation of the virtual temperature $\delta \Theta$ we obtain

$$\mathcal{U}_e^{ext} = \sum_{a=1}^n \delta \Theta_a \int_{\mathcal{B}_e} [D_{loc}^p - 3\kappa\alpha\Theta \text{div} \dot{\mathbf{u}} + \rho_0 r] M_a d\Omega. \quad (2.9.35)$$

Here the first and the second term of this equation are temperature dependent, such that they must be considered in the linearization prozess, whereas the boundary term is assumed to be given and is unimportant for the linearization. The temperature derivative of the dissipation yields

$$\partial_{\Theta} D_{loc}^p = \partial_{\Theta} \left[\frac{\Delta \gamma}{\Delta t} \chi \sqrt{\frac{2}{3}} Y_n(\xi, \Theta) \right] = \sqrt{\frac{2}{3}} \frac{\chi}{\Delta t} \left[\frac{\partial \Delta \gamma}{\partial \Theta} + \Delta \gamma \frac{\partial Y_n}{\partial \Theta} + \Delta \gamma \frac{\partial Y_n}{\partial \xi} \frac{\partial \xi}{\partial \Delta \gamma} \frac{\partial \Delta \gamma}{\partial \Theta} \right]. \quad (2.9.36)$$

Here the derivative of the plastic multiplier needs to be determined and this quantity can be calculated from the yield function, whereby we differentiate the yield function with respect to the temperature and obtain for the corresponding derivative

$$\frac{\partial \Delta \gamma}{\partial \Theta} = - \frac{\sqrt{\frac{2}{3}} \partial_{\Theta} Y_n}{2\mu + \frac{2}{3} \partial_{\xi} Y_n} \quad (2.9.37)$$

This relation inserted into eqn. 2.9.36 completes the linearization of the dissipation. Finally we have to linearize the second term in eqn. 2.9.35, that describes the thermoelastic coupling of the external energy contribution. The linearization of this term is straight forward and we obtain

$$\partial_{\Theta} Q_{eth} = -3\kappa\alpha \text{tr}(\mathbf{d}^p). \quad (2.9.38)$$

This completes the linearization of the external energy contribution, such that in the end we obtain a tangent stiffness matrix of the thermal subproblem with respect to the temperature

$$\mathbf{K}_e^{\Theta\Theta} = \bigcup_{a=1}^n \bigcup_{b=1}^n \left[\int_{\mathcal{B}_e} M_a \left[\frac{\rho c_p}{\Delta t} + \partial_{\Theta} D_{loc}^p + \partial_{\Theta} Q_{eth} \Delta t \right] M_b d\Omega + \int_{\mathcal{B}_e} \chi \nabla_x M_a \cdot \mathbf{b} \cdot \nabla_x M_b d\Omega \right] \quad (2.9.39)$$

As already suggested in eqn. 2.9.29 the thermal subproblem also depends on the deformation, such that we need to linearize the energy balance equation additionally with respect to the displacements. This yields the thermo-mechanical coupling between both subproblems beneath the

thermo-mechanical interaction of the mechanical subproblem, that also yields a coupling contribution. These two coupling terms are derived in the sequel and we start with the linearization of the thermal field with respect to the displacements. At first we consider the heat conduction term in eqn. 2.9.24, that depends on the temperature gradient with respect to the spatial configuration and the corresponding material formulation was derived in eqn. 2.9.28. Here it is straight forward to see that this term does not depend on the displacement field, such that the corresponding linearization becomes zero ¹¹

$$D_x [\mathcal{U}_{con}] \Delta \mathbf{u} = 0. \quad (2.9.40)$$

Furthermore, there is the thermoelastic contribution, that depends on J and therefore also on the deformation. The corresponding linearization can be derived from

$$D_x [J] \cdot \Delta \mathbf{u} = J [\mathbf{f}^\sharp]^t \cdot [\mathbf{F}^\sharp]^t \text{grad} \Delta \mathbf{u} = J \text{div} \Delta \mathbf{u} \quad (2.9.41)$$

and by taking this result into account, the linearization of the elasto-thermal contribution yields

$$D_x [\mathcal{Q}_{eth}] \cdot \Delta \mathbf{u} = \frac{\partial \mathcal{Q}_{eth}}{\partial J} \frac{\partial J}{\partial \mathbf{u}} \Delta \mathbf{u} = \frac{\partial \mathcal{Q}_{eth}}{\partial J} J \text{div} \Delta \mathbf{u} = \frac{\partial \mathcal{Q}_{eth}}{\partial J} J \mathbf{g}^\sharp : \text{grad} \Delta \mathbf{u}. \quad (2.9.42)$$

The linearization of the dissipation with respect to the mechanical field is a little bit more complicated and needs some additional considerations, since we can replace the derivative of D_{loc}^p with respect to the displacement field by the differentiation with respect to the spatial metric tensor

$$\frac{\partial D_{loc}^p}{\partial \mathbf{u}} \Delta \mathbf{u} = 2 \frac{\partial D_{loc}^p}{\partial \mathbf{g}^b} : \text{grad} \Delta \mathbf{u} \quad (2.9.43)$$

The corresponding derivative renders

$$\frac{\partial D_{loc}^p}{\partial \mathbf{g}^b} = \frac{\chi}{\Delta t} \sqrt{\frac{2}{3}} \left[Y_n(\xi, \Theta) + \Delta \gamma \frac{\partial Y_n}{\partial \xi} \frac{\partial \xi}{\partial \Delta \gamma} \right] \frac{\partial \Delta \gamma}{\partial \mathbf{g}^b}, \quad (2.9.44)$$

where we obtain the problem to determine the derivative of the plastic multiplier $\Delta \gamma$ with respect to the spatial metric tensor. This information emanates from the differentiation of the yield condition

$$\frac{\partial \Phi}{\partial \mathbf{g}^b} = \frac{\partial \|\tilde{\boldsymbol{\tau}}^\sharp\|}{\partial \mathbf{g}^b} - 2\mu \frac{\partial \Delta \gamma}{\partial \mathbf{g}^b} - \sqrt{\frac{2}{3}} \frac{\partial Y_n}{\partial \xi} \frac{\partial \xi}{\partial \Delta \gamma} \frac{\partial \Delta \gamma}{\partial \mathbf{g}^b} = 0. \quad (2.9.45)$$

The only task left to do is to perform the differentiation of the norm of the deviatoric Kirchhoff stress with respect to the spatial metric tensor. It can be calculated from

$$2 \frac{\partial \|\tilde{\boldsymbol{\tau}}^\sharp\|}{\partial \mathbf{g}^b} = \partial_{\mathbf{g}^b} \sqrt{[\tilde{\boldsymbol{\tau}}^\sharp \cdot \mathbf{g}^b] : [\mathbf{g}^b \cdot \tilde{\boldsymbol{\tau}}^\sharp]} = 2\mu \boldsymbol{\nu} + 2\|\tilde{\boldsymbol{\tau}}^\sharp\| \boldsymbol{\nu}^2 \quad (2.9.46)$$

and with this at hand we can obtain the needed derivative of the local dissipation with respect to the spatial metric tensor

$$2 \frac{\partial D_{loc}^p}{\partial \mathbf{g}^b} = \frac{4\chi}{\Delta t} \frac{\beta_1}{\beta_0} [\mu \boldsymbol{\nu} + \|\tilde{\boldsymbol{\tau}}^\sharp\| \boldsymbol{\nu}^2], \quad \text{with}$$

¹¹This is valid, since we have chosen an isotropic constitutive law of the Fourier type with respect to the reference configuration ($\boldsymbol{\kappa}_0 = \kappa \mathbf{G}^b$). It is also conceivable to postulate isotropy with respect to the spatial configuration ($\boldsymbol{\kappa} = \kappa \mathbf{g}^\sharp$), that would yield a corresponding contribution to linearization.

$$\beta_0 = \left[\mu + \frac{2}{3} \partial_\xi Y_n \right], \quad \text{and} \quad \beta_1 = \sqrt{\frac{2}{3}} [Y_n + \partial_\xi Y_n \Delta \xi] \quad (2.9.47)$$

This relation makes up the linearization of the thermal subproblem and since we considered here the term describing the thermoplastic coupling, in the corresponding discretization we find combinations of the mechanical and the thermal shape functions in the mixed element tangent matrix

$$\mathbf{K}_e^{\Theta \mathbf{u}} = \bigcup_{a=1}^n \bigcup_{b=1}^n \delta \Theta_a \left[\int_{\mathcal{B}_e} \mathbf{M}_a [2\partial_{g^b} \mathbf{D}_{loc}^p + \partial_J \mathbf{Q}_{eth} J \mathbf{I}] \cdot \nabla_x \mathbf{N}_b - J \nabla_x \mathbf{M}_a \cdot \overline{\nabla_x \mathbf{N}_a} \cdot \mathbf{q} \right] \Delta \mathbf{u}_b d\Omega,$$

where

$$\overline{\nabla_x \mathbf{N}_a} = \frac{1}{2} [\nabla_x \mathbf{N}_a \otimes \mathbf{I} + \mathbf{I} \otimes [\nabla_x \mathbf{N}_a]^t]. \quad (2.9.48)$$

According to the purely mechanical problem we obtain the global set of linearized equations by assembling over all elements analogous to eqn. 2.8.49, whereby still the linearization of the mechanical balance equation needs to be performed with respect to the temperature field. For an exhaustive treatment we have to mention here, that in general we have to take the heat convection into account. Therefore one can make an approach for the boundary terms q_n , which are assumed to be prescribed in the previous considerations. In this case the heat convection, that we want to denote by $\mathcal{U}_{surf}(\Theta)$, which acts at the boundaries has also to be linearized with respect to the temperature field and the displacement field as well, such that we obtain additional terms in the thermomechanical tangent matrix. Here we just want to sketch the linearization of the boundary contribution with respect to the displacement field. For this we obtain

$$D_x [da] \cdot \Delta \mathbf{u} = [\text{div} \Delta \mathbf{u} - \mathbf{n} \cdot [\text{grad} \Delta \mathbf{u}]^t \cdot \mathbf{n}] da, \quad (2.9.49)$$

that emanates from the subsequent argumentation. The deformations are related to the surface over which we need to integrate. Therefore we rewrite $da = \mathbf{n} \cdot [\mathbf{n} da]$ and by differentiating we get

$$D_x [da] \cdot \Delta \mathbf{u} = \mathbf{n} \cdot D_x [\mathbf{n} da] \cdot \Delta \mathbf{u} = \mathbf{n} \cdot D_x [J [\mathbf{f}^\sharp]^t \cdot \mathbf{N} dA] \cdot \Delta \mathbf{u}, \quad (2.9.50)$$

whereby in the last step the Nanson formula was applied. Of course we also have to linearize the spatial normal vector, but since $\Delta \mathbf{n} \cdot \mathbf{n} = 0$ we obtain no further contributions. Here J and $[\mathbf{f}^\sharp]^t$ are the quantities depending on the deformation and for the corresponding linearization we can resort to eqn. 2.9.41 and the derivation of the linearized $[\mathbf{f}^\sharp]^t$ can be performed by resorting on eqn. 2.8.18 and the relation $D_x [[\mathbf{F}^\sharp]^t \cdot [\mathbf{f}^\sharp]^t] = 0$, such that we obtain

$$D_x [[\mathbf{f}^\sharp]^t] \cdot \Delta \mathbf{u} = - [\text{grad} \Delta \mathbf{u}]^t \cdot [\mathbf{f}^\sharp]^t. \quad (2.9.51)$$

These results inserted again into eqn. 2.9.50 finally leads to eqn. 2.9.49. Since we assume the boundary values q_n as given this linearization is not relevant here. But for a complete linearization, these terms should have taken into account. Accordingly, also the element stiffness matrix needs to be complemented by these surface contributions.

The linearization of the mechanical field equation with respect to the temperature still needs to be performed and this would be the last step to accomplish the thermo-mechanical problem. There is only the internal virtual work in eqn. 2.9.62, that makes one suppose, that it is temperature dependent. Therefore we have to calculate

$$D_\Theta [\mathcal{G}_{int}] \Delta \Theta = \int_{\mathcal{B}_t} \text{grad} \delta \mathbf{u} : D_\Theta [\boldsymbol{\tau}^\sharp] \Delta \Theta dV, \quad (2.9.52)$$

whereby here the internal virtual work is expressed in terms of the Kirchhoff stress tensor. Since the Kirchhoff stress can be divided into a volumetric and a deviatoric part it is easy to see the explicit dependence of the volumetric stress on the temperature, what follows from the thermo-mechanical potential chosen eqn. 2.9.9. Here the thermomechanical stress can be derived from

$$\tau_{eth}^\# = \frac{\partial W}{\partial J} = \frac{\partial W_{vol}}{\partial J} + \frac{\partial W_{eth}}{\partial J} = \tau_{vol}^\# - 3\kappa\alpha\Delta\vartheta\mathbf{g}^\# \quad (2.9.53)$$

and the linearization of this term with respect to the temperature finally yields

$$D_\Theta [\tau_\Theta^\#] \Delta\Theta = -3\kappa\alpha\mathbf{g}^\#. \quad (2.9.54)$$

According to this there is an implicit dependence of the deviatoric stress field on the temperature, namely, since the plastic flow depends on the temperature. The update of the deviatoric stress is given by

$$\tilde{\tau}^\# = \hat{\tau}^{\#,tr} - 2\mu\Delta\gamma\boldsymbol{\nu} \quad (2.9.55)$$

such that the linearization is restricted to the term including the plastic flow. For the directional derivative of the deviatoric stress contribution we obtain

$$D_\Theta [\tilde{\tau}^\#] = -2\mu D_\Theta \Delta\gamma\boldsymbol{\nu}. \quad (2.9.56)$$

and this term was already determined in eqn. 2.9.37. This completes the linearization process and the corresponding element stiffness matrix is given by

$$\mathbf{K}_e^{\mathbf{u}\Theta} = \sum_{a=1}^n \sum_{b=1}^n \delta \mathbf{u}_a \cdot \int_{\mathcal{B}_e} \nabla_x \mathbf{N}_a \cdot [-3\kappa\alpha\mathbf{I} - 2\mu\partial_\Theta \Delta\gamma\boldsymbol{\nu}] \mathbf{M}_b \Delta\Theta_b d\Omega \quad (2.9.57)$$

such that we are able to construct the complete element stiffness matrix for the thermo-mechanical problem and to apply the standard Newton-Raphson iteration scheme. The total thermomechanical stiffness element stiffness matrix is composed by the contributions in the eqns. 2.9.48, 2.9.57, 2.9.39 and 2.8.62

$$\begin{bmatrix} \mathbf{K}_e^{\mathbf{u}\mathbf{u}} & \mathbf{K}_e^{\mathbf{u}\Theta} \\ \mathbf{K}_e^{\Theta\mathbf{u}} & \mathbf{K}_e^{\Theta\Theta} \end{bmatrix} \begin{bmatrix} \mathbf{u}_e \\ \Theta \end{bmatrix} = - \begin{bmatrix} \mathbf{R}_e^{\mathbf{u}} \\ \mathbf{R}_e^{\Theta} \end{bmatrix} \quad (2.9.58)$$

whereby in this context the purely mechanical part of the stiffness matrix $\mathbf{K}_e^{\mathbf{u}\mathbf{u}}$ coincides with the element stiffness matrix derived in eqn. 2.8.62. By assembling these equations we obtain the global set of coupled algebraic equations, that is solved by the Newton-Raphson iteration or an quasi-Newton algorithm. This described method is usually denoted by *monolithic* algorithm, since the thermal and the mechanical subproblem are solved simultaneously. This algorithm enforces a mixed discretization with the consequence, that the tangent stiffness matrix in general is not symmetric anymore and in addition to that, in general it is bad conditioned, since both subproblems are of different order. This requires solvers which are able to treat nonsymmetric problems and to improve the condition number specific algorithms like pivoting are necessary. To avoid these effects another approach is possible, that is denoted by *staggered* algorithm, where one subproblem is solved at first and serves as initial condition for the second subproblem. The benefit of this algorithm is, that each subproblem can be solved by stable algorithms oriented on the particular requirements, since they are independent from each other. From this emanates another advantage, which is the symmetry of both subproblems, which can be maintained, whereas in the monolithic algorithm the symmetry of the stiffness matrix gets lost.

2.9.5 Adiabatic Processes

Adiabatic temperature evolution A special case of thermomechanical processes are so-called adiabatic ones. In general a process is called adiabatic, if no heat exchange with the surrounding environment takes place due to isolation for instance. In the case, that we like to consider here, it is assumed, that no external heat is induced, but the deformation velocity is so high, such that the heat flux out of the system during the deformation process is negligible. This assumption leads to a simpler temperature evolution equation and the main advantage of this formulation is, that the temperature does not appear as an additional primary variable like the displacements, but it can be introduced as an additional internal variable. This means, that the linear momentum balance equation remains the only global balance equation, which needs to be fulfilled, in contrast to the thermo-mechanically coupled problem, where the temperature is introduced as a global primary variable and its evolution is another global balance equation, that needs to be taken into account. Finally, the made assumptions yields

$$\dot{\Theta} = \frac{1}{\rho_0 c_p} \left[\dot{\gamma} \sqrt{\frac{2}{3}} Y_0(\Theta) + \Theta \partial_{\Theta} \boldsymbol{\tau}^{\#} : \mathbf{d}^p \right] \quad (2.9.59)$$

for the temperature evolution equation. If this is embedded into the von-Mises plasticity we obtain three residuals, where the first one coincides with the yield condition. Here it is taken into account, that the linear and non-linear hardening moduli depend on temperature, as they were introduced in eqn. 2.6.76. Therefore we obtain the representation of the residuals for the local iteration

$$\begin{aligned} r_1 &= \|\tilde{\boldsymbol{\tau}}^{\#}\| - 2\mu\Delta\gamma - \sqrt{\frac{2}{3}} Y_n(\Theta, \xi) \\ r_2 &= \xi_n - \xi + \sqrt{\frac{2}{3}} \Delta\gamma \\ r_3 &= \Theta_n - \Theta + \frac{1}{\rho_0 c_p} \left[\Delta\gamma \sqrt{\frac{2}{3}} Y_0 + \Theta_0 \partial_{\Theta} \boldsymbol{\tau}^{\#} : \mathbf{d}^p \right]. \end{aligned} \quad (2.9.60)$$

Here we also introduced a reference temperature Θ_0 to simplify the equation

Algorithmic tangent operator Analogous to damage models, where the damage variable was introduced as an additional internal variable, here we have to consider the temperature-dependence in the representation of the algorithmic tangent operator of the adiabatic material model. As the dilatation due to temperature increase shows, we have to consider the volumetric part of the free energy as temperature-dependent. Therefore we adopt the formulation of thermoelastic contribution of the free helmholtz energy as

$$W_{elth} = \kappa \ln J \left[\frac{\ln J}{2} - 3\alpha \Delta\vartheta \right], \quad \text{with} \quad \Delta\vartheta = \Theta - \Theta_0, \quad (2.9.61)$$

whereby we combined it here with the volumetric part of the isothermal formulation. As a consequence the volumetric part of the spatial adiabatic elasto-plastic algorithmic tangent operator becomes

$$\mathbb{C}_{vol}^{adep} = \sum_{\beta=1}^3 \sum_{\gamma=1}^3 \varphi_{\beta\gamma}^{vol} \mathbf{m}^{\beta} \otimes \mathbf{m}^{\gamma}. \quad (2.9.62)$$

In eqn. 2.9.61 α denotes the heat expansion coefficient and of course only the volume dilatation with respect to the initial temperature has to be considered, such that only the temperature difference is inserted into this approach.

In addition we have to consider the temperature dependence of the resulting yield stress, if the derivative of the plastic multiplier with respect to the principal stretches are calculated. This derivative yields

$$\frac{\partial \Delta \gamma}{\partial \lambda_\beta} = \frac{2\mu\nu_\alpha}{2\mu + \sqrt{\frac{2}{3}} \left[\frac{\partial Y_n}{\partial \xi} \frac{\partial \xi}{\partial \Delta \gamma} + \frac{\partial Y_n}{\partial \Theta} \frac{\partial \Theta}{\partial \Delta \gamma} \right]} \quad (2.9.63)$$

whereas the rest of the isothermal elasto-plastic tangent operator in eqn. 2.6.72 remains unchanged and can be adopted to the adiabatic material model. Therefore we find the well-known structure

$$\mathbb{C}_{iso}^{adep} = \sum_{\alpha=1}^3 \sum_{\beta=1}^3 \varphi_{\alpha\beta}^{iso} \mathbf{m}^\alpha \otimes \mathbf{m}^\beta + \sum_{\alpha=1}^3 2\tilde{\tau}_\alpha \frac{\partial \mathbf{m}^\alpha}{\partial \mathbf{g}^b}, \quad \text{with}$$

$$\varphi_{\alpha\beta}^{iso} = 2\mu \left[\delta_{\alpha\beta} - \frac{1}{3} \right] - \frac{4\mu^2 \Delta \gamma}{\|\tilde{\tau}^\# \|^2} [\delta_{\alpha\beta} - \nu_\alpha \nu_\beta] - 2\mu \left[2\mu + \sqrt{\frac{2}{3}} \left[\frac{\partial Y_n}{\partial \xi} \frac{\partial \xi}{\partial \Delta \gamma} + \frac{\partial Y_n}{\partial \Theta} \frac{\partial \Theta}{\partial \Delta \gamma} \right] \right]^{-1} \nu_\alpha \nu_\beta \quad (2.9.64)$$

for the isochoric part of the algorithmic spatial tangent operator for an adiabatic hyperelasto-plastic material formulation. The total tangent operator is given by the sum of the volumetric and the isochoric contribution and this completes the adiabatic modification of the J_2 plasticity.

2.10 Applications

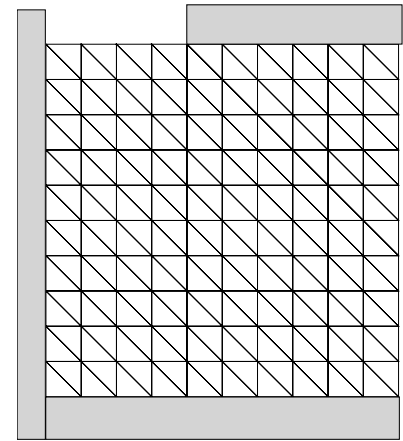
In the last section of this chapter we like to present the effects of the different material models, that were derived in the previous sections, by means of some numerical examples. Here we tried to choose some examples which we recover in later chapters of this work in a modified way, whereby then interface elements are taken into account. Especially, the thermo-mechanical coupling and the different characters of the inelastic formulations of the Lemaitre and the Gurson type are in the center of interest and last but not least the influence of the rate-dependence should be investigated. Some of the examples in this work were developed within a project about the tearing and cutting of ductile materials, where a validation of the models by experimental results was performed. In this context the deepdrawing problem of polypropylen was calculated, whereby some results are also presented in this section. Finally, we like to investigate the tension test of a plate with a hole and the tension of a notched shell, whereby also here the two damage formulations were applied taking elasto-viscoplastic effects into account. As mentioned before we like to start with a thermo-mechanically coupled problem, whereby only mechanical loads are imposed.

2.10.1 Thermo-Elasto-Plasticity

Description The first example is illustrated in fig. 2.8b) and it shows a 2-dimensional quadratic block of 10×10 units of length, discretized by 200 6-node triangular finite elements. The left and lower boundaries are fixed in vertical as well as in horizontal direction. The loading is imposed by means of 300 displacement steps a 0.001 units in vertical direction, such that in total the deformation

Parameter	Dimension	Value
E	kN/mm ²	206.9
ν	[—]	0.29
Yield stress Y_∞	kN/mm ²	0.450
lin. Hardening modulus h	kN/mm ²	-0.0129
nonlin. Hardening modulus κ	[—]	16.93
Conductivity k	[W/°K]	0.045
Heat expansion coefficient α	[°K ⁻¹]	0.000012
Θ_0	[°K]	293.15
ω_y	[1/°K]	0.002
ω_h	[1/°K]	0.002
c_p	[W/°K]	0.003855

a)



b)

Figure 2.8. a) Thermo-mechanically coupled von-Mises model: Table with the applied material parameters b) initial problem

takes 0.3 units of lengths. The applied material parameters are depicted in fig. 2.8c whereby the chosen values corresponds to the typical parameter values of steel.

The results are depicted in fig. 2.9 that shows the initial configuration, the deformed block after 125 load steps and the final configuration after 250 load steps, whereby the colors highlight the temperature distributions in the block. One can observe, that a band evolves, where the temperature increases and it coincides with the zone of plastic deformation. In plasticity theory this band is called localization band and it indicates the zone where the material possibly localizes, i.e. an accumulation of plastic strains take place¹². Since the load is quasistatically superposed the temperature increase is not very pronounced, but sufficient for the qualitative demonstration of the thermo-mechanical coupling.

Interpretation The imposed loading leads to the typical development of a localization zone, that means a pronounced accumulation of plastic strains, such that the upper part nearly tends to move like a rigid body, if the intermediate and the final state is considered. Nevertheless, due to the continuous discretization of the primary field of unknowns the failure mode is not fully developed. Since the temperature is related to the plastic strains due to the yield function or the resulting yield stress, respectively, finally the plastic strains induce an increase of temperature. Of course this evolves in the localization zone where the localization takes place. Since we applied a fully thermo-mechanically coupled material model, the heat flux has to be taken into account, such that the temperature also increases in regions beyond the plastic zone, whereas in the case of an adiabatic formulation, the temperature increase would be restricted to the plastic zone. In fact this effect is not very pronounced here since the thermal conductivity was chosen quite low. If the conductivity was increased and additionally a rate-dependent formulation was chosen, this effect would have been more obviously.

¹²A detailed consideration on localization is given in chapter 4

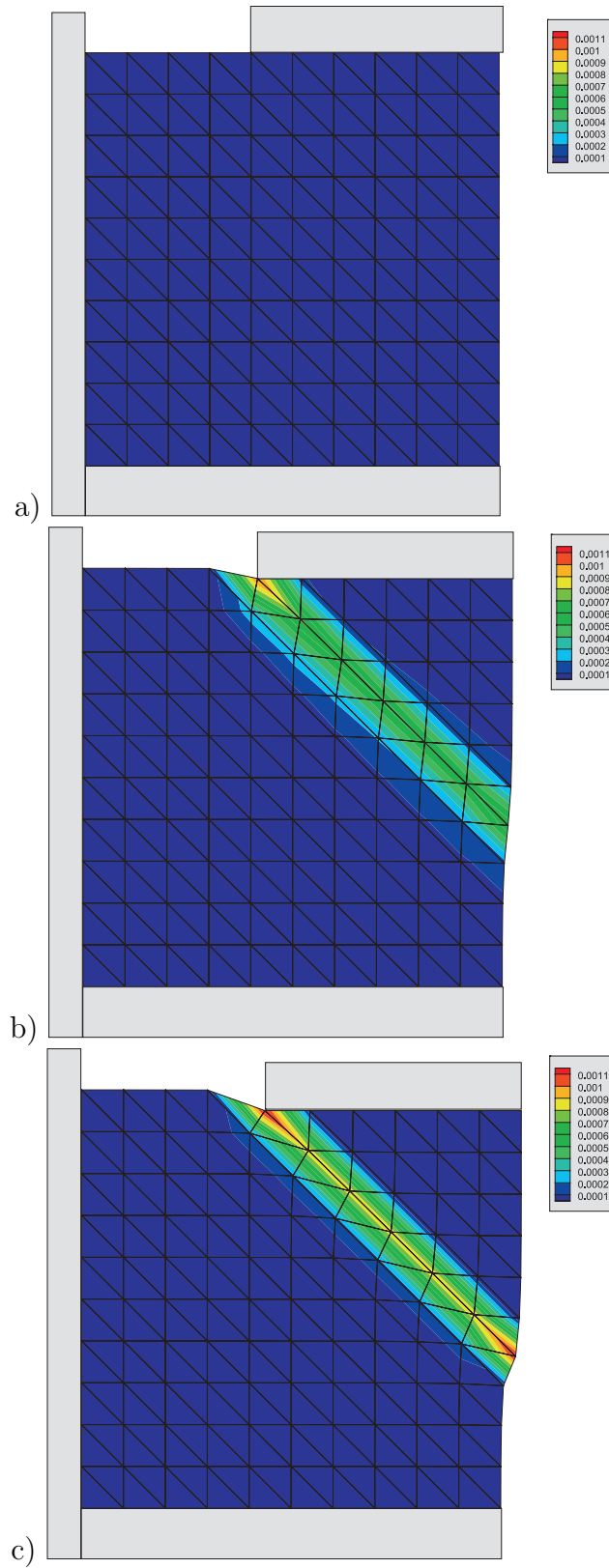


Figure 2.9. Thermo-mechanically coupled von-Mises model: Temperature evolution due to the deformation a) initial state b) after 150 load steps c) after 300 load steps.

2.10.2 The Lemaitre Model and the Gurson Model

Description In the next step we want to apply the rigid footing test to a purely isothermal problem, but taking damage and other inelastic effects into account. Therefore the thermo-mechanical material law is replaced by the Lemaitre-type or the Gurson-type Model, respectively. The boundary conditions and the loading are chosen exactly the same as before. Only the material parameters are chosen with respect to the Lemaitre-type or the Gurson-type model and the corresponding values are summarized in figure 2.10. The crucial parameters for the Lemaitre-type Model defining the energy release rate are given by $S_0 = 50$ and the corresponding exponent was chosen as $s_0 = 1$. Accordingly, we recover the parameters of the Gurson-like Model also in fig. 2.10, whereby here the crucial quantity is the initial void volume fraction $d_0 = 4 \cdot 10^{-4}$ and the slope $k = 1.5$ determining the development of the void volume fraction. The rest of the parameters are chosen in the ranges, recommended by Mahnen [Mah99].

The results are depicted in fig. 2.12 or 2.13, respectively, representing the initial state, the state after 150 load steps and the final state after 300 load steps. The coloring highlights the distribution of the damage variable or the void volume fraction, respectively, during the deformation.

Parameter	Value	Lemaitre	Gurson
E	1600	x	x
ν	0.3	x	x
Y_0	8	x	x
Y_{infy}	20	x	x
h	12	x	x
κ	9.6	x	x
S_0	50	x	-
s_0	1	x	-
d_0	$4 \cdot 10^{-4}$	-	x
d_c	$5 \cdot 10^{-4}$	-	x
Δd	$8 \cdot 10^{-5}$	-	x
v_c	1.5	-	x
q_1	1.2	-	x
q_2	1.2	-	x
q_3	0.5	-	x
k	1.5	-	x

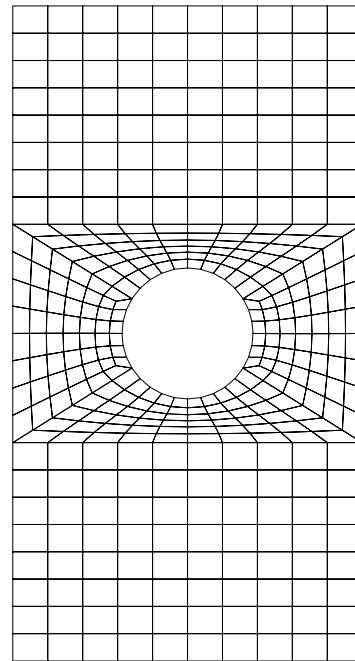


Figure 2.10. a) Parameters for the Lemaitre-type and the Gurson-type model b) initial geometry of a plate with a hole

Interpretation The evolution equation of the Lemaitre-type damage model depends on the energy release rate which is a function of the stress or the strain field, respectively. Therefore it seems plausible, that the damage evolve in zones of increasing stresses as they occur in the upper area where the force is imposed and high stresses due to tension are induced.

A more interesting result delivers the same calculation taking the Gurson model into account. Since the model assumes, that there are voids in the material in the initial state, we obtain an orange colouring of the block. These voids increase due to tension, but desintegrate if pressure is imposed. In the particular example only pressure is imposed, such that the initial voids decrease

and finally desintegrate. Accordingly the color changes from orange to green and finally to blue, that corresponds to much smaller void volume fraction than the initial one. There is only one little zone, where tensile stress occur and it is plausible, that this zone coincides with the red colored zone indicating an increasing void volume. Here the main difference of the Lemaitre-type damage formulation and the Gurson-type formulation can be easily realized, since the Lemaitre-type model starts from the undamaged material, which is indicated by the red colour and the damaged zone can not regress, whereas in the assumption of voids this is conceivable. On the other hand within the Gurson-type model the voids can totally vanish, such that a kind of 'healing' takes place, that physically does not make any sense, at least not in this context. Therefore the Gurson-type model is not appropriate for the modelling of squeezing problems. Nevertheless it seems useful if ductile or porous materials like polypropylen or alluminium alloys are considered.

Description Another application that seems more appropriate for the application of the Gurson-type model is the tensile test of a plate with a centered whole as depicted in fig. 2.10b. The plate was discretized by 376 quadrilateral 4-node elements, where the length of the plate consists of 18 units and it has a width of 10 units. The diameter of the inner whole is 3.75 units. The loading was applied by 200 steps of 0.01 units until a maximum displacement of 2.0 units was reached. In this numerical example the three different material laws were applied: 1) the Gurson-type model 2) the Lemaitre-type model and 3) rate-dependent modification of the Lemaitre-type model. We used the same parameter values as they were already used in the previous example and as they are summarized in fig. 2.10a. For the last calculation we additionally assumed a viscosity $\eta = 500 \text{ N/mm}^2 \text{ s}$ and a $\Delta t = 0.01 \text{ s}$ to perform the rate-dependent calculation. The corresponding results are summarized in fig. 2.14 in the previously mentioned order.

Interpretation Here we can see, that the void volume fraction and the damage variable in the first two calculation evolve similarly, however, the corresponding variables are not of the same order. What one can find in both calculations is, that the development of the considered internal variable shows the shape of an 'x', that is characteristic for this kind of problem. The evolution of the internal variables begins at the middle of the plate due to the hole, that weakens the shell essentially and that induces locally higher stresses that initiate the weakening of the material and finally leads to the failure of the material in these specific zones. This coincides with experimental observations. In this kind of problem we find the Gurson-type model behaving similar to the Lemaitre-type model, since this time only tensile stresses are superposed.

The extremely high values for the damage variable in the last calculation, where viscous effects were taken into account, bases on the fact that due to the high deformation velocity the material gets stiffer, such that higher stresses are induced. Therefore in the zones of increased stresses, the material accordingly suffers an increased damage evolution and also here we find the maximum in the zones where the material is weakened the most, i.e. at the boundary of the hole.

2.10.3 Deepdrawing Process

Description The last example, that should be discussed here is an application requiring all the effects provided by the material models we derived before: cutting and deepdrawing processes. This kind of problems are quite complex, since a lot of mechanical effects occur in a combined manner. In fig. 2.11b the corresponding geometry and the boundary conditions are depicted and the results of such an deepdrawing process can be find in fig. 2.16 - 2.18. The calculation was performed with the quasistatic adiabatic Lemaitre-type model using the same material parameters as they are

Parameter	Dimension	Value
E	kN/mm^2	206.9
ν	—	0.29
Yield stress Y_∞	kN/mm^2	0.450
lin. Hardening modulus h	kN/mm^2	0.0129
nonlin. Haredening modulus κ	—	16.93
Heat expansion coefficient α	$^\circ\text{K}^{-1}$	0.000012
Θ_0	$^\circ\text{K}$	293.15
ω_y	$^\circ\text{K}^{-1}$	0.002
ω_h	$^\circ\text{K}^{-1}$	0.002
c_p	$\text{W/}^\circ\text{K}$	0.04
S_0	W	200
s_0	—	1

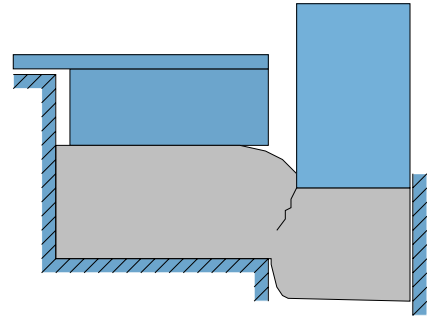


Figure 2.11. a) List of applied parameters for the adiabatic Lemaitre-type modell b) Initial geometry of deepdrawing prozess

collected in fig. 2.11a. The specimen was discretized by 875 linear quadrilateral 4-node elements. The specimen possesses a height of 5 units and a entire length of 15 units whereby the finite element mesh was adequately refined in the cutting zone between the stator and the blade. The loading was applied at the upper boundary as it is illustrated in fig. 2.11 by means of 300 steps of 0.01 units in vertical direction. Since the problem is axially symmetric the calculation only had to be performed for one half. Therefore the right boundary was fixed in horizontal direction. Furthermore the left boundary of the specimen was fixed in vertical and horizontal direction as well as the part of the lower boundary which is connected to the stator. The rest of the lower boundary is free.

Interpretation In analogy to the previous examples of the footing test we find the typical shear band in the cutting zone where strain localization would be expected and accordingly the hardening variable evolves along the cutting zone, as it is illustrated in fig. 2.16. The damage variable within the Lemaitre formulation depends on the stresses, therefore the damage variable evolves as well as the temperature in the localization zone (s. fig.2.17 and 2.18). Since the loading was performed quasistatically here the temperature increase is not as significant as in the case of higher loading velocities. Nevertheless, in the cutting zone plastic strains accumulate and localization takes place and the internal variables, like hardening variable, damage and temperature evolves in this particular region of course.

The material models are able to cover these kind of problems quite well. Of course, it depends on the set of parameters, whether the simulation can be performed or not. Especially, taking the adiabatic effects and the thermo-mechanical coupling into account, often induces numerical difficulties, since the slope of the force-displacement curve can become negativ. This induces negative eigenvalues in the stiffness matrix, such that the Newton-Raphson method fails. In this case it is recommended to apply the arclength method to handle these kinds of problems.

At last a comparison of a real deepdrawing process of polypropylen and a calculation is presented in fig. 2.10.3, whereby it should not be discussed in detail here. Here a simple geometrically nonlinear von-Mises frmulation was chosen, whereby the softening was induced due to a negative hardening

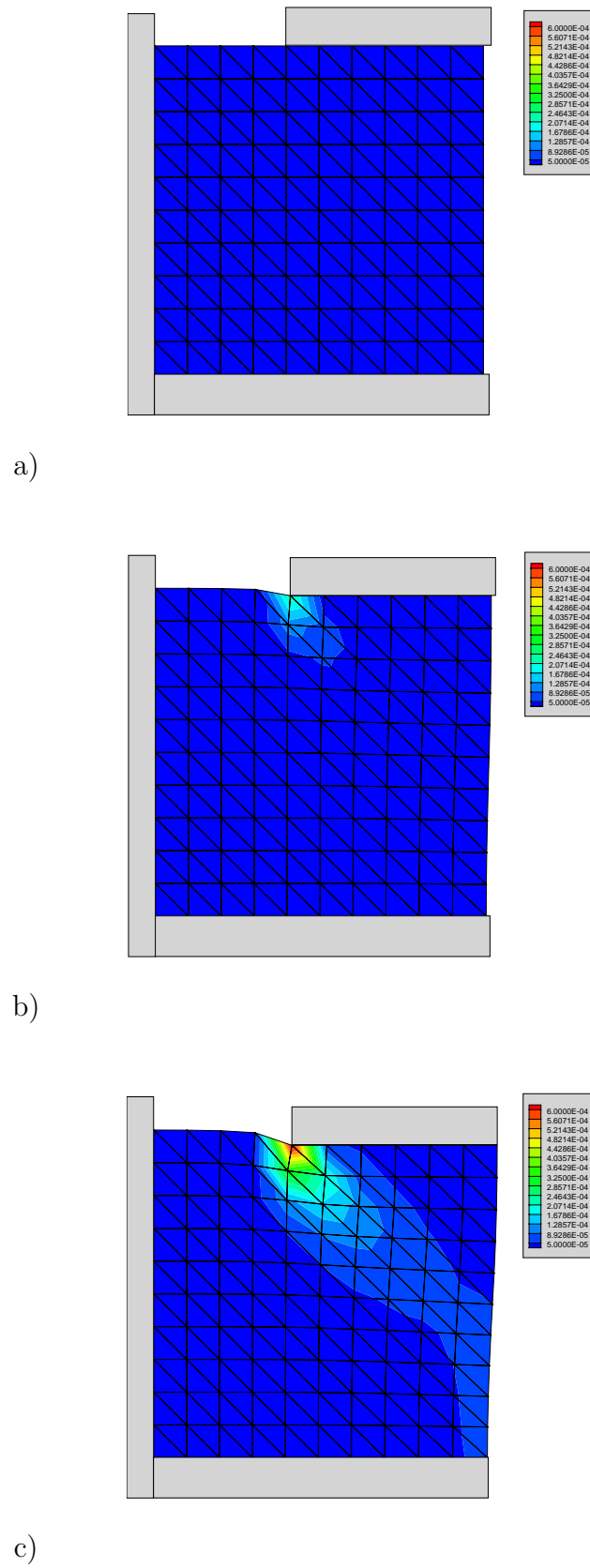


Figure 2.12. Lemaitre-type model: Evolution of the damage variable d in the a) initial state b) after 150 load steps c) after 300 load steps.

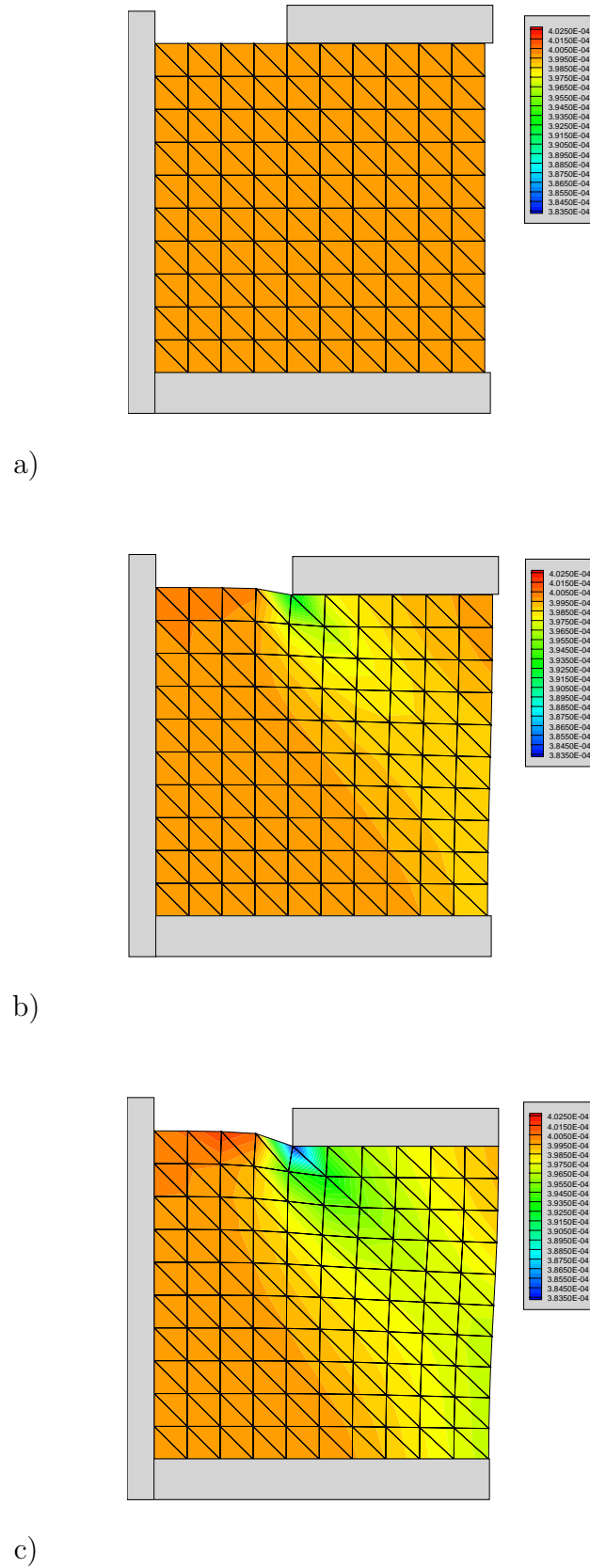


Figure 2.13. Gurson- type model: Evolution of the void volume fraction d in the a) initial state b) after 150 load steps c) after 300 load steps.

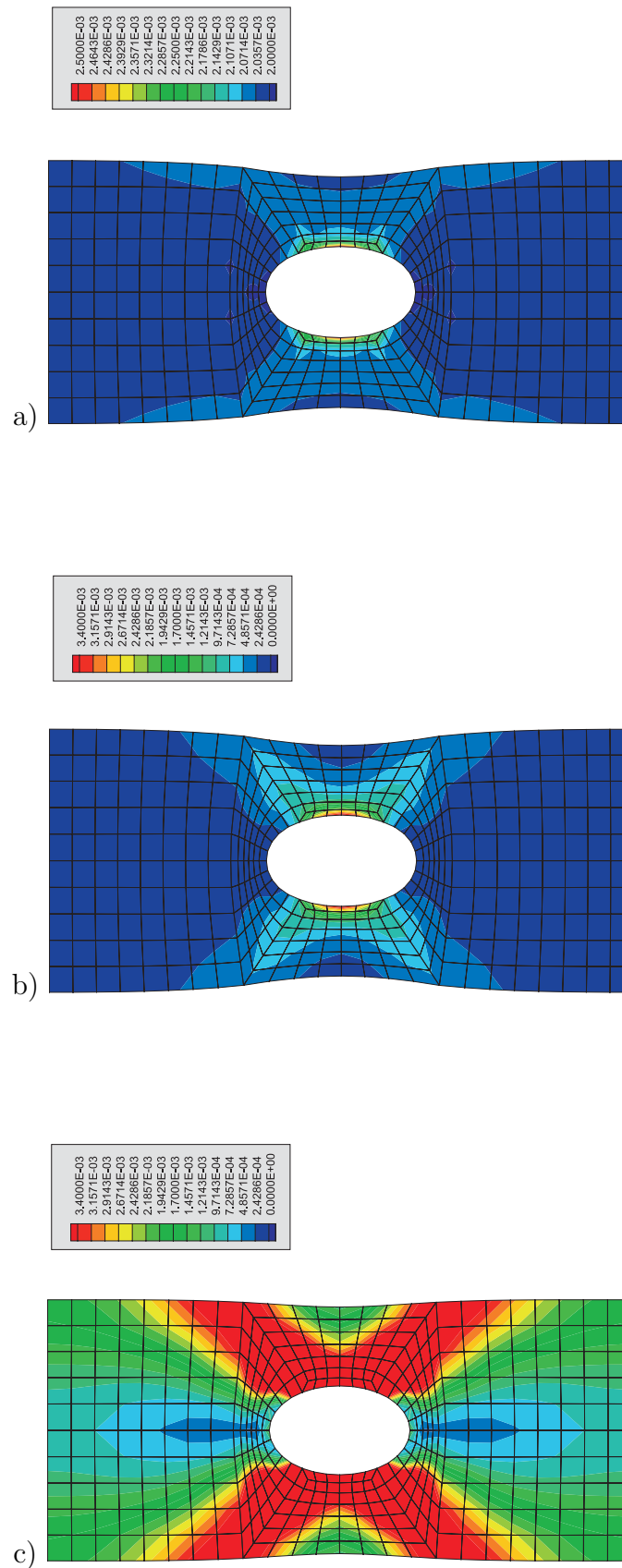
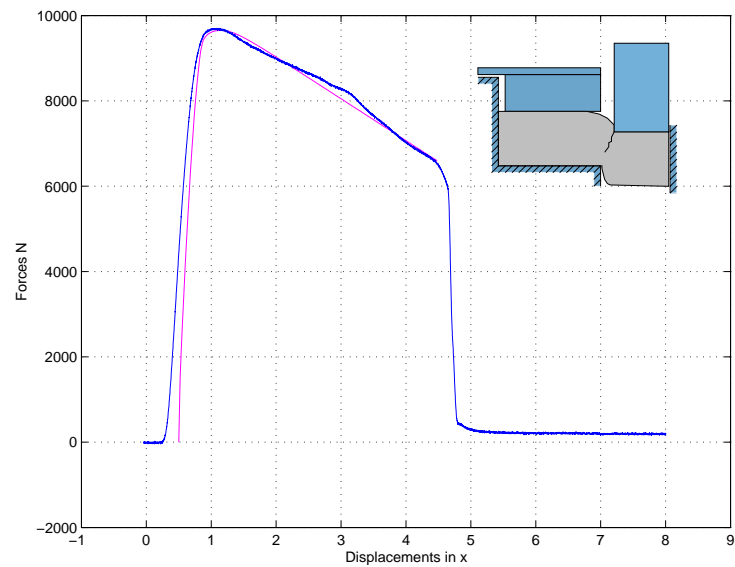
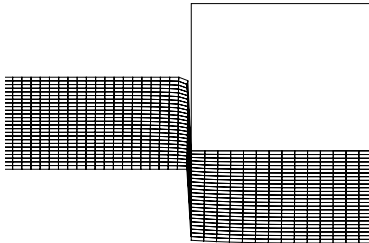


Figure 2.14. Evolution of the damage variable of a) the Gurson-type model b) the Lemaitre-type model and c) the rate-dependent Lemaitre-type model

Parameter	Parameter Value
E	1000 N/mm ²
ν	0.3
Y_0	52 N/mm ²
Y_∞	55 N/mm ²
κ	1.6
h	-1. N/mm ²
von-Mises Model	



Cutting Geometry					
angle of blade	specimen thickness	gap width	velocity	material	specimen end
90°	5 mm	0.2 mm	50 mm/s	Polypropylen	horizontally fixed

Figure 2.15. Comparison of experiment and simulation: The diagramm shows the force- displacement- curve of a cutting process of PP

modulus as it can be seen in table 2.10.3a. Furthermore the probe was fixed as in the last example and the loading was imposed quasistatically. Due to the softening effects it was necessary to apply the arclength method for the solution. The parameters were chosen by the hand-fitting method and the match between simulation and real process is quite good. But the parametrization would have to be chosen completely different if a higher loading velocity was chosen. Therefore it would have been necessary to perform a parameter optimization that was not topic of the particular project.

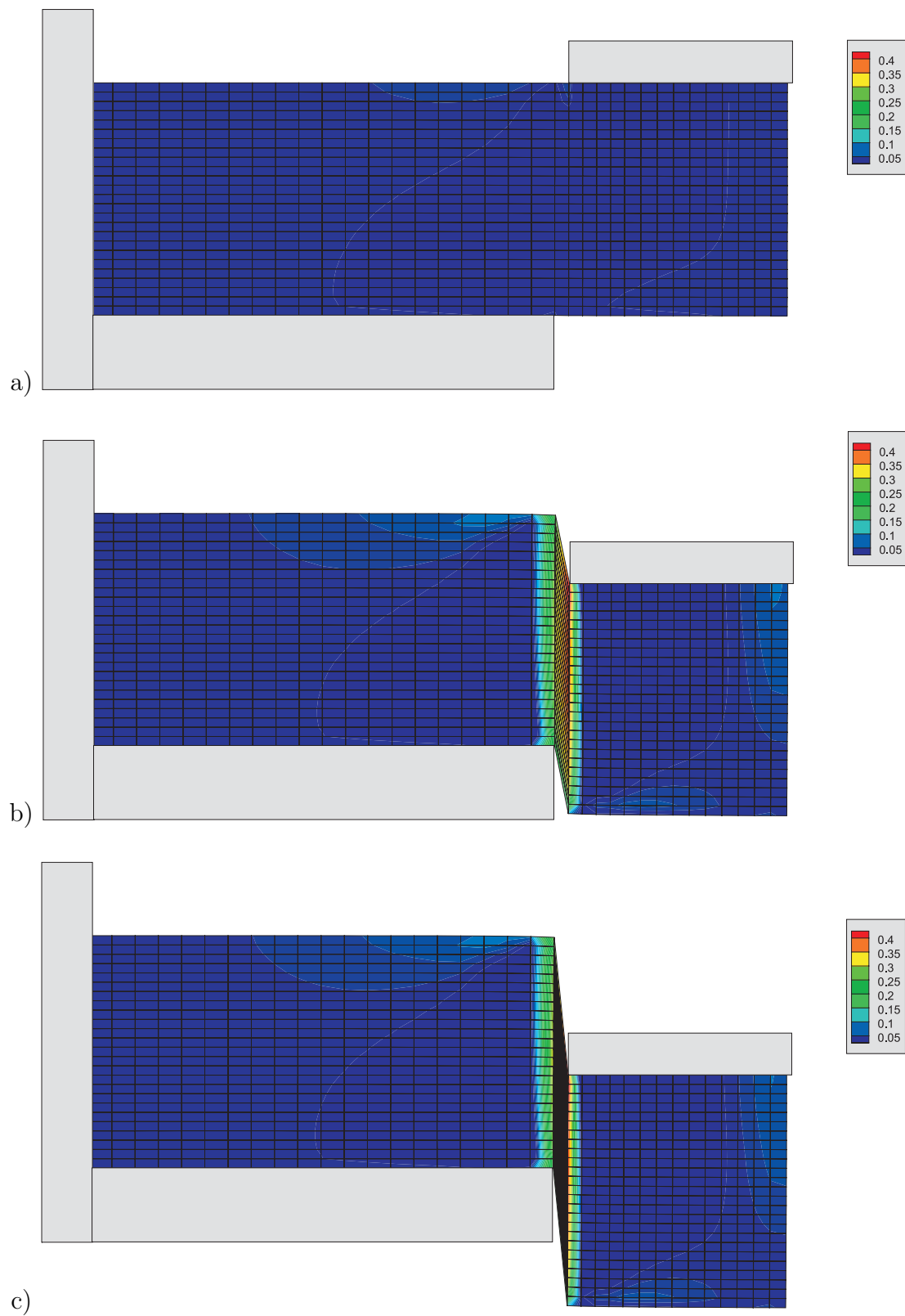


Figure 2.16. Axial symmetric adiabatic Lemaitre-type model: Evolution of the hardening variable during a deepdrawing process: a) at initial state b) after 150 load steps c) after 300 load steps.

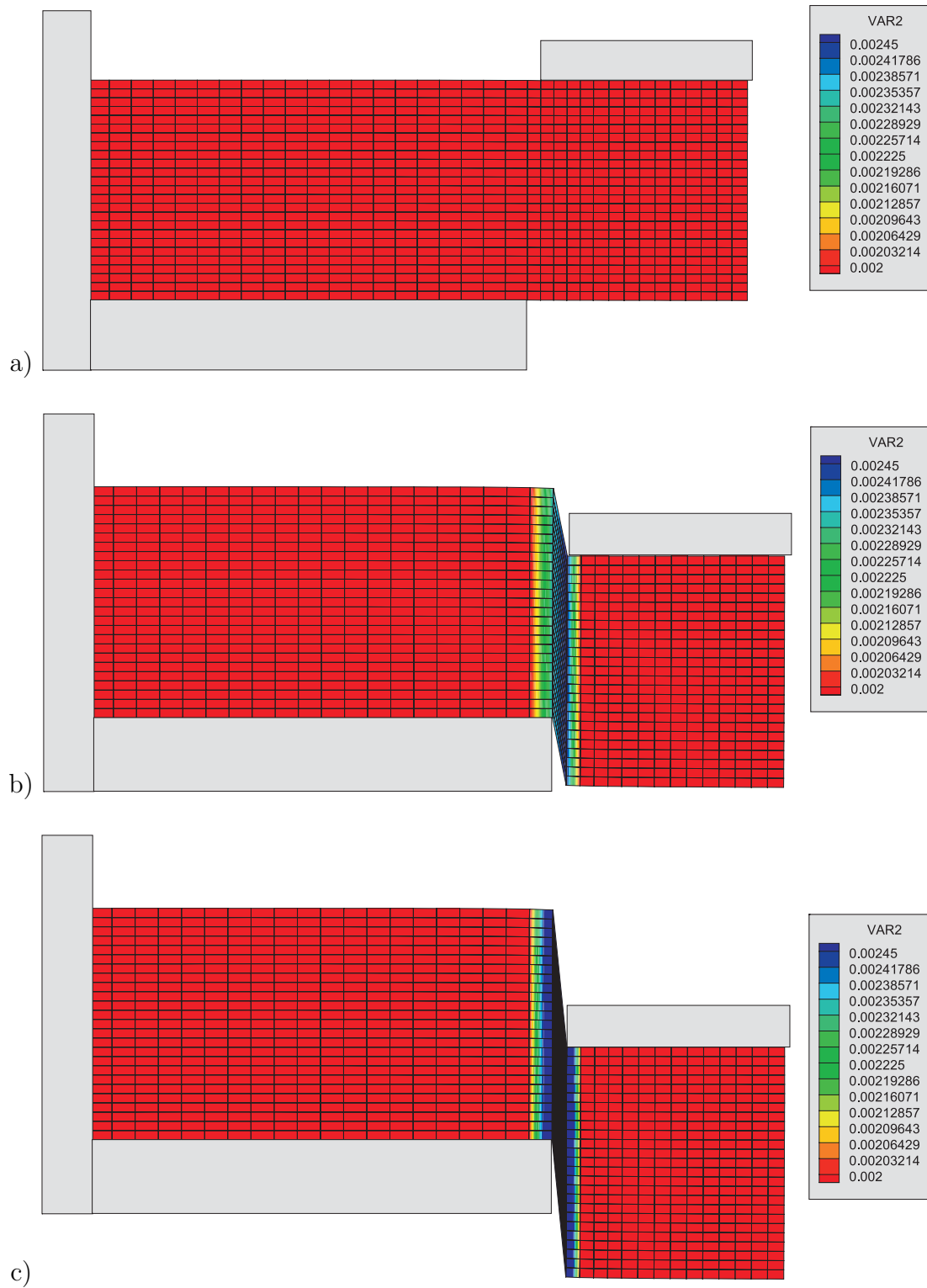


Figure 2.17. Axial symmetric adiabatic Lemaitre-type modell: Evolution of the damage variable during a deepdrawing process: a) at initial state b) after 150 load steps c) after 300 load steps.

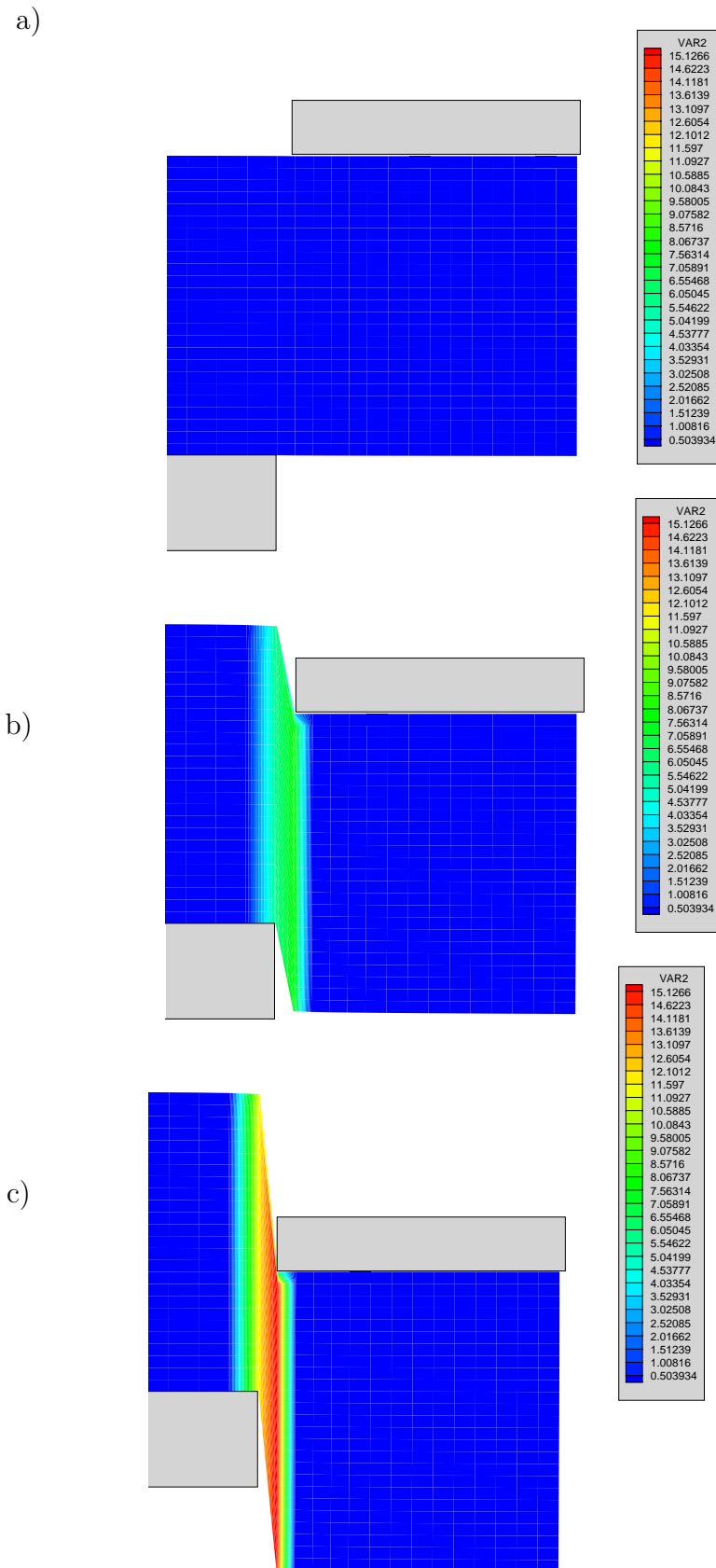


Figure 2.18. Axial symmetric adiabatic Lemaitre-type modell: Evolution of the temperature during a deepdrawing process: a) at initial state b) after 150 load steps c) after 300 load steps.

3 Interface Formulations

3.1 Overview

In the sequel we like to take discontinuities into account, which are embedded in the ambient continuum. These discontinuities can emerge from a different material behaviour, whereby their volumetric size can be neglected with respect to the ambient material. In this spirit they are predestinated for the modelling of composites and in general for all problems, where different orders of magnitudes are considered but the influence on the total behaviour of a certain structure can not be neglected. Another application of discontinuities is the modelling of material separation processes as they occur within shear deformations for instance. Here the stresses within an inelastic material locally increase so, that the yield stress locally is exceeded and so-called *shear bands* evolve, which are characteristic limited zones. This occurrence is called *localization* and in general it induces damage effects, which finally leads to macroscopic failure of the material. The numerical description of the failure and the implied discrete separation of the material can not be covered by standard finite element formulations and their numerical treatment requires particular interface elements, which are able to record such effects. As mentioned before discontinuities are fields or properties which obeys a jump of the particular quantity and interfaces relate these jumps to dependent quantities. The subsequent chapter bases on a publication of Steinmann & Häsner [SH05] and here we like to develop the main tools for the treatment of discontinuities and interfaces, which are specified with respect to different applications in the subsequent chapters. At first we introduce some kinematical quantities and some mathematical issues needed for the modelling of discontinuities and interfaces. Then we like to represent the momentum balance equations and the balance of mechanical energy, which have to be modified in consideration of the discontinuities and interfaces. Likewise we have to adopt the laws of thermodynamics to the formulations taking discontinuities and interfaces into account. The derived representations are transformed to weak formulations, whereby, as we will see, the introduction of an interface temperature yields two possible definitions, which induce two different possible weak formulations of the thermal subproblem. The modified balance equations represented in this chapter are very general and shall be apprehended as an overview and framework to discontinuous and interface problems. The given formulations will be adopted to the specific problems discussed in the subsequent chapters concerned with localization and composite behaviour.

3.2 Introduction

In the previous chapter we investigated the mechanical behaviour of solids based on the formulations and methods in continuum mechanics. In the classical context it is assumed that the corresponding

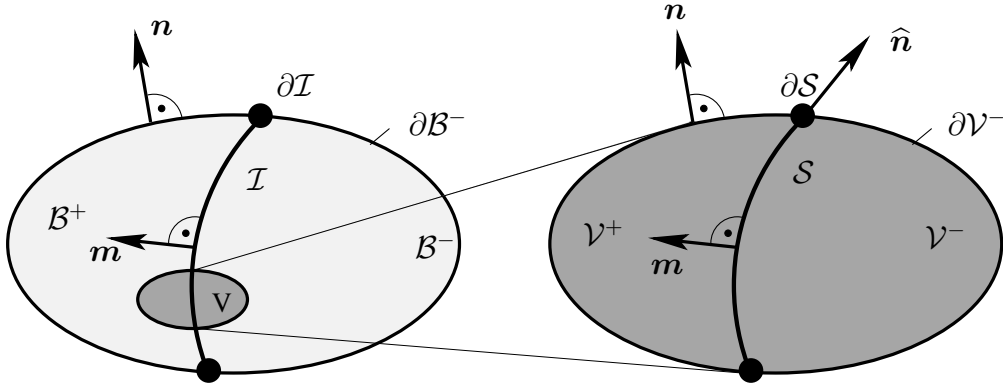


Figure 3.1. Strong discontinuity

displacement field is continuous. In the sequel we also take discontinuities into account, that are represented by a *material* surface \mathcal{I} embedded in the body \mathfrak{B} . The body \mathfrak{B} is represented by certain configuration \mathcal{B} , whereby here and in the sequel we firstly do not distinguish between the reference and the current configuration anymore: $\mathcal{B}_0 = \mathcal{B}_t = \mathcal{B}$. Therefore the notation *material* surface has to be declared and adopted to the current context. Here the term material indicates that the motion of the interface depends on the motion of the surrounding continuum by kinematic slavery. Let the material surface be fixed within the body and its position in \mathbb{E}^3 is given by the placement vector $\mathbf{x}(\theta^\alpha)$, where $\theta^\alpha, \alpha = 1, 2$ denote convected coordinates. With this parametrization at hand a possible representation of the material surface is given by

$$\mathcal{I} = \mathcal{I}(\mathbf{x}, t) = 0. \quad (3.2.1)$$

The tangent vectors on this surface are defined by the derivatives of the placement vector with respect to the corresponding coordinate lines, such that we obtain the contravariant basis vectors analogously to the first section in chapter 2. Here we like to denote them by $\mathbf{t}_\alpha = \partial_{\theta^\alpha} \mathbf{x}$ (instead of the \mathbf{g}_i) and from the tangent vectors it is straightforward to derive the corresponding normal vector \mathbf{m} by

$$\mathbf{m} = \frac{\mathbf{t}_1 \times \mathbf{t}_2}{\|\mathbf{t}_1 \times \mathbf{t}_2\|}. \quad (3.2.2)$$

The material surface divides the body into two disjoint parts \mathcal{B}^+ and \mathcal{B}^- and accordingly, the boundary consists of the two parts $\partial\mathcal{B} = \partial\mathcal{B}^- \cup \partial\mathcal{B}^+$. The interfacial normal vector \mathbf{m} is assumed to point from \mathcal{B}^- to \mathcal{B}^+ . Furthermore, in the sequel we shall consider arbitrary subbodies \mathfrak{V} taking the subconfigurations $\mathcal{V} \subset \mathcal{B}$ with the corresponding boundary $\partial\mathcal{V}$. If the subconfiguration contains a part of the interface $\mathcal{S} \subset \mathcal{I}$, its intersection with the boundary $\partial\mathcal{V}$ is denoted by $\partial\mathcal{S}$. Thereby we adopt the notations and definitions of the previously defined normal vector \mathbf{n} and \mathbf{m} to $\partial\mathcal{V}$ and \mathcal{S} . Moreover, we introduce the outward normal vector $\hat{\mathbf{n}}$ to the interfacial boundary $\partial\mathcal{S}$ pointing in tangential direction. The angles enclosed by the two normal vectors \mathbf{n} and $\hat{\mathbf{n}}$ are arbitrary and in general, both point in different directions. Before we can go on we have to introduce two relevant notations, since we have to distinguish between jump quantities $[[\bullet]]$ across the interface \mathcal{S} and interfacial average quantities $\{[\bullet]\}$. For the corresponding definitions we approach the interface from \mathcal{V}^+ or \mathcal{V}^- and obtain

$$\left. \begin{aligned} [\bullet]^+ (\mathbf{x}, t) &= \lim_{\epsilon \rightarrow 0} [\bullet] (\mathbf{x} - \epsilon \mathbf{m}) \\ [\bullet]^- (\mathbf{x}, t) &= \lim_{\epsilon \rightarrow 0} [\bullet] (\mathbf{x} + \epsilon \mathbf{m}) \end{aligned} \right\} \quad \forall \mathbf{x} \in \mathcal{S}. \quad (3.2.3)$$

With this at hand we are able to define the jump and the average of $[\bullet]$ by

$$[[[\bullet]]] := [\bullet]^+ - [\bullet]^- \quad \text{and} \quad \{[\bullet]\} := \frac{1}{2} [[[\bullet]] + [\bullet]^-]. \quad (3.2.4)$$

An important relation, that is needed for the subsequent derivations, between the jump and the average of the quantities $[\bullet]$ and $[\circ]$ with respect to an appropriate multiplicative operation \star is given by

$$[[[\bullet] \star [\circ]]] = [[[\bullet]]] \star \{[\circ]\} + \{[\bullet]\} \star [[[\circ]]]. \quad (3.2.5)$$

Furthermore, in the sequel it will be necessary to consider the limits of integrals extending over \mathcal{V}^\pm or $\partial\mathcal{V}^\pm$, respectively, containing parts of the interface $\mathcal{S} \subset \mathcal{I}$. Then for an integral extending over either \mathcal{V} or $\partial\mathcal{V}$, i.e. for a volume and a surface integral we obtain

$$\lim_{\mathcal{V} \rightarrow 0} \int_{\mathcal{V}} [\bullet] dv = 0 \quad \lim_{\mathcal{V} \rightarrow \mathcal{S}} \int_{\mathcal{V}} [\bullet] dv = \int_{\mathcal{S}} [[[\bullet]]] \cdot \mathbf{m} da \quad (3.2.6)$$

From this relations we learn, that the interfacial kinematics depend on the ambient continuum motion. Another important tool is the relation between volume and surface integrals by applying the Gauss theorem, that transforms a flux $[\bullet]$ through the boundary $\partial\mathcal{V}$ to its divergence $\text{div} [\bullet]$ in \mathcal{V} . Taking a possible jump of the flux $[\bullet]$ into account the Gauss theorem is represented by

$$\int_{\partial\mathcal{V}} [\bullet] \cdot \mathbf{n} da = \int_{\mathcal{V}} \text{div} [\bullet] dv + \int_{\mathcal{S}} [[[\bullet]]] \cdot \mathbf{m} da. \quad (3.2.7)$$

In analogy to this we can apply the Gauss theorem to the interface, such that a flux $\widehat{[\bullet]}$ through the interfacial boundary $\partial\mathcal{S}$ is related to the interface divergence $\widehat{\text{div}}[\bullet]$ in the interface \mathcal{S} by

$$\int_{\partial\mathcal{S}} \widehat{[\bullet]} \cdot \widehat{\mathbf{n}} dl = \int_{\mathcal{S}} \widehat{\text{div}}[\bullet] da. \quad (3.2.8)$$

Here $\widehat{[\bullet]}$ either denotes a tangential vector field or a superficial tensor field in the sense of Gurtin [Gur00], such that $\widehat{[\bullet]} \cdot \mathbf{m} = \mathbf{0}$ and $\widehat{\nabla} [\bullet]$ and $\widehat{\text{div}} [\bullet]$ are the surface gradient and the divergence of $[\bullet]$, respectively. These two operators can be defined by taking the covariant basis vectors \mathbf{t}^α into account, such that the interfacial gradient and divergence operators of a vector field $[\bullet]$, for instance, is given by

$$\widehat{\nabla} [\bullet] = [\bullet]_{,\alpha} \otimes \mathbf{t}^\alpha \quad \text{and} \quad \widehat{\text{div}} [\bullet] = [\bullet]_{,\alpha} \cdot \mathbf{t}^\alpha. \quad (3.2.9)$$

Then in particular if $[\bullet]$ is smooth in a three dimensional neighbourhood of \mathcal{S} , the surface gradient and divergence expands into $\widehat{\nabla} [\bullet] = \nabla [\bullet] \cdot \mathbf{P}$ and $\widehat{\text{div}} [\bullet] = \widehat{\nabla} [\bullet] : \mathbf{P}$, where

$$\mathbf{P} = [\mathbf{I} - \mathbf{m} \otimes \mathbf{m}] \quad (3.2.10)$$

is called a projection tensor. In passing it is noted that if the geometrical properties of the interface \mathcal{I} are concerned, its curvature tensor $\mathbf{L} = -\widehat{\nabla} \mathbf{m}$ and its total curvature (twice the mean curvature) $K = -\widehat{\text{div}} \mathbf{m}$ are given by the negative surface gradient and surface divergence of the normal \mathbf{m} to \mathcal{I} , respectively.

3.3 Modified Balance Equations

3.3.1 Momentum Balance Equations

For the derivation of the momentum balance equation we consider the work done by the external mechanical forces as there are volume forces \mathbf{b} and $\hat{\mathbf{b}}$ acting on the bulk material \mathcal{V} and on the interface \mathcal{S} , respectively. Additionally we have to consider tractions on $\partial\mathcal{V}$ and $\partial\mathcal{S}$ that are denoted by $\mathbf{t} = \boldsymbol{\sigma}^t \cdot \mathbf{n}$ and $\hat{\mathbf{t}} = \hat{\boldsymbol{\sigma}}^t \cdot \hat{\mathbf{n}}$. Here the assumption is taken into account, that the Cauchy theorem holds for the standard bulk stress $\boldsymbol{\sigma}^t$ as well as for the non-standard interfacial stress $\hat{\boldsymbol{\sigma}}^t$. Therefore we obtain for the resulting external mechanical power

$$P^{ext} = \frac{dW^{ext}}{dt} = \int_{\mathcal{V}} \mathbf{b} \cdot \mathbf{v} \, dv + \int_{\mathcal{S}} \hat{\mathbf{b}} \cdot \hat{\mathbf{v}} \, da + \int_{\partial\mathcal{V}} \mathbf{t} \cdot \mathbf{v} \, da + \int_{\partial\mathcal{S}} \hat{\mathbf{t}} \cdot \hat{\mathbf{v}} \, dl \quad \forall \mathbf{v}, \hat{\mathbf{v}}, \quad (3.3.1)$$

whereby \mathbf{v} is the time derivative of the standard displacement field and $\hat{\mathbf{v}}$ denotes the according interfacial velocity field that is not specified so far. Performing a change of observer by a superposed rigid body motion as it is defined by

$$\mathbf{v}^* = \mathbf{v} + \mathbf{c} + \boldsymbol{\omega} \times \mathbf{r} \quad \text{and} \quad \hat{\mathbf{v}}^* = \hat{\mathbf{v}} + \mathbf{c} + \boldsymbol{\omega} \times \mathbf{r} \quad (3.3.2)$$

we get another expression for the external mechanical power $P^{ext}(\mathbf{v}^*, \hat{\mathbf{v}}^*)$. Here \mathbf{c} and $\boldsymbol{\omega}$ are the angular and translational velocity vectors of the superposed rigid body motion and \mathbf{r} describes the distance vector to a fixed point in \mathbb{E}^3 . Due to the restriction of material objectivity both expressions have to coincide with each other, such that

$$P^{ext}(\mathbf{v}, \hat{\mathbf{v}}) - P^{ext}(\mathbf{v}^*, \hat{\mathbf{v}}^*) = 0. \quad (3.3.3)$$

We note here, that the interfacial velocity vector $\hat{\mathbf{v}}$ is affected by the rigid body motion the same as the bulk velocities \mathbf{v} . From the difference in eqn. 3.3.3 we separate all terms that are multiplied by the transversal velocity \mathbf{c} from the contributions that are multiplied by the resulting vector $\boldsymbol{\omega} \times \mathbf{r}$ and obtain the global formulations of the linear momentum balance equation

$$\int_{\mathcal{V}} \mathbf{b} \, dv + \int_{\partial\mathcal{V}} \mathbf{t} \, da + \int_{\mathcal{S}} \hat{\mathbf{b}} \, da + \int_{\partial\mathcal{S}} \hat{\mathbf{t}} \, dl = \mathbf{0} \quad (3.3.4)$$

and the balance of angular momentum

$$\int_{\mathcal{V}} \mathbf{r} \times \mathbf{b} \, dv + \int_{\partial\mathcal{V}} \mathbf{r} \times \mathbf{t} \, da + \int_{\mathcal{S}} \mathbf{r} \times \hat{\mathbf{b}} \, da + \int_{\partial\mathcal{S}} \mathbf{r} \times \hat{\mathbf{t}} \, dl = \mathbf{0}. \quad (3.3.5)$$

By shrinking the subconfiguration \mathcal{V} , that does not contain the interface, to zero we obtain the local form of the linear and angular momentum balance equations

$$\operatorname{div} \boldsymbol{\sigma}^t + \mathbf{b} = \mathbf{0} \quad \text{and} \quad \boldsymbol{\sigma}^t = \boldsymbol{\sigma}, \quad (3.3.6)$$

whereby here the Cauchy theorem $\mathbf{t} = \boldsymbol{\sigma} \cdot \mathbf{n}$ and the (standard) Gauss theorem were taken into account. For the derivation of the local angular balance equation we used the identity $\operatorname{div}(\mathbf{r} \times \boldsymbol{\sigma}^t) = \mathbf{r} \times \operatorname{div} \boldsymbol{\sigma}^t - 2\boldsymbol{\sigma}^{axl}$, whereby $\boldsymbol{\sigma}^{axl}$ was already introduced as the axial vector in eqn. 2.3.22.

To obtain the interfacial formulation of the balance equations we chose a corresponding subconfiguration \mathcal{V} containing the interface $\mathcal{S} \subset \mathcal{V}$ and by taking the limit $\mathcal{V} \rightarrow \mathcal{S}$ we analogously obtain the local interface balance equations of linear and angular momentum

$$[\![\boldsymbol{\sigma}^t]\!] \cdot \mathbf{m} + \widehat{\text{div}} \hat{\boldsymbol{\sigma}}^t + \hat{\mathbf{b}} = \mathbf{0} \quad \text{and} \quad \hat{\boldsymbol{\sigma}}^t = \hat{\boldsymbol{\sigma}}. \quad (3.3.7)$$

For the derivation of the interfacial relations in eqn. 3.3.7 we analogously applied the interface Cauchy theorem $\hat{\mathbf{t}} = \hat{\boldsymbol{\sigma}}^t \cdot \hat{\mathbf{n}}$ together with the corresponding interface Gauss theorem, that was already introduced in eqn. 3.2.8. Finally we applied the relation $\widehat{\text{div}}(\mathbf{r} \times \hat{\boldsymbol{\sigma}}^t) = \mathbf{r} \times \widehat{\text{div}} \hat{\boldsymbol{\sigma}}^t - 2\hat{\boldsymbol{\sigma}}^{axl}$ that yields the symmetry of the interfacial stress $\hat{\boldsymbol{\sigma}}^t$, whereby the axial vector is defined in analogy to the bulk formulation. Therefore $\hat{\boldsymbol{\sigma}}^t$ can be identified as a purely tangential superficial tensor field, that does not possess any normal contributions $\hat{\boldsymbol{\sigma}}^t \cdot \mathbf{m} = \hat{\boldsymbol{\sigma}} \cdot \mathbf{m} = \mathbf{0}$ and also the interface traction vector $\hat{\mathbf{t}} = \hat{\boldsymbol{\sigma}}^t \cdot \hat{\mathbf{n}}$ acting at $\partial\mathcal{S}$ is tangent to \mathcal{S} as well.

To derive the internal mechanical power we firstly introduce an abbreviation for the displacement jump $[\![\mathbf{u}]\!]$ and its energetically conjugate traction $\{\boldsymbol{\sigma}^t\} \cdot \mathbf{m}$, that subsequently are denoted by

$$\tilde{\mathbf{u}} := [\![\mathbf{u}]\!] \quad \text{and} \quad \tilde{\mathbf{t}} := \{\boldsymbol{\sigma}^t\} \cdot \mathbf{m}. \quad (3.3.8)$$

Furthermore, here we want to determine the interface displacement $\hat{\mathbf{u}}$ as the average of the bulk displacements when approaching the interface from \mathcal{V}^+ and \mathcal{V}^- , i.e.

$$\hat{\mathbf{u}} := \{\mathbf{u}\}. \quad (3.3.9)$$

This assumption seems feasible, since the limit of continuous displacements across the interface \mathcal{S} is captured correctly. With these definitions at hand and the above local bulk and interface balances of linear and angular momentum we can derive the internal mechanical power in terms of the bulk stress power and the corresponding interface stress power, such that we obtain

$$\mathbf{P}^{int}|_{\mathcal{V}} = \int_{\mathcal{V}} \nabla \mathbf{v} : \boldsymbol{\sigma}^t \, dv + \int_{\mathcal{S}} [\widehat{\nabla} \hat{\mathbf{v}} : \hat{\boldsymbol{\sigma}}^t + \tilde{\mathbf{v}} \cdot \tilde{\mathbf{t}}] \, da. \quad (3.3.10)$$

Here we find that the interface part is divided into contributions along the interface in tangential direction and across the interface in normal direction to \mathcal{S} .

In order to describe dynamical processes the momentum balance equation has to be extended by the corresponding inertial terms, whereby also here we have to distinguish between the standard bulk formulation and a non-standard interfacial contribution, such that the sum of external forces causes a change of linear momentum

$$\frac{d}{dt} \left[\int_{\mathcal{V}} \rho \mathbf{v} \, dv + \int_{\mathcal{S}} \hat{\rho} \hat{\mathbf{v}} \, da \right] = \int_{\mathcal{V}} \mathbf{b} \, dv + \int_{\partial\mathcal{V}} \mathbf{t} \, da + \int_{\mathcal{S}} \hat{\mathbf{b}} \, da + \int_{\partial\mathcal{S}} \hat{\mathbf{t}} \, dl. \quad (3.3.11)$$

This consideration yields the problem, that we have to distinguish between the interfacial and the standard bulk velocity \mathbf{v} and $\hat{\mathbf{v}}$, respectively, which were introduced previously only in a formal way. Of course, we have to make a difference between the motion of the body on the one hand and the motion of the surface, since it is conceivable, that the surface moves through the body. The example of an freezing lake where the ice front, characterized by another mass density than water, can be considered as moving surface, while the water „stands still“. Another example is the wave front

moving through a body with a certain expansion velocity, that is different from the body motion. In general the total interfacial velocity consists of

$$\widehat{\mathbf{v}} \cdot \mathbf{m} = [\mathbf{v} + \mathbf{w}] \cdot \mathbf{m}. \quad (3.3.12)$$

Here \mathbf{w} denotes the expansion velocity of the surface, describing the movement of the interface through the ambient material. If the interfacial velocity coincides with the bulk velocity

$$[\mathbf{v} - \widehat{\mathbf{v}}] \cdot \mathbf{m} = 0 \quad (3.3.13)$$

the surface is fixed with respect to the body. In this case the surface is called a *material surface*. This notation bases on the idea that materials can not penetrate and move through each other. A wave moving through a material is an example of a *non-material* surface. The case we like to investigate, assumes that the interfacial velocity coincides with the motion of the body and therefore we restrict ourselves to material surfaces.

3.3.2 Balance of Mechanical Energy

Following the concept described in section 2.3.4, the balance of mechanical energy coincides with the power done by the external forces which is equal to the change of internal energy and the kinetic energy in time. The external power was still derived in eqn. 3.3.1 and the internal energy accordingly can be found in eqn. 3.3.10. In the sequel we only consider quasistatic deformations, but for completeness we like to specify the kinetic energy by

$$K(t) = \frac{1}{2} \int_{\mathcal{V}} \rho \mathbf{v} \cdot \mathbf{v} dv + \frac{1}{2} \int_S \widehat{\rho} \widehat{\mathbf{v}} \cdot \widehat{\mathbf{v}} da. \quad (3.3.14)$$

As mentioned before we solely consider material surfaces and in addition to this, we assume quasistatic deformations, such that the kinetic energy contribution can be neglected. Therefore the resulting balance of mechanical energy can be written as

$$\begin{aligned} \int_{\mathcal{V}} \mathbf{b} \cdot \mathbf{v} dv + \int_S \widehat{\mathbf{b}} \cdot \widehat{\mathbf{v}} da + \int_{\partial \mathcal{V}} \mathbf{t} \cdot \mathbf{v} da + \\ \int_{\partial S} \widehat{\mathbf{t}} \cdot \widehat{\mathbf{v}} dl = \int_{\mathcal{V}} \nabla \mathbf{v} : \boldsymbol{\sigma}^t dv + \int_S \left[\widehat{\nabla} \widehat{\mathbf{v}} : \widehat{\boldsymbol{\sigma}}^t + \widetilde{\mathbf{v}} \cdot \widetilde{\mathbf{t}} \right] da, \end{aligned} \quad (3.3.15)$$

whereby the power due to external forces is written on the left hand side and the internal contributions can be found on the right hand side.

3.4 Thermodynamical Modifications

3.4.1 The 1st Law in Consideration of Interfaces

The 1st law of thermodynamics for closed systems coincides with the balance of internal energy. The rate of the internal energy, as mentioned before in section 2.4.1, is caused by the heat power Q and the internal due to mechanical forces. Adopting the notation of section 2.4.1 the rate of internal energy can be represented by

$$\int_{\mathcal{V}} \rho \partial_t u dv + \int_S \hat{\rho} \partial_t \hat{u} da = Q + P^{int}, \quad (3.4.1)$$

whereby the terms Q and P^{int} include the contribution due to the discontinuity, such that the heat power consists of the regular part derived in eqn.2.4.6 and the interfacial part that can be written analogously to the regular one, such that the total heating is given by

$$Q = - \int_{\partial \mathcal{V}} q(\mathbf{x}, t, \mathbf{n}) da + \int_{\mathcal{V}} \rho r(\mathbf{x}, t) dv - \int_{\partial \mathcal{S}} \hat{q}(\hat{\mathbf{x}}, t, \mathbf{m}) dl + \int_S \hat{\rho} \hat{r}(\hat{\mathbf{x}}, t) da. \quad (3.4.2)$$

Here \hat{r} denotes the non-standard heat source in the interface and $\hat{\rho}$ is the corresponding interface mass density. The interface heat flux can be decomposed in analogy to the bulk heat flux by the Cauchy theorem, such that $\hat{q} = \hat{\mathbf{q}} \cdot \hat{\mathbf{n}}$. We emphasize here that we made three distinctive assumptions of an extra contribution to internal energy in the interface \hat{u} , an extra heat source $\hat{\rho} \hat{r}$ and the interface heat flux $\hat{\mathbf{q}}$, that solely acts in tangential direction \mathcal{I} . The local form of the regular part can be found in eqn. 2.9.3 and the corresponding local interface formulation can be obtained by choosing \mathcal{V} containing \mathcal{S} and taking the limit $\mathcal{V} \rightarrow \mathcal{S}$. This yields the local interface balance of internal energy

$$\hat{\rho} \partial_t \hat{u} = \hat{\nabla} \hat{\mathbf{v}} : \hat{\boldsymbol{\sigma}}^t - \hat{\text{div}} \hat{\mathbf{q}} + \hat{\rho} \hat{r} + \partial_t \hat{\mathbf{u}} \cdot \hat{\mathbf{t}} - \llbracket \mathbf{q} \rrbracket \cdot \mathbf{m}. \quad (3.4.3)$$

Here we take the Cauchy theorem and the corresponding Gauss theorem for the interface heat flux into account, which was already introduced in eqn. 3.2.8. It resembles to eqn. 2.9.3, whereby we have to recognize that the first three terms represent internal energy production and sources along the interface, whereas the last two terms are related to the internal energy production and energy sources across the interface.

3.4.2 The 2nd Law in Consideration of Interfaces

Similar to the rate of internal energy the entropy rate also has to be modified with respect to interface contributions. In contrast to the balance of internal energy the entropy is not a conserving quantity, such that in addition to the entropy flux and entropy source, a production term, which is denoted by Y , has to be taken into account. Therefore the rate of total entropy renders eqn. 2.4.14, such that we have to specify the entropy production and entropy input \bar{Q} in consideration of the interface contribution. The entropy input consists of the standard entropy flux h and entropy source g and the corresponding interface entropy input is determined by \hat{h} and \hat{g} , which describe the entropy flux and source in the interface. The resulting entropy input can be written as

$$\bar{Q} = \int_{\mathcal{V}} \rho g dv + \int_{\partial \mathcal{V}} h da + \int_S \hat{\rho} \hat{g} da + \int_{\partial \mathcal{S}} \hat{h} dl. \quad (3.4.4)$$

Analogous to the internal energy, the entropy rate consists of an regular bulk contribution and the additional interface contribution. The corresponding production term can also be decomposed into a standard bulk contribution η and the interface contribution $\hat{\eta}$. With this at hand we can write the entropy production as the difference of the entropy rate and the entropy input

$$\int_{\mathcal{V}} \eta dv + \int_{\mathcal{S}} \hat{\eta} da = \int_{\mathcal{V}} \rho \partial_t s dv + \int_{\mathcal{S}} \hat{\rho} \partial_t \hat{s} da - \bar{Q} \geq 0. \quad (3.4.5)$$

Clearly, the assumption of a separate interface entropy \hat{s} , interface entropy production $\hat{\eta}$, interface entropy source \hat{g} and interface entropy flux \hat{h} are the distinctive features, here. In the next step we can localize the global statement of total entropy for an arbitrary subconfiguration \mathcal{V} , that does not contain \mathcal{S} , and obtain the familiar bulk entropy balance equation

$$\rho \partial_t s = -\operatorname{div} \mathbf{h} + \rho g + \eta \quad \text{with} \quad \eta \geq 0, \quad (3.4.6)$$

whereby we again applied the Cauchy theorem to the entropy flux $h = \mathbf{h} \cdot \mathbf{n}$ and the standard Gauss theorem transforms the integral over $\partial \mathcal{V}$ into a integral over \mathcal{V} . Analogous we applied the non-standard interface Cauchy theorem to the interface entropy flux $\hat{h} = \hat{\mathbf{h}} \cdot \hat{\mathbf{n}}$ and afterwards we transform the integral over $\partial \mathcal{S}$ into an integral over \mathcal{S} by applying the non-standard Gauss theorem. Taking the limit $\mathcal{V} \rightarrow \mathcal{S}$, whereby this time the subconfiguration \mathcal{V} contains the interface \mathcal{S} , and localizing for an arbitrary \mathcal{S} we get the local entropy balance equation for the interface

$$\hat{\rho} \partial_t \hat{s} = -\operatorname{div} \hat{\mathbf{h}} + \hat{\eta} + \hat{\rho} \hat{g} - \llbracket \mathbf{h} \rrbracket \cdot \mathbf{m} \quad \text{with} \quad \hat{\eta} \geq 0. \quad (3.4.7)$$

Again we like to point out, that in this representation the first three terms describe the entropy input and entropy production along the interface, reflecting the format of the bulk balance of entropy, whereas the last term describes the entropy flux across the interface.

3.4.3 Modified Clausius-Duhem Inequality

In order to proceed we have to specify the entropy flux and entropy production terms by constitutive assumptions. It is quite common to relate the entropy fluxes and sources to the heat fluxes and sources, as already mentioned in section 2.4.3. From this emanates the subsequent relations

$$\mathbf{h} := \frac{1}{\Theta} \mathbf{q}, \quad g := \frac{1}{\Theta} r, \quad \hat{\mathbf{h}} := \frac{1}{\Theta} \hat{\mathbf{q}}, \quad \hat{g} := \frac{1}{\Theta} \hat{r}, \quad (3.4.8)$$

defining the entropy flux and entropy source for the bulk and the interface, respectively. Here $\hat{\Theta}$ denotes the non-standard interface temperature in \mathcal{S} , which has to be specified exactly later on. The given approach for the entropy flux is somehow arbitrary and generally questionable. However, it is widely accepted. In addition to that, it is motivated by the corresponding p-V-T thermodynamics. For the purposes of this work this ansatz is sufficient and derives reasonable results. Therefore we shall accept the given assumption in the spirit of simplicity and clearness.

Furthermore we have to define the entropy production terms η and $\hat{\eta}$ and in general it is related to the dissipation D , whereby we introduce here an extra interface dissipation \hat{D} , such that the production terms can be defined by

$$\eta := \frac{1}{\Theta} D \geq 0 \quad \text{and} \quad \hat{\eta} := \frac{1}{\Theta} \hat{D} \geq 0. \quad (3.4.9)$$

With the above given constitutive assumptions at hand the local bulk and interface balance equations can be rewritten as

$$\begin{aligned}\Theta \rho \partial_t s &= -\operatorname{div} \mathbf{q} + \nabla \ln \Theta \cdot \mathbf{q} + \rho r + D & \text{with } D &\geq 0, \\ \widehat{\Theta} \widehat{\rho} \partial_t \widehat{s} &= -\widehat{\operatorname{div}} \widehat{\mathbf{q}} + \widehat{\nabla} \ln \widehat{\Theta} \cdot \widehat{\mathbf{q}} + \widehat{\rho} \widehat{r} + \widehat{D} - \widehat{\Theta} \llbracket \mathbf{h} \rrbracket \cdot \mathbf{m} & \text{with } \widehat{D} &\geq 0.\end{aligned}\quad (3.4.10)$$

The derived balance equations of the bulk and interface entropy can be related to the internal energy balance equations and the free Helmholtz energy by means of the Legendre transformation

$$u = \Psi + \Theta s \quad \text{and} \quad \widehat{u} = \widehat{\Psi} + \widehat{\Theta} \widehat{s}, \quad (3.4.11)$$

whereby this also requires the distinction between the standard bulk free energy Ψ and an interface free energy contribution $\widehat{\Psi}$. The corresponding rate formulations are given by

$$\partial_t u = \partial_t \Psi + \Theta \partial_t s + s \partial_t \Theta \quad \text{and} \quad \partial_t \widehat{u} = \partial_t \widehat{\Psi} + \widehat{\Theta} \partial_t \widehat{s} + \widehat{s} \partial_t \widehat{\Theta}. \quad (3.4.12)$$

Inserting these expressions in eqn. 3.4.10, 3.4.3 and 2.9.3 into the corresponding rate formulations and solving for the dissipation powers, finally yields

$$\begin{aligned}D &= [\nabla \mathbf{v}]^{sym} : \boldsymbol{\sigma}^t - \rho \partial_t \Psi - s \rho \partial_t \Theta - \nabla \ln \Theta \cdot \mathbf{q} \geq 0, \\ \widehat{D} &= [\widehat{\nabla} \widehat{\mathbf{v}}]^{sym} : \widehat{\boldsymbol{\sigma}}^t - \widehat{\rho} \partial_t \widehat{\Psi} - \widehat{s} \widehat{\rho} \partial_t \widehat{\Theta} - \widehat{\nabla} \ln \widehat{\Theta} \cdot \widehat{\mathbf{q}} + \partial_t \widehat{\mathbf{u}} \cdot \widehat{\mathbf{t}} - \llbracket \mathbf{q} \rrbracket \cdot \mathbf{m} + \widehat{\Theta} \llbracket \mathbf{h} \rrbracket \cdot \mathbf{m} \geq 0.\end{aligned}\quad (3.4.13)$$

Analogous to the entropy rate and the internal energy balance, in the interface dissipation power we can identify the first four terms, which are related to the dissipation along the interface resembling the format of the bulk dissipation inequality, whereas the last three terms stem from the dissipation associated with jumps of displacement, heat and entropy flux across the interface. In section 2.4.3 we splitted the dissipation into a local and a convective part and this decomposition is also applied to the interface dissipation power. Therefore, analogous to eqn. 2.4.25 and 2.4.26 we have to distinguish the local interface dissipation

$$\widehat{D}_{loc} = [\widehat{\nabla} \widehat{\mathbf{v}}]^{sym} : \widehat{\boldsymbol{\sigma}}^t - \widehat{\rho} \partial_t \widehat{\Psi} - \widehat{s} \widehat{\rho} \partial_t \widehat{\Theta} + \partial_t \widehat{\mathbf{u}} \cdot \widehat{\mathbf{t}} \geq 0. \quad (3.4.14)$$

from the non-local or convective interface dissipation contribution

$$\widehat{D}_{con} = \underbrace{\widehat{\Theta} \llbracket \mathbf{h} \rrbracket \cdot \mathbf{m} - \llbracket \mathbf{q} \rrbracket \cdot \mathbf{m}}_{\widehat{D}_{con}^\perp} - \underbrace{\widehat{\nabla} \ln \widehat{\Theta} \widehat{\mathbf{q}}}_{\widehat{D}_{con}^\parallel} \geq 0, \quad (3.4.15)$$

whereby we want to distinguish additionally the dissipation contribution in tangential direction $\widehat{D}_{con}^\parallel$ and normal direction \widehat{D}_{con}^\perp . In these expressions the definition of the interface temperature $\widehat{\Theta}$, that was not specified so far, plays a crucial role and that shall be investigated in the following section.

3.4.4 Remarks on the Interface Temperature

For the description of the thermal subproblem further constitutive assumptions with respect to the heat flux are necessary. Therefore we resort to the Fourier heat conduction law and adopt it to the interface heat flux, such that we obtain

$$\mathbf{q} \propto -\nabla \Theta \quad \text{and} \quad \widehat{\mathbf{q}} \propto -\widehat{\nabla} \widehat{\Theta}, \quad (3.4.16)$$

whereby the heat flux is assumed depending linearly of the temperature gradient and the interface temperature gradient, respectively. Inserting this assumptions into the reduced bulk dissipation inequality shows

$$D_{con} \propto \nabla \ln \Theta \cdot \nabla \Theta \geq 0, \quad (3.4.17)$$

that a positive bulk convective dissipation power is ensured. This conclusion can be extended to the complete interface formulation, but solely for the tangent part $\hat{D}_{loc}^{\parallel}$, since we get

$$\hat{D}_{con} \neq \hat{D}_{con}^{\parallel} \propto \hat{\nabla} \ln \Theta \cdot \hat{\nabla} \hat{\Theta} \geq 0. \quad (3.4.18)$$

The second part of the convective interface dissipation describing the perpendicular contributions leads to the sufficient requirement

$$\hat{D}_{con}^{\perp} = -\llbracket \mathbf{q} \rrbracket \cdot \mathbf{m} + \hat{\Theta} \llbracket \frac{\mathbf{q}}{\Theta} \rrbracket \cdot \mathbf{m} \geq 0, \quad (3.4.19)$$

whereby we replaced the entropy flux by the constitutive assumption made in eqn. 3.4.8. This condition is fulfilled if an appropriate interface temperature $\hat{\Theta}$ is chosen and subsequently we investigate two reasonable alternatives with respect to the thermodynamical consistency of eqn. 3.4.19

Hypothesis I The simplest attempt to find an interface temperature is to define it by the average temperature when approaching the interface from \mathcal{V}^- and \mathcal{V}^+

$$\hat{\Theta} := \{\Theta\}. \quad (3.4.20)$$

Inserting this approach into eqn. 3.4.19 we obtain an expression, in which the term $\{\Theta\} \llbracket \frac{\mathbf{q}}{\Theta} \rrbracket$ occurs and applying the relation in eqn. 3.2.5, we can replace it by

$$\{\Theta\} \llbracket \frac{\mathbf{q}}{\Theta} \rrbracket = \llbracket \Theta \frac{\mathbf{q}}{\Theta} \rrbracket - \llbracket \Theta \rrbracket \{\frac{\mathbf{q}}{\Theta}\}, \quad (3.4.21)$$

such that the convected dissipation power across the interface reduces to

$$\hat{D}_{con}^{\perp} = -\llbracket \Theta \rrbracket \{\frac{\mathbf{q}}{\Theta}\} \cdot \mathbf{m} \geq 0. \quad (3.4.22)$$

This equation is fulfilled, if the average entropy flux across the interface is proportional to the negative temperature jump

$$\tilde{h} := \{\mathbf{h}\} \cdot \mathbf{m} \propto -\llbracket \Theta \rrbracket. \quad (3.4.23)$$

Hypothesis II The second obvious choice for the interface temperature is the inverse of the average coldness

$$\hat{\Theta} := \{\Theta^{-1}\}^{-1}. \quad (3.4.24)$$

Inserting this choice into the reduced interface dissipation inequality and applying the relation

$$\llbracket \frac{\mathbf{q}}{\Theta} \rrbracket = \llbracket \Theta^{-1} \rrbracket \{\mathbf{q}\} + \{\Theta^{-1}\} \llbracket \mathbf{q} \rrbracket \quad (3.4.25)$$

we obtain for the convective dissipation power due to jumps of heat and entropy flux across the interface

$$\widehat{D}_{con}^{\perp} = -\llbracket \Theta \rrbracket \frac{\{\mathbf{q}\}}{\{\Theta\}} \cdot \mathbf{m} \geq 0. \quad (3.4.26)$$

A natural choice to satisfy this equation is a Fourier type behaviour for the average heat flux across the interface

$$\widetilde{q} := \{\mathbf{q}\} \cdot \mathbf{m} \propto -\llbracket \Theta \rrbracket. \quad (3.4.27)$$

Summarizing adopting one of the hypotheses I or II for the interface temperature together with the assumption of Fourier type behaviour in the bulk, along and across the interface identically satisfies the reduced dissipation inequalities for the bulk and in the interface.

3.5 Weak Form of the Coupled Problem

Likewise the continuous case the described problem has to be solved numerically by the finite element method. For this we have to derive the weak form, which has to be extended by the interface contributions and in analogy to the continuous case we like to distinguish between the mechanical subproblem and the thermal one. Here we want to consider the different formulations emerging from the two approaches for the interface temperature $\widehat{\Theta}$.

3.5.1 Mechanical Subproblem

For representation of the virtual mechanical work we need to introduce some abbreviations for the virtual bulk and interface displacements as there are $\delta \mathbf{u}$, $\delta \widehat{\mathbf{u}} := \{\delta \mathbf{u}\}$ and $\delta \widetilde{\mathbf{u}} = \llbracket \delta \mathbf{u} \rrbracket$. The strong formulations of the balance of linear momentum for the bulk and the interface

$$\operatorname{div} \boldsymbol{\sigma}^t + \mathbf{b} = \mathbf{0} \quad \text{and} \quad \widehat{\operatorname{div}} \widehat{\boldsymbol{\sigma}}^t + \widehat{\mathbf{b}} + \llbracket \boldsymbol{\sigma}^t \rrbracket \cdot \mathbf{m} = \mathbf{0} \quad (3.5.1)$$

are tested by the virtual displacements and the resulting representation of the mechanical virtual work is given by

$$\begin{aligned} 0 &= \int_{\mathcal{B}} [\nabla \delta \mathbf{u} : \boldsymbol{\sigma}^t - \delta \mathbf{u} \cdot \mathbf{b}] \, dv - \int_{\partial \mathcal{B}} \delta \mathbf{u} \cdot \mathbf{t} \, da \\ &+ \int_{\mathcal{I}} [\widehat{\nabla} \delta \widehat{\mathbf{u}} : \widehat{\boldsymbol{\sigma}}^t - \delta \widehat{\mathbf{u}} \widehat{\mathbf{b}} + \delta \widetilde{\mathbf{u}} \cdot \{\boldsymbol{\sigma}^t\} \cdot \mathbf{m}] \, da - \int_{\partial \mathcal{I}} \delta \widehat{\mathbf{u}} \cdot \widehat{\mathbf{t}} \, dl. \end{aligned} \quad (3.5.2)$$

This equation is the point of departure for the application of numerical iteration schemes to the mechanical subproblem.

3.5.2 The Thermal Subproblem based on Hypothesis I

If adopting hypothesis I for the interface temperature it turns out that the following version of the entropy evolution leads eventually to the most convenient definition of the thermal virtual work expressions

$$\rho \partial_t s = -\operatorname{div} \mathbf{h} + \eta + \rho g \quad \text{and} \quad \widehat{\rho} \partial_t \widehat{s} = -\widehat{\operatorname{div}} \widehat{\mathbf{h}} + \widehat{\eta} + \widehat{\rho} g - \llbracket \mathbf{h} \rrbracket \cdot \mathbf{m}. \quad (3.5.3)$$

Testing these equations with virtual entropies δs and $\delta \hat{s} := \{\delta s\}$ renders after some straight forward manipulations the thermal virtual work statement, whereby we used the abbreviation $\delta \tilde{s} := \llbracket \delta s \rrbracket$ for the jump of the virtual entropy

$$\begin{aligned}
 \int_{\mathcal{B}} \delta s \rho \partial_t s \, dv + \int_{\mathcal{I}} \delta \hat{s} \partial_t \hat{s} \, da &= \int_{\mathcal{B}} [\nabla \delta s \cdot \mathbf{h} + \delta s \eta + \delta s \rho g] \, dv \\
 &- \int_{\partial \mathcal{B}} \delta s h \, da \\
 &+ \int_{\mathcal{I}} \left[\widehat{\nabla} \delta \hat{s} \cdot \widehat{\mathbf{h}} + \delta \hat{s} \widehat{\eta} + \delta \hat{s} \widehat{\rho} g + \delta \hat{s} \widehat{h} \right] \, da \\
 &- \int_{\partial \mathcal{I}} \delta \hat{s} \widehat{h} \, dl.
 \end{aligned} \tag{3.5.4}$$

This version of the thermal virtual work statment is on the one hand most suited for hypothesis I, i.e. the probably naive assumption $\widehat{\Theta} := \{\Theta\}$, since it allows to incorporate directly the Fourier type behaviour for the average entropy flux across the interface $\widehat{h} \propto \llbracket \Theta \rrbracket$. On the other hand the necessity to specify constitutive laws for the entropy flux in the bulk and along the interface together with the difficulty to prescribe entropy fluxes across the Neumann boundaries and to evaluate the entropy production terms makes this formulation less attractive.

3.5.3 The Thermal Subproblem based on Hypothesis II

In analogy it turns out that adopting hypothesis II for the interface temperature an alternative version of the entropy evolution equations leads eventually to a more convenient definition of the thermal virtual work expression

$$\rho \Theta \partial_t s = -\operatorname{div} \mathbf{q} + r \quad \text{and} \quad \widehat{\rho} \widehat{\Theta} \partial_t \widehat{s} = -\widehat{\operatorname{div}} \widehat{\mathbf{q}} + \widehat{\rho} \widehat{r} - \llbracket \mathbf{q} \rrbracket \cdot \mathbf{m}. \tag{3.5.5}$$

Testing these equations with virtual entropies δs and using the same abbreviations as before it renders after some straight forward manipulations the thermal virtual work statement

$$\begin{aligned}
 \int_{\mathcal{B}} \delta s \rho \Theta \partial_t s \, dv + \int_{\mathcal{I}} \delta \hat{s} \widehat{\rho} \widehat{\Theta} \partial_t \widehat{s} \, da &= \int_{\mathcal{B}} [\nabla \delta s \cdot \mathbf{q} + \delta s \rho r] \, dv \\
 &- \int_{\partial \mathcal{B}} \delta s q \, da \\
 &+ \int_{\mathcal{I}} \left[\widehat{\nabla} \delta \hat{s} \cdot \widehat{\mathbf{q}} + \delta \hat{s} \widehat{\rho} \widehat{r} + \delta \hat{s} \widehat{q} \right] \, da \\
 &- \int_{\partial \mathcal{I}} \delta \hat{s} \widehat{q} \, dl
 \end{aligned} \tag{3.5.6}$$

This version of the thermal virtual work statement is most suited for the hypothesis II, i.e. the somewhat unexpected assumption $\widehat{\Theta} := [\Theta^{-1}]^{-1}$, since it allows to incorporate directly the Fourier type behaviour for the average heat flux across the interface $\widehat{q} \propto \llbracket \Theta \rrbracket$.

3.5.4 The Thermal Subproblem in Terms of Temperature

The formulation of the thermal subproblem was performed in terms of the entropy rate, which is not very useful for realistic calculations, which usually require a formulation of the measurable and controllable quantities temperature and heat flux. The corresponding temperature evolution equation can be derived from the entropy rate equation of hypothesis II. Point of departure for this is the entropy rate equations in eqn. 3.4.10, where we insert the bulk and interface dissipation inequalities from eqn. 3.4.13, such that we obtain

$$\begin{aligned} \rho\Theta\partial_t s &= \rho r - \operatorname{div} \mathbf{q} + [\nabla \mathbf{u}]^{sym} : \boldsymbol{\sigma}^t - \rho\partial_t \Psi - \rho s \partial_t \Theta \\ \widehat{\rho}\widehat{\Theta}\partial_t \widehat{s} &= \widehat{\rho} r - \widehat{\operatorname{div}} \widehat{\mathbf{q}} + [\widehat{\nabla} \widehat{\mathbf{u}}]^{sym} : \widehat{\boldsymbol{\sigma}}^t - \widehat{\rho}\partial_t \widehat{\Psi} - \widehat{\rho} \widehat{s} \partial_t \widehat{\Theta} + \partial_t \widehat{\mathbf{u}} \cdot \widehat{\mathbf{t}} - \llbracket \mathbf{q} \rrbracket \cdot \mathbf{m}. \end{aligned} \quad (3.5.7)$$

Analogous to the bulk free energy function, that depends on the displacement and the temperature field, the interface free energy function depends on the interface displacement and temperature field and in addition to that also on the displacement jump across the discontinuity. According to this we can express the rates of the free energy functions by

$$\begin{aligned} \partial_t \Psi &= \frac{\partial \Psi}{\partial [\nabla \mathbf{u}]^{sym}} \partial_t [\nabla \mathbf{u}]^{sym} + \frac{\partial \Psi}{\partial \Theta} \partial_t \Theta \quad \text{and} \\ \partial_t \widehat{\Psi} &= \frac{\partial \widehat{\Psi}}{\partial [\widehat{\nabla} \widehat{\mathbf{u}}]^{sym}} : \partial_t [\widehat{\nabla} \widehat{\mathbf{u}}]^{sym} + \frac{\partial \widehat{\Psi}}{\partial \widehat{\mathbf{u}}} \cdot \partial_t \widehat{\mathbf{u}} + \frac{\partial \widehat{\Psi}}{\partial \widehat{\Theta}} \partial_t \widehat{\Theta} \end{aligned} \quad (3.5.8)$$

whereby we define the appearing derivatives of the interface free energy in analogy to the continuous quantities

$$\begin{aligned} \rho \frac{\partial \Psi}{\partial [\nabla \mathbf{u}]^{sym}} &:= \boldsymbol{\sigma}^t, & \rho \frac{\partial \Psi}{\partial \Theta} &:= -\rho s, \\ \widehat{\rho} \frac{\partial \widehat{\Psi}}{\partial [\widehat{\nabla} \widehat{\mathbf{u}}]^{sym}} &:= \widehat{\boldsymbol{\sigma}}^t, & \widehat{\rho} \frac{\partial \widehat{\Psi}}{\partial \widehat{\mathbf{u}}} &:= \widehat{\mathbf{t}}, & \widehat{\rho} \frac{\partial \widehat{\Psi}}{\partial \widehat{\Theta}} &:= -\widehat{\rho} \widehat{s}. \end{aligned} \quad (3.5.9)$$

Inserting these quantities in eqn. 3.5.8 the entropy rate equations reduce to

$$\begin{aligned} \rho\Theta\partial_t s &= \rho r - \operatorname{div} \mathbf{q} \\ \widehat{\rho}\widehat{\Theta}\partial_t \widehat{s} &= \widehat{\rho} r - \widehat{\operatorname{div}} \widehat{\mathbf{q}} - \llbracket \mathbf{q} \rrbracket \cdot \mathbf{m}, \end{aligned} \quad (3.5.10)$$

whereby here two interface heat fluxes occur describing the heat conduction behaviour across and along the interface. But still the rate equation is formulated in terms of the entropies. Therefore we use now the definitions of the entropies $s := -\partial_\Theta \Psi$ and $\widehat{s} := -\partial_{\widehat{\Theta}} \widehat{\Psi}$ for replacing it by expressions in terms of the free energies, such that we obtain

$$\rho\partial_t s = -\rho \frac{\partial^2 \Psi}{\partial \Theta \partial [\nabla \mathbf{u}]^{sym}} : \partial_t [\nabla \mathbf{u}]^{sym} - \rho \frac{\partial^2 \Psi}{\partial \Theta^2} \partial_t \Theta \quad (3.5.11)$$

$$\widehat{\rho}\partial_t \widehat{s} = -\widehat{\rho} \frac{\partial^2 \widehat{\Psi}}{\partial \widehat{\Theta} \partial [\widehat{\nabla} \widehat{\mathbf{u}}]^{sym}} : \partial_t [\widehat{\nabla} \widehat{\mathbf{u}}]^{sym} - \widehat{\rho} \frac{\partial^2 \widehat{\Psi}}{\partial \widehat{\Theta} \partial \widehat{\mathbf{u}}} \cdot \partial_t \widehat{\mathbf{u}} - \widehat{\rho} \frac{\partial^2 \widehat{\Psi}}{\partial \widehat{\Theta}^2} \partial_t \widehat{\Theta}. \quad (3.5.12)$$

Solving these expression for the terms containing the temperature rates, we obtain the temperature evolution equations for the bulk and the interface

$$\begin{aligned} \rho c \partial_t \Theta &= \rho r^* - \operatorname{div} \mathbf{q} \\ \widehat{\rho} \widehat{c} \partial_t \widehat{\Theta} &= \widehat{\rho} \widehat{r}^* - \widehat{\operatorname{div}} \widehat{\mathbf{q}} - \llbracket \mathbf{q} \rrbracket \cdot \mathbf{m} \end{aligned} \quad (3.5.13)$$

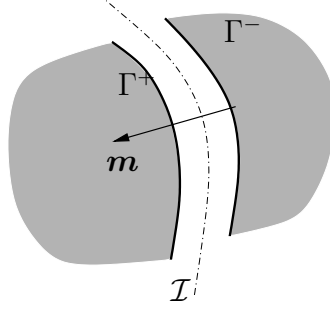


Figure 3.2. Shape of a strong discontinuity

These equations are the temperature evolution equations for the bulk and the interface. Here we assumed a thermo-elastic material where no further internal variables are taken into account. The terms of thermo-mechanical coupling are collected in the modified source terms r^* and \widehat{r}^* , which are defined by

$$\begin{aligned}\rho r^* &= \rho r + \Theta \boldsymbol{\beta} : \partial_t [\nabla \mathbf{u}]^{sym} \\ \widehat{\rho r}^* &= \widehat{\rho r} + \widehat{\Theta} \left[\widehat{\boldsymbol{\beta}} \cdot \partial_t [\widehat{\nabla} \widehat{\mathbf{u}}]^{sym} + \widetilde{\boldsymbol{\beta}} : \partial_t \widetilde{\mathbf{u}} \right].\end{aligned}\quad (3.5.14)$$

It seems feasible, that we obtain two contributions to the interface temperature evolution due to the mechanical work done across and along the interface which are covered by the interface stress $\widehat{\boldsymbol{\sigma}}^t$ and the traction vector $\widetilde{\mathbf{t}}$ or the corresponding temperature derivatives $\widehat{\boldsymbol{\beta}}$ and $\widetilde{\boldsymbol{\beta}}$. These are the local temperature rate equations describing the thermal subproblem.

In the next step we derive the variational form of the temperature balance equation by multiplying it by a virtual temperature and integrating it over the corresponding domains. After applying once more the partial integration scheme and the standard Gauss theorem we obtain the weak form consisting of the three following contributions

$$\mathcal{U}^{ext}(\delta\Theta) - \mathcal{U}^{int}(\delta\Theta) + \mathcal{U}^{dis}(\delta\Theta) = 0, \quad \forall \delta\Theta. \quad (3.5.15)$$

Here we recover the terms for the external virtual power as we derived them in eqn. 2.9.23 and we rewrite them here just for clarity

$$\mathcal{U}^{int} = \int_{\mathcal{B}_t} \left[-\rho c_p \dot{\Theta} \delta\Theta + \mathbf{q} \cdot \text{grad} \delta\Theta \right] dv, \quad \mathcal{U}^{ext} = \int_{\partial\mathcal{B}_t} q_n \delta\Theta da - \int_{\mathcal{B}_t} r^* \delta\Theta dv.$$

Furtheron we also get additional contributions of virtual thermal power due to the discontinuity, that arise from the integral over the internal boundaries Γ^+ and Γ^- (fig. 3.2), such that we obtain

$$\mathcal{U}^{dis} = - \int_{\Gamma^+} \delta\Theta^+ \mathbf{q}^+ \cdot \mathbf{m}^+ da - \int_{\Gamma^-} \delta\Theta^- \mathbf{q}^- \cdot \mathbf{m}^- da \quad (3.5.16)$$

Analogous to the mechanical subproblem we assume $-\mathbf{m}^+ = \mathbf{m}^- = \mathbf{m}$ and taking eqn. 3.2.9 into account we can rewrite the thermal discontinuous virtual power contribution as

$$\mathcal{U}^{dis} = - \int_{\mathcal{I}} \left[\delta\widehat{\Theta} [\mathbf{q}] \cdot \mathbf{m} + \llbracket \delta\Theta \rrbracket \{ \mathbf{q} \} \cdot \mathbf{m} \right] da. \quad (3.5.17)$$

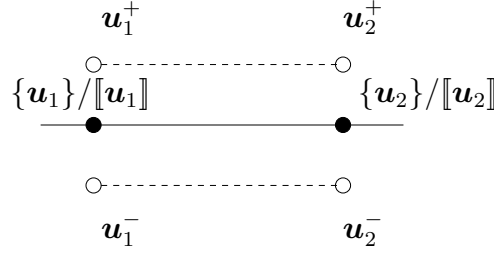


Figure 3.3. Construction of interface element

Here we like to replace the first term by the interface temperature evolution equation in eqn. 3.5.13, that we accordingly solve for $[[\mathbf{q}]] \cdot \mathbf{m}$. This yields for the discontinuous contribution to the weak form of the thermal subproblem

$$\mathcal{U}(\delta\Theta) = - \int_{\mathcal{I}} \left[\delta\hat{\Theta} [\hat{\rho}\hat{r}^* - \hat{\rho}c\partial_t\hat{\Theta}] + [[\delta\Theta]]\{\mathbf{q}\} \cdot \mathbf{m} + \widehat{\text{div}}\hat{\mathbf{q}} \right] da. \quad (3.5.18)$$

The last term in this relation can be replaced by applying the partial integration scheme such that the weak form of the thermal subproblem, in consideration of interfaces, can be represented by

$$\begin{aligned} \int_{B_t} [\rho c_p \partial_t \Theta - r^*] \delta\Theta dv + \int_{\mathcal{I}} [\hat{\rho}c_p \partial_t \hat{\Theta} - \hat{r}^*] da &= \int_{\partial B} q_n \delta\Theta da - \int_{B_t} \mathbf{q} \nabla \delta\Theta dv - \int_{\mathcal{I}} [[\delta\Theta]] \{\mathbf{q} \cdot \mathbf{m}\} da \\ &+ \int_{\partial \mathcal{I}} \delta\hat{\Theta} \hat{q}_n dl - \int_{\mathcal{I}} \hat{\nabla} \delta\hat{\Theta} \cdot \hat{\mathbf{q}} da \end{aligned} \quad (3.5.19)$$

Here $\hat{q}_n = \hat{\mathbf{q}} \cdot \hat{\mathbf{n}}$ describes the heat flux over the interface boundary. This is the point of departure for the numerical realization of the thermal problem in consideration of thermo-mechanical coupling and interfaces. As mentioned before, we considered the simple case of thermo-elastic coupling, such that the introduction of additional internal variables is not necessary. If we apply the presented theory to the subject of localization problems (domain-dependent formulation), we will find the formulation of yield condition indicating the onset of slip. This initiates the postcritical behaviour and in the following proceeding the slip zone can behave inelastic requiring additional internal variables describing inelastic effects (hardening, damage, etc.). According to this the list of arguments of the interface free energy function has to be extended. Here for the sake of clearness, we restricted the presentation to the thermo-elastic case.

3.6 Numerical Aspects

The numerical treatment of discontinuities and interfaces requires, as mentioned above, certain finite element formulations that are able to cover discrete separation of materials. On the one hand we need element formulations describing the jump contributions and on the other hand there is some necessity for elements, which are able to describe the material behaviour of the interface in mean by the average quantities. Since we investigate the linear theory, we do not need any linearization, such that it is sufficient to present the discrete representation of the corresponding elements. For the spatial discretization of the displacements and temperatures in the interface we resort to the isoparametric concept. For the discretization of the bulk displacement and temperature fields we

use the standard Legendre interpolations. The geometry of the interface element is described by

$$\mathbf{x}|_{\mathcal{I}_e} \approx \sum_{a=1}^n N_a(\xi_i) \mathbf{x}_a \quad \mathcal{I} = \bigcup_e \mathcal{I}_e. \quad (3.6.1)$$

whereby \mathbf{x} denotes an isoparametric finite element interpolation and \mathbf{x}_a are the coordinates of a typical finite element node. Since no derivatives of higher order are needed the choice of linear shape functions for the interpolation of the interface displacements and temperatures are sufficient. At first we approximate the tangent vector \mathbf{m} within the interface by

$$\hat{\mathbf{n}}|_{\mathcal{I}_e} = \sum_{a=1}^n \nabla_x N_a(\xi_i) \mathbf{x}_a \quad (3.6.2)$$

and by following the standard finite element approach we discretize the actual and virtual displacement jumps

$$\tilde{\mathbf{u}}|_{\mathcal{I}_e} = \sum_{a=1}^{n/2} N_a(\xi_i) [\![\mathbf{u}]\!]_a \quad \text{and} \quad \delta \tilde{\mathbf{u}}|_{\mathcal{I}_e} = \sum_{a=1}^{n/2} N_a(\xi_i) [\![\delta \mathbf{u}]\!]_a \quad (3.6.3)$$

and analogously the temperature jump and the corresponding variation are interpolated by

$$\tilde{\Theta}|_{\mathcal{I}_e} = \sum_{a=1}^{n/2} M_a(\xi_i) [\![\Theta]\!]_a \quad \text{and} \quad \delta \tilde{\Theta}|_{\mathcal{I}_e} = \sum_{a=1}^{n/2} M_a(\xi_i) [\![\delta \Theta]\!]_a. \quad (3.6.4)$$

Here again the quantities $[\![\mathbf{u}]\!]_a = \mathbf{u}_a^+ - \mathbf{u}_a^-$ and $[\![\Theta]\!]_a = \Theta_a^+ - \Theta_a^-$ comply with the jump of the particular variable at the a -th node of a typical interface element. That is also the reason why the summation only runs over $n/2$ nodes.

To approximate averages of the interfacial quantities we transfer the discretization of the jump to the average terms, such that we obtain for the average displacements

$$\hat{\mathbf{u}}|_{\mathcal{I}_e} = \sum_{a=1}^{n/2} N_a(\xi_i) \{\mathbf{u}\}_a, \quad \delta \hat{\mathbf{u}}|_{\mathcal{I}_e} = \sum_{a=1}^{n/2} N_a(\xi_i) \{\delta \mathbf{u}\}_a. \quad (3.6.5)$$

The interface temperature $\hat{\Theta}$ can be chosen in different ways, whereby here for the reasons mentioned before we chose it in the spirit of hypothesis II, such that the numerical approximation is given by

$$\hat{\Theta}|_{\mathcal{I}_e} = \sum_{a=1}^{n/2} M_a(\xi_i) \{\Theta^{-1}\}_a^{-1} \quad \text{and} \quad \delta \hat{\Theta}|_{\mathcal{I}_e} = \sum_{a=1}^{n/2} M_a(\xi_i) \{\delta \Theta^{-1}\}_a^{-1}. \quad (3.6.6)$$

We calculate the average of the displacements by $\{\mathbf{u}\}_a = \frac{1}{2}[\mathbf{u}_a^+ + \mathbf{u}_a^-]$ and the discrete interfacial temperature can be determined by $\hat{\Theta} = \{\Theta^{-1}\}_a^{-1} = [\frac{1}{2}[1/\Theta_a^+ + 1/\Theta_a^-]]^{-1} = [2\Theta_a^+ \Theta_a^-]/[\Theta_a^+ + \Theta_a^-]$. The theory developed so far did not need the averages of the displacements and here the discretization is just written for completeness. In contrast to that, for the thermal subproblem the temperature average is needed for the determination of the average-based thermomechanical stress.

Finally, we are interested in the finite element interpolation of the tangential gradients of the interface quantities. Also here we apply the standard finite element interpolation whereby the derivatives of

the shape functions are needed. The gradient of the tangent interface displacements is interpolated by

$$\widehat{\nabla} \widehat{\mathbf{u}} \Big|_{\mathcal{I}_e} = \sum_{a=1}^{n/2} \nabla \mathbf{N}_a(\xi_i) \{\mathbf{u}\}_a \quad \text{and} \quad \widehat{\nabla} \delta \widehat{\mathbf{u}} \Big|_{\mathcal{I}_e} = \sum_{a=1}^{n/2} \nabla \mathbf{N}_a(\xi_i) \{\delta \mathbf{u}\}_a \quad (3.6.7)$$

and the corresponding interface temperature gradients are discretized as follows

$$\widehat{\nabla} \widehat{\Theta} = \sum_{a=1}^{nen/2} \nabla \mathbf{M}_a(\xi_i) \{\Theta^{-1}\}_a^{-1} \quad \text{and} \quad \widehat{\nabla} \delta \widehat{\Theta} = \sum_{a=1}^{n/2} \nabla \mathbf{M}_a(\xi_i) \{\delta \Theta^{-1}\}_a^{-1} \quad (3.6.8)$$

Since we consider generally a time-dependent thermal subproblem we also have to discretize the entropy \widehat{s} or the temperature $\widehat{\Theta}$, respectively in time

$$\partial_t \widehat{s} = \frac{1}{\Delta t} [\widehat{s}^{n+1} - \widehat{s}^n] \quad \text{and} \quad \partial_t \widehat{\Theta} = \frac{1}{\Delta t} [\widehat{\Theta}^{n+1} - \widehat{\Theta}^n] \quad (3.6.9)$$

where Δt is the given time-step and \widehat{s}^{n+1} or $\widehat{\Theta}^{n+1}$ denote the interface entropy or interface temperature at the new time step and \widehat{s}^n and $\widehat{\Theta}^n$ are the corresponding values for the old times step. For the time integration of the non-mechanical variable the generalized midpoint rule was applied.

4 Interfaces in Localisation Problems

4.1 Overview

There are a lot of technical problems which can not be treated with the tools of the classical continuum mechanics or solid mechanics, respectively, since the presetting of continuity is not given anymore. Of course the continuous inelastic material models presented in the previous chapter are able to indicate localization phenomena due to damage evolution. But in particular the description of discrete cracks in materials or material separation occurring in cutting and machining processes require additional tools to describe the appearing jumps in the corresponding displacement fields. The aim of this section is to present possibilities of modelling such kind of phenomena, which in general are denoted by *strong discontinuities*. J. Oliver defines them in [Oli96a] & [Oli96b] as „... jumps in the displacement field appearing at a certain time, in general unknown before the analysis, of the loading history and developing across paths of the solid which are material (fixed) surfaces. They have to be distinguished from weak discontinuities that correspond to jumps in the strain field (the displacement remaining continuous) which develop along moving surfaces.” We present numerical techniques accomplishing the modelling of discrete postcritical material separation by interface elements. The presented formulations are oriented on the paper Miehe and Schröder [MS94]. They compared two methods for modelling the postcritical behaviour of discontinuities in materials by interface elements. They distinguish between so-called *domain-dependent* and *domain-independent* interface formulations. The first formulation proposes a projection of the constitutive law of the ambient material into the discontinuity. From this projection emerges the *acoustic* or *localization tensor* that can be interpreted as a stiffness of the discontinuity. The singularity of the localisation tensor finally indicates the failure of the corresponding interface element. Furthermore, this formulation can be understood as a bifurcation problem, since the singularity of the localization tensor also indicates, that the type of differential equation changes.

In the domain-independent formulation a separate constitutive law for the interface is assumed depending on the displacement jump. Here the key idea is to split the displacement jump into an elastic and an inelastic contribution analogously to linear plasticity theory. The failure in this formulation occurs as soon as the traction vector exceeds a certain threshold value.

Before we start presenting the different formulations we give a brief definition of localization phenomena, we want to apply the general form of the weak formulations in chapter 3 to localization problems, such that a simpler formulation emerges. Afterwards we present the domain-dependent and the domain-independent interface formulation separately. The differences of both formulations emerge, as we will see, from the kinematical assumptions, such that we concentrate on this topic before we derive the corresponding constitutive relations. Since we like to consider thermo-mechanically

processes, we tried to extend the corresponding formulations to thermomechanical behaviour. After that we derive the numerical realisation of both formulations and finish this chapter with some numerical examples comparing both formulations.

4.2 Localization Requirement

As mentioned before the localization criteria coincides with the loss of ellipticity of the governing differential equation. For the determination of reliable localization criteria, we resort to the assumption of a discontinuous displacement field

$$\partial_t \mathbf{u}(\theta^1, \theta^2, \theta^3) = \partial_t \mathbf{u}_c(\theta^1, \theta^2, \theta^3) + \mathcal{R}(\theta^3) \gamma(\theta^1, \theta^2) \mathbf{s}(\theta^1, \theta^2). \quad (4.2.1)$$

parametrized in terms of the convective coordinates. Here $\partial_t \mathbf{u}_c$ denotes the regular and smooth velocity field and $\mathcal{R}(\theta^3)$ is the ramp function, which is defined as follows

$$\mathcal{R}(\theta^3) := \begin{cases} \theta^3 & \text{with } \theta^3 > 0, \\ 0 & \text{with } \theta^3 \leq 0. \end{cases} \quad (4.2.2)$$

Here $\gamma(\theta^1, \theta^2)$ is assumed to be a smooth function describing the amount of the discontinuity, whereas $\mathbf{s}(\theta^1, \theta^2)$, $|\mathbf{s}| = 1$ defines its direction. In the framework of the linear theory the strains are defined by the gradient of the displacement field such that applying the gradient operator to the given displacement field in eqn. 4.2.2 we obtain an expression

$$\nabla \partial_t \mathbf{u} = \nabla \partial_t \mathbf{u}_c + \mathcal{R}_{\partial \theta^\alpha}(\gamma \mathbf{s}) \otimes \mathbf{t}^\alpha + \gamma \mathcal{H}(\theta^3) \mathbf{s} \otimes \mathbf{t}^3, \quad \text{with } \alpha = 1, 2 \quad (4.2.3)$$

where \mathcal{H} defines the Heaviside function

$$\mathcal{H}(\theta^3) := \begin{cases} 1 & \text{with } \theta^3 > 0, \\ 0 & \text{with } \theta^3 \leq 0, \end{cases} \quad (4.2.4)$$

that emanates from the gradient of the ramp function $\partial_{\theta^3} \mathcal{R}(\theta^3)$. Since the first two terms in eqn. 4.2.3 are smooth we assume, that these contributions describe the regular strain field, whereas the last term covers the discontinuous part of the strain field. Furthermore, we assume that there is a stress-strain-relation given by an inelastic constitutive law, such that we can express the stress rate in terms of the strain rate field and the corresponding rate of the traction vector can be derived from the Cauchy theorem

$$\partial_t \mathbf{t} = \mathbf{m} \cdot \mathbb{C}^{in} : \nabla \partial_t \mathbf{u}. \quad (4.2.5)$$

Here \mathbb{C}^{in} denotes the inelastic continuous material tensor of the ambient constitutive material law. Taking eqn. 4.2.3 into account, we can derive the limits of the traction vector at the positive and negative surfaces Γ^+ and Γ^- , which shape the material surface \mathcal{I} and with this at hand we can define the jump of the traction rate vector $[[\partial_t \mathbf{t}]] = [\mathbf{t}^+ - \mathbf{t}^-] = \mathbf{0}$, that has to equal zero for fulfilling the equilibrium requirement. If we finally assume, that $\mathbb{C}^{in+} = \mathbb{C}^{in-} = \mathbb{C}^{in}$ when the discontinuity starts to evolve, the subsequent relation can be derived

$$[[\partial_t \mathbf{t}]] = \mathbf{m} \cdot \mathbb{C}^{in} : [[\nabla \partial_t \mathbf{u}]] = \mathbf{0}, \quad (4.2.6)$$

The jump of the rate traction vector has to equal zero, since we still consider the continuous case, where the displacement field is still assumed to be continuous $[[\partial_t \mathbf{u}]] = \mathbf{0}$. In eqn. 4.2.4 we identified

the last term as responsible for the discontinuity of the strain field, such that we can identify the rate of the displacement jump with

$$[\partial_t \mathbf{u}] = \gamma \mathbf{s} \otimes \mathbf{m}, \quad \text{with} \quad \mathbf{t}^3|_{\theta^3=0} = \mathbf{m}. \quad (4.2.7)$$

Inserting this expression again into eqn. 4.2.6, we obtain the requirement

$$[[\partial_t \mathbf{t}]] = \mathbf{m} \cdot \mathbb{C}^{in} : [\gamma \mathbf{s} \otimes \mathbf{m}] = \gamma [\mathbf{m} \cdot \mathbb{C}^{in} \cdot \mathbf{m}] \cdot \mathbf{s} = \gamma \mathbf{Q}^{in} \cdot \mathbf{s} = \mathbf{0} \quad \forall \mathbf{s}. \quad (4.2.8)$$

Here \mathbf{Q}^{in} denotes the acoustic tensor and the equation is only fulfilled for arbitrary directions $\mathbf{s} \neq \mathbf{0}$, if \mathbf{Q}^{in} gets singular, i.e. an eigenvalue gets zero. This indicates the loss of ellipticity and the onset of localization. As a consequence thereof the determinant of the localization tensor changes its sign from positive to negative.

These presented relations are the essence of very interesting investigations on localization phenomena. For a more detailed insight to this subject we like to refer to Belytschko et al. [BFE87] and the referred literature. In the work of Steinmann & Willam [SW91a], [SW91b] and Steinmann [Ste92] one can find some numerical investigations with respect to localization phenomena and in particular the behaviour of different types of finite elements to localization. In the sequel we like to investigate the so-called postcritical behaviour and the description in means by the domain-dependent and the domain-independent formulation.

4.3 Domain-Dependent Interfaces

Beneath the previously denoted publications of Oliver and Miehe & Schröder treating the modelling of strong discontinuities and their numerical realisation, the representation of the domain-dependent strategy can be found in a paper of Larson et al. [LRO93] or Leppin [Lep00]. An essential work dealing with the numerical realization of discontinuities was made by Schellekens [Sch92] and in Schellekens and de Borst [SDB93]. An extension to geometrically non-linear formulations in the framework of elastoplasticity was performed by Steinmann in [SLR97], [Ste99] or in Steinmann & Betsch [SB00]. The treatment of coupled problems with respect to porous media can be found in Steinmann [Ste98]. Another numerical approach, which is summarized by the term embedded discontinuity element technique, can be found in the publications of Wells et al. [WS00], [WS01c], [WS01a], [WS01d], [WS01b] and [Wel01].

4.3.1 Kinematical Aspects

For the derivation of the kinematical relations, we follow the representation of Leppin [Lep00], that assumes, that the material points \mathbf{x} are parametrized in terms of the convective coordinates θ^1, θ^2 and θ^3 . The discontinuity is divided into equal halves by the reference surface, that is defined by $\theta^3 = 0$. The convective coordinates $\theta^\alpha, \alpha = 1, 2$ describes the material surface in tangential direction and the derivatives of \mathbf{x} with respect to $\theta^\alpha, \alpha = 1, 2$ defines the tangent vectors \mathbf{t}_α . With this parametrization of the placement vector a material point of the localization surface is given by

$$\mathbf{x}(\theta^1, \theta^2, \theta^3) = \hat{\mathbf{x}}(\theta^1, \theta^2) + \theta^3 \mathbf{m}(\theta^1, \theta^2). \quad (4.3.1)$$

Here $\hat{\mathbf{x}}$ is the corresponding placement vector of the middle surface and the normal vector \mathbf{m} points from \mathcal{B}^- to \mathcal{B}^+ . In the sequel we assume the localization zone as constant in time and additionally due to the assumption of geometrically linear deformations the interfacial normal vector \mathbf{m} remains

constant as well. Therefore the time parameter is neglected in the following derivations. For the consideration of the discontinuities in the context of the domain-dependent interface formulation, the crucial kinematical assumption is made, that the displacement field can be decomposed into a continuous and a discontinuous part. Thus the interface displacement field is represented by

$$\mathbf{u}(\theta^1, \theta^2) = \hat{\mathbf{u}}(\theta^1, \theta^2) + \frac{\theta^3}{w} \tilde{\mathbf{u}}(\theta^1, \theta^2), \quad (4.3.2)$$

where w denotes the width of the localization zone and the definitions of $\hat{\mathbf{u}}$ and $\tilde{\mathbf{u}}$ were already given in eqn.3.3.8 and 3.3.9, respectively. The corresponding expression describing the discontinuous strain field emanates from the gradient of the displacement field by differentiating the displacement field with respect to \mathbf{x} , such that we obtain

$$\varepsilon_\delta = \nabla \mathbf{u} = \partial_{\theta^\alpha} \hat{\mathbf{u}} \otimes \mathbf{t}^\alpha + \frac{1}{w} \tilde{\mathbf{u}} \otimes \mathbf{t}^3 + \frac{\theta^3}{w} \partial_{\theta^\alpha} \tilde{\mathbf{u}} \otimes \mathbf{t}^\alpha. \quad (4.3.3)$$

Here the \mathbf{t}^α and \mathbf{t}^3 denote the covariant base vectors, whereby the direction of \mathbf{t}^3 coincides with the direction of \mathbf{m} . In general only the second term is considered, since the derivatives of the displacement jump are neglected $\partial_{\theta^\alpha} \tilde{\mathbf{u}} \approx \mathbf{0}$ as well as the derivatives of the corresponding displacement average $\partial_{\theta^\alpha} \hat{\mathbf{u}} = \mathbf{0}$ ¹, such that the interface strain field reduces to

$$\varepsilon_\delta = \nabla \mathbf{u} = \frac{1}{w} [\tilde{\mathbf{u}} \otimes \mathbf{m}], \quad \text{with} \quad \mathbf{m} \approx \mathbf{t}^3. \quad (4.3.4)$$

This term dominates the process of strain localization and for the description of postcritical processes it seems sufficient.

An alternative approach to derive the interface strain field in eqn. 4.3.4 can be found in the paper of Larson et al. [LRO93] or in the work of Wells [WS01c]. Here the discontinuity of the displacement field is taken into account by the Heaviside function, such that the total displacement field is given by

$$\mathbf{u}(\mathbf{x}) = \mathbf{u}_c(\mathbf{x}) + \mathcal{H}(\theta^3) \tilde{\mathbf{u}}, \quad (4.3.5)$$

where \mathcal{H} denotes the Heaviside function as it was introduced in eqn. 4.2.4 and \mathbf{u} is the continuous displacement field of the ambient domain. From this point of departure we can derive the strain field by differentiation of the displacement field. Therefore we get the expression

$$\varepsilon = \nabla \mathbf{u} = \nabla \mathbf{u}_c + \mathcal{H}(\theta^3) [\nabla \tilde{\mathbf{u}}] + \delta(\theta^3) [\tilde{\mathbf{u}} \otimes \mathbf{m}] \quad (4.3.6)$$

and here δ denotes the Dirac-Delta, which emanates from the gradient of the Heaviside function and which is defined by

$$\delta(\theta^3) := \begin{cases} \infty & \text{with} \quad \theta^3 = 0, \\ 0 & \text{with} \quad \theta^3 \neq 0. \end{cases} \quad (4.3.7)$$

The first two terms in eqn.4.3.6 are assumed to describe the continuous part of the displacement field, whereas the last one records the kinematical properties of the localization zone ε_δ . For $w \rightarrow 0$ we find the accordance of the results for ε_δ in eqn. 4.3.4 and eqn. 4.3.7

¹We also want to note here, that derivatives of the average displacement field describes the deformation due to bending and disregarding this term is questionable. For the sake of simplicity here we follow the proceeding of Miehe & Schröder [MS94] and Larson [LRO93] et al.. A representation taking the bending terms into account is given by Leppin [Lep00]

4.3.2 Constitutive Equations

Like the notation makes one suppose, the domain-dependent postcritical surface formulation is determined by the constitutive equations of the ambient material, since it is projected into the *cohesive zone*. For this projection we resort to the localization requirement, where we introduced the acoustic tensor \mathbf{Q} as an indicator of localization. This localization tensor was derived by the definition of the traction vector via the Cauchy theorem and the corresponding jump condition across the discontinuity, such that we obtained eqn. 4.2.6. Now we have to formulate constitutive relations for the interface in terms of the interface strain field $\boldsymbol{\varepsilon}_\delta$ in eqn. 4.3.4 and the internal variable

$$\widehat{\Psi} = \widehat{\Psi}(\boldsymbol{\varepsilon}_\delta, \xi) = \widehat{\Psi}_{vol}(\text{tr } \boldsymbol{\varepsilon}_\delta) + \widehat{\Psi}_{iso}(\widetilde{\boldsymbol{\varepsilon}}_\delta) + \Psi_{mic}(\xi). \quad (4.3.8)$$

Here $\text{tr } (\boldsymbol{\varepsilon}_\delta)$ and $\widetilde{\boldsymbol{\varepsilon}}_\delta$ denote the volumetric and deviatoric parts of the interface strain field $\boldsymbol{\varepsilon}_\delta$. The corresponding stress field can be obtained by differentiating eqn. 4.3.8 with respect to the interface strain field. But since the quantity of interest is not the stress field but the traction vector, the result has to be contracted by the normal vector such that the algorithmic traction vector increment is given by

$$[\dot{\mathbf{t}}]_{n+1} = \frac{1}{w} \mathbf{m} \cdot \mathbb{C}_{n+1}^{in} : [\llbracket \dot{\mathbf{u}} \rrbracket_{n+1} \otimes \mathbf{m}]^{sym} = \mathbf{Q}_{n+1}^{in} \cdot [\dot{\mathbf{u}}]_{n+1}, \quad (4.3.9)$$

where we refine the algorithmic localization tensor $\mathbf{Q}_{n+1}^{in} = \mathbf{m} \cdot \mathbb{C}_{n+1} \cdot \mathbf{m}$. In the interface context we can identify the acoustic tensor as the corresponding interface stiffness operator that relates the interface traction vector to the interface displacement jump. From these derivations we find that the interface behaviour depends from the constitutive law in the ambient material, which is given by the tangent operator \mathbb{C}^{in} . The corresponding interface stiffness represented by the acoustic tensor requires the tangent operator \mathbb{C}^{in} of the bulk material as they are derived in chapter 2 (in terms of large deformations). Therefore the constitutive law in the bulk is projected into the discontinuity, such that the interface behaviour adopts the bulk behaviour. According to this, effects like damage, viscosity or adiabatic behaviour can be simply taken into account, without requiring a specific interface modelling. In contrast to this, the domain-independent interface formulation needs appropriate material models to cover the corresponding effects like the domain-dependent formulation. Of course, for the investigation of (thermo-mechanically) coupled problems we need a corresponding kinematical extension, which includes an extension of the interface stiffness.

4.3.3 Thermo-mechanical Extension

For completeness we want to sketch the thermo-mechanical problem for a domain-dependent interface formulation. The thermo-mechanical extension of the domain-dependent formulation includes, that the stresses are temperature dependent, such that the list of arguments of the free energy function has to be extended by the corresponding interface temperature

$$\widehat{\Psi} = \widehat{\Psi}(\boldsymbol{\varepsilon}_\delta, \xi, \widehat{\Theta}) \quad (4.3.10)$$

In contrast to the previous chapter, here the interface temperature only depends on the temperature values of the boundary limiting the discontinuity, such that it seems feasible, that

$$\widehat{\Theta} := \llbracket \Theta \rrbracket \quad (4.3.11)$$

With this at hand we are able now to specify the corresponding free energy function. For this we simply transform the approach of thermo-mechanical coupling presented in eqn. 2.9.9 to the linear theory, such that the free energy function consists of the subsequent contributions

$$\widehat{\Psi} = \widehat{\Psi}_{vol}(\text{tr}(\boldsymbol{\varepsilon}_\delta)) + \widehat{\Psi}_{iso}(\widetilde{\boldsymbol{\varepsilon}}_\delta) + \widehat{\Psi}_{mic}(\xi) + \widehat{\Psi}_{eth}(\text{tr}(\boldsymbol{\varepsilon}_\delta), \widehat{\Theta}) + \widehat{\Psi}_{th}(\widehat{\Theta}). \quad (4.3.12)$$

We note here, that the three first contributions, recording the elasto-plastic behaviour, are assumed to be independent on the temperature field. The thermal effects are solely covered by the contribution $\widehat{\Psi}_{eth}$, which records the thermo-elastic coupling and $\widehat{\Psi}_{th}$, that solely depends on the temperature field. Adopting these contributions to the framework of the linear theory finally gains

$$\widehat{\rho}\widehat{\psi}_{th} = \widehat{\rho}\frac{\widehat{c}}{2}\frac{\widehat{\Theta}^2}{\widehat{\Theta}_0} \quad \text{and} \quad \widehat{\rho}\widehat{\psi}_{eth} = -3\widehat{\alpha}\Delta\widehat{\vartheta}\kappa\text{tr}(\boldsymbol{\varepsilon}_\delta)\mathbf{m} \otimes \mathbf{m}, \quad \text{with} \quad \Delta\widehat{\vartheta} = [\widehat{\Theta} - \widehat{\Theta}_0] \quad (4.3.13)$$

The total stress can be derived from the strain energy function by differentiation with respect to the elastic strain field $\boldsymbol{\varepsilon}_\delta$. But since we consider discontinuities, we are interested in the traction vector, that can be determined by the projection of the resulting stress field on normal direction by twice contraction with the normal vector \mathbf{m} , such that we obtain

$$\widehat{\mathbf{t}} = \frac{\partial \widehat{\Psi}}{\partial \boldsymbol{\varepsilon}_\delta} \cdot \mathbf{m} = \frac{1}{\delta} \mathbf{Q}^{in} \cdot [\widehat{\mathbf{u}}] - \mathbf{m} \cdot \beta_\delta \Delta\widehat{\vartheta}, \quad \text{with} \quad \beta_\delta = 3\widehat{\alpha}\kappa\mathbf{m} \otimes \mathbf{m}. \quad (4.3.14)$$

Hereby Θ_0 corresponds to the reference temperature, β_δ denotes the thermal interface stress and \mathbf{Q}^{in} is the acoustic tensor, which was already introduced in the previous section. To complete the description of the thermal subproblem we need to define the heat flux in the localization zone. In the continuous case usually a constitutive law of the Fourier type is installed where the heat flux is assumed to be proportional to the negative temperature gradient. In the discontinuous case it is assumed that the heat flux in the discontinuity only depends on the temperature jump in normal direction to the material surface. Therefore we want to introduce the „interface temperature gradient“, that is defined by

$$\mathbf{h}_\delta := -\frac{1}{\delta} [[\Theta]] \mathbf{m}. \quad (4.3.15)$$

To obtain a thermodynamical consistent temperature model, we have to demand the non-local interface dissipation as non-negative, which is guaranteed by the constitutive relation of the Fourier type

$$\widetilde{q} = -\frac{\partial \widehat{\Psi}}{\partial \mathbf{h}_\delta} \cdot \mathbf{m} = -\frac{1}{\delta} k_\delta [[\Theta]], \quad (4.3.16)$$

from which the corresponding potential can be easily constructed. Here k_δ denotes the specific interface conductivity parameter and the vector \mathbf{h}_δ can be understood as the interface temperature gradient, that naturally points in direction across the interface. This completes the modelling of thermo-mechanical processes in the context of domain-dependent interface formulations.

4.4 Domain-Independent Interfaces

The domain-independent interface formulation allows to introduce an extra material law for the cohesive zone, which differs from the ambient constitutive assumptions. In particular formulations

are used, which base on the concepts of plasticity. In the framework of plasticity theory we introduced a yield condition, that is formally adopted to the cohesive zone model and if the yield function gets zero this accords to the slip of a gliding plain. Likewise the plasticity theory we apply the principle of maximum dissipation from which we can derive an associated flow rule for the displacement jump and associated evolution equations for possible internal variables.

The subsequent representation bases on the paper of Miehe & Schröder [MS94] and on the work of Leppin [Lep00]. In the publications of Janson [Jan01], [Jan02], [Jan], Larsson & Jansson [LJ02] and Jansson & Larsson [JL] the interface formulations were applied to the delamination analysis in composite structures. In order to show the agreement of the linear plasticity and the domain-independent post-critical localization formulation we will assume an inelastic bulk material of the von-Mises type and perform the corresponding procedure for the derivation of the governing equations.

4.4.1 Kinematical Aspects

The crucial kinematical assumption in the domain-independent approach is, that the displacement jump can be splitted into an elastic and an inelastic contribution, such that we obtain

$$\tilde{\mathbf{u}} = \tilde{\mathbf{u}}_e + \tilde{\mathbf{u}}_p. \quad (4.4.1)$$

The material behaviour is mainly determined by the traction vector acting in the material surface. For the computation of stresses or tractions, respectively, we assume an interface free energy Ψ_δ in terms of the elastic displacement jump and an internal variable ξ , that is able to record any hardening or softening effects within the cohesive zone $\Psi_\delta(\tilde{\mathbf{u}}_e, \xi)$. Furthermore, it is assumed, that the free energy describing the post-critical behaviour of the localization zone only depends on the displacement jump. Since we like to describe the onset of slip with methods of the linear plasticity theory we have to introduce a threshold like the resulting yield stress denoted by \tilde{Y}_n , such that the free energy functions are given by

$$\Psi = \Psi([\nabla \mathbf{u}]_e^{sym}, \xi, [\bullet]) \quad \text{and} \quad \hat{\Psi} = \hat{\Psi}(\tilde{\mathbf{u}}, \hat{\xi}). \quad (4.4.2)$$

Since we consider a domain-independent formulation the list of arguments of the free energy functions, do not have to coincide with each other, such that it is conceivable, that there are additional variables the bulk free energy depends on. In the sequel we like to restrict ourselves to the explicit denoted variables. The simplest choice of an inelastic model is given by the subsequent specification of the free energy function

$$\Psi := \frac{1}{2} [\nabla \mathbf{u}]_e^{sym} : \mathbb{E} : [\nabla \mathbf{u}]_e^{sym} + \frac{1}{2} h \xi^2 \quad \text{and} \quad \hat{\Psi} := \frac{1}{2} \tilde{\mathbf{u}}_e \cdot \tilde{\mathbf{E}} \cdot \tilde{\mathbf{u}}_e + \frac{1}{2} \hat{h} \hat{\xi}^2 \quad (4.4.3)$$

From this we can derive the bulk stress and the interface stress-like quantity by differentiating the free energy functions with respect to the work-conjugated elastic strains and elastic displacement jump, respectively. Therefore we obtain

$$\boldsymbol{\sigma}^t = \frac{\partial \Psi}{\partial [\nabla \mathbf{u}]_e^{sym}} = \mathbb{E} : [\nabla \mathbf{u}]_e^{sym} \quad \text{and} \quad \tilde{\mathbf{t}} = \frac{\partial \hat{\Psi}}{\partial \tilde{\mathbf{u}}} = \tilde{\mathbf{E}} \cdot \tilde{\mathbf{u}}_e \quad (4.4.4)$$

where $\tilde{\mathbf{t}}$ emerges as the interface traction vector. \mathbb{E} denotes the fourth order elasticity tensor and the corresponding interface elasticity tensor is denoted by $\tilde{\mathbf{E}}$ which shall be defined by

$$\tilde{\mathbf{E}} = \tilde{E}_\perp \mathbf{m} \otimes \mathbf{m} + \tilde{E}_\parallel \mathbf{P}, \quad \text{with} \quad \mathbf{P} = \mathbf{I} - \mathbf{m} \otimes \mathbf{m} \quad (4.4.5)$$

whereby \mathbf{P} defines the projection tensor into the material surface and \tilde{E}_\perp and \tilde{E}_\parallel are parameters describing the elastic behaviour across the interface and along the material surface in tangential direction. We emphasise here, that \mathbf{E} is a second order tensor, that maps the displacement jump vector to the traction vector, whereas the material tensor in general is fourth order tensor, that maps the strain tensor on the corresponding stress tensor. Furthermore we assumed a linear hardening law and with this at hand we can evaluate the corresponding isothermal local dissipation inequalities for the bulk and the interface in eqn. 3.4.13 and obtain

$$\begin{aligned} D_{loc} &= \boldsymbol{\sigma}^t : \partial_t [\nabla \mathbf{u}]^{sym} - \rho \partial_t \Psi \geq 0 \quad \text{and} \\ \widehat{D}_{loc} &= \tilde{\mathbf{t}} \cdot \partial_t \tilde{\mathbf{u}} - \hat{\rho} \partial_t \widehat{\Psi}(\tilde{\mathbf{u}}_e, \widehat{\xi}) = \tilde{\mathbf{t}} \cdot \partial_t \tilde{\mathbf{u}}_p - \hat{\rho} \partial_{\widehat{\xi}} \widehat{\Psi} \partial_t \widehat{\xi} \geq 0. \end{aligned} \quad (4.4.6)$$

In analogy to the linear plasticity theory we have to define a yield function, that defines the onset of slip. In contrast to the continuous inelastic constitutive material laws the given threshold is compared with the tangential projection of traction vector on the material surface $\mathbf{s} \cdot \widehat{\mathbf{n}}$ and not with the magnitude of the deviatoric stress tensor. Hence the yield condition, proposed by Miehe and Schröder has the following structure

$$\Phi := |\boldsymbol{\sigma}^t| - \sqrt{\frac{2}{3}} Y_n(\xi) \leq 0 \quad \text{and} \quad \widehat{\Phi} := |\tilde{\mathbf{t}} \cdot \widehat{\mathbf{n}}| - \widehat{Y}_n(\widehat{\xi}) \leq 0, \quad \text{with} \quad \widehat{Y}_n = \widehat{Y}_0 - \widehat{h} \widehat{\xi} \quad (4.4.7)$$

where \widehat{Y}_0 denotes the initial yield traction or „slip-stress“ and \widehat{h} can be understood as a hardening modulus. In order to derive the evolution equations we follow the procedure of plasticity theory and rewrite the local dissipation inequality as Lagrange functional, where the yield conditions corresponds to the side conditions. From this we can determine the evolution equations for the plastic bulk strains and the plastic displacement jump of the interface

$$\partial_t [\nabla \mathbf{u}]_p^{sym} = \dot{\gamma} \mathbf{n}^{dev} \quad \text{and} \quad \partial_t \tilde{\mathbf{u}}_p = \dot{\gamma} \text{sign}(\tilde{\mathbf{t}} \cdot \widehat{\mathbf{n}}) \widehat{\mathbf{n}}, \quad (4.4.8)$$

whereby the interface flowrule can also be denoted as *slip rule*. According to this we obtain for the evolution equations of the internal variables

$$\partial_t \xi = \sqrt{\frac{2}{3}} \dot{\gamma} \quad \text{and} \quad \partial_t \widehat{\xi} = \dot{\gamma}. \quad (4.4.9)$$

From the yield condition, where only the tangential projection of the traction vector is taken into account and was compared with the yield stress, follows, that the slip rule only includes the tangential contribution of the displacement jump. With this at hand we can also calculate the corresponding rate of the traction vector

$$\partial_t \tilde{\mathbf{t}} = \tilde{\mathbf{C}}^{in} \cdot \partial_t \tilde{\mathbf{u}}, \quad \text{with} \quad \tilde{\mathbf{C}}^{in} = \tilde{E}_\perp \mathbf{m} \otimes \mathbf{m} + \mathbf{P} \left[1 - \frac{\tilde{E}_\parallel}{\tilde{E}_\parallel + \widehat{h}} \right] \quad (4.4.10)$$

where $\tilde{\mathbf{C}}^{in}$ denotes the consistent algorithmic interface tangent operator. Note that we can split the traction vector into a contribution perpendicular to the material surface and a tangent contribution along the interface. For the description of the slip mechanism within the cohesive zone this formulation is completely sufficient. In order to apply this formulation also to more general problems like cutting processes, in the sequel we like to modify the given yield function, such that also contributions in normal direction are considered.

In contrast to the domain-dependent formulation the domain-independent formulation can be developed from the general theory in chapter 3. Since the general formulation also includes extra-energy contributions which are treated in detail in the subsequent chapter, we like to consider the nonlinear extension of domain-dependent interface formulation in the framework of the more generalised representation in chapter 5.

4.4.2 Constitutive Modifications

The governing equations within this formulation remain unchanged and the procedure of deriving them keeps the same as well, such that we restrict ourselves to the modifications according to the interface description. But, as mentioned before, in the sequel also contributions in normal direction have to be considered in the yield condition. Thus we have modified the interface yield function as follows

$$\widehat{\Phi} = k\nu \widetilde{\mathbf{t}} \cdot \mathbf{m} + [1 - k] [\widetilde{\mathbf{t}} \cdot \widehat{\mathbf{n}}]^2 - (\widehat{Y}_0 + \widehat{h}\widehat{\xi}) \quad (4.4.11)$$

Here ν is a dimension factor and k denotes a weighting parameter, such that the influence of the different contributions can be controlled. We introduced the squared tangential contribution of the traction vector for numerical reasons. Accordingly we obtain a modified slip rule, that also consists of contributions that correspond to the normal direction and the tangential direction

$$\partial_t \widetilde{\mathbf{u}}_p = \dot{\gamma} [k\nu \mathbf{m} + 2[1 - k][\widetilde{\mathbf{t}} \cdot \widehat{\mathbf{n}}]^2 \widehat{\mathbf{n}}. \quad (4.4.12)$$

Obviously also the evolution equation of the internal variable changes and we finally obtain

$$\partial_t \widehat{\xi} = \dot{\gamma} \quad (4.4.13)$$

From this it is straightforward to calculate the rate of the traction vector of this formulation if we know the interface tangent operator, that of course also becomes a little bit more complicated

$$\begin{aligned} \partial_t \widetilde{\mathbf{t}} &= \mathbf{C}^{in} \cdot \partial_t \widetilde{\mathbf{u}} \\ &= \left[\widetilde{E}_\perp \left[1 - \frac{\widetilde{E}_\perp [k\nu]^2}{N} \right] \mathbf{m} \otimes \mathbf{m} + \widetilde{E}_\parallel \left[1 - \frac{4\widetilde{E}_\parallel [1 - k]^2 [\widetilde{\mathbf{t}} \cdot \widehat{\mathbf{n}}]^2 \widehat{\mathbf{n}} \cdot \mathbf{P} \cdot \widehat{\mathbf{n}}}{N} \right] \mathbf{P} \right] \cdot \partial_t \widetilde{\mathbf{u}} \end{aligned} \quad (4.4.14)$$

whereby the denominator N can be computed by

$$N = \widetilde{E}_\perp [k\nu]^2 + 4\widetilde{E}_\parallel [1 - k]^2 [\widetilde{\mathbf{t}} \cdot \widehat{\mathbf{n}}]^2 \widehat{\mathbf{n}} \cdot \mathbf{P} \cdot \widehat{\mathbf{n}} + \widehat{h}. \quad (4.4.15)$$

This formulation also takes normal contributions of the traction vector into account, such that not only slip behaviour can occur but also real separation. In the next step we extend this formulation to the adiabatic case where locally the material can be heated, but no heat flux is considered.

4.4.3 Adiabatic Extension

The main task in this formulation is, that the material can get warm, but the heat flux to the ambient material is neglected. We already investigated adiabatic formulations in the continuous setting and there we learned that in this case the temperature can be treated as an additional internal variable. Therefore we have to extend the list of arguments for the free energy functions

$$\Psi = \Psi([\nabla \mathbf{u}]^{sym}, \Theta, \xi) \quad \text{and} \quad \widehat{\Psi} = \widehat{\Psi}(\widetilde{\mathbf{u}}, \widehat{\Theta}, \widehat{\xi}) \quad (4.4.16)$$

In particular we like to specify the thermoelastic potential by

$$\begin{aligned} \Psi &= \frac{1}{2} [\nabla \mathbf{u}]^{sym} : \mathbb{E} : [\nabla \mathbf{u}]^{sym} + \frac{1}{2} h_0 [1 - \omega_h \vartheta] \xi^2 - \frac{c}{\Theta_0} \frac{\vartheta^2}{2} - \vartheta \alpha \mathbf{I} : \mathbb{E} : [\nabla \mathbf{u}]^{sym} \\ \widehat{\Psi} &= \frac{1}{2} \widetilde{\mathbf{u}} \cdot \widetilde{\mathbf{E}} \cdot \widetilde{\mathbf{u}} + \frac{1}{2} \widehat{h}_0 [1 - \widehat{\omega}_h \widehat{\vartheta}] \widehat{\xi}^2 - \frac{\widehat{c}}{\widehat{\Theta}_0} \frac{\widehat{\vartheta}^2}{2} - \widehat{\vartheta} \widehat{\alpha} \mathbf{m} \cdot \widetilde{\mathbf{E}} \cdot \widetilde{\mathbf{u}} \end{aligned} \quad (4.4.17)$$

$$\text{with } \vartheta = [\Theta - \Theta_0] \quad \text{and} \quad \hat{\vartheta} = \hat{\Theta} - \hat{\Theta}_0$$

Here c and \hat{c} denote the bulk and interface heat capacity and α and $\hat{\alpha}$ are the corresponding heat expansion coefficients. ω_h and $\hat{\omega}_h$ approximates the decrease of the hardening modulus due to thermal effects and also here we introduced reference temperatures Θ_0 and $\hat{\Theta}_0$ for the bulk and the interface. Secondly we have to adopt the yield function of the previous section to the adiabatic case by assuming the yield stress and the linear hardening modulus as temperature-dependent, such that we get

$$\hat{\Phi} = k\nu\tilde{\mathbf{t}} \cdot \mathbf{m} + [1 - k][\tilde{\mathbf{t}} \cdot \hat{\mathbf{n}}]^2 - [Y_0(\Theta) + h(\Theta)\hat{\xi}] \quad (4.4.18)$$

Since we introduced the temperature as an additional internal variable an evolution equation is required, that should be derived from the modified interface Clausius-Duhem inequality, that we already introduced in eqn. 3.4.13₂. Inserting this expression into eqn. 3.4.10 and solving for the entropy rate we finally obtain

$$\hat{\Theta}\hat{\rho}\partial_t\hat{s} = \hat{\rho}\hat{r} + [\hat{\nabla}\partial_t\tilde{\mathbf{u}}]^{sym} : \hat{\boldsymbol{\sigma}}^t - \hat{\rho}\partial_t\hat{\Psi} - \hat{\rho}\hat{s}\partial_t\hat{\Theta} + \tilde{\mathbf{t}} \cdot \partial_t\tilde{\mathbf{u}}. \quad (4.4.19)$$

Since we consider the adiabatic case, we can disregard any temperature flux terms and additionally, in the given context, we can neglect any average-based contributions. Furthermore we assume that there are no further artificial interface heat sources, such that the entropy evolution can be reduced to

$$\hat{\Theta}\hat{\rho}\partial_t\hat{s} = \tilde{\mathbf{t}} \cdot \partial_t\tilde{\mathbf{u}} - \hat{\rho}\partial_t\hat{\Psi} - \hat{\rho}\hat{s}\partial_t\hat{\Theta}. \quad (4.4.20)$$

As we derived in the previous sections we can identify the traction vector with the derivative of the free energy function with respect to the elastic displacement jump and the hardening modulus \hat{h} corresponds to the derivative with respect to the hardening variable. Due to the temperature contribution in the free energy stress or stress-like quantities are modified and we get the following expressions

$$\boldsymbol{\sigma}^t = \mathbb{E} : [[\nabla\mathbf{u}]^{sym} - \alpha\vartheta\mathbf{I}] \quad \text{and} \quad \tilde{\mathbf{t}} = \tilde{\mathbf{E}} \cdot [\tilde{\mathbf{u}} - \hat{\alpha}\vartheta\mathbf{m}] \quad (4.4.21)$$

For the specification of the entropy we want to follow the familiar definition, where it emerges from the differentiation of the free energy function with respect to the temperature

$$s = -\frac{\partial\Psi}{\partial\Theta} = \frac{c}{\Theta_0}\vartheta + \alpha\mathbf{I} : \mathbb{E} : [\nabla\mathbf{u}]^{sym} \quad \text{and} \quad \hat{s} := -\frac{\partial\hat{\Psi}}{\partial\hat{\Theta}} = \frac{\hat{c}}{\hat{\Theta}_0}\hat{\vartheta} + \hat{\alpha}\mathbf{m} \cdot \tilde{\mathbf{E}} \cdot \tilde{\mathbf{u}} \quad (4.4.22)$$

With this definition at hand the bulk entropy rate is given by

$$\partial_t s = -\frac{\partial^2\Psi}{\partial\Theta\partial[\nabla\mathbf{u}]} \partial_t[\nabla\mathbf{u}] - \frac{\partial^2\Psi}{\partial\Theta\partial\xi} \partial_t\xi - \frac{\partial^2\Psi}{\partial\Theta^2} \partial_t\Theta \quad (4.4.23)$$

and for the interface we obtain

$$\partial_t\hat{s} = -\frac{\partial^2\hat{\Psi}}{\partial\Theta\partial\tilde{\mathbf{u}}} \partial_t\tilde{\mathbf{u}} - \frac{\partial^2\hat{\Psi}}{\partial\hat{\Theta}\partial\hat{\xi}} \partial_t\hat{\xi} - \frac{\partial^2\hat{\Psi}}{\partial\hat{\Theta}^2} \partial_t\hat{\Theta}. \quad (4.4.24)$$

Inserting this expression into eqn. 4.4.19 the interface temperature evolution equation results in

$$\hat{\rho}\hat{c}\partial_t\hat{\Theta} = \tilde{\mathbf{t}} \cdot \partial_t\tilde{\mathbf{u}}_p - h\partial_t\hat{\xi} + \hat{\Theta}_0\tilde{\boldsymbol{\beta}} \cdot \partial_t\tilde{\mathbf{u}} - \hat{\Theta}_0\partial_\Theta [\tilde{\mathbf{t}} \cdot \partial_t\tilde{\mathbf{u}}_p - \hat{h}\partial_t\hat{\xi}] \quad \text{with} \quad \hat{c} = -\hat{\Theta}\frac{\partial^2\hat{\Psi}}{\partial\hat{\Theta}^2} \quad (4.4.25)$$

Here we introduced the notation $\tilde{\beta}$ for the thermomechanical stress in the interface. It can be defined by

$$\tilde{\beta} = \tilde{\alpha} \tilde{\mathbf{E}} \cdot \mathbf{m} = \tilde{\alpha} \tilde{E}_\perp \mathbf{m} \quad (4.4.26)$$

Finally we have to determine the corresponding consistent tangent operator that emerges from the above introduced governing equations. By using the consistency condition of the yield function we can determine the Lagrange multiplier and by inserting this into

$$\partial_t \tilde{\mathbf{t}} = \tilde{\mathbf{E}} \cdot \partial_t \tilde{\mathbf{u}}_e = \tilde{\mathbf{E}} \cdot \left[\partial_t \tilde{\mathbf{u}} - \dot{\gamma} [\nu k \mathbf{m} + 2[1 - k]^2 [\tilde{\mathbf{t}} \cdot \mathbf{m}] \mathbf{m}] \right] = \mathbf{C}^{in} \cdot \partial_t \tilde{\mathbf{u}} \quad (4.4.27)$$

we can finally determine the consistent tangent operator

$$\mathbf{C}^{in} = \tilde{E}_\perp \left[1 - \frac{\tilde{E}_\perp k^2 \nu^2 + \hat{\Theta}_0 \tilde{\alpha} \tilde{E}_\perp k \nu [\hat{\rho} \hat{c}]^{-1}}{N} \right] \mathbf{m} \otimes \mathbf{m} + E_\parallel \left[1 - \frac{4 \tilde{E}_\parallel [1 - k]^2 [\tilde{\mathbf{t}} \cdot \hat{\mathbf{n}}] \hat{\mathbf{n}} \cdot \mathbf{P} \cdot \hat{\mathbf{n}}}{N} \right] \mathbf{P}, \quad (4.4.28)$$

where the denominator N is given by

$$N = K \nu \tilde{E}_\perp - 4 \tilde{E}_\parallel [1 - k]^2 [\tilde{\mathbf{t}} \cdot \hat{\mathbf{n}}]^2 + \hat{h} + L P. \quad (4.4.29)$$

The appearing functions L and P occur due to the adiabatic contributions and they are defined by

$$L = [\hat{Y}_{00} \hat{\omega}_y + \hat{h}_0 \hat{\omega}_h \hat{\xi}] \quad \text{and} \quad P = [\hat{\rho} \hat{c}]^{-1} [\hat{Y}_0(\hat{\Theta}) + \hat{\Theta} \hat{\omega}_y \hat{Y}_{00}] \quad (4.4.30)$$

From the approach of the free energy function where the thermoelastic contribution only is associated with the normal direction, we find the corresponding contribution in the consistent tangent operator. In the yield function for the adiabatic case we have squared the tangential contribution of the traction vector for numerical reasons.

4.5 Weak Form for localization problems

The numerical treatment of discontinuities within thermo-mechanical solids in the framework of finite elements requires the corresponding weak formulations of the mechanical and thermal subproblem and since we reduced the list of arguments for the description of localization phenomena the corresponding weak formulations can be simplified.

4.5.1 Weak Form of the Mechanical Subproblem

For the derivation of numerical approaches the weak form is required and beneath the standard terms we obtain additional contribution due to the localization zone or discontinuity, respectively. Starting point here is the interfacial linear momentum balance equation derived in 3.3.7, whereby we can neglect all the terms along the interface or discontinuity, respectively, such that it reduces to

$$[\![\boldsymbol{\sigma} \cdot \mathbf{m}]\!] = 0. \quad (4.5.1)$$

Considering the balance equation of the regular parts \mathcal{B}^+ and \mathcal{B}^- , where Γ^+ and Γ^- denotes the boundaries rendering the discontinuity \mathcal{S} and therefore the weak form can be written as

$$\mathcal{G}^{ext}(\delta \mathbf{v}) - \mathcal{G}^{int}(\delta \mathbf{v}) + \mathcal{G}^{dis}(\delta \mathbf{v}) = 0. \quad (4.5.2)$$

The contribution due to external forces can be written as

$$\mathcal{G}^{ext}(\delta \mathbf{v}) = \int_{\mathcal{B}^+ \cup \mathcal{B}^-} \delta \mathbf{v} \cdot \mathbf{b} dv + \int_{\partial \mathcal{B}^+ \cup \partial \mathcal{B}^-} \delta \mathbf{v} \cdot \mathbf{t} da \quad (4.5.3)$$

and the internal virtual work is given by

$$\mathcal{G}^{int} = \int_{\mathcal{B}^+ \cup \mathcal{B}^-} \nabla \delta \mathbf{v} : \boldsymbol{\sigma} dv. \quad (4.5.4)$$

The contribution due to the discontinuity emanates from the integral of the virtual mechanical energy over the internal boundaries Γ^+ and Γ^- , such that we obtain

$$\mathcal{G}^{dis}(\delta \mathbf{v}) = \int_{\Gamma^+} \delta \mathbf{v}^+ \cdot \boldsymbol{\sigma}^+ \cdot \mathbf{m}^+ da + \int_{\Gamma^-} \delta \mathbf{v}^+ \cdot \boldsymbol{\sigma}^- \cdot \mathbf{m}^- da. \quad (4.5.5)$$

By assuming $-\mathbf{m}^+ = \mathbf{m}^- = \mathbf{m}$ and taking eqn. 3.2.9 into account, we can rewrite the discontinuous contribution in the subsequent form

$$\mathcal{G}^{dis}(\delta \mathbf{v}) = - \int_{\mathcal{I}} [\{\delta \mathbf{v}\} \cdot \llbracket \boldsymbol{\sigma} \cdot \mathbf{m} \rrbracket + \llbracket \delta \mathbf{v} \rrbracket \{\boldsymbol{\sigma} \cdot \mathbf{m}\}] da, \quad (4.5.6)$$

such that in consideration of eqn. 4.3.2, we only obtain a single additional contribution due to the discontinuity. Thus, the virtual complete mechanical power can be represented by

$$\mathcal{G}(\delta \mathbf{v}) = \int_{\mathcal{B}} \delta \mathbf{v} \cdot \mathbf{b} dv + \int_{\partial \mathcal{B}} \delta \mathbf{v} \cdot \mathbf{t} da - \int_{\mathcal{B}} \nabla \delta \mathbf{v} : \boldsymbol{\sigma} dv - \int_{\mathcal{I}} \delta \tilde{\mathbf{v}} \cdot \{\boldsymbol{\sigma} \cdot \mathbf{m}\} da, \quad (4.5.7)$$

where $\delta \tilde{\mathbf{v}} = \llbracket \delta \mathbf{v} \rrbracket$ denotes the time derivative of the corresponding virtual displacement jump $\tilde{\mathbf{u}}$. Comparing the weak form of the mechanical subproblem in eqn. 4.5.7 with the more general formulation in eqn. 3.5.2 we see that the resulting formulation only contains the interface contributions describing the traction in direction across the interface, such that no inner contributions are taken into account here.

4.5.2 Weak Form of the Thermal Subproblem

By completing the formulation with the specification of the weak form of the thermal subproblem, we are able to consider thermo-mechanically coupled problems in the framework of localization problems.

In chapter 3 we already introduced the weak formulation of the thermal subproblem, but this formulation was given in terms of the entropy and this is less helpful for the solution of realistic problems, since it is hard to define reasonable entropy boundary conditions. Therefore we have to reformulate the entropy rate equation in terms of the temperature, such that we finally obtain a temperature

evolution equation. This finally represents the balance equation for the thermal subproblem, that we have to transform to the weak form and that we like to discretize in terms of the temperature. Analogous to the mechanical subproblem we can neglect any contribution along the interface, such that the local entropy evolution equation for the bulk and the interface in eqn. 3.4.10 reduce to

$$\begin{aligned} \Theta \rho \partial_t s &= -\operatorname{div} \mathbf{q} + \nabla \ln \Theta \cdot \mathbf{q} + \rho r + D & \text{with } D \geq 0, \\ 0 &= +\widehat{D} - \Theta \llbracket \mathbf{h} \rrbracket \cdot \mathbf{m} & \text{with } \widehat{D} \geq 0. \end{aligned} \quad (4.5.8)$$

According to this also the dissipation inequality changes, since also here any tangential contributions along the interfaces are not taken into account. The corresponding expressions of the dissipation inequalities ineqn. 3.4.13 results in

$$\begin{aligned} D &= [\nabla \mathbf{v}]^{sym} : \boldsymbol{\sigma}^t - \rho \partial_t \Psi - \rho s \partial_t \Theta - \nabla \ln \Theta \cdot \mathbf{q} \geq 0, \\ \widehat{D} &= \partial_t \tilde{\mathbf{u}} \cdot \tilde{\mathbf{t}} - \widehat{\rho} \partial_t \widehat{\Psi} - \widehat{\rho} s \partial_t \widehat{\Theta} - \llbracket \mathbf{q} \rrbracket \cdot \mathbf{m} + \widehat{\Theta} \llbracket \mathbf{h} \rrbracket \cdot \mathbf{m} \geq 0. \end{aligned} \quad (4.5.9)$$

Inserting the dissipation into the entropy rate equation we finally obtain

$$\begin{aligned} \Theta \rho \partial_t s &= [\nabla \mathbf{v}]^{sym} : \boldsymbol{\sigma}^t - \operatorname{div} \mathbf{q} + \rho r - \rho \partial_t \Psi - \rho s \partial_t \Theta, \\ \widehat{\Theta} \widehat{\rho} \partial_t \widehat{s} &= \partial_t \tilde{\mathbf{u}} \cdot \tilde{\mathbf{t}} - \llbracket \mathbf{q} \rrbracket \cdot \mathbf{m} + \widehat{\rho} \widehat{r} - \widehat{\rho} \partial_t \widehat{\Psi} - \widehat{\rho} s \partial_t \widehat{\Theta}, \end{aligned} \quad (4.5.10)$$

whereby it seems as if we did not win anything so far. The crucial trick is, that we can express the entropy rates in terms of the free energy functions as in eqn. 4.4.23 and eqn. 4.4.24, whereby we assumed the list of arguments in the form of eqn. 4.4.14. But since we assumed that the discontinuity is independent of any interface contributions we also have to remove the interface temperature from the list of arguments. Inserting this expression into eqn. 4.5.10 the entropy evolution can be replaced by an expression in terms of the temperature rate, such that in analogy to the adiabatic case in eqn. 4.4.25 we get the following bulk and interface temperature evolution equations

$$\begin{aligned} \rho c \partial_t \Theta &= r^* - \operatorname{div} \mathbf{q}, \\ \widehat{\rho} \widehat{c} \partial_t \widehat{\Theta} &= \widehat{r}^* - \llbracket \mathbf{q} \rrbracket \cdot \mathbf{m}. \end{aligned} \quad (4.5.11)$$

These equations are the point of departure for the derivation of the weak form of the thermal subproblem, whereby we introduced the abbreviations

$$\begin{aligned} r^* &= [\nabla \mathbf{v}]_p^{sym} : \boldsymbol{\sigma}^t - h \partial_t \xi + \Theta_0 \boldsymbol{\beta} : \partial_t [\nabla \mathbf{u}]^{sym} - \Theta_0 \partial_\Theta [\nabla \mathbf{v}]_p^{sym} : \boldsymbol{\sigma}^t - h \partial_t \xi + \rho r \\ \widehat{r}^* &= \partial_t \tilde{\mathbf{u}}_p : \tilde{\mathbf{t}} - \widehat{h} \partial_t \widehat{\xi} + \Theta_0 \widehat{\boldsymbol{\beta}} : \partial_t \tilde{\mathbf{u}} - \Theta_0 \partial_{\widehat{\Theta}} [\partial_t \tilde{\mathbf{u}}_p : \tilde{\mathbf{t}} - h \partial_t \xi] + \widehat{\rho} \widehat{r}. \end{aligned} \quad (4.5.12)$$

The above proceeding is completely analogous to the continuous nonlinear case as it was described in chapter 2 and one can easily see that by removing all heat flux terms $\operatorname{div} \mathbf{q} = \llbracket \mathbf{q} \rrbracket \cdot \mathbf{m}$ and additional heat sources $r = \widehat{r} = 0$ the adiabatic formulation in eqn. 4.4.25 remains.

For the derivation of the weak form, we follow the proceeding presented in section 3.5.4, whereby we have to consider the modified temperature balance equation, where no contributions along the interface are taken into account. Therefore we solve eqn. 4.5.12₂ for the interface heat flux term and accordingly replace the power contribution due to the jump in the heat flux in eqn. 3.5.17, such that we obtain for the virtual power contribution due to the discontinuity

$$\mathcal{U}^{dis}(\delta \Theta) = - \int_{\mathcal{I}} \left[\delta \widehat{\Theta} [\widehat{\rho} \widehat{r}^* - \widehat{\rho} \widehat{c} \partial_t \widehat{\Theta}] + \llbracket \delta \Theta \rrbracket \{ \mathbf{q} \cdot \mathbf{m} \} \right] da. \quad (4.5.13)$$

Summarizing all contributions to the virtual thermal power the weak form can be represented by

$$\int_{\mathcal{B}_t} [\rho c_p \partial_t \Theta - r^*] \delta \Theta dv + \int_{\mathcal{I}} [\widehat{\rho c_p} \partial_t \widehat{\Theta} - \widehat{r}^*] da = \int_{\partial \mathcal{B}} q_n \delta \Theta da - \int_{\mathcal{B}_t} \mathbf{q} \nabla \delta \Theta dv - \int_{\mathcal{I}} \llbracket \delta \Theta \rrbracket \{ \mathbf{q} \cdot \mathbf{m} \} da, \quad (4.5.14)$$

whereby here the interface contributions can be clearly distinguished from the bulk contributions. In this expression the heat conduction term needs to be specified and in general a material law of the Fourier type is chosen. A possible specification is given in the next chapter, where explicit thermomechanical coupled problems are treated.

4.6 Nonlinear Formulation

For the geometrically nonlinear formulation we want to restrict ourselves to the domain dependent formulation and resort to the decomposition of the displacement field in eqn. 4.3.5 into an continuous contribution and a discontinuous one, indicated by the Heaviside function. Furthermore we have to distinguish between the reference configuration and the spatial configuration, which are connected by the mapping $\mathbf{x}(t) := \boldsymbol{\varphi}(\mathbf{X}, t) : \mathcal{B}_0 \times \mathbb{R} \rightarrow \mathcal{B}_t$ as it is written in eqn. 2.2.4. The deformation map considering an embedded discontinuity within the body and taking eqn. 4.3.5 into account we can rewrite eqn. 2.2.4 as

$$\boldsymbol{\varphi}(\mathbf{X}, t) = \mathbf{x}(t) = \mathbf{X} + \mathbf{u}(\mathbf{X}, t) + \mathcal{H}(\mathbf{X}) \widetilde{\mathbf{u}}(\mathbf{X}, t). \quad (4.6.1)$$

The crucial quantity in the nonlinear theory was the deformation gradient, that was derived by the derivative of the deformation map with respect to material coordinates. Applying this to the deformation map given in eqn. 4.3.10 we obtain analogously to the strain field of the linear theory the deformation gradient

$$\mathbf{F}^{\natural} = \nabla_{\mathbf{X}} \boldsymbol{\varphi} = \mathbf{F}_c^{\natural} + \mathcal{H}(\mathbf{X}) \widetilde{\mathbf{F}}^{\natural} + \delta(\mathbf{X}) [\widetilde{\mathbf{u}} \otimes \mathbf{M}], \quad (4.6.2)$$

whereby here we introduced the material normal vector on the material surface \mathbf{M} in the reference configuration. Furthermore \mathbf{F}_c^{\natural} denotes the standard deformation gradient and $\widetilde{\mathbf{F}}^{\natural} = \nabla_{\mathbf{X}} \widetilde{\mathbf{u}}$ coincides with the gradient of the displacement jump with respect to the material coordinates. The crucial task in the nonlinear theory is the determination of the normal unit vector on the material surface in the deformed configuration, since it is conceivable in contrast to the linear theory, that the normal vectors on Γ^+ and Γ^- do not coincide anymore. In principle the normal vectors can be transformed by the Nanson formula, but in the case of the discontinuity the normal vector is not unique and therefore we have to distinguish between the transformations

$$\mathbf{m}^- = \det(\mathbf{F}_c^{\natural}) [\mathbf{F}_c^{\natural}]^{-t} \cdot \mathbf{M} \frac{dA}{da^-} \quad \text{and} \quad \mathbf{m}^+ = \det(\mathbf{F}_c^{\natural} + \widetilde{\mathbf{F}}^{\natural}) [\mathbf{F}_c^{\natural} + \widetilde{\mathbf{F}}^{\natural}]^{-t} \cdot \mathbf{m} \frac{dA}{da^+}. \quad (4.6.3)$$

These relations can be found in the work of Wells [Wel01] and they are most general. In contrast to that one can find the accordance of the normal vectors $\mathbf{m}^+ = \mathbf{m}^-$ in the publications of Steinmann et al. [SLR97] or Larson et al [LRO93]. In general this assumption seems questionable. On the other hand within numerical investigations, it is necessary to define an particular normal vector within the

open discontinuity, since the forces on both boundaries, which are given by the traction vector, have to be equal in their direction and magnitude. Wells [?] defines the average normal vector \mathbf{m}^* by

$$\mathbf{m}^* = \det(\mathbf{F}^\natural + \frac{1}{2}\tilde{\mathbf{F}}^\natural) \left[\mathbf{F}^\natural + \frac{1}{2}\tilde{\mathbf{F}}^\natural \right]^{-t} \mathbf{M} \frac{dA}{da^*} \quad (4.6.4)$$

This normal vector is finally used to define a local base system and the traction vector at the discontinuity. This assumptions seems questionable as well as the accordance of the positive and negative normal vectors at the discontinuity and seems to be a matter of taste, which assumption has to be made.

The Weak formulations In any case it is necessary to derive the corresponding weak formulation for the nonlinear theory. Following the propositions of Wells [Wel01] the virtual work equation in the reference configuration can be written as

$$\mathcal{G} = \int_{\mathcal{B}_0} \mathbf{P}^\natural : \delta \mathbf{F}^\natural dV - \int_{\partial \mathcal{B}_0} \mathbf{t}_0 \cdot \delta \mathbf{u} dA - \int_{\mathcal{B}_0} \mathbf{b}_0 \cdot \delta \mathbf{u} dV = 0, \quad \forall \delta \mathbf{u}. \quad (4.6.5)$$

Here \mathbf{P}^\natural denotes the first Piola-Kirchhoff stress tensor and $\delta \mathbf{F}^\natural = \text{Grad} \delta \mathbf{u}$ is the material gradient of the displacement field, that can be expressed in terms of the deformation gradient, which includes also the discontinuous contributions. Inserting the expression derived in eqn. 4.3.11 we obtain the subsequent virtual work formulation

$$\begin{aligned} \mathcal{G} = \int_{\mathcal{B}_0} [\delta \mathbf{F}_c^\natural : \mathbf{P}^\natural + \mathcal{H}(\mathbf{X}) \delta \tilde{\mathbf{F}}^\natural : \mathbf{P}^\natural + \delta(\mathbf{X}) [\delta \tilde{\mathbf{u}} \otimes \mathbf{m}_0] : \mathbf{P}^\natural] dV \\ - \int_{\partial \mathcal{B}_0} [\mathbf{t}_0 \cdot \delta \mathbf{u} + \mathbf{t}_0 \cdot [\mathcal{H}(\mathbf{X}) \delta \tilde{\mathbf{u}}]] dA - \int_{\mathcal{B}_0} [\mathbf{b}_0 \cdot \delta \mathbf{u}_c + \mathbf{b}_0 \cdot [\mathcal{H}(\mathbf{X}) \delta \tilde{\mathbf{u}}]] dV = 0. \end{aligned} \quad (4.6.6)$$

In this equation we can eliminate the Dirac-delta $\delta(\mathbf{X})$ by integrating over the domain \mathcal{B}_0 and the Heaviside Function disappears by changing the domain of integration from \mathcal{B}_0 to \mathcal{B}_0^+ , such that we finally obtain

$$\begin{aligned} \mathcal{G} = \int_{\mathcal{B}_0} \delta \mathbf{F}_c^\natural : \mathbf{P}^\natural dV + \int_{\mathcal{B}_0^+} \delta \tilde{\mathbf{F}}^\natural : \mathbf{P}^\natural dV + \int_{\mathcal{B}_0} \delta \tilde{\mathbf{u}} [\mathbf{P}^\natural \cdot \mathbf{m}_0] dV \\ - \int_{\partial \mathcal{B}_0} [\mathbf{t}_0 \cdot \delta \mathbf{u} + \mathbf{t}_0 \cdot [\mathcal{H}(\mathbf{X}) \delta \tilde{\mathbf{u}}]] dA - \int_{\mathcal{B}_0} [\mathbf{b}_0 \cdot \delta \mathbf{u}_c + \mathbf{b}_0 \cdot [\mathcal{H}(\mathbf{X}) \delta \tilde{\mathbf{u}}]] dV = 0. \end{aligned} \quad (4.6.7)$$

This equation can be splitted into an continuous contribution

$$\int_{\mathcal{B}_0} \delta \mathbf{E}_c^\flat : \mathbf{S}^\sharp dV - \int_{\mathcal{B}_0} \mathbf{b}_0 \cdot \delta \mathbf{u}_c dV - \int_{\partial \mathcal{B}_0} \mathbf{t}_0 \cdot \delta \mathbf{u}_c dA = 0 \quad (4.6.8)$$

and a contribution due to the discontinuity

$$\begin{aligned} \int_{\mathcal{B}_0^+} \delta \tilde{\mathbf{E}}^\flat : \mathbf{S}^\sharp dV + \int_{\mathcal{I}_0} \delta \tilde{\mathbf{u}} \cdot [\mathbf{F}^\natural \cdot \mathbf{S}^\sharp \cdot \mathbf{m}_0] dA \\ - \int_{\partial \mathcal{B}_0} \mathcal{H}(\mathbf{X}) \delta \tilde{\mathbf{u}} \cdot \mathbf{t}_0 dA - \int_{\mathcal{B}_0} \mathcal{H}(\mathbf{X}) \delta \tilde{\mathbf{u}} \cdot \mathbf{b}_0 dV = 0. \end{aligned} \quad (4.6.9)$$

The corresponding spatial formulations for the continuous and the discontinuous contributions are given by the following relations

$$\int_{B_t} \delta \mathbf{e}^b : \boldsymbol{\sigma}^\sharp dv - \int_{\partial B_t} \mathbf{t} \cdot \delta \mathbf{u}_c da - \int_{B_t} \mathbf{b} \cdot \delta \mathbf{u}_c dv = 0 \quad (4.6.10)$$

and

$$\int_{B_t^+} \delta \mathbf{e}^b : \boldsymbol{\sigma}^\sharp + \int_{\mathcal{I}} \delta \tilde{\mathbf{u}} \cdot \tilde{\mathbf{t}} da - \int_{\partial B_t} \mathcal{H}(\mathbf{X}) \delta \tilde{\mathbf{u}} \cdot \mathbf{t} da - \int_{B_t} \mathcal{H}(\mathbf{X}) \delta \tilde{\mathbf{u}} \cdot \mathbf{b} dv = 0 \quad (4.6.11)$$

whereby the following transformations were used

$$\text{Grad} \delta \mathbf{u}_c = \text{grad} \delta \mathbf{u}_c \cdot \mathbf{F}^\sharp \quad \text{and} \quad \mathbf{m} da = J \mathbf{M} \cdot [\mathbf{f}^\sharp]^t dA \quad \text{and} \quad dv = J dV. \quad (4.6.12)$$

We applied the Cauchy theorem $\tilde{\mathbf{t}} = \boldsymbol{\sigma}^\sharp \cdot \mathbf{m}$ to calculate the true traction vectors in the discontinuity and here we have to determine the normal vector in the spatial configuration, which is not unique. We want to cite the work of Wells [WS01c] here: „... Conceptually, it is necessary to deviate from classical mechanics when applying a traction force at a discontinuity which is opening. Classically, two bodies can only transmit forces, if the bodies are in contact, and being in contact implies that at the point of contact the outward normal vectors to the surfaces of two bodies are identical in direction and opposite in sign. However here it is possible that forces are transmitted between bodies for which the outward normal vectors are not in the same direction...”. For the numerical implementation he suggests to take the normal vector not from the boundaries Γ^+ and Γ^- but from the center surface of the discontinuity, that leads to the relation in eqn. 4.6.4.

Linearizations In section 2.8 we already derived that in the nonlinear theory the balance equations need to be linearized, such that they can be solved by numerical methods as there is the Newton-Raphson iteration scheme. The linearization of the continuous contributions to the virtual work was already derived in chapter 2. For the sake of completeness we want to add the linearization of the discontinuous contributions without any derivations. The corresponding derivations can be also found in the work of Wells [WS01c]. Furthermore, we assume that the external loads are independent of the deformation, such that their contributions are zero in the linearized form and only contributions due to the internal virtual work and the discontinuity remain. Linearizing the material formulation of the weak form including the discontinuity finally leads to

$$\begin{aligned} D_x [\mathcal{G}^{dis}(\bar{\varphi})] \cdot \Delta \mathbf{u} &= \int_{B_0} \left[\delta \widetilde{\mathbf{E}}^b : \mathbb{C} : [[\mathbf{F}^\sharp]^t \cdot \text{Grad} \Delta \mathbf{u}] + \mathbf{S}^\sharp : [[\text{Grad} \Delta \mathbf{u}]^t \cdot \text{Grad} \delta \tilde{\mathbf{u}}]^{sym} \right] dV \\ &+ \int_{\mathcal{I}_0} \delta \tilde{\mathbf{u}} \cdot [\text{Grad} \Delta \mathbf{u} \cdot \mathbf{S}^\sharp + \mathbf{F}^\sharp \mathbb{C} : [[\mathbf{F}^\sharp]^t \cdot \text{Grad} \Delta \mathbf{u}]^{sym}] \cdot \mathbf{M} da \end{aligned} \quad (4.6.13)$$

whereby the linearizations $D_x \mathbf{S}^\sharp$ can be found in section 2.8. Furthermore we still need the linearization of the spatial formulation and this is given by

$$\begin{aligned} D_x [\mathcal{G}^{dis}(\bar{\varphi})] \cdot \Delta \mathbf{u} &= \int_{B_t} [\text{grad} \delta \tilde{\mathbf{u}} : \text{grad} \Delta \mathbf{u} \cdot \boldsymbol{\sigma}^\sharp + \text{grad} \delta \tilde{\mathbf{u}} : \mathbb{c} : \text{grad} \Delta \mathbf{u}] dv \\ &+ \int_{\mathcal{I}} \delta \tilde{\mathbf{u}} \cdot [\text{grad} \delta \mathbf{u} \cdot \boldsymbol{\sigma}^\sharp + \mathbb{c} : \text{grad} \Delta \mathbf{u}] \cdot \mathbf{m} da \end{aligned} \quad (4.6.14)$$

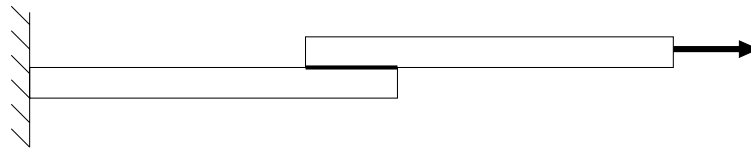


Figure 4.1. Arrangement of tension test of jointed sheets

For the linearization of the particular terms we resort to the relations already given in section 2.8. In this representation the normal vector is not specified so far. But within the numerical treatment the application of the normal vector on the centered material surface is useful. With this relations we like to finish the investigations of discontinuities within the framework of the nonlinear theory.

4.7 Applications

The applications, which are presented in the sequel emanate from investigations, which were performed in the framework of a project supported by the german research foundation (DFG) and which were concerned with the modeling and numerical treatment of cutting and tearing processes of ductile materials. In particular we want to perform a comparison of the domain-dependent and domain-independent interface formulation by the problem of jointed sheets and by the more complex application of cutting processes, where also a contact problem has to be taken into account and a brief description of the applied contact algorithm is given in the corresponding section.

4.7.1 Problem of Jointed Sheets

The interface formulations given above are predestined for the modelling of failure processes as they occur within an tension test of jointed sheets. In the sequel we apply the different interface formulations to the modelling of such processes comparing the properties of the different formulations. In fig. 4.1 the arrangement of such a tension test can be found whereby in the presented example the used parameters remain the same (as far as possible) and only the interface formulation was exchanged. For the sheets themselves a simple linear elastic material law was chosen and to the interfaces we applied the following models

- domain-dependent interface elements
- the domain-independent interface elements **without** normal contributions and
- the domain-dependent interface elements **with** normal contributions.

The sheets were discretized by 11×4 quadrilateral 4-node elements and they are connected by a single layer of 6 linear interface elements. The tension force is superposed by 20 displacement increments à 0.02 units in x-direction on the right boundary of the upper sheet, whereby here plane strains were assumed. The left boundary of the lower sheet was fixed in both directions.

Observations and interpretations

1. In fig. 4.2 we find the tension test of jointed sheets taking the domain-dependent interface formulation into account, whereby we assumed an elasto-plastic standard von-Mises material

law for the interface whereas as mentioned before, linear elastic law was applied to model the sheets behaviour. One can observe, that the upper sheet slips along the horizontal direction and in addition to this the system rotates slightly. This rotation is caused by angular forces, appearing in the interface layer. Furthermore the plotted hardening variable indicates that the inelastic range in the interface layer is reached (picture a) and b)), whereas in the sheets no plastic deformation can occur. If the same material was chosen in the interface as in the bulk the rotation of the probe would have been much stronger than in the presented case, since the stress of failure would have been reached much later.

2. In fig. 4.3 we find the same problem whereby in this calculation the domain-independent interface formulation was applied, whereby no contributions of the traction vector in normal direction was taken into account. Therefore one can observe, that the upper sheet more or less solely slips in horizontal direction, whereby almost no rotation of the system takes place, because of the missing normal contributions of the traction vector.
3. In fig. 4.4 we finally find the deformation of the jointed sheets with the application of the domain-independent interface formulation with additional contributions in normal direction of the traction vector. Here one can observe, that the sheets get much more deformed than in the previous case. Since the load is distributed in normal and tangential direction, the system can be loaded much more and according to this it is deformed much more than in the previous case before the yield stress in the interface is reached and they fail.

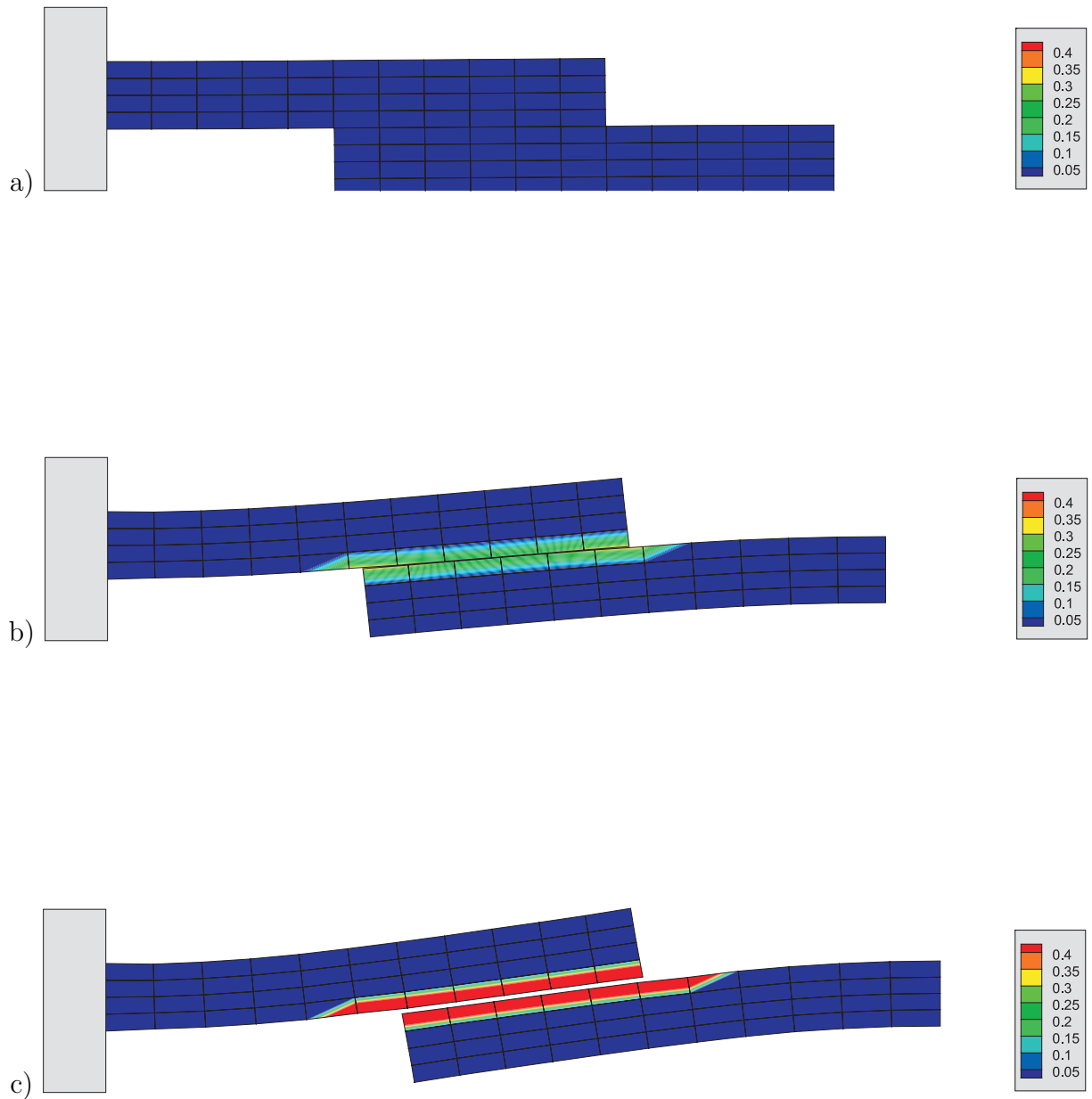


Figure 4.2. Evolution of the hardening variable in the a) initial state b) after 10 load steps c) after 20 load steps. The interface layer was modelled by 6 linear interface elements of the domain-dependent type.

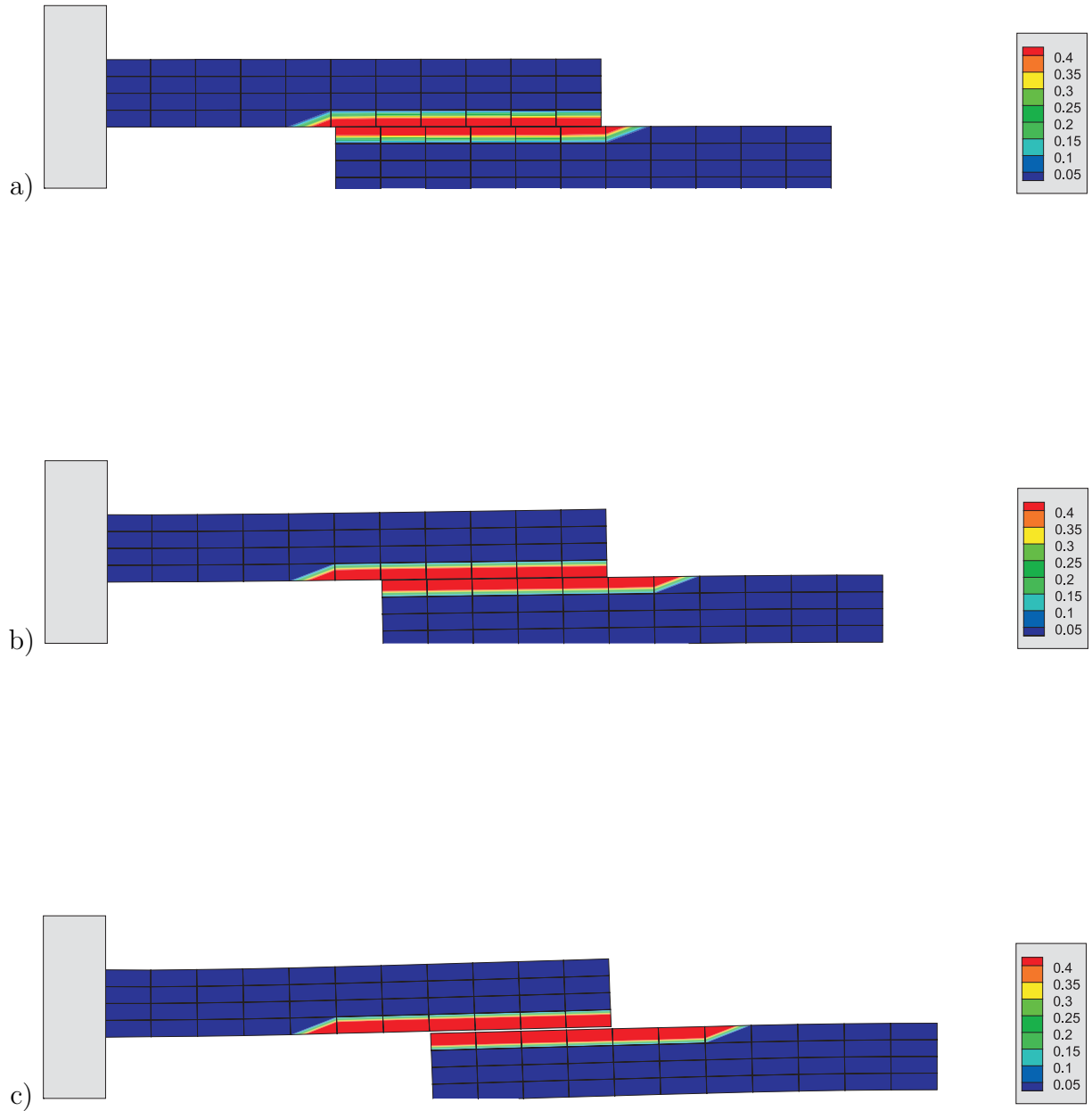


Figure 4.3. Evolution of the hardening variable in the a) initial state b) after 10 load steps c) after 20 load steps. The interface layer was modelled by 6 linear interface elements of the domain-independent type without considering normal contributions of the traction vector.

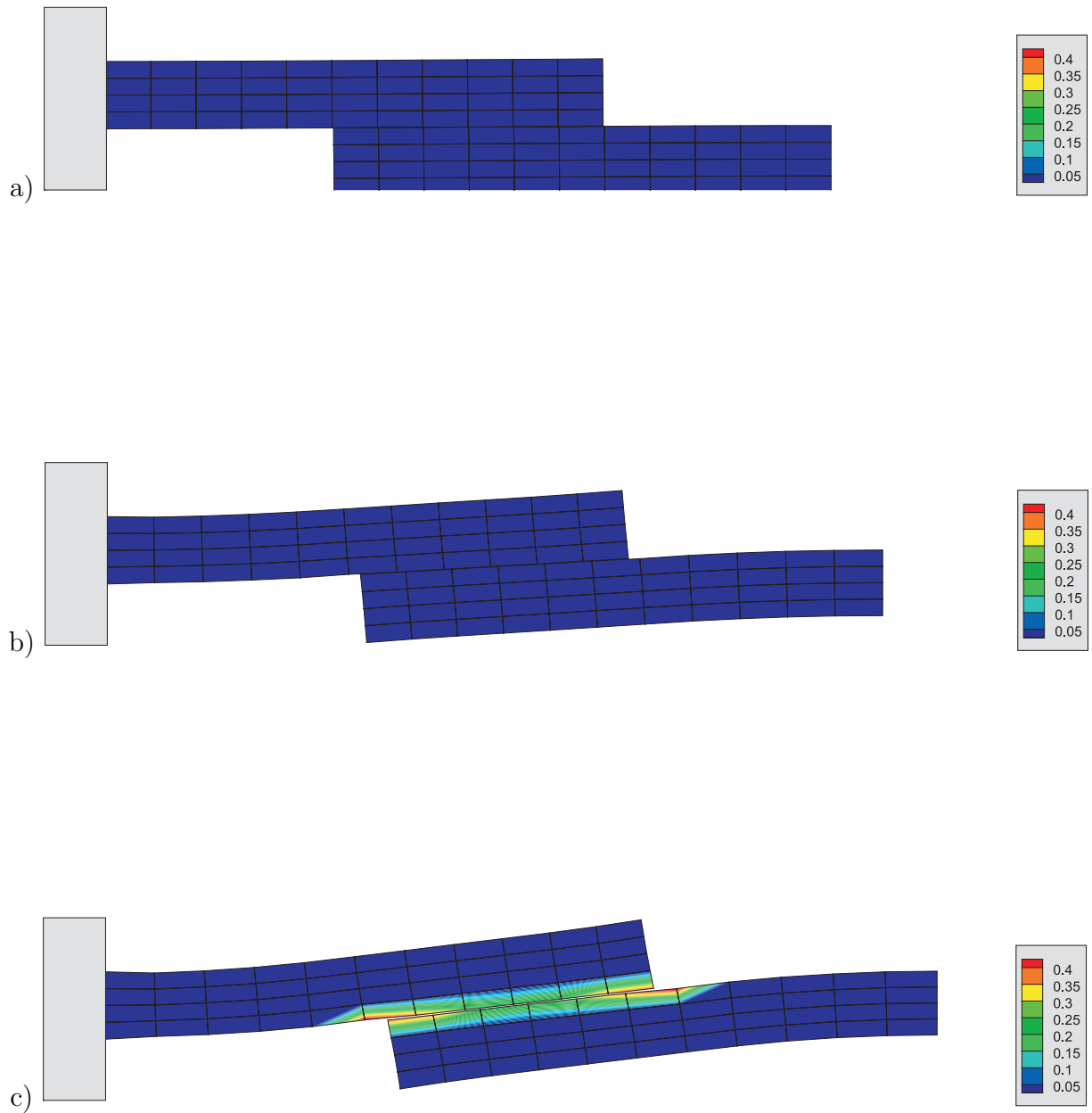


Figure 4.4. Evolution of the hardening variable in the a) initial state b) after 10 load steps c) after 20 load steps. The interface layer was modelled by 6 linear interface elements of the domain-independent type in consideration of normal contributions of the traction vector.

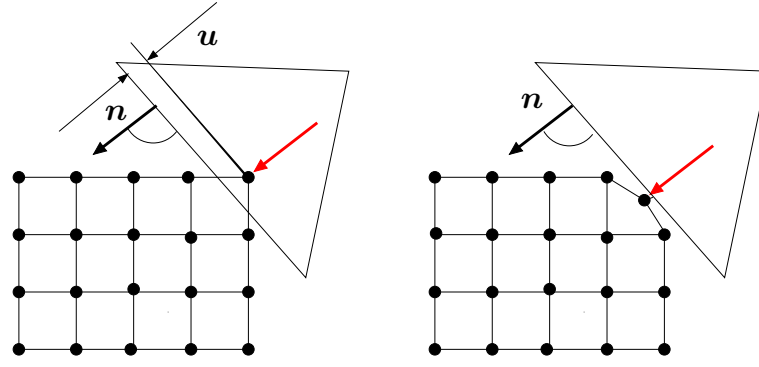


Figure 4.5. Contact problem between cutting tool and ductile probe

4.7.2 Cutting Problems

Contact problem The modelling of cutting and tearing processes is a more complex subject where also the contact problem between cutting tool and the probe has to be taken into account. Since we consider ductile materials like polypropylen (PP), which is less stiff than any steel-like materials we can assume that the cutting tool is rigid in comparison to the probe material. In order to describe the penetration of the cutting knife into the material we applied the following numerical strategy, which is illustrated in fig. 4.6. We start by introducing a so-called gap function $g_N = \mathbf{g}(\mathbf{x}) \cdot \mathbf{n}$ that measures the distance of the considered boundary of the cutting tool for instance and the nodes of the probe, which possibly get in contact with the knife. With this gap function at hand we can distinguish the following three cases:

$$\begin{aligned} g_N > 0 &\implies \text{no contact} \\ g_N = 0 &\implies \text{contact} \\ g_N < 0 &\implies \text{penetration.} \end{aligned} \tag{4.7.1}$$

Obviously, the last possibility is not admissible and therefore the gap function has to be $g_N \geq 0$. For the fulfillment of this equation we introduce an artificial force F_c which acts in direction of the boundary and that moves the corresponding nodes back to the boundary $g_N = 0$. This force should be proportional to g_N and has the direction $-\mathbf{n}$, such that it is defined by

$$\mathbf{F}_c = \epsilon A_c \langle -g_N \rangle \mathbf{n}, \tag{4.7.2}$$

where ϵ denotes the penalty parameter that has to be chosen sufficiently great, such that the contact condition is fulfilled. Usually, some problems arise due to an increasing the condition number, such that the convergency of the Newton-Raphson iteration becomes worse. Therefore often an alternative formulation is applied, denoted by augmented Lagrange algorithm, where the penalty value is increased step by step after each iteration until the contact condition is fulfilled. This method ensures that the penalty parameter only increases as much as necessary, whereby the contact condition is fulfilled exactly and the problem remains numerically well-conditioned. In the discussed formulations no friction is taken into account. For a closer treatment of this topic we refer to the publications of Hallquist, Goudreau & Benson & [HGB85] and Benson & Hallquist [BH90], who firstly considered the numerical treatment of contact problems. A very enclosing treatment of contact problems can be found in Simo & Laurson [LS93a], [LS93b], in the publications of Laurson [Lau94] and Laursen & Oancea [LG94], where also friction was taken into account. An

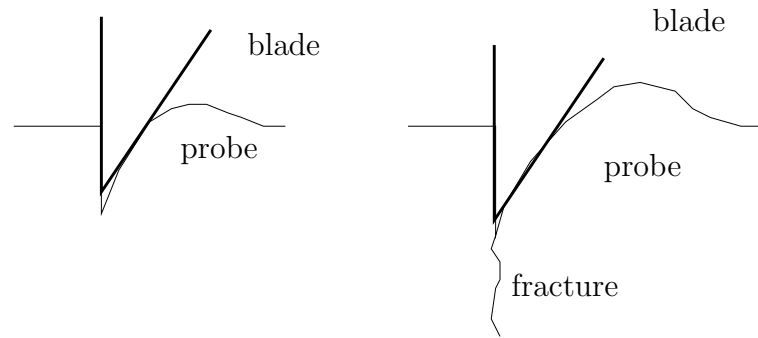


Figure 4.6. Contact problem between cutting tool and ductile probe

overview on small and large strain contact formulations is given by Laursen [Lau02] and in the publications of Wriggers [Wri86], [Wri95], [Wri96] [Wri02], Wriggers & Scherf [WS98] and Wriggers & Miehe [WM94], where especially thermomechanically coupled contact problems were investigated.

The phenomenology Basically, observing the phenomenology of cutting processes two kinds of failure occur. On the one hand the failure takes place at the tip of the cutting tool and on the other hand the failure goes ahead the cutting blade. Moreover, the failure changes from the first type to second one by an increasing cutting velocity, such that the process is highly rate-dependent. This effect is illustrated in fig. 4.9.

With the increase of the cutting velocity the temperature in the cutting zone increases as well and materials like polypropylen reach their melting point and accordingly the stiffness of the material decreases. These are the most important effects if cutting processes are investigated. Furthermore we can summarize the main results of the experimental investigation in the following rules:

The maximum cutting force

- increases with the thickness of the probe
- increases with the applied cutting velocity
- decreases with increasing ambient temperature
- increases with angle of the cutting blade
- decreases with decreasing cutting radius of the blade.

The results of the modelling of cutting process, which we like to discuss here, are depicted in fig. 4.9 and fig. 4.7.2. In this example we restrict ourselves to the quasi-static case, such that the rate-dependent and thermal effects can be neglected here. Therefore the simple von-Mises material law can be applied to the complex problem. In contrast to the previous problem of jointed sheets the separation of the material takes place and so the corresponding failing interface elements have to be taken from the calculation. This problem was solved by introducing an fixed threshold stress (not the yield stress) and as soon as the interface traction has reached the threshold value, this particular element was ignored in the following iterations. This effect can be seen clearly in the diagram in fig. 4.7.2 where the calculated curve of the cutting force is compared to the experimental curve. In this curve the failure of an interface element can be seen in the sudden decrease of the curve.

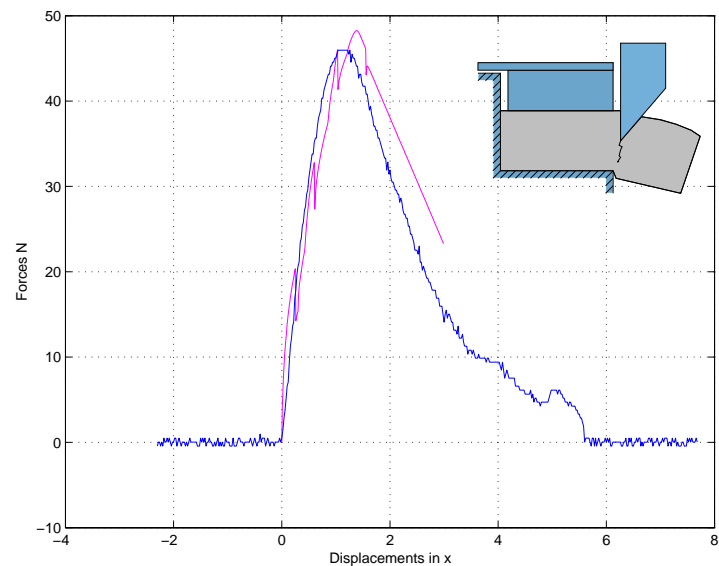
² Additionally, we want to mention here, that the used material parameters extremely differ to the specific material parameters as they are used to characterize the particular material. Thus the elastic modulus for polypropylene for instance, usually is specified by $16000 - 20000 \text{ N/mm}^2$. For the simulation of cutting process it had to be reduced to the number of 1000 N/mm^2 . According to this also the other material parameters like the yield stress and the linear hardening modulus in particular had to be corrected to cover the real cutting process by the finite element model. These effects are caused by the fact, that the material fails nearly immediately after the penetration of the blade takes place, such that the inelastic range is not reached. On the other hand the penetration induces stresses in the material regions which are not reached by the blade, such that the material there behaves in an elasto-plastic manner. For the investigations of cutting processes, which were performed for polypropylene and aluminium alloys the elastic modulus can be estimated by 10% of the standard values. In addition to this the corresponding set of parameters for a particular problem also depends on the geometric parameters of the cutting process. In addition to this one obtains different force- displacement curves in dependency of the blade angle, cutting gap, the material thickness and so on. Therefore it is a difficult task to define a reliable set of parameters which is valid for all real cutting processes. Probably it would be necessary to perform a parameter identification procedure, which was not aim of this present work. In order to minimize the number of parameters we decided to chose the simple geometrically nonlinear isotropic von-Mises material model for the description of the cutting process, whereby for the interfaces the domain-dependent formulation with a negative hardening modulus was applied which requires the arc-length solution method.

Discretization For the modelling of the cutting problem we discretized the modelling as follows. The probe was divided into three blocks whereby the left block consists of 25 rows and 20 columns of rectangular 4-node elements. The height of the whole probe was chosen by 2 units and its length is 15 units. The length of the first block is 10 units, whereas the second block was introduced to realize a variable gap between the rotor blade and the static blade. In the particular calculation the second block simply consists of a single column and it has a width of 0.2 units. The last block models the free end of the probe, that is separated and which consists of 14 columns of elements. It is connected to the second block by a single interface layer of linear domain-dependent 4-node interface elements. The load was superposed by vertical displacement increments of 0.01 units of the blade until the separation of the probe was performed, that is indicated by the divergence of the corresponding iteration step. The used material parameter are summarized in fig. 4.7.2

Interpretation The interpretation of the results is performed by fig. 4.9, that illustrates different states of the cutting of polypropylene. After 5 load steps one can observe, that the cutting tool penetrates the probe slightly and induces stresses in vertical direction along the interface layer. The more the blade penetrates into the material the stresses increase. But due to the modified interface formulation the material relaxes, where the separation is finished and the stress disappear at the corresponding interface elements (s. fig 4.9b). After 44 load steps the stresses in the material are increased so much (s. fig 4.9c) that in the next load step the calculation stops due to divergency and we can interpret it as the complete failure of the material. This corresponds to experimental experience, where after some time of ductile failure at the tip of the cutting tool, the stresses in

²Of course, there are better criteria which can be found to indicate the failure of an interface. An appropriate criteria of failure could be the singularity of the interface stiffness. But for the sake of a better understanding and control of the calculation, we decided simply to introduce the threshold value.

Parametername	Parametervalue
E	1000 N/mm ²
ν	0.3
Y_0	34 N/mm ²
Y_∞	35 N/mm ²
κ	9.6
h	-10 N/mm ²
E^{int}	1000 N/mm ²
Y_0^{int}	20 N/mm ²
Y_∞^{int}	20 N/mm ²
κ^{int}	0
h^{int}	-10 N/mm ²
von-Mises model	



Cutting-geometrie					
angle of blade	thickness of probe	width of gap	velocity	material	Lagerung
30°	5 mm	0.2 mm	quasistatic	Polypropylen	free

Figure 4.7. Comparison of experiment and simulation: The diagramm shows the force- displacement- curve of a cutting process of PP

the remaining material are increased so much that it fails due to sudden fracture. The divergency indicates that the separated material behaves like a separate body, that can not be treated within an quasistatic formulation, since there are no sufficient boundary conditions for the „new” body. We want to note here, that the interface elements are also able to cover the separation processes as they occur in the framework of material cutting processes. The force- displacement curve in fig 4.9 shows a good accommodation of the experimental and numerical data, whereby the parameters had to be adapted to the complex problem for the before mentioned reasons.

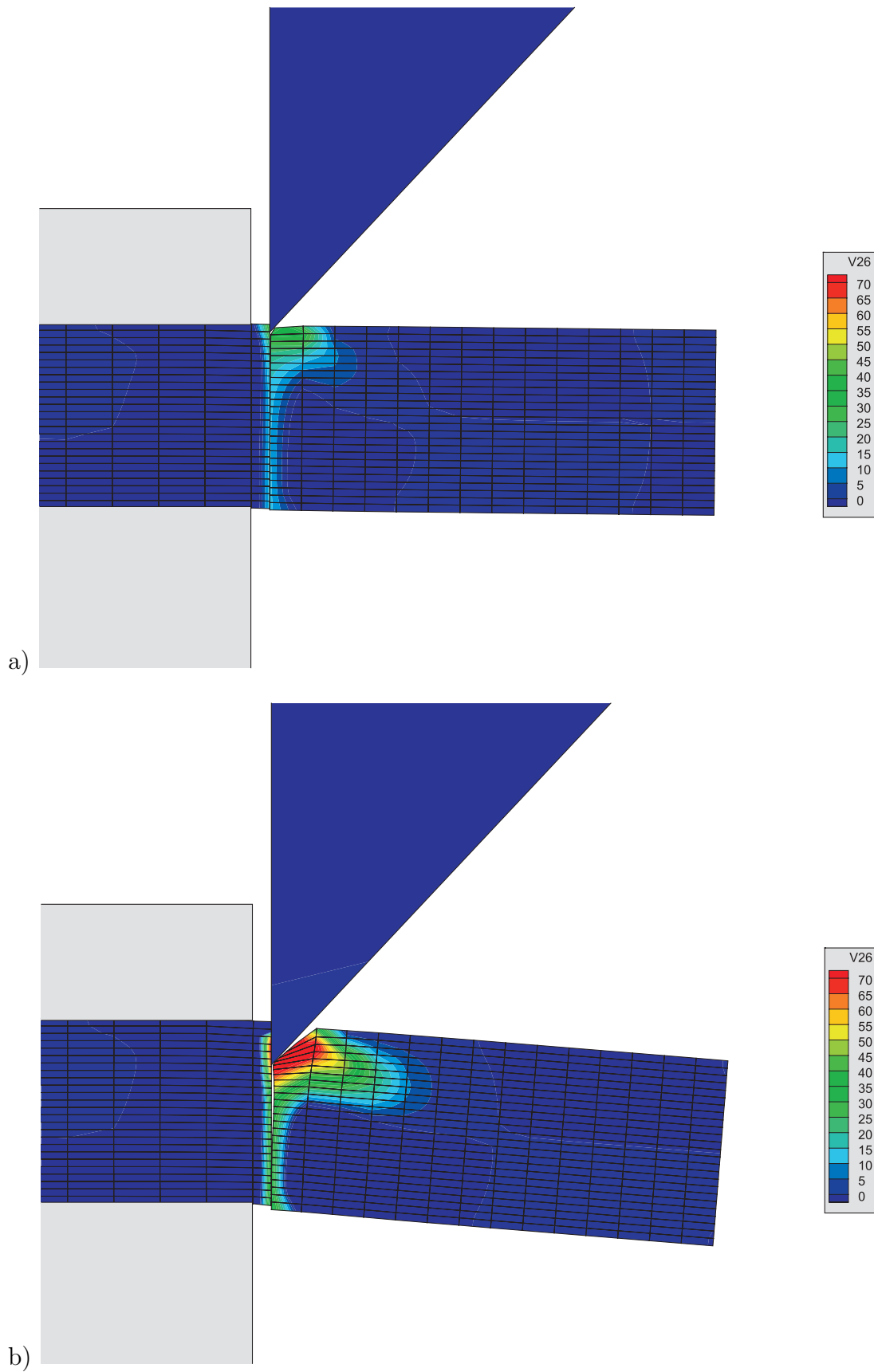


Figure 4.8. Stress distribution during a cutting process a) after 5 load steps b) after 25 load steps

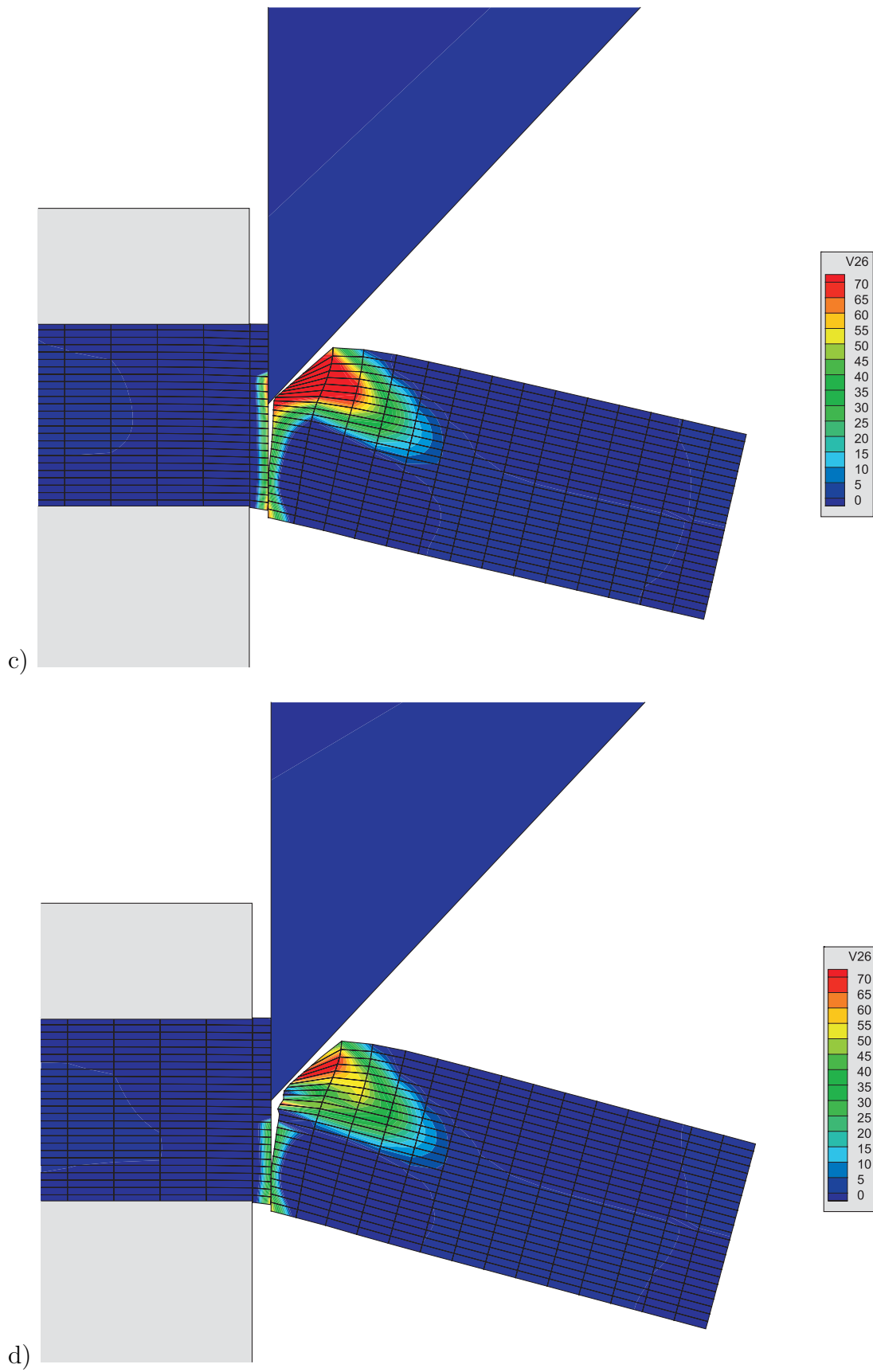


Figure 4.9. Stress distribution during a cutting process a) after 44 load steps b) after 45 load steps

5 Interfaces with Extra-Energy Contributions

5.1 Overview

In chapter 3 we introduced the kinematics of interfaces which have certain properties in tangential direction of the material surface. These contributions were neglected within the description of localization phenomena, since they are not relevant for this kind of problems. In the context we like to investigate in this chapter we need these additional contributions. One can imagine the material surface which feature these extra contributions as a kind of membrane or fibre embedded in the ambient material. Therefore this kind of interfaces is predestinated for the description of composites, where the material properties are relevant, whereas the volumetric dimension is neglectable. The given kinematical introduction from chapter 3 is completely taken to this description, such that there is no need to derive any kinematical tools anymore, since they can be taken from chapter 3 one by one. Also the thermodynamical features are completely given, such that the only thing left to do is to derive some constitutive laws for the mechanical and thermal subproblem. In particular for the thermal subproblem we want to resort to hypothesis II for the interface temperature $\hat{\Theta}$, since it is difficult to predict Neumann boundary conditions for the entropy flux in a reasonable way. Afterwards we will show some applications of this formulation, discussing the mechanical and the thermal subproblem and finally we give some simple examples of thermo-mechanically coupled problems.

5.2 Constitutive Equations

In order to exploit the above derived dissipation inequality we specify the constitutive model by selecting a particular list of arguments for the free energy functions for the bulk and the interface. Moreover, an appropriate heat conduction law has to be chosen, that depends on the choice of the interface temperature that is assumed in the spirit of hypothesis II: $\hat{\Theta} = \{\Theta^{-1}\}^{-1}$. In the sequel, for sake of simplicity we will restrict ourselves to the thermoelastic case, whereby in principle also inelastic models are conceivable. Furthermore, we tried to construct the interface constitutive laws analogously to the corresponding bulk formulations. However, for the thermoelastic case the free energy for the bulk and the interface depends on

$$\Psi := \Psi([\nabla \mathbf{u}]^{sym}, \Theta) \quad \text{and} \quad \hat{\Psi} := \Psi([\hat{\nabla} \hat{\mathbf{u}}]^{sym}, \tilde{\mathbf{u}}, \hat{\Theta}) \quad (5.2.1)$$

From these assumptions and the corresponding dissipation inequalities the following familiar constitutive laws of the bulk stress and the bulk entropy emanate

$$\boldsymbol{\sigma}^t = \rho \frac{\partial \Psi}{\partial [\nabla \mathbf{u}]^{sym}} \quad \text{and} \quad s = -\frac{\partial \Psi}{\partial \Theta} \quad (5.2.2)$$

In analogy to the bulk formulation the interface dissipation inequality yields the following interface entropy

$$\hat{s} = -\frac{\partial \hat{\Psi}}{\partial \hat{\Theta}}, \quad (5.2.3)$$

whereas we have to distinguish between the tangential interface stress $\hat{\boldsymbol{\sigma}}^t$ along the interface \mathcal{S} and the stress contribution that we obtain from the traction vector $\tilde{\mathbf{t}}$ acting across the interface and which we already introduced in the previous chapter. We finally obtain for the mechanical forces in the interface

$$\hat{\boldsymbol{\sigma}}^t = \hat{\rho} \frac{\partial \hat{\Psi}}{\partial [\hat{\nabla} \hat{\mathbf{u}}]^{sym}} \quad \text{and} \quad \tilde{\mathbf{t}} = \llbracket \boldsymbol{\sigma}^t \rrbracket \cdot \mathbf{m} = \hat{\rho} \frac{\partial \hat{\Psi}}{\partial \hat{\mathbf{u}}}. \quad (5.2.4)$$

The free energy functions for standard linear thermo-elastic bulk materials can be assumed by

$$\rho \Psi := \frac{1}{2} [\nabla \mathbf{u}]^{sym} : \mathbb{E} : [\nabla \mathbf{u}]^{sym} - \rho \frac{c}{\Theta_0} \frac{\vartheta^2}{2} - \vartheta \alpha \mathbf{I} : \mathbb{E} : [\nabla \mathbf{u}]^{sym}, \quad (5.2.5)$$

whereby \mathbb{E} denotes the fourth order elasticity tensor for linear elastic materials, that can be specified by

$$\mathbb{E} = L \mathbb{I} + 2G \mathbf{I} \otimes \mathbf{I}. \quad (5.2.6)$$

Here L and G denote elastic material parameters, α denotes the heat expansion coefficient and c is the heat capacity of the bulk material. According to this we can prescribe also a free energy function for the interface which in principle has the same structure

$$\hat{\rho} \hat{\Psi} := \frac{1}{2} [\hat{\nabla} \hat{\mathbf{u}}]^{sym} : \hat{\mathbf{E}} : [\hat{\nabla} \hat{\mathbf{u}}]^{sym} - \hat{\vartheta} \hat{\alpha} \mathbf{P} : \hat{\mathbf{E}} : [\hat{\nabla} \hat{\mathbf{u}}]^{sym} - \frac{\hat{c}}{\hat{\Theta}_0} \frac{\hat{\vartheta}^2}{2} + \frac{1}{2} \tilde{\mathbf{u}} \cdot \tilde{\mathbf{E}} \cdot \tilde{\mathbf{u}} - \hat{\vartheta} \tilde{\alpha} \mathbf{m} \cdot \tilde{\mathbf{E}} \cdot \tilde{\mathbf{u}}. \quad (5.2.7)$$

The appearing second order tensor $\tilde{\mathbf{E}}$ was already introduced in the previous chapter and was defined by

$$\tilde{\mathbf{E}} = \tilde{E}_{\parallel} \mathbf{P} + \tilde{E}_{\perp} \mathbf{m} \otimes \mathbf{m}, \quad \text{with} \quad \mathbf{P} = \mathbf{I} - \mathbf{m} \otimes \mathbf{m}. \quad (5.2.8)$$

It relates the displacement jump to the interface traction vector $\tilde{\mathbf{t}}$, whereby \tilde{E}_{\parallel} and \tilde{E}_{\perp} are elastic parameters describing the elastic behaviour perpendicular and tangential to the material surface. The fourth order isotropic elasticity tensor $\hat{\mathbf{E}}$ relates the symmetric interface displacement gradient $[\hat{\nabla} \hat{\mathbf{u}}]^{sym}$ to the tangent interface stress contribution $\hat{\boldsymbol{\sigma}}^t$ and is defined in analogy to the continuous elasticity tensor in eqn. 5.2.6

$$\hat{\mathbf{E}} = \hat{L} \mathbb{I} + 2\hat{G} \mathbf{P} \otimes \mathbf{P}. \quad (5.2.9)$$

Here \widehat{L} and \widehat{G} are the corresponding material parameter and $\widehat{\mathbb{I}} = \mathbf{P} \otimes \mathbf{P} + \mathbf{P} \otimes \mathbf{P}$. From the given free energy functions we can derive the bulk stress and the bulk entropy in the manner of equation 5.2.2 by performing the differentiation of the free energy with respect to the displacement gradient and the temperature, such that the specified expressions are given by

$$\boldsymbol{\sigma}^t = \mathbb{E} : [[\nabla \mathbf{u}]^{sym} - \alpha \vartheta \mathbf{I}] \quad \text{and} \quad s = \frac{c}{\Theta_0} \vartheta + \alpha \mathbf{I} : \mathbb{E} : [\nabla \mathbf{u}]^{sym}. \quad (5.2.10)$$

Furthermore, from the interface free energy function we can derive the specified expressions for the interface entropy and the interface stress quantities. They emanate analogously from the derivatives of the interface free energy function with respect to the interface temperature, the interface gradient of the average displacement field and the displacement jump, such that we obtain according to eqn. 5.2.3 and 5.2.3 the interface stress tensor and the interface traction vector

$$\widehat{\boldsymbol{\sigma}}^t = \widehat{\mathbf{E}} : [[\widehat{\nabla} \widehat{\mathbf{u}}]^{sym} - \widehat{\alpha} \widehat{\vartheta} \widehat{\mathbf{P}}] \quad \text{and} \quad \widetilde{\mathbf{t}} = \widetilde{\mathbf{E}} \cdot [\widetilde{\mathbf{u}} - \widetilde{\alpha} \widehat{\vartheta} \mathbf{m}] \quad (5.2.11)$$

and finally the interface entropy is given by

$$\widehat{s} = \widehat{\rho} \frac{\widehat{c}}{\Theta_0} \widehat{\vartheta} + \widehat{\alpha} \mathbf{P} : \widehat{\mathbf{E}} : [\widehat{\nabla} \widehat{\mathbf{u}}]^{sym} + \widetilde{\alpha} \widetilde{\mathbf{m}} \cdot \widetilde{\mathbf{E}} \cdot \widetilde{\mathbf{u}}. \quad (5.2.12)$$

Note that the interface temperature is related to the heat expansion along the interface and across the interface. By selecting the various material parameters properly, different linear thermoelastic submodels can be established. As mentioned before we like to assume the interface temperature in the spirit of hypothesis II, from which the definition of the tangential heat flux $\widehat{\mathbf{q}}$ and the heat flux across the interface $\widetilde{\mathbf{q}}$ emerges. As mentioned before we chose a constitutive formulation of the Fourier type, such that they are given by

$$\widehat{\mathbf{q}} = -\widehat{\kappa} \widehat{\nabla} \widehat{\theta} \quad \text{and} \quad \widetilde{\mathbf{q}} = [\mathbf{q}] \cdot \mathbf{m} = -\widetilde{\kappa} [\theta], \quad (5.2.13)$$

where $\widehat{\kappa}$ and $\widetilde{\kappa}$ denote the heat conduction coefficients along and across the interface. They are material specific parameters.

5.3 Applications

In this section we want to give some numerical examples, where the before shown extended interface formulation is applied, whereby the emphasis is on the illustration of the influence due to the additional interface contributions indicated by $[\bullet]$. The parameters in the following examples were chosen in a way to emphasize the qualitative effect of the interface formulation. A validation of the presented results in the spirit of comparing them with experimental data, did not take place and a corresponding application would be a subject of future work. Therefore the given examples are solely investigated with respect to plausibility.

The subsequent presented calculations are restricted to the 2-dimensional case, such that the interface elasticity tensors for the case of isotropy reduces to

$$\widehat{\mathbf{E}} = \widehat{E} \widehat{\mathbf{n}} \otimes \widehat{\mathbf{n}} \quad \text{and} \quad \widetilde{\mathbf{E}} = \widetilde{E}_{\parallel} \widehat{\mathbf{n}} \otimes \widehat{\mathbf{n}} + \widetilde{E}_{\perp} \mathbf{m} \otimes \mathbf{m}, \quad (5.3.14)$$

whereby the constants \widehat{E} , $\widetilde{E}_{\parallel}$ and \widetilde{E}_{\perp} are independent from each other and can be chosen arbitrarily. Furthermore we need to specify the heat conduction vectors for the thermal subproblem, which are assumed of the Fourier type

$$\{\mathbf{q}\} \cdot \mathbf{m} = -\widetilde{\kappa} [\theta] \quad \text{and} \quad \widehat{\mathbf{q}} = -\widehat{\kappa} \cdot \widehat{\nabla} \widehat{\theta}, \quad \text{with} \quad \widehat{\kappa} = \widehat{\kappa} \widehat{\mathbf{n}} \otimes \widehat{\mathbf{n}}. \quad (5.3.15)$$

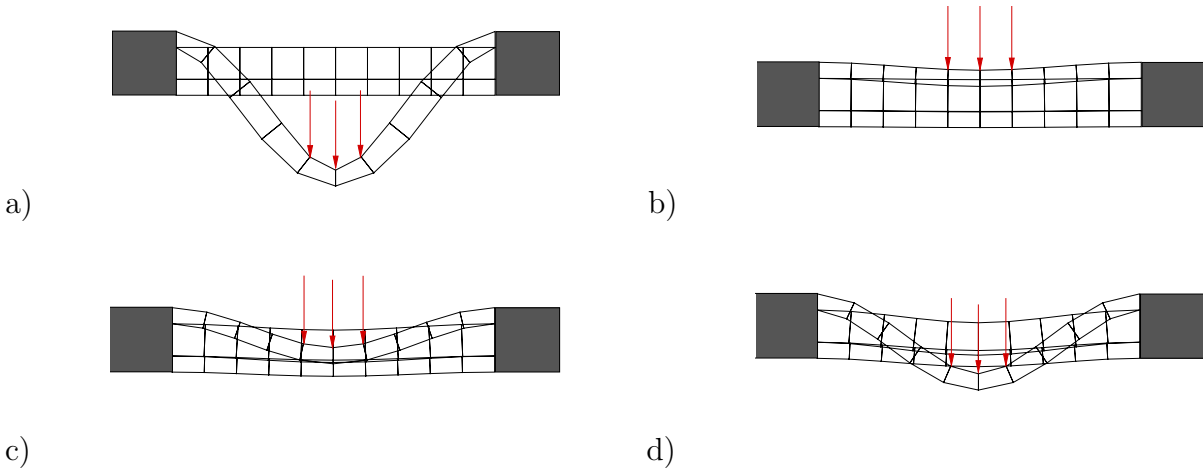


Figure 5.1. Bending of a beam with a) $\tilde{E}_{\parallel} = \tilde{E}_{\perp} = \hat{E} = 0$ b-d) $\tilde{E}_{\parallel} = \tilde{E}_{\perp} = 0, \hat{E} \neq 0$

The remaining parameters are scalar quantities and they are specified within the particular problem. We begin by investigating the purely mechanical problem of a bended beam and continue to consider some heat flux problems representing the thermal subproblem. Finally, two simple examples of thermomechanically coupled problems are presented.

5.3.1 Mechanical Problem

We start with a pure mechanical example of a bending beam that is fixed at both ends and loaded as it is depicted in fig. 5.1. The beam has a thickness of 3 units of lengths and a length of 10. For demonstration of the interface influence we insert two layers of interfaces into the finite element mesh and vary their stiffness in tangential direction by changing the elastic parameters \tilde{E}_{\parallel} , \tilde{E}_{\perp} and \hat{E} . The other parameters for the bulk and the interface remain unchanged and they are collected in table 5.1. The thermal parameters are neglected and set to zero. The continuous part is discretised by three rows of ten 9-Node quadrilateral elements and these are connected accordingly by two rows of ten 6-Node interface-elements. The stiffness for the tangential jump-based contributions \tilde{E}_{\perp} was set to zero, such that the effects of the jump-based and the average based contributions can be distinguished more easily.

In the first step also the interface stiffness \hat{E} and \tilde{E}_{\perp} are set to zero and the beam is load by means of displacement boundary conditions, such that the three continuous parts the beam consisting of, are disconnected and behave as depicted in fig. 5.1a). We note here, that the lower parts of the beam are not affected by the deformation. This example is physically not reasonable, since the different parts may not penetrate each other, but it is appropriate as point of departure to illustrate

Parameter	Bulk-Material	Interface (jump-based)	Interface (average-based)
Youngs Modulus [N/mm ²]	$E = 10$	$\tilde{E}_{\parallel} = 0, 10, \tilde{E}_{\perp} = 0$	$\hat{E} = 10, 100, 1000$
Poissonzzahl ν	0.29	-	-

Table 5.1. Parameter for linear elastic material

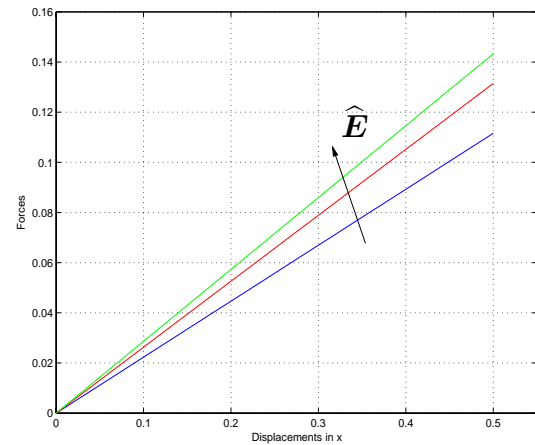
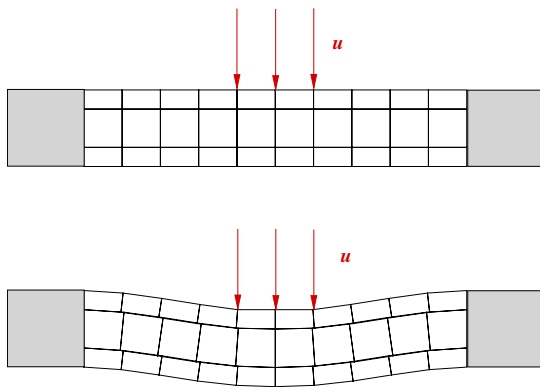


Figure 5.2. a) Undeformed and deformed Beam b) Increasing stiffness

the influence of the different interface contributions. Therefore in fig. 5.1b)-d) we can see the beam at different load steps, whereby the loading is the same as in the previous example, but in contrast to the previous example, the tangential interface stiffness is chosen $\hat{E} > 0$.

Interpretation In contrast to the first calculation we can see, that also the lower part of the beam is affected by the loading. That means, that \hat{E} contributes to the interface stiffness, but the penetration prevented by this parameter. Naturally, this example is not physically reasonable at all, but it indicates the influence of \hat{E} , that controls the tangential interface stiffness.

In the next example we set the parameter $\tilde{E}_\perp = 10$ and as in the previous calculation we imposed displacements as depicted in fig. 5.2 and we measured the reaction forces acting at the fixed element nodes in the middle row during the deformation.

Interpretation There are two phenomena we can observe in this example.

- At first one can see, that the different parts of the beam do not penetrate anymore, such that the increase of the interface stiffness parameter \tilde{E} seems to control the contact condition between the different layers.
- On the other hand one expects that the stiffness of the beam increases according to the increase of the interface stiffness. This is verified by the diagramm in fig. 5.2 where the stiffness increase induces a higher slope of the curves.

5.3.2 Thermal Problems

Now we show an example for the pure thermal heat conduction problem. For this we consider a plate with a height and width of ten units of length and discretize it by 10×10 quadrilateral 4-node-elements. In the middle of the plane we insert again an interface layer of ten 4-node interface-elements. On this plate we apply a one-time temperature increment of 100 degrees at the left

Parameter	Bulk-Material	Interface (jump-based)	Interface (jump-based)
Heat Conduction coefficient	$\kappa = 0.01$	$\tilde{\kappa} = 0.001$	$\hat{\kappa} = 0.005, 0.50$
Heat Expansion Coefficient	$\alpha = 0.000012$	$\tilde{\alpha} = 0.000012$	$\hat{\alpha} = 0.000012$
Reference Temperature [$^{\circ}$ K]	293.15		
Heat Capacity [kJ/ K]	$c = \hat{c} = 0.0036$		

Table 5.2. Parameter for linear elastic material

boundary for a time-increment of 0.01 seconds. After that we consider the heat conduction for the next 0.29 seconds. This problem was computed for different values of the tangential heat conduction parameter $\hat{\kappa}$ of the interface layer direction while the other parameter remained unchanged. The used parameters for the computation are collected in table 5.2 whereby the same values for the mechanical subproblem were applied as in the previous numerical example.

Interpretation The calculations in fig. 5.3 show the temperature distribution of the system after 10, 20 and 30 seconds, whereby in the left series a)-c) the average interface heat conduction parameter was chosen by $\hat{\kappa} = 0.005$, such that is of the same order than in the ambient bulk material. In the second calculation that is represented in the right series d)-f) the interface heat conduction parameter was set to $\hat{\kappa} = 5.0$, where as the heat conduction parameter in the bulk remained constant. If we compare the second calculations d)- f) to the first series, it is easy to observe, that the heat conduction in the interface layer is much higher than in the bulk material, where the heat conduction parameter is chosen as before. The interface heat conduction coefficient is chosen much higher than in the bulk material to show the qualitative effect.

In other calculations the interface heat conduction parameter $\hat{\kappa}$ was decreased to a value much lower than the heat conduction parameter in the bulk material, such that the interface heat flux was expected to be less developed after 30 s than the heat flux in the ambient bulk material. But the interface heat flux is effected by the temperature jump and thus it also depends on the bulk temperature distribution, such that the interface behaviour was superimposed by the bulk behaviour. The resulting effect was marginal, such that we pass on without presenting the corresponding calculations.

In the next example we investigate the influence of the interface component across the interface with respect to the heat conduction behaviour. For this we consider the same system as before, whereby this time a homogenous temperature field of 100° K in ten time steps $\Delta t = 0.1$ s at the lower boundary is superposed. Afterwards the system is left on its own for further 30 s. The corresponding calculation is represented in fig. 5.4, whereby the left series a)-c) again represents the reference calculation without any interface contribution, whereas the right series shows the system, where an interface layer is integrated. The interface heat conduction coefficients $\tilde{\kappa}$ and $\hat{\kappa}$ are set to zero. The remaining parameters are listed in table 5.2. Like in the previous example also here the temperature distribution in the plate is plotted, indicating the heat flux within the system. One can observe that in the reference calculation due to the heat flux the temperature in the upper part of the plate increases after some time. In the calculation including the interface layer, presented in the series d)-e), the heat flux to the upper part of the plate is prevented by the interface layer.

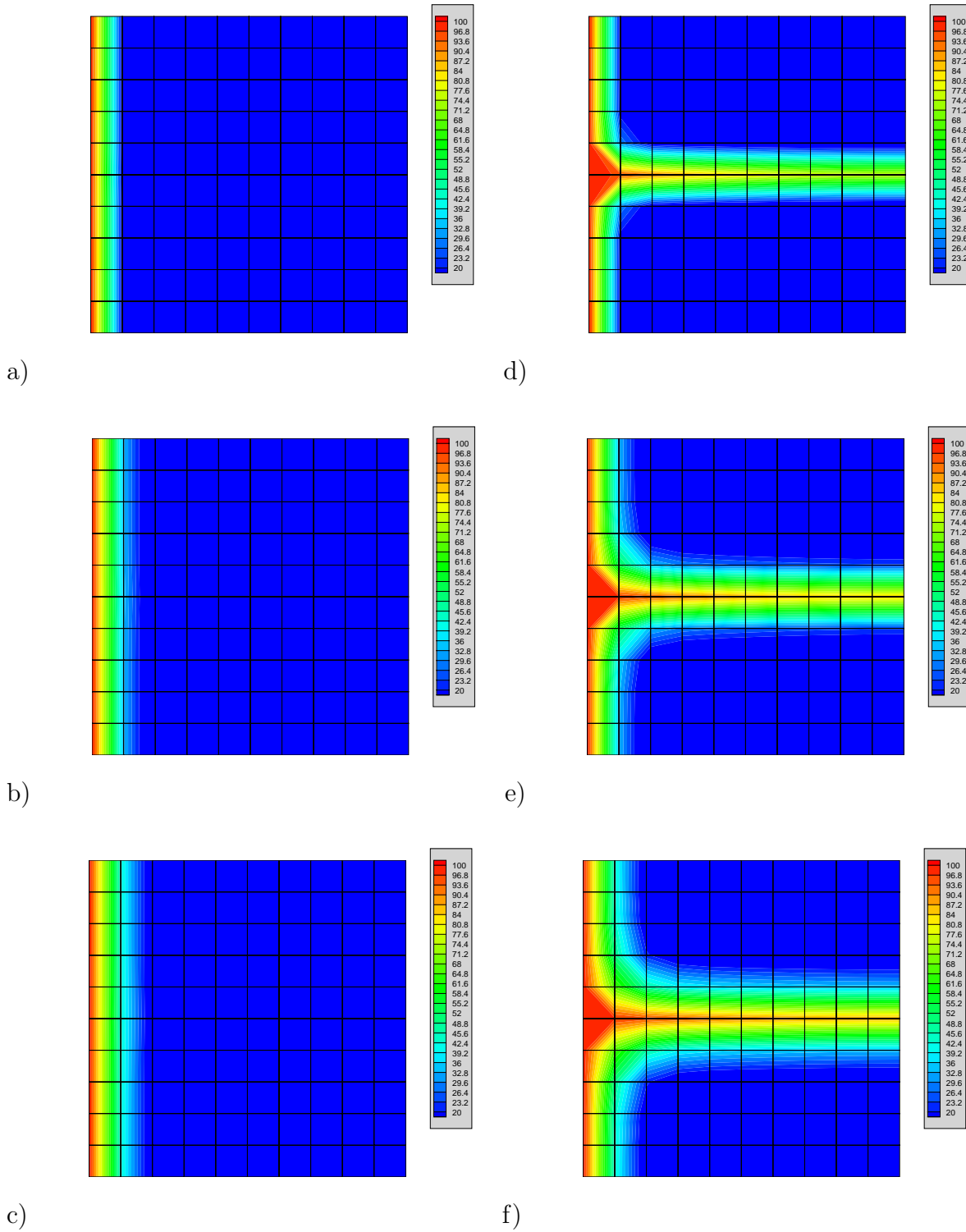
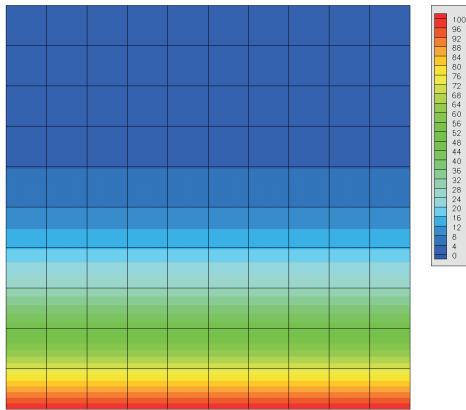
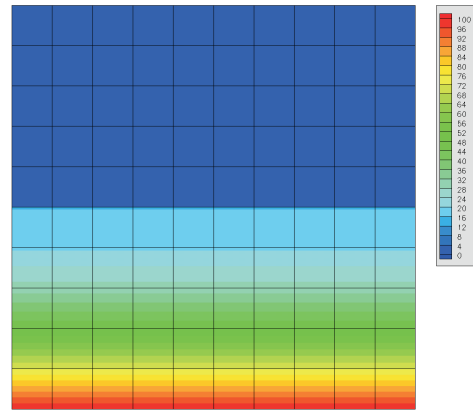


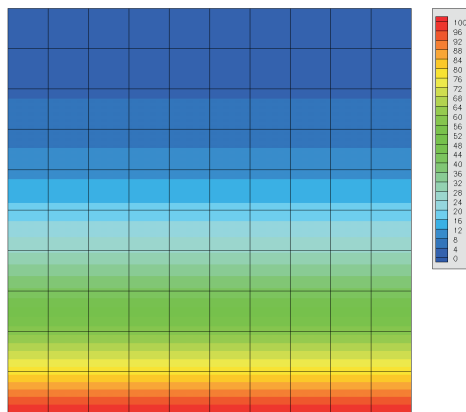
Figure 5.3. Thermal Problem with average-based heat conduction a-c) Temperature distribution after 10s, 20s and 30s with $\hat{\kappa} = 0.005$ d-f) Temperature distribution after 10s, 20s and 30s with $\hat{\kappa} = 0.5$



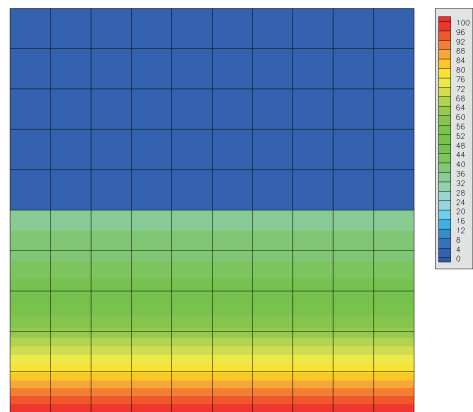
a)



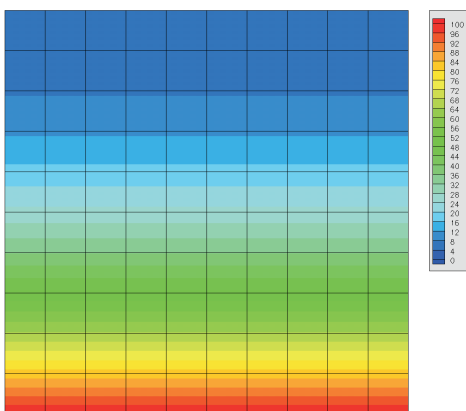
d)



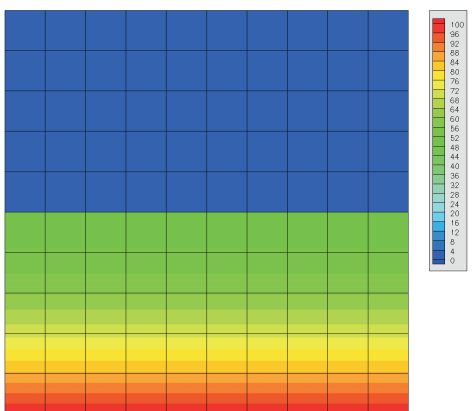
b)



e)



c)



f)

Figure 5.4. Temperature distribution a)-c) without interface layer after 2s, 3s and 4s d)-e) with interface heat conduction $\tilde{\kappa} = 0$ after 1s, 2s and 3s

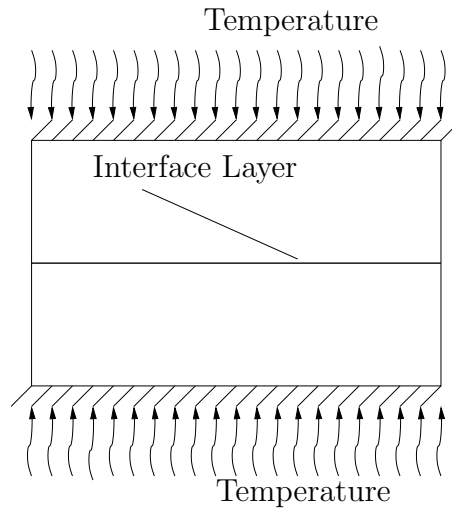


Figure 5.5. a) Arrangement of coupled problem

Interpretation Since the heat conduction coefficients in the interface is set to zero no heat exchange with the upper part of the plate can take place and the heat accumulates in the lower part. Therefore the interface works as an insulator preventing the heat flux to the upper system part.

Also for this example we investigated the inverse problem, where the interface heat conduction coefficient in normal direction was chosen much higher than in the ambient bulk material. One expects an „acceleration” of the heat flux due to higher heat conduction in the interface. But also here, the effect was likewise marginal, such that we pass on the representation of the corresponding calculations.

5.3.3 Coupled Problems

For the investigation of the thermoelastic coupled problem we choose the arrangement depicted in fig. 5.6 a). Here again a single interface layer consisting of ten 4-node-interface elements is inserted between two continuous plates that are fixed at the boundaries at the top and at the bottom. The two continuous domains are discretized symmetrically by 10×5 quadrilateral 4-node-elements and they have a height and width of 10 units of length. The boundaries at the side are free and at the top and bottom boundary twenty temperature increments of 25° are imposed during 2 seconds. The parameters for the mechanical and the thermal problem are chosen as in the previous examples

Parameter	Bulk-Material	Interface (jump-based)	Interface (average-based)
Youngs Modulus [N/mm ²]	$E = 10$	$\tilde{E}_\perp = 50, \tilde{E}_\parallel = 0$	$\hat{E} = 10$
Poissonzzahl ν	0.29	-	-
Heat Conduction coefficient	$\kappa = 0.002$	$\tilde{\kappa} = 0.002$	$\hat{\kappa} = 0.002$
Heat Expansion Coefficient	$\alpha = 0.00001$	$\tilde{\alpha} = 0.00001$	$\hat{\alpha} = 0.00101$
Reference Temperature [° K]	293.15		

Table 5.3. Parameter for linear thermo-elastic material

except for the heat expansion coefficient of the average-based interface contribution that is chosen much higher than the heat expansion coefficients α and $\tilde{\alpha}$ for the bulk material and for jump-based interfacial contributions. All parameters are collocated in table 5.3.

Interpretation Due to the extremely high interface heat expansion coefficient the fibre, represented by the interface layer, expands much more than the bulk material as it can be seen in fig 5.6 b). Since the interface heat expansion coefficient across the interface $\tilde{\alpha}$ is chosen from the same order than the bulk the fibre is solely able to expand in tangential direction, where no boundary conditions are prescribed, a tension stress is induced in the bulk material that is fixed at the upper and lower boundaries. If the stiffness of the interfaces is not high enough, these stresses cause an opening of the interfaces. This can be avoided by an increase of the jump-based elastic modulus \tilde{E}_\perp .

In a last example treating a thermodynamically coupled problem we consider the „inverse” problem and exchange the parameters of the previous example in the spirit, that the tangent interface heat expansion coefficient is chosen much lower than in the ambient bulk material. The corresponding boundary conditions and time steps are retained unchanged, such that we obtain the different deformed configurations at different time steps as they are depicted in fig. 5.7.

Interpretation Due to its lower tangent heat expansion coefficient the interface is not able to expand as much as the surrounding bulk material. This causes a necking in the middle of the plate. But since the interface lives in kinematical slavery to the bulk material, it is superposed by the bulk deformation. Thus naturally the interface can not remain completely undeformed as well.

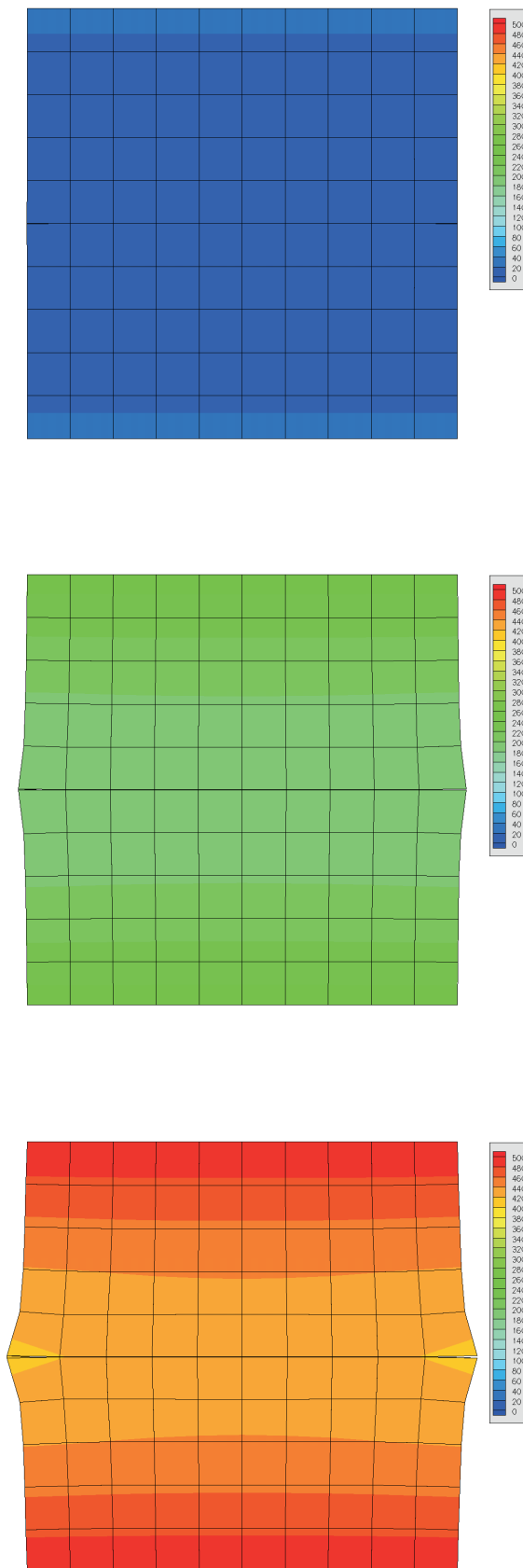


Figure 5.6. Distribution of absolute temperature in the a) initial configuration and after b) 10 seconds and c) 20seconds

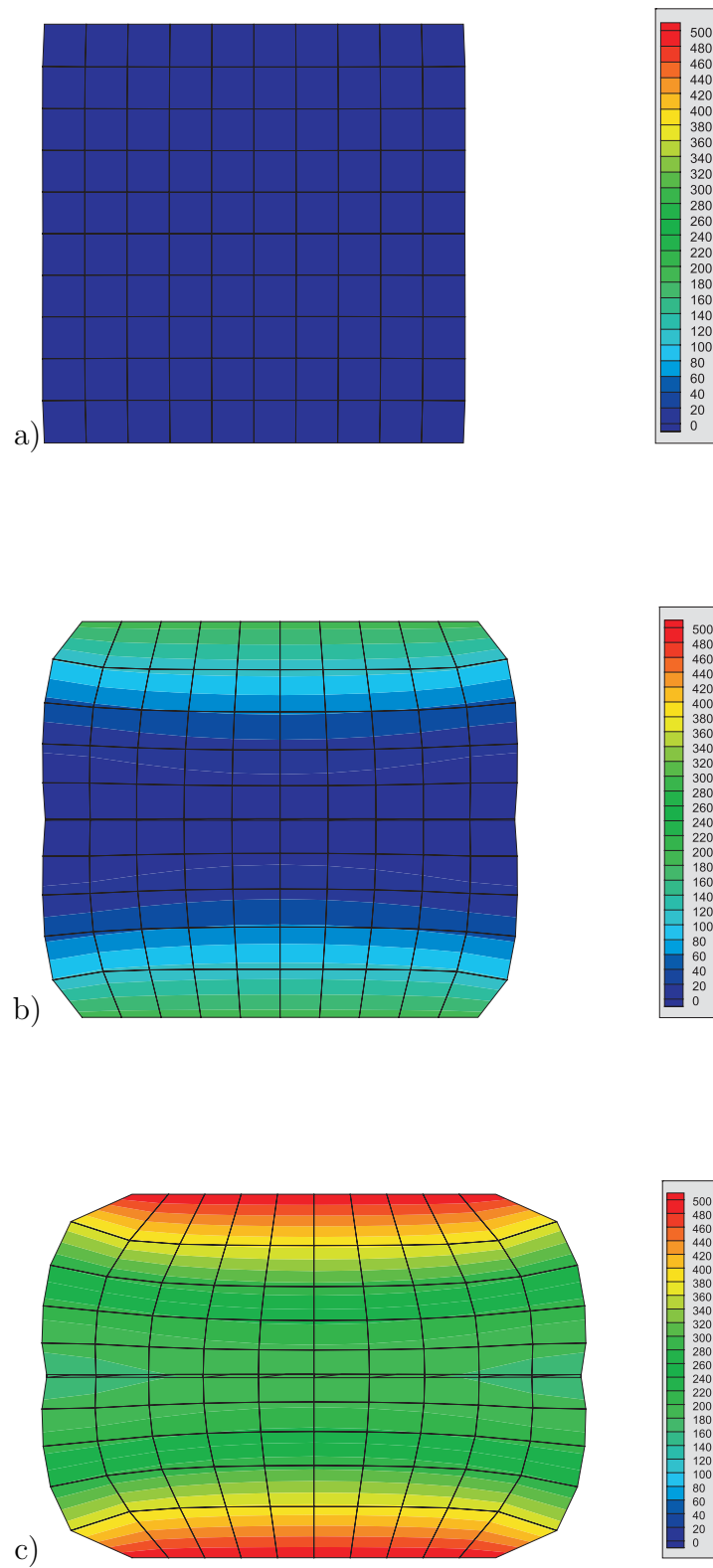


Figure 5.7. Distribution of absolute temperature in the a) initial configuration and after b) 10 seconds and c) 20seconds

6 Summary and Conclusions

The submitted work is divided into two parts whereby the first part is concerned with the preparation of a continuum mechanical framework where discontinuities and interfaces can be integrated. We started with the general description of geometrically nonlinear deformation and the inherent distinction of material and spatial configurations. From these two point of views different nonlinear strain and stress measures and the corresponding rate formulations emerge. In this context the two essential concepts of isotropy and material objectivity were introduced. With these tools at hand the fundamental mechanical and thermo-mechanical balance equations could be formulated, which are the foundations of material theory. Especially, the 2nd law of thermodynamics, in terms of the Clausius-Duhem-Inequality, delivers important constraints for the modeling of materials. Firstly we applied the previous concepts of nonlinear (isothermal) continuum mechanics to elastic problems. Here the spectral decomposition of kinematical quantities led to a stress-strain-relation in terms of the eigenvalues, which simplify the transformation of terms in the initial configuration to the spatial one and vice versa. With respect to the numerical solution methods, where usually the Newton-Raphson-Scheme is applied, the derivation of the corresponding tangent operators is necessary. These were derived for the spatial and the material formulation, in terms of the eigenvalues and the corresponding eigenbases. These material tensors were also used for the inelastic constitutive laws in consideration of the corresponding inelastic modifications. Afterwards the fundamental concepts for the geometrically linear plasticity theory was resumed, before they were applied to the nonlinear theory. The main ideas in plasticity are the additive decomposition of the strains into an elastic and a plastic part, the concept of internal variables and the principle of maximum dissipation, that yields the normality rule providing a unique relation between the (deviatoric) stresses and the plastic strain rate. The main difference of the linear and the nonlinear plasticity theory consists in the more complex nonlinear kinematics that require an additional plastic configuration and the introduction of strain measures describing the accumulated plastic strains. In the linear plasticity theory, the strains consist of the sum of elastic and plastic contributions, whereas in the nonlinear theory the deformation gradient is decomposed multiplicatively. Hereby the plastic deformation gradient maps from the reference configuration to the intermediate configuration, where plastic strains are described by the plastic right Cauchy-Green tensor as the usual plastic strain measure. The elastic deformation gradient maps quantities from the plastic configuration to the spatial one. By introducing a logarithmic strain measure the multiplicative structure is reduced to a sum again, such that the concepts of the linear plasticity theory can be applied. For updating the internal variables the implicit Euler-backward scheme was used and with the resulting plastic multiplier the consistent algorithmic tangent operator could be computed. The solution of the momentum balance equation was performed by the finite element method. In this context the weak forms of the spatial and the material configuration had to be derived and the corresponding linearizations had to be carried out.

Hereby the general form was restricted to quasistatic problems. In order to take thermal effects into account, a temperature evolution equation was derived, that also led to a modified Clausius-Duhem inequality. Here in addition to the isothermal standard local dissipation a nonlocal or convective dissipation was derived induced by the entropy flux, that was related to the heat flux by appropriate constitutive assumptions. Within the consideration of thermo-mechanical problems two different kinds of thermo-mechanical coupling have to be distinguished, which also induces different ways in numerical treatment. In the first case we assumed that the temperature increase in a particular point does not effect its neighbourhood, since heat flux is neglected. This adiabatic assumption usually can be made if the investigated processes are very fast. Since the temperature only depends on the location itself and not on the neighbourhood, it can be introduced as an additional internal variable and its rate can be determined by a local iteration algorithm. In contrast to this, in the second case the temperature can also be introduced as an additional primary variable. With this at hand we can also describe the heat flux within a material. The numerical realization proves to be analogous to the isothermal problem, whereby in addition to the linear momentum balance equation the temperature evolution needs to be transformed to the weak form in consideration of coupling terms connecting both types of subproblems. Afterwards the corresponding linearization procedure was performed and finally, the additional primary variable required to be discretized in an appropriate way. This concluded the theoretical description of bulk modelling of elasto-plastic and thermo-elasto-plastic materials. Finally the derived models were applied in numerical calculations. In the second part of this work the given mechanical and thermodynamical framework was extended to enable the consideration of discontinuities and interfaces, whereby we restricted ourselves to the geometrically linear theory. At first we started with the reformulation of the momentum balance equation, whereby the discontinuities were considered as boundaries cutting through the continuous body. From the kinematical point of view finally two interfacial displacement contributions, namely across and along the interface emanated. The first contribution was given by the displacement jump, that results from the difference of the boundary displacement values and the second was defined by the gradient of the averaged displacements. From these two interfacial kinematical quantities emerged two corresponding tractions or stress contributions, respectively, in the interfacial linear momentum balance equation.

In consideration of the additional interface contributions, we derived the modified balance equations of internal energy and entropy. These balances formally contain, in analogy to the balance of linear momentum, an average-based and a jump-based heat flux, whereby these terms were not defined up to this point, since the interface temperature was not defined so far. This definition was performed in the next step, whereby two possible definitions were investigated leading to two corresponding forms of the interface heat flux or the interface entropy flux, respectively. The simplest assumption was that the interface temperature coincides with the average of the boundary temperature values. But this led to a formulation that required a presetting of entropy boundary conditions, such that this choice rather was of less practical interest. The second approach was that the inverse interface temperature coincides with the average of the inverse boundary temperature values. This assumption yielded a formulation involving boundary conditions of the interface heat flux. For the numerical investigations within the finite element method the derived balance equations had to be transformed into the weak form and afterwards the corresponding discretization was performed, whereby especially the additional interfacial primary variables had to be taken into account. Finally the interface formulation was adopted to localization problems and to the description of thermo-mechanical composites.

This thesis can be understood as an introductory framework for the description of discontinuities and interfaces within inelastic thermo-mechanical materials. The derived concepts were transformed

to corresponding numerical formulations and they were successfully applied to realistic problems. Although the given representation was as capacious as possible, there are still some aspects which were not considered so far. Further investigations could be concerned with:

- The transformation of the interface formulations from the linear to the geometrically nonlinear context as far as it was not performed so far. Especially from the consideration of the average-based contributions within the nonlinear theory some problems emanate since a reasonable determination of the average values from the initially related boundary values after deformation often is not unique anymore in the framework of large deformations.
- The numerical behaviour of thermo-mechanical interfaces with respect to different types of finite elements taking interfaces with extra energy contributions into account.
- A numerically stable interface formulation that is able to cover mechanism of complete material separation.
- Interaction of interfaces and contact formulations as they arise from cutting problems as they were discussed fundamentally in this thesis.

A Appendix

A.1 Spectral Decomposition

A lot of kinematical quantities introduced in chapter 2 are tensors of second order and if they are symmetric, they can be represented by the spectral decomposition of the form

$$\mathbf{A} = \sum_{\alpha=1}^3 \lambda_{\alpha} \mathbf{N}^{\alpha} \otimes \mathbf{N}^{\alpha}, \quad \text{with} \quad \mathbf{A} \in \mathbb{S}^3 \quad (\text{A.1.1})$$

where λ_{α} denotes the *eigenvalues* and \mathbf{N}^{α} ($\alpha = 1, 2, 3$) are the corresponding *eigenvectors* or *principal directions*. Since the triple of the eigenvectors are generally orthogonal to each other, the co- and contravariant eigenvectors coincide and the position of the index can be chosen arbitrarily, but it is common to mark the eigenvectors by superscripts. In spectral decomposed form the tensor is a linear combination of the *eigenbase* $\mathbf{M}^{\alpha} = \mathbf{N}^{\alpha} \otimes \mathbf{N}^{\alpha}$ multiplied by the corresponding eigenvalue as the linear factor. Every particular eigenbase is a rank one tensor and therefore we obtain the following properties

$$\mathbf{M}^{\alpha} \cdot \mathbf{M}^{\beta} = \mathbf{N}^{\alpha} \otimes \mathbf{N}^{\alpha} \cdot \mathbf{N}^{\beta} \otimes \mathbf{N}^{\beta} = \begin{cases} \mathbf{M}^{\alpha} & \text{if } \alpha = \beta \\ \mathbf{0} & \text{if } \beta \neq \alpha \end{cases}, \quad \sum_{\alpha=1}^3 \mathbf{M}^{\alpha} = \mathbf{I} \quad (\text{A.1.2})$$

with the consequence, that \mathbf{A} to the power of n is equivalent to raising the eigenvalue λ_{α} to the power of n and remaining the eigenbase unaltered. Therefore we obtain

$$\mathbf{A}^n = \sum_{\alpha=1}^3 \lambda_{\alpha}^n \mathbf{N}^{\alpha} \otimes \mathbf{N}^{\alpha}. \quad (\text{A.1.3})$$

Before we can reformulate the tensor in this form, we need to calculate the eigenvalues λ_{α} and the corresponding eigenvectors \mathbf{N}^{α} . For the determination of the eigenvalues of \mathbf{A} we firstly calculate the determinant of the eigenvalue problem represented by

$$\det [\mathbf{A} - \lambda_{\alpha} \mathbf{I}] = \lambda_{\alpha}^3 - I_1 \lambda_{\alpha}^2 + I_2 \lambda_{\alpha} - I_3 = 0, \quad (\text{A.1.4})$$

whereby the I_1, I_2 and I_3 denote the *principal invariants* that are defined by

$$\begin{aligned} I_1 &= \text{tr}(\mathbf{A}) &= \lambda_1 + \lambda_2 + \lambda_3 \\ I_2 &= \frac{1}{2} [\text{tr}^2(\mathbf{A}) - \text{tr}(\mathbf{A}^2)] &= \lambda_1 \lambda_2 + \lambda_2 \lambda_3 + \lambda_3 \lambda_1 \\ I_3 &= \det(\mathbf{A}) &= \lambda_1 \lambda_2 \lambda_3. \end{aligned} \quad (\text{A.1.5})$$

From this expression the eigenvalues can be determined analytically by

$$\lambda_\alpha = \frac{1}{3} \left[I_1 + 2\sqrt{I_1 - 3I_2} \cos \frac{1}{3} [\psi + 2\pi\alpha] \right] \quad \text{with} \quad \psi = \arccos \left[\frac{\frac{1}{2} [2I_1^3 - 9I_1I_2 + 27I_3]}{\sqrt{[I_1^2 - 3I_2]^3}} \right] \quad (\text{A.1.6})$$

and the corresponding eigenbase \mathbf{M}^α can be obtained by the following relation

$$\mathbf{M}^\alpha = \frac{\sum_{\zeta=1 \setminus \alpha}^3 [\mathbf{A} - \lambda_\zeta \mathbf{I}]}{\sum_{\zeta=1 \setminus \alpha}^3 [\lambda_\alpha - \lambda_\zeta]} = \frac{\mathbf{A}^2 - [I_1 - \lambda_\alpha] \mathbf{A} + I_3 \lambda_\alpha^{-1} \mathbf{I}}{2\lambda_\alpha^2 - I_1 \lambda_\alpha + I_3 \lambda_\alpha^{-1}}. \quad (\text{A.1.7})$$

Here we have to remark that for the denominator in eqn. A.1.7 the eigenvalues shall not be equal. For this case the eigenvalues have to be perturbed by a small number δ , such that we obtain $\lambda_\alpha = \lambda_\alpha [1 + \delta]$, $\lambda_\beta = \lambda_\beta [1 - \delta]$ and $\lambda_\gamma = \lambda_\gamma / [1 - \delta] [1 + \delta]$. Another remark we like to do here is that it is usually sufficient with respect to numerical applications to calculate the eigenbase \mathbf{M}_α and not the eigenvectors. The expression given in eqn A.1.7 is very crucial for the numerical determination of stress-rates. A detailed discussion can be found in the publication of Miehe [Mie93] and the main results are represented in section 2.5.3. Another crucial relation, we want to mention here is the Cayley-Hamilton-theorem that states that the characteristic polynomial is solved by the tensor \mathbf{A} itself, such that

$$\mathbf{A}^3 - I_1 \mathbf{A}^2 + I_2 \mathbf{A} - I_3 \mathbf{I} = \mathbf{0} \rightsquigarrow \mathbf{A}^3 = I_1 \mathbf{A}^2 - I_2 \mathbf{A} + I_3 \mathbf{I}. \quad (\text{A.1.8})$$

Here we have to take into account, that if I_3 gets zero, \mathbf{A}^{-1} is singular. With this at hand it is possible to express the exponent \mathbf{A}^m for every integer m in terms of the invariants and \mathbf{I} , \mathbf{A} and \mathbf{A}^2 . Hence, the inverse \mathbf{A}^{-1} can easily be represented by

$$\mathbf{A}^{-1} = \frac{1}{I_3} [\mathbf{A}^2 - I_1 \mathbf{A} + I_2 \mathbf{I}]. \quad (\text{A.1.9})$$

These results are applicable to symmetric tensors, like the right Cauchy Green tensor or the strain measures derived in Chapter 2.

A.2 Differentiation of Base Tensors

Material Description The implementation of constitutives requires the knowledge of the elasticity tensor, that is determined by the derivative of the stress measure with respect to the corresponding strain measure. Performing this differentiation it is necessary to determine also the derivative of the eigenbase with respect to the corresponding strain measure. Here we want to start with the material formulation where the derivative of the material eigenbase with respect to the right Cauchy Green tensor $\partial \mathbf{S}^\# / \partial \mathbf{M}^\alpha$ has to be computed. For this we start with the expression for the eigenbase in eqn. A.1.7, whereby we want to rewrite it here in terms of the right Cauchy Green tensor \mathbf{C}^b and therefore we must insert here the squared eigenvalues. Furthermore we have to take into account that the derivation of the modified eigenbase has to be calculated here. That means, that we have to multiply the equation by λ_α^{-2} and therefore we obtain

$$\mathbf{M}^\alpha = \frac{\mathbf{G}^\# \cdot \mathbf{C}^b - [I_1 - \lambda_\alpha^2] \mathbf{G}^\# + I_3 \lambda_\alpha^{-2} [\mathbf{C}^b]^{-1}}{2\lambda_\alpha^4 - I_1 \lambda_\alpha^2 + I_3 \lambda_\alpha^{-2}} = \frac{\mathbf{K}^\alpha}{D_\alpha} \quad (\text{A.2.10})$$

Of course, the invariants are also formulated in terms of the squared eigenvalues. At first we can determine the derivative by using the product rule again

$$\frac{\partial \mathbf{M}^\alpha}{\partial \mathbf{C}^b} = \frac{1}{D_\alpha} \frac{\partial \mathbf{K}^\alpha}{\partial \mathbf{C}^b} - \mathbf{K}^\alpha \otimes \frac{1}{D_\alpha^2} \frac{\partial D_\alpha}{\partial \mathbf{C}^b}, \quad (\text{A.2.11})$$

whereby the derivatives of \mathbf{K}^α and D_α with respect to the right Cauchy Green tensor have to be computed. We start with the computation of the nominators derivative that is

$$\begin{aligned} \frac{\partial \mathbf{K}^\alpha}{\partial \mathbf{C}^b} &= \mathbb{I}_{\mathbf{C}^{-1}}^{sym} - \mathbf{G}^\# \otimes \mathbf{G}^\# + \lambda_{(\alpha)}^2 \mathbf{M}^\alpha \otimes \mathbf{G}^\# - \lambda_{(\alpha)}^{-2} I_3 \mathbf{M}^\alpha \otimes [\mathbf{C}^b]^{-1} \\ &+ I_3 \lambda_\alpha^{-2} [\mathbf{C}^b]^{-1} \otimes [\mathbf{C}^b]^{-1} - \lambda_\alpha^{-2} I_3 \mathbb{I}_{\mathbf{C}^{-1}}^{sym}. \end{aligned} \quad (\text{A.2.12})$$

Here we get the fourth order tensor $\mathbb{I}_{\mathbf{C}^{-1}}^{sym}$ that was already introduced in eqn. 2.5.75 and that results from the derivative of the inverse right Cauchy Green tensor with respect to the right Cauchy Green tensor itself $\partial [\mathbf{C}^b]^{-1} / \partial [\mathbf{C}^b]$. To determine this derivative we start with the identity $[\mathbf{C}^b]^{-1} \cdot \mathbf{C}^b = \mathbf{I}$ and consider its derivative with respect to the right Cauchy Green tensor, whereby we take the definition of the fourth order identity tensor in eqn. 2.5.45 into account. With this at hand we obtain the expression we are looking for, such that ¹

$$\mathbb{I}_{\mathbf{C}^{-1}}^{sym} = \frac{\partial [\mathbf{C}^b]^{-1}}{\partial \mathbf{C}^b} = -\frac{1}{2} \left[[\mathbf{C}^b]^{-1} \bar{\otimes} [\mathbf{C}^b]^{-1} + [\mathbf{C}^b]^{-1} \underline{\otimes} [\mathbf{C}^b]^{-1} \right]. \quad (\text{A.2.13})$$

Taking eqn.2.5.47 and eqn. 2.5.37_{1,3} into account also the derivative of the denominator can be calculated by

$$\frac{\partial D_\alpha}{\partial \mathbf{C}^b} = [4\lambda_\alpha^4 - I_1 \lambda_\alpha^2 - I_3 \lambda_\alpha^{-2}] \mathbf{M}^\alpha - \lambda_\alpha^2 \mathbf{G}^\# + \lambda_\alpha^{-2} I_3 [\mathbf{C}^b]^{-1}. \quad (\text{A.2.14})$$

¹Here $\mathbb{I} = \mathbf{I} \bar{\otimes} \mathbf{I}$ denotes the fourth order unit tensor, that maps a second order tensor to itself $\mathbf{A} = \mathbb{I} : \mathbf{A}$, whereas $\mathbb{I}^t = \mathbf{I} \underline{\otimes} \mathbf{I}$ maps a second order tensor to its tranposed: $[\mathbf{A}]^t = \mathbb{I}^t : \mathbf{A}$. Therefore the given definition yields a symmetric fourth order unit tensor.

Now the relations in eqn. A.2.12 and A.2.14 can be inserted into eqn. A.2.11 and by using the identity $\mathbf{K}_\alpha/D_\alpha = \mathbf{M}^\alpha$ we can rewrite it as

$$\begin{aligned} \frac{\partial \mathbf{M}^\alpha}{\partial \mathbf{C}^b} &= \frac{1}{D_\alpha} [\mathbb{I}_C^{sym} - I_3 \lambda_\alpha^{-2} \mathbb{I}_{C^{-1}}^{sym} - \mathbf{G}^\# \otimes \mathbf{G}^\# + \lambda_\alpha^2 [\mathbf{M}^\alpha \otimes \mathbf{G}^\# + \mathbf{G}^\# \otimes \mathbf{M}^\alpha] \\ &+ I_3 \lambda_\alpha^{-2} [\mathbf{C}^b]^{-1} \otimes [\mathbf{C}^b]^{-1} - I_3 \lambda_\alpha^{-2} [[\mathbf{C}^b]^{-1} \otimes \mathbf{M}^\alpha + \mathbf{M}^\alpha \otimes [\mathbf{C}^b]^{-1}] \\ &+ [2I_3 \lambda_\alpha^{-2} - 2\lambda_\alpha^4] \mathbf{M}^\alpha \otimes \mathbf{M}^\alpha - \mathbf{M}^\alpha \otimes \mathbf{M}^\alpha]. \end{aligned} \quad (\text{A.2.15})$$

This result corresponds to the representation derived by Miehe [Mie93], whereby here the derivative with respect to the material strain tensor is considered. Following Miehe [Mie93] equation A.2.15 can be rewritten as

$$\frac{\partial \mathbf{M}^\alpha}{\partial \mathbf{C}^b} = \frac{1}{D_\alpha} [\mathbb{I}_C^{sym} - I_3 \lambda_\alpha^{-2} \mathbb{I}_{C^{-1}}^{sym}] - \sum_{\beta=1}^3 [I_3 \lambda_\alpha^{-2} - \lambda_\beta^4] \mathbf{M}^\beta \otimes \mathbf{M}^\beta - \mathbf{M}^\alpha \otimes \mathbf{M}^\alpha, \quad (\text{A.2.16})$$

such that the derivative of the eigenbase with respect to the strain tensor can be reduced to a sum of the eigenbases themselves and the fourth order unit tensors \mathbb{I}_C^{sym} and $\mathbb{I}_{C^{-1}}^{sym}$. In favour of brevity the author abandons to discuss the derivatives of the eigenbases for plane problems and the numerical treatment of identical eigenvalues. These investigations are accomplished in detail by Miehe [Mie93] or in the publication of Betsch & Steinmann [BS98].

Spatial Description For the determination of the spatial formulation we simply push forward the results of the material setting, whereby we employ the relation

$$\mathbf{m}^\alpha = \mathbf{F}^\natural \cdot \mathbf{M}^\alpha \cdot [\mathbf{F}^\natural]^t. \quad (\text{A.2.17})$$

Performing the push forward operation term by term the derivative of the spatial eigenbase with respect to the spatial metric tensor can be computed by

$$\varphi^* \left(\frac{\partial \mathbf{M}^\alpha}{\partial \mathbf{C}^b} \right) = \frac{\partial \mathbf{m}^\alpha}{\partial \mathbf{g}^b} = [\mathbb{I}_b - I_3 \lambda_\alpha^{-2} \mathbb{I}_g] - \frac{1}{D_\alpha} \sum_{\beta=1}^3 [I_3 \lambda_\alpha^{-2} - \lambda_\beta^4] \mathbf{m}^\beta \otimes \mathbf{m}^\beta - \mathbf{m}^\alpha \otimes \mathbf{m}^\alpha \quad (\text{A.2.18})$$

The spatial fourth order unit tensor $\mathbb{I}_{g^\#}$ is given by the push forward of the material fourth order unit tensor $\mathbb{I}_{C^b}^{sym}$.

A.3 Convexity

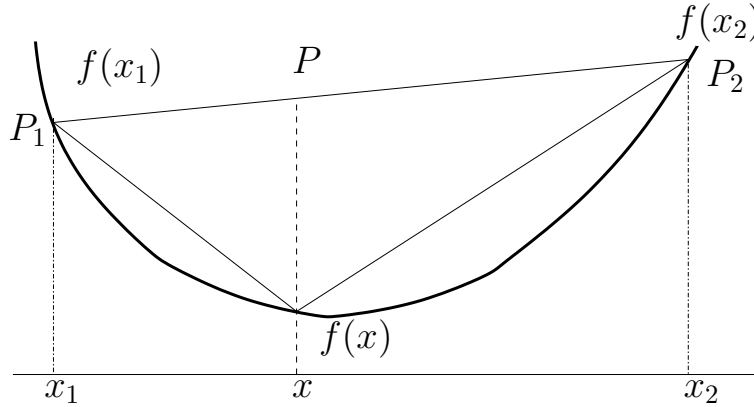


Figure A.1. Definition of a konvex function

In the framework of plasticity convexity is a very important condition which the yield function has to fulfill. In Königsberger [KÖ1] it is defined as follows. For a given scalarvalued function $f(x)$, as it is illustrated in fig. A.3 the convexity is ensured if there are two arbitrary values $f(x_1)$ and $f(x_2)$ that are connected by a line

$$L(x) = f(x_1) + \frac{f(x_2) - f(x_1)}{[x_2 - x_1]}[x - x_1] \quad (\text{A.3.19})$$

and every value $f(x)$ for any $x_1 < x < x_2$ lies below the line

$$L(x) \geq f(x) \quad (\text{A.3.20})$$

A more comfortable formulation of the convexity criterion can be obtained by introducing a scalar parameter λ and expressing x in terms of λ . This yields $x = x_1 + [1 - \lambda]x_2$, $\lambda \in [0, 1]$, that is inserted in eqn. A.3.19, such that we obtain

$$L(x) = f(x_1) + \lambda [f(x_2) - f(x_1)] \geq f(x_1 + \lambda[x_2 - x_1]) \quad \lambda \in [0, 1] \quad (\text{A.3.21})$$

This representation is also valid if vector- and tensorvalued functions $f(\mathbf{x})$ are considered. Another equivalent definition is given by Simo & Hughes [SH98] where the function $f(\mathbf{x})$ for any $\mathbf{x}_1 < \mathbf{x} < \mathbf{x}_2$ is convex if the

$$f(\mathbf{x}_2) \geq f(\mathbf{x}_1) + \text{grad}f(\mathbf{x}_1) \cdot [\mathbf{x} - \mathbf{x}_1]. \quad (\text{A.3.22})$$

This equation describes that if the gradient at $f(\mathbf{x}_1)$ is less than the values $f(\mathbf{x})$ for any $\mathbf{x}_1 < \mathbf{x} < \mathbf{x}_2$ then convexity is ensured. Of course the function $f(\mathbf{x})$ needs to be smooth in $[\mathbf{x}_1, \mathbf{x}_2]$, such that the gradient exists. This relation can be derived from eqn. A.3.21 that can be transformed to

$$\frac{f(\mathbf{x}_1 + \lambda[\mathbf{x}_2 - \mathbf{x}_1]) - f(\mathbf{x}_1)}{\lambda} \leq f(\mathbf{x}_2) - f(\mathbf{x}_1), \quad \lambda \in [0, 1]. \quad (\text{A.3.23})$$

By considering the limes of $\lambda \rightarrow 0$ we obtain the presented result in eqn. A.3.22.

Bibliography

- [AA94] J. Altenbach and H. Altenbach. *Einführung in die Kontinuumsmechanik*. B. G. Teubner Verlag Stuttgart Leipzig Wiesbaden, 1994.
- [AA02] H. Askes and E. C. Aifantis. Numerical modelling of size effects with gradient elasticity - formulation, meshless discretization and examples. *International Journal of Fracture*, 117:347–358, 2002.
- [AD81] J. H. Argyris and J. St. Doltsinis. On the natural formulation and analysis of large deformation coupled thermomechanical problems. *Comp. Meth. Appl. Mech. Engrg.*, 25:pp. 195–253, 1981.
- [ADPW82] J. H. Argyris, J. St. Doltsinis, P.M. Pimenta, and H. Wüstenberg. Thermomechanical response of solids at high strains - natural approach. *Comp. Meth. Appl. Mech. Engrg.*, 32:pp. 3–57, 1982.
- [AS00] H. Askes and B. Sluys. Remeshing strategies for adaptive ale analysis of strain localisation. *European Journal of Mechanics A/Solids*, 19:447–467, 2000.
- [Ask00] H. Askes. *Advanced spatial discretisation strategies for localised failure*. PhD thesis, Faculty of Civil Engineering and Geosciences, Technical University of Delft,, 2000.
- [BB75] V. Becker and W. Bürger. *Kontinuumsmechanik*. B. G. Teubner Verlag Stuttgart Leipzig Wiesbaden, 1975.
- [Bet02] P. Betsch. *Computational Methods for Flexible Multibody Dynamics*. Habilitationsschrift am Lehrstuhl für Technische Mechanik, Universität Kaiserslautern, 2002.
- [BFE87] T. Belytschko, J. Fish, and B. Engelmann. A finite element with embedded localization zones. *Comp. Meth. Appl. Mech. Engrg.*, Vol. 70:pp. 59–89, 1987.
- [BH90] D. J. Benson and J. O. Hallquist. A singel surface contact algorithm for the post-buckling analysis of shell structures. *Comp. Meth. Appl. Mech. Engrg.*, 78:141–163, 1990.

- [BLM00] T. Belytschko, W. K. Liu, and B. Moran. *Nonlinear Finite Elements for Continua and Structures*. John Wiley & Sons, 2000.
- [BS98] P. Betsch and P. Steinmann. Derivation of the fourth-order tangent operator based on a generalized eigenvalue problem. *International Journal of Solids and Structures*, Vol. 37:pp. 1615–1628, 1998.
- [BS00a] P. Betsch and P. Steinmann. Conservation properties of a time FE method. Part I: Time stepping scheme for n-body problems. *Int. J. Numer. Meth. Eng.*, 49:599–638, 2000.
- [BS00b] P. Betsch and P. Steinmann. Inherently energy conserving time finite elements for classical mechanics. *Journal for Computational Physics*, 160:88–116, 2000.
- [BS02a] P. Betsch and P. Steinmann. Conservation properties of a time FE method. Part II: Time-stepping for nonlinear elastodynamics. *Int. J. Numer. Meth. Eng.*, 53:2271–2304, 2002.
- [BS02b] P. Betsch and P. Steinmann. Conservation properties of a time FE method. Part III: Mechanical systems with holonomic constraints. *Int. J. Numer. Meth. Eng.*, 53:2271–2304, 2002.
- [BWed] J. Bonet and R. D. Wood. *Nonlinear Continuum Mechanics for Finite Element Analysis*. Cambridge Press, 2000 Reprinted.
- [Cel98] C. C. Celigoj. Finite deformation coupled thermomechanical problems and 'generalized standard materials'. *Int. J. Numer. Meth. Eng.*, 42:pp. 1025–1043, 1998.
- [Cia82] Geymonat G. Ciarlet, P. G. Sur les lois de comportement en élasticité non linéaire compressible. In *Comptes Rendus Hebdomadaires des Séances de l'Académie des Sciences*, volume 295, pages 423–426. Paris Séries II, 1982.
- [CN63] B. D. Coleman and W. Noll. The thermodynamics of elastic materials with heat conduction and viscosity. *Arch. Rational Mech. Anal.*, 13:pp. 167–178, 1963.
- [DS96] J. E. Dennis and R. B. Schnabel. *Numerical Methods for Unconstrained Optimaization and Nonlinear Equations*. Society for Industrial and Applied Mathematics, 1996.
- [Eri67] A. C. Eringen. *Mechnics of Continua*. John Wiley & Sons, 1967.
- [Eri02] A.C. Eringen. *Nonlocal Continuum Field Theories*. Springer, 2002.
- [Fel93] D. Feldmann. *Repetitorium der Ingenieurmathematik*, volume II. Binomi Verlag, 4. edition, 1993.
- [GN64] A. E. Green and P. M. Naghdi. A general theory of an elastic-plastic continuum. *Arch. rat. Mech. Phys.*, 18:251–281, 1964.
- [Gon96a] O. Gonzales. *Design and Analysis of Conserving Algorithms for Nonlinear Hamiltonian Systems with Symmetry*. PhD thesis, 1996.
- [Gon96b] O. Gonzales. Time integration and discrete hamiltonian systems. *Journal of nonlinear science*, 6:449–467S, 1996.

- [Gon00] O. Gonzales. On the stability of symplectic and energy-momentum algorithms for non-linear hamiltonian systems with symmetry. *Comp. Meth. Appl. Mech. Engrg.*, 190:1763–1783, 2000.
- [Gre03] R. Greve. *Kontinuumsmechanik*. Springer-Verlag, Springer-Verlag Berlin Heidelberg New York 2003.
- [Gro04] M. Groß. *Conserving Time Integrators for Nonlinear Elastodynamics*. PhD thesis, Lehrstuhl für Technische Mechanik, Universität Kaiserslautern, 2004.
- [GS00] O. Gonzales and J. C. Simo. Exact energy and momentum conserving integrators for general models in nonlinear elasticity. *Comp. Meth. Appl. Mech. Engrg.*, 190:1763–1783, 2000.
- [Gur77] A. L. Gurson. Continuum theory of ductile rupture by void nucleation and growth: Part 1 - yield criteria and flow rules for porous ductile media. *Engng. Materials Technology*, Vol. 99:pp. 2–15, 1977.
- [Gur00] M. E. Gurtin. *Configurational Forces as Basic Concepts of Continuum Physics*, volume 137 of *Applied Mathematical Sciences*. Springer-Verlag, 2000.
- [Hau02] P. Haupt. *Continuum Mechanics and Theory of Materials*. Springer-Verlag, 2. edition, 2002.
- [HGB85] J.O. Hallquist, G.L. Goudreau, and D. J. Benson. Sliding interfaces with contact-impact in large-scale lagrangian computations. *Comp. Meth. Appl. Mech. Engrg.*, 51:pp. 107–137, 1985.
- [Hol01] G. A. Holzapfel. *Nonlinear Solid Mechanics*. John Wiley & Sons, Reprint in 2001.
- [HR99] W. Han and B. D. Reddy. *Plasticity, Mathematical Theory and Numerical Analysis*. Springer-Verlag, 1999.
- [Hug00] T. J. R Hughes. *The Finite Element Method*. Dover Publications, Reprinted in 2000.
- [Hut77] K. Hutter. The foundations of thermodynamics, its basic postulates and implications. a review of modern thermodynamics. *Acta Mech.*, 27:pp. 1–54, 1977.
- [IC02] A. Imbrahimbegovic and L. Chorfi. Covariant principal axis formulation of associated coupled thermoplasticity at finite strains and its numerical implementation. *Int. J. Solid Structures*, 39:pp.499–528, 2002.
- [ICG01] A. Imbrahimbegovic, L. Chorfi, and F. Gharzeddine. Thermomechanical coupling at finite elastic strain: Covariant formulation and numerical implementation. *Commun. Numer. Meth. Engng.*, 17:pp.275–289, 2001.
- [Jan] N. Jansson. A shell- interface formulation for delamination analysis of composite laminates. *Computers & Structures*.
- [Jan01] N. Jansson. A damage model for simulation of mixed-mode delamination growth. *Composite Structures*, 53(4):409–417, 2001.

- [Jan02] N. Jansson. *Modelling of Delamination Growth in Composite Structures*. PhD thesis, Chalmers University of Technology, Göteborg, Sweden, 2002.
- [JL] N. Jansson and R. Larsson. Rotational interface formulation for delamination analysis of composite laminates. *Computers & Structures*.
- [JL01] M. Jung and U. Langer. *Methode der Finiten Elemente für Ingenieure*. B. G. Teubner Verlag Stuttgart Leipzig Wiesbaden, 2001.
- [Kö1] K. Königsberger. *Analysis*, volume 1. Springer-Verlag, 5. edition, 2001.
- [Lau94] T. A. Laursen. The convected description in large deformation frictional contact problems. *Int. J. Solid Structures*, 31:pp. 669–681, 1994.
- [Lau02] T. A. Laursen. *Computational Contact and Impact Mechanics*. Springer-Verlag, 2002.
- [Lee67] E. H. Lee. Elastic-plastic deformations at finite strains. *J. Appl. Mech.*, 36:1–6, 1967.
- [Lem84] J. Lemaitre. Coupled elasto-plasticity and damage constitutive equations. *Comp. Meth. Appl. Mech. Engrg.*, Vol. 51:pp. 31–49, 1984.
- [Lem85] J. Lemaitre. A continuous damage mechanics model for ductile fracture. *J. Eng. Mater. Technol.*, Vol. 107:pp. 83–89, 1985.
- [Lep00] C. Leppin. *Ein diskontinuierliches Finite-Element-Modell für Lokalisierungsversagen in metallischen und granularen Materialien*. PhD thesis, Universität Hannover, 2000.
- [LG94] T. A. Laursen and Oancea V. G. Automation and assessment of augmented lagrangian algorithms for frictional contact problems. *J. Appl. Mech.*, 61:pp. 956–963, 1994.
- [Lie03] T. Liebe. *Theory and Numerics of Higher Gradient Inelastic Material Behaviour*. PhD thesis, Lehrstuhl für Technische Mechanik, Universität Kaiserslautern, 2003.
- [LJ02] R. Larsson and N. Jansson. Geometrically nonlinear damage interface based on regularized strong discontinuities. *Int. J. Numer. Meth. Engrg.*, 54:473–497, 2002.
- [LRO93] R. Larson, K. Runesson, and N. S. Ottosen. Discontinuous displacement approximation for capturing plastic localization. *Int. J. Numer. Meth. Eng.*, 36:2087–2105, 1993.
- [LS93a] T. A. Laursen and J. C. Simo. Algorithmic symmetrization of coulomb frictional problems using augmented lagrangians. *Comp. Meth. Appl. Mech. Engrg.*, 108:pp. 133–146, 1993.
- [LS93b] T. A. Laursen and J. C. Simo. A continuum-based finite element formulation for the implicit solution of multi-body, large deformation frictional contact problems. *Int. J. Numer. Meth. Eng.*, 36:pp. 3451–3485, 1993.
- [Lub90] J. Lubliner. *Plasticity Theory*. MacMillan Publishing Company, 1990.
- [Mah99] R. Mahnen. Aspects on the finite-element implementation of the gurson model including parameter identification. *International Journal of Plasticity*, Vol. 15:pp. 1111–1137, 1999.

- [Men02] A. Menzel. *Modelling and Computation of Geometrically Nonlinear Anisotropic Inelasticity*. PhD thesis, Lehrstuhl für Technische Mechanik, Universität Kaiserslautern, 2002.
- [MH94] J. E. Marsden and T. J. R. Hughes. *Mathematical Foundations of Elasticity*. Dover Publications, 1994.
- [Mie88] C. Miehe. *Zur numerischen Behandlung thermomechanischer Prozesse*. PhD thesis, Dissertation am Fachbereich Bauingenieur- und Vermessungswesen, Universität Hannover, 1988.
- [Mie92] C. Miehe. *Kanonische Modelle multiplikativer Elastizität. Thermodynamische Formulierung und Numerische Implementierung*. Habilitationsschrift am Fachbereich Bauingenieur- und Vermessungswesen, Universität Hannover, 1992.
- [Mie93] C. Miehe. Computation of isotropic tensor functions. *Commun. Numer. Meth. Engng*, Vol. 9:pp. 889–896, 1993.
- [Mie94] C. Miehe. A theory of large-strain isotropic thermoplasticity based on metric transformation tensors. *Arch. Appl. Mech.*, Vol. 66:pp. 45–64, 1994.
- [Mie95] C. Miehe. Entropic thermoelasticity at finite strains. aspects of the formulation and numerical implementation. *Comp. Meth. Appl. Mech. Engrg.*, Vol. 120:pp. 243–269, 1995.
- [Mie98a] C. Miehe. A constitutive frame of elastoplasticity at large strains based on the notion of plastic metric. *Int. J. Solids Structures*, Vol. 35:pp. 3859–3897, 1998.
- [Mie98b] C. Miehe. A formulation of finite elastoplasticity based on dual co- and contra-variant eigenvector triads normalized with respect to a plastic metric. *Comp. Meth. Appl. Mech. Engrg.*, Vol. 159:pp. 223–260, 1998.
- [MS92] C. Miehe and E. Stein. A canonical model of multiplicative elasto-plasticity. formulation and aspects of the numerical implementation. *Eur. J. Mech. A/Solids*, Vol. 11:pp. 25–43, 1992.
- [MS94] C. Miehe and J. Schroeder. Postcritical discontinuous localization analysis of small-strain softening elastoplastic solids. *Arch. Appl. Mech.*, Vol. 64:pp. 267–285, 1994.
- [Nag90] P. M. Naghdi. A critical review of the state of finite plasticity. *J. Appl. Math. Phys.*, 41:315–394, 1990.
- [Ode72] J. T. Oden. *Finite Elements of Nonlinear Continua*. McGraw-Hill, 1972.
- [Ogd97] R. W. Ogden. *Nonlinear Elastic Deformations*. Dover Publications, 1997.
- [Oli96a] J. Oliver. Modelling strong discontinuities in solid mechanics via strain softening constitutive equations. part 1: Fundamentals. *Int. J. Numer. Meth. Eng.*, Vol. 39:pp. 3575–3600, 1996.
- [Oli96b] J. Oliver. Modelling strong discontinuities in solid mechanics via strain softening constitutive equations. part 2: Numerical simulation. *Int. J. Numer. Meth. Eng.*, Vol. 39:pp. 3601–3623, 1996.

- [OR76] J. T. Oden and J. N. Reddy. *An Introduction to the Mathematical Theory of Finite Elements*. John Wiley & Sons, 1976.
- [Par03] H. Parisch. *Festkörper-Kontinuumsmechanik*. B. G. Teubner Verlag Stuttgart Leipzig Wiesbaden, 2003.
- [Per63] P. Perzyna. The constitutive equations for rate sensitive plastic materials. *Quart. Appl. Mechanics*, 20:321–332, 1963.
- [Per66] P. Perzyna. Fundamental problems in viscoplasticity. In G. Kuerti, editor, *Advances in Applied Mechanics*, volume 9, pages 243–377, 1966.
- [PG00] P. Podio-Guidugli. *A Primer in Elasticity*. Kluwer Academic Publishers, Dordrecht-Boston -London, 2000.
- [PW68] P. Perzyna and W. Wonjo. Thermodynamics of rate sensitive plastic material. *Arch. Appl. Mech.*, 20:499–511, 1968.
- [RBD03] M. Rappaz, M. Bellet, and M. Deville. *Numerical Modelling in Material Science and Engineering*. Springer Series in Computational Mathematics. Springer-Verlag, 2003.
- [Red93] J. N. Reddy. *An Introduction to Finite Element Method*. McGraw-Hill, 2. edition, 1993.
- [Ree01] S. Reese. *Thermomechanische Modellierung gummiartiger Polymerstrukturen*. Habilitationsschrift am Institut für Baumechanik und Numerische Methoden, Universität Hannover, 2001.
- [RS99] H. G. Roos and H. Schwetlick. *Numerische Mathematik*. Mathematik für Ingenieure und Naturwissenschaftler. B. G. Teubner Verlag Stuttgart Leipzig Wiesbaden, 1999.
- [SB00] P. Steinmann and P. Betsch. A localization capturing fe-interface based on regularized strong discontinuities at large inelastic strains. *Int. J. Solids Structures*, Vol. 37:pp. 4061–4082, 2000.
- [Sch92] J. C. J. Schellekens. *Computational Strategies for Composite Structures*. PhD thesis, Technical University Delft, Netherlands, 1992.
- [Sch97] H. R. Schwarz. *Numerische Mathematik*. B. G. Teubner Verlag Stuttgart Leipzig Wiesbaden, 4. edition, 1997.
- [SDB93] J. C. J. Schellekens and R. De Borst. On the numerical integration of interface elements. *Int. J. Numer. Meth. Eng.*, Vol. 36:pp. 43–66, 1993.
- [SH98] J.C. Simo and T. J. R Hughes. *Computational Inelasticity*. Interdisciplinar Applied Mathematics. Springer-Verlag, 1998.
- [SH05] P. Steinmann and O. Häsner. On material interfaces in thermomechanical solids. *Arch. Appl. Mech.*, July 2005.
- [Sim88a] J. C. Simo. A framework for the finite dtrain elastoplasticity based on maximum plastic dissipation and multiplicative decomposition: Part 1. computational aspects. *Comp. Meth. Appl. Mech. Engrg.*, 68:1–31, 1988.

- [Sim88b] J. C. Simo. A framework for the finite strain elastoplasticity based on maximum plastic dissipation and multiplicative decomposition: Part I. continuum formulation, numerical algorithms. *Comp. Meth. Appl. Mech. Engrg.*, 66:199–219, 1988.
- [Sim92] J. C. Simo. Algorithms for static and dynamic multiplicative plasticity that preserve the classical return mapping schemes of the infinitesimal theory. *Comp. Meth. Appl. Mech. Engrg.*, Vol. 99:pp. 61–112, 1992.
- [Sim98] J. C. Simo. *Numerical Analysis And Simulation Of Plasticity*. Number VI in Handbook of Numerical Analysis. Elsevier Science, 1998.
- [SLR97] P. Steinmann, R. Larsson, and K. Runesson. On the localization properties of multiplicative hyperelastoplastic continua with strong discontinuities. *Int. J. Solids Structures*, 34(8):969–990, 1997.
- [SM92] J. C. Simo and C. Miehe. Associative coupled thermoplasticity at finite strains: Formulation, numerical analysis and implementation. *Comp. Meth. Appl. Mech. Engrg.*, 98:pp. 41–104, 1992.
- [SMS94] P. Steinmann, C. Miehe, and E. Stein. Comparison of different finite deformation inelastic damage models within multiplicative elastoplasticity for ductile materials. *Comp. Mech.*, Vol. 13:pp. 458–474, 1994.
- [ST92] J. C. Simo and N. Tarnow. The discrete energy momentum method. conserving algorithms for nonlinear elastodynamics. *Z. angew. Math. Phys.*, 43:757–792, 1992.
- [ST94] J. C. Simo and N. Tarnow. A new energy and momentum conserving algorithm for the nonlinear dynamics of shells. *Int. J. Numer. Meth. Eng.*, 37:2527–2549, 1994.
- [Ste92] P. Steinmann. *Lokalisierungsprobleme*. PhD thesis, Fakultät für Bauingenieur- und Vermessungswesen, University of Karlsruhe, 1992.
- [Ste98] P. Steinmann. A model adaptive strategy to capture strong discontinuities at large inelastic strains. In E. Onate und E. Dvorkin S. Idelsohn, editor, *Comp. Mech. CIMNE*, Barcelona, Spain, 1998.
- [Ste99] P. Steinmann. A finite element formulation for strong discontinuities in fluid-saturated porous media. *Mechanics of Cohesive-Frictional Materials*, Vol. 4:pp. 133–152, 1999.
- [SW91a] P. Steinmann and K. Willam. Finite elements for capturing localized failure. *Arch. Appl. Mech.*, 61:259–275, 1991.
- [SW91b] P. Steinmann and K. Willam. Performance of enhanced finite element formulations in localized failure computations. *Comp. Meth. Appl. Mech. Engrg.*, 90:845–867, 1991.
- [TN84] V. Tvergaard and A. Needleman. Analysis of the cup-cone fracture in a round tensile bar. *Acta Metallurgica*, Vol. 32:pp. 157–169, 1984.
- [WA90] G. Weber and L. Anand. Finite deformation constitutive equations and a time integration procedure for isotropic hyperelastic-viscoplastic solids. *Comp. Meth. Appl. Mech. Engrg.*, Vol. 79:pp. 173–202, 1990.

- [Wel96] F. Weller. *Numerische Mathematik für Ingenieure und Naturwissenschaftler*. Vieweg Verlag, 1996.
- [Wel01] G. N. Wells. *Discontinuous Modelling of Strain Localization and Failure*. PhD thesis, Technical Univeristy of Delft, 2001.
- [Wil99] K. Wilmanski. *Thermomechanics of Continua*. Springer-Verlag, 1999.
- [WM94] P. Wriggers and C. Miehe. Contact constraints within coupled thermomechanical analysis- a finite element model. *Comp. Meth. Appl. Mech. Engrg.*, 113:pp. 301–319, 1994.
- [Wri86] P. Wriggers. Konsistente Linearisierungen in der Kontinuumsmechanik und ihre Anwendung. Habilitationsschrift, 1986.
- [Wri95] P. Wriggers. Finite element algorithms for contact problems. In *Archive of Computational Methods in Engineering*, 1995.
- [Wri96] P. Wriggers. Finite element methods for contact problems with friction. *Tribology International*, Vol. 29:pp. 651–658, 1996.
- [Wri01] P. Wriggers. *Nichtlineare Finite-Element-Methode*. Springer-Verlag, 2001.
- [Wri02] P. Wriggers. *Computational Contact Problems*. John Wiley & Sons, 2002.
- [WS98] P. Wriggers and O. Scherf. Adaptive finite element techniques for frictional contact problems involving large elastic strains. *Comp. Meth. Appl. Mech. Engrg.*, Vol. 151:pp. 593–603, 1998.
- [WS00] G. N. Wells and L. J. Sluys. Application of embedded discontinuities for softening solids. *Eng. Fract. Mech.*, 2000.
- [WS01a] G. N. Wells and L. J. Sluys. Analysis of slip planes in three-dimensional solids. *Comp. Meth. Appl. Mech. Engrg.*, 190:pp. 3591–3606, 2001.
- [WS01b] G. N. Wells and L. J. Sluys. Discontinuous analysis of softening solids under impact loading. *Int. J. Numer. Anal. Meth. Geomech.*, 2001.
- [WS01c] G. N. Wells and L. J. Sluys. A new method for modelling cohesive cracks using finite elements. *Int. J. Numer. Engng*, 50:pp. 2667–2682, 2001.
- [WS01d] G. N. Wells and L. J. Sluys. Three-dimensional embedded discontinuity model for brittle fracture. *Int. J. Solids Structures*, 38:pp. 897–913, 2001.
- [WT73] C. C. Wang and C. Truesdell. *Introduction to Rational Elasticity*. Noordhoff International Publishing Leyden, 1973.
- [Zem68] M. W. Zemansky. *Heat and Thermodynamics*. McGraw-Hill, 5. edition, 1968.
- [ZT02a] O. C. Zienkiewicz and R. L. Taylor. *The Finite Element Method, Volume I: The Basis*. Butterworth-Heinemann, 5th edition, Reprinted in 2002.

Bibliography

- [ZT02b] O. C. Zienkiewicz and R. L. Taylor. *The Finite Element Method, Volume II: Solid Mechanics*. Butterworth-Heinemann, 5th edition, Reprinted in 2002.
- [ZT02c] O. C. Zienkiewicz and R. L. Taylor. *The Finite Element Method, Volume III: Fluid Dynamics*. Butterworth-Heinemann, 5th edition, Reprinted in 2002.

Curriculum Vitae

Birth name	Häsner
Surname	Krol
Forename	Oliver
Nationality	German
Date of Birth	8.6.1973 in Berlin
07/1979 - 06/1983	Valentin-Ostertag-Grundschule, Bad Dürkheim
07/1983 - 06/1992	Werner-Heisenberg-Gymnasium, Bad Dürkheim
07/1992 - 10/1993	Civil Service, Bad Dürkheim Hospital
10/1993 - 10/1999	Studies of Mechanical Engineering, Emphasis: Combustion Engines University of Kaiserslautern
11/1999 - 12/2004	Research Associate, University of Kaiserslautern Department of Mechanical and Process Engineering Chair of Applied Mechanics (Prof. Dr.-habil. P. Steinmann)
since 01/2005	Fraunhofer Institute for Information and Data Processing in Karlsruhe, Systems for Measurement, Control and Diagnosis (MRD) (Dr. H.-B. Kuntze)

bereits veröffentlicht wurden:

- 1 Menzel, A.: Modelling and Computation of Geometrically Nonlinear Anisotropic Inelasticity.
2002, ISBN 3-925178-86-4
- 2 Betsch, P.: Computational Methods for Flexible Multibody Dynamics.
2002, ISBN 3-925178-92-9
- 3 Liebe, T.: Theory and numerics of higher gradient inelastic material behavior.
2003, ISBN 3-936890-09-9
- 4 Groß, M.: Conserving Time Integrators for Nonlinear Elastodynamics.
2004, ISBN 3-936890-37-4
- 5 Kuhl, E.: Theory and Numerics of Open System Continuum Thermodynamics – Spatial and Material Settings –
2004, ISBN 3-936890-42-0
- 6 Sunyk, R.: On Aspects of Mixed Continuum-Atomistic Material Modelling.
2004, ISBN 3-936890-51-X
- 7 Arockiarajan, A.: Computational Modeling of Domain Switching Effects in Piezoceramic Materials – A Micro-Macro Mechanical Approach.
2005, ISBN 3-936890-92-7
- 8 Mergheim, J.: Computational Modeling of Strong and Weak Discontinuities.
2006, ISBN 3-939432-02-4; 978-3-939432-02-4-9
- 9 Delibas, B.: Rate dependent nonlinear properties of perovskite tetragonal piezoelectric materials using a micromechanical model.
2006, ISBN 3-939432-05-9; 978-3-939432-05-0
- 10 Leyendecker, S.: Mechanical integrators for constrained dynamical systems in flexible multibody dynamics.
2006, ISBN 3-939432-09-1; 978-3-939432-09-8
- 11 Denzer, R.: Computational Configurational Mechanics
2006, ISBN 3-939432-12-1; 978-3-939432-12-8

- 12 Krol, O.: Thermo-Mechanical Modelling of Solids and Interfaces
– Theory, Numerics and Applications –
2007, ISBN 978-3-939432-45-6